2025 Volume 2

# MORGANTON SCIENTIFIC

JOURNAL OF STUDENT STEM RESEARCH AT THE
NORTH CAROLINA SCHOOL OF SCIENCE AND MATHEMATICS

# Morganton Scientific

North Carolina School of Science and Mathematics

Journal of Student STEM Research

https://doi.org/10.62329/dwgm3685

Cover image by Arjun Rao

## Table of Contents


4 *Words from the Editors*

**Interviews**

6 *An Interview with Mrs. Erika Cummings (PA) from the Duke Neurology Department on Clinical Neuroscience*

12 *An Interview with Dr. Kathryn Moore (MD) from the Duke Neurology Department on Clinical Neuroscience and Research*

**Essays**

27 *Designer Babies A Tale of Horrific Immoralities*
GANGA NAIR

30 *Rewiring Eating Disorder Recovery: Neuroethical Implications of tDCS in ED Treatment*
LEYLA URMANOVA

**Papers**

38 *An Examination of the Enzymatic Degradation of PET Plastic via PETase and MHETase*
RUBY ALLRED

43 *The Psychological Profile of a Future Abuser*
NAVYA BANSAL

49 *Risk Factors of Frequent Poor Mental Health Days Among Adults in the United States*
ANIL CHINTAPALLI

61 *Exploring the Use of Immunotherapy Techniques in Lymphocytic Leukemia*
ENOCH EDWIN

66 *In Silico Exploration of L-Valine Ester Prodrug Designs for Enhanced Pharmacokinetics in BCS Class IV Nucleoside Antivirals.*
KEVIN GENCEL

76 *Modeling Shifts in Reversible Chemical Reactions and Economic Markets*
RADHIKA GOEL

85 *Evaluating the Effects of Lactic Acid Fermented Foods on Type 2 Diabetes Mellitus using Bombyx Mori Silkworms*
VIVEK GOTTUMUKKALA

95 *Utilizing Alkaline Hydrolysis to Recover Terephthalic Acid Monomer From PET-Based Textile Waste*
SARRAH KITCHELL

104 *Utilizing Enzymatic and Chemical Delignification Methods on Fibrous Plants for Decentralized Production of Absorbent Materials for Menstrual Pads in Semi-Arid Regions*

PRERANA KULLA

120 *Binding Affinity and Selectivity of Peptide Ligands for G-Protein-Coupled Receptors*

LILY LI

130 *Green synthesis of decomposing rubber; comparing processing using carboxymethyl cellulose and Ipomoea pes-caprae*

ZUZANNA A. MIKOLAJEC

142 *Optimizing Photovoltaic Output Through the Integration of Passive Optical Tools for Enhanced Photon Capture in Solar Cells*

PRAHAS RAMIDI, AKHILESH KARTHIK

155 *Evaluating the Effect of an Externally Applied Electric Field on Fluorescing Alpha-Synuclein Aggregates in NL5901 Parkinson's Disease Model of Caenorhabditis elegans*

ADRIJA SARKAR

168 *Harvesting Energy with Affordable Piezoelectric Sensors for Low-Power Biosensors*

ANANYA SRIRAM

180 *Exploring The Gut-Brain Axis in C. elegans— Probiotics as a Therapeutic Approach to Alpha-Synuclein Aggregation in Parkinson's Disease*

LEYLA URMANOVA

189 *Computationally Modeling Factors of Aging that Affect the Population of T-cells and B-cells of Humans Age 60 and Older*

FELICE ZHU

## A Note from the Editors

Welcome to the second volume of The Morganton Scientific, NCSSM-Morganton's research journal. Since last year, the journal has grown—not just in size, but in how we work. More students submitted papers. More editors joined the team. The process became more focused, more collaborative, and more deliberate from start to finish.

As with last year, students from both the Morganton and Online programs contributed research across all areas of STEM. The topics and approaches vary, but each paper is the result of consistent effort and a clear interest in the subject. Every author took their work seriously and saw it through with care.

We are grateful to Mrs. Erika Cummings and Dr. Kathryn Moore for taking the time to speak with our team. Their conversations added valuable perspective to this year's edition. We also thank Mr. Christopher Collins and Mrs. Jennifer Williams for their steady support throughout the editorial process. This journal would not exist without them.

This volume builds on the foundation laid last year. It reflects the kind of work students at NCSSM are capable of, and we hope it encourages future contributors to keep writing and keep pushing their ideas forward.

Armaan Gera, Laira Lee, and Mickayla Belus

Editors-in-Chief

# INTERVIEWS

Morganton Scientific

North Carolina School of Science and Mathematics

Journal of Student STEM Research

# An Interview with Mrs. Erika Cummings (PA) from the Duke Neurology Department on Clinical Neuroscience

**Keywords** Interview, Clinical neurology, Neurodegenerative diseases, Deep brain stimulation, Hospital neurology, Healthcare

## 1. Introduction

On Tuesday, March 25th, Mrs. Erika Cummings from the Duke Neurology Department visited the NCSSM Morganton Campus. During her visit, she spoke with authors of the Morganton Scientific. Both Adrija Sarkar and Leyla Urmanova conducted original research to better understand therapies for Parkinson's Disease; their articles are included in the 2nd Edition of the Morganton Scientific. Additionally, Leyla Urmanova and Navya Bansal wrote literature reviews evaluating topics important to clinical psychology and neuroscience. Laira Lee, one of the chief editors of the Morganton Scientific, and Mr. Christopher Collins, a member of the science faculty at NCSSM Morganton, assisted during the interview. A great thanks goes to Mr. Collins for helping set up the interview and reaching out to Mrs. Cummings.

Mrs. Erika Cummings is a Physicians Associate (PA) practicing on the inpatient General Neurology team. She is also involved in PA training. She graduated with a Master of Medical Science degree from Wake Forest University and graduated from Duke's APP residency program.

## 2. Interview

### *2.1. [Laira]: What does your typical day in the hospital look like?*

**[Mrs. Cummings]:** We see people with anything from disorders of consciousness or alertness, changes in their behavior or personality, dramatic injuries, brain bleeds, people with strokes, people with seizures, severe migraines and headaches, tremors, trouble walking, trouble swallowing, weakness, numbness that's unexplained. They come to us and we try to figure it out. We also take care of patients who have brain tumors and tumors in the spinal cord .

I work seven days on and seven days off usually, alternating with a colleague. So one of us is there providing continuity to the rest of the big academic team that only be there for a week or so, they're kind of rotating more quickly and there's a lot of learners, and so part of our role, as the PAs is to give that continuity to the the new people coming on and kind of let them know what happened last week, when they weren't there.

A big group of us will round in the morning, and what that looks like is we show up at seven and we get the sign out from the night team. That tells us about any new patients that came in and then if there were any problems that our old patients might have had overnight.

Then we'll go see all of our patients, one by one, kind of stand outside the room, talk about what happened the night before, what their plan is for the day, what their medications are on or should be on. Additionally, we talk about questions such as:

How close are they to leaving the hospital? How can we help get out of the hospital? And then who needs to be involved in the patient's care?

**Published** Jun 27, 2024

**Figure 1**. *Adrija Sarkar, Navya Bansal, Mrs. Erika Cummings, Leyla Urmanova, and Laira Lee (from left to right) on March 25th.*

So that's the medical providers, we would be consulting the rest of the interdisciplinary team, asking them to come in and weigh in. That could be physical therapists, occupational therapists, speech therapists, respiratory therapists, and social workers.

And so we'll keep going. And we'll see maybe 20 patients on average in a morning, so that probably takes us till around noon. Then we will write notes on all these patients documenting our plans. Then the afternoons are kind of free flowing.

When new patients come in, we're ready to go see them and make a plan for them, or we might be educating some of the learners on the team, taking some time for teaching. Then at 7 PM, we sign off to the night team. And that's the flow of our day, so sometimes it can be really busy, sometimes it has a lot more free time, but it's always with a lot of people.

There's always a lot of signing out and communicating the right information to whoever you're talking to. You have to be able to change your communication style based on who you are talking to, including the patient.

*2.2. [Laira]: What is one disease, whether the symptoms or treatments, that you wish neuroscience researchers focused more on?*

**[Mrs. Cummings]:** Yes. So ALS has a lot of research dedicated to it, right?

Do you remember the ice bucket challenge from a couple years ago?

That was to raise awareness for Lou Gehrig's disease or amyotrophic lateral sclerosis (ALS) and ALS research. So, after that, a lot of more money went into ALS research, but we need more research into, not just new treatments, but also, alternative treatments, because it's such a devastating disease that usually leads to death within a couple of years, people will try anything.

They will try whatever the Internet tells them might work, and so I think we need more research into definitively proving that those things may or may not help someone so that they don't waste their time and their money when they don't have a lot of time left.

*2.3. [Leyla]: What is the most urgent ethical, systemic challenge there is in healthcare, specifically in the care of neurodegenerative diseases? And how do you think we should go about addressing that challenge?*

**[Mrs. Cummings]:** There's a lot of new ideas, new technology, new therapeutics, for example, for Alzheimer's, we have a new treatment for Alzheimer's as of last year. A treatment that we're still learning about in the long term, how well it works.

That's the first big breakthrough treatment we've had in decades.

But a lot of people who have Alzheimer's can't get the treatment for various reasons.

Just access to centers where the stuff is being offered. Access to clinical trials is limited by where people live and how much money they have sometimes to get to somewhere where these innovations and new treatments are being offered.

So, I think to increase equity in healthcare research, we have to find ways to involve people who don't have the means to physically get to or afford the things that are being offered.

*2.4. [Mr. Collins]: Do you come across issues where individuals that do not have any immediate family members and it is difficult to get consent, where you are left wondering whether or not they fully understand what you are asking?*

**[Mrs. Cummings]:** Here's a good tie in with neurology, so patients who have aphasia for various reasons, maybe from most commonly a stroke affecting the speech center of the brain.

One type of aphasia is broken speech, but they can fully understand everything that's going on.

They are not different from someone who has trouble speaking for a structural reason, like their muscles aren't working, right?

Or there's another type where they have no trouble producing words and they just have this word salad and they just say a bunch of random words in a string it doesn't make sense and they can't understand what you're saying, even though they might be nodding, they can't actually follow commands.

But I have seen, even recently, a patient who had a brain tumor in her speech center and she was being asked big picture questions about her goals of care. For example, did she want a feeding tube?

Did she want to live at home or in a facility?

And the initial evaluation of her capacity for decision making did not account for her aphasia.

And so our team stepped in and was like, oh, she knows what we're saying.

Like, if you give her the time and the repetition, and a little bit of patience, she understands what you're asking her, but just needs a different way to communicate.

We, the medical community, have great understanding of aphasia, but I think, others like patients and their families need a better understanding of aphasia and strategies to communicate their wishes. And so yeah, this issue of capacity, capacity to make difficult medical decisions for yourself, we run into it in patients with aphasia or patients with dementia.

Yeah, so if grandma said that she never ever wanted to be in a nursing home, ever, but now there's no one to take care of her. Family members can't get off work, and she doesn't have an otherwise safe place to be, and she's falling all the time at home and hurting herself.

What is the ethical thing to do in that situation?

*2.5. [Adrija]: What drew you to neuroscience, specifically hospital neurology? What part do you find the most rewarding?*

**[Mrs. Cummings]:** Yeah, just that the hospital setting it's fast pace, it's interesting.

If you order a test, you get it back right away, some of that instant gratification. Getting to see people from day to day how they're doing instead of seeing them in a clinic and then seeing them again in three months. Everything in the hospital happens quickly. Also, the people that come in are scared, you know, if you suddenly can't walk or talk or are having trouble breathing, these things are scary, and so you can be there for people during these moments.

It's very difficult for them. You can help them know what to expect.

Also, hospital neurology is just like a team sport. You're working with big teams, everyone has a really important role and is so much more efficient when we're working together as a team than if we're in our own silo roles. And to see that come together every day is very satisfying. So, yeah, those are the things that make me like my job.

*2.6. [Navya]: So neurology is obviously really complex. It comes with the job, and sometimes it can be really, high stakes, like you're literally grappling life and death in your hands. So, how exactly do you approach your difficult cases or your uncertain clinical situations?*

**[Mrs. Cummings]:** Well, so again, not alone, I've never dealt with anything alone.

I always have a team that I can bounce ideas off of.

We can work together. That's important.

We can also support each other emotionally when a case might affect one of us more than more than it would another person for, you know, whatever personal connection we might have to that condition. I think something I try to live by is that some of my patients

really do have devastating conditions, and I might not be able to make their whole life better.

It's pretty unrealistic, but I could make their day better, pretty reliably, I could find some way to make someone's stay better.

So, that helps me, kind of stay grounded in my goals to try to help them.

I can make their day better and I can help them understand their disease better, which will help them in their long term recovery even after they're not under my care anymore.

*2.7. [Leyla]: I was wondering what specific technologies you typically use for treating neurological conditions? I've been reading that deep brain stimulations (DBS) are very prevalent, but are there any modifications or advancements that you're making to that technology, like closed loop DBS, I've heard is becoming more popular, and like there's this thing transcranial ultrasound stimulation also becoming popular.*

**[Mrs. Cummings]:** Yeah, at least in my career, eight years, I have seen these technologies become more prevalent.

I've seen it increase quite a bit. I remember the first patient I saw who had a DBS early on in my career, was in the ICU because they got an infection from the treatment.

And that made a big impact on me like, wow, there's a lot of dangers to these things.

I think that it is still possible to get an infection from a deep brain stimulator, but in the last decade, our understanding of the surgical process and how to use them for different conditions has advanced significantly.

It is really effective for Parkinson's tremors. If you can find a video, it's crazy. Like an on and off switch, where the tremor stabilizes. It's so cool.

So that's more of an outpatient thing, like movement disorders specialists would be working with the surgeons, to get that placed, but then following up at the clinic to fine tune it.

And in the hospital in terms of technology, we use electroencephalograms (EEGs), to look at brain waves and try to make a spell characterization, if a patient is admitted because they have some kind of shaking spell.

We use an EEG to answer questions such as is it an epileptic seizure or are the brain waves abnormal? Or is it something else like a heart problem? We use EEGs every day in the hospital.

And obviously imaging.

I mean, functional MRIs is something you might have read about, so, we're not using that so much for clinic patients, but in research, that's exploded in recent years. Using functional MRI to see in real time what's happening in the brain. Instead of just looking at the structure.

*2.8. [Leyla]: Do you see those procedures becoming more noninvasive, too?*

**[Mrs. Cummings]:** That's always the goal. That is what biomedical engineers and researchers are looking for is how can it be the least invasive, but most effective as possible, because surgeries are not without risk.

Thank you to Mrs. Erika Cummings for taking the time to drive to NCSSM Morganton and speak with our authors. Additionally, thank you to Adrija, Leyla, and Navya for creating

insightful questions for Mrs. Cummings and leading the conversation. A special thanks to Mr. Christopher Collins for making this opportunity possible.

Morganton Scientific

North Carolina School of Science and Mathematics

Journal of Student STEM Research

# An Interview with Dr. Kathryn Moore (MD) from the Duke Neurology Department on Clinical Neuroscience and Research

**Keywords** Interview, Clinical neurology, Neurodegenerative diseases, Deep brain stimulation, Hospital neurology, Healthcare, Parkinsons, Dystonia, Neurologist, Motor Disorders

## 1. Introduction

On Tuesday, April 1st, Dr. Kathyrn Moore (MD, Msc) from the Duke Neurology Department virtually spoke with three authors of the Morganton Scientific. Both Adrija Sarkar and Leyla Urmanova conducted original research to better understand therapies for Parkinson's Disease; their articles are included in the 2nd Edition of the Morganton Scientific. Additionally, Leyla Urmanova and Navya Bansal wrote literature reviews evaluating topics important to clinical psychology and neuroscience. Laira Lee, one of the chief editors of the Morganton Scientific, and Mrs. Jennifer Williams, the sponsor of the Morganton Scientific, assisted during the interview. A great thanks goes to Mr. Christopher Collins for helping set up the interview and reaching out to Dr. Moore.

Dr. Moore is a Movement Disorders Neurologist and works with patients with a variety of diseases, including Huntington's and Parkinson's. She is a graduate of NCSSM Durham in 2003. Since then, Dr. Moore has pursued an undergraduate degree at Duke University and medical training at UNC Chapel Hill and the University of Florida.

## 2. Interview

### 2.1. *[Laira]: Since I think we have three budding clinicians on the call just like how do you feel about keeping an open mind to various specialties along your medical journey, or do you feel like you started out in college, knowing neuroscience was your thing? Can you speak on developing your interest into motor disorders, etc?*

**[Dr. Moore]:** I discovered the brain in about the sixth grade. And I just thought it was the coolest thing. And what makes you tick? What makes you as a person? And I think many students get into the neuroscience aspect of like what is the seat of me, right? Whereas the Greeks thought it was in the liver and now we're thankfully aware it's the brain.

And over time what I found is like what my scientific interests are and what my clinical interests are, like who do I like taking care of. What kind of space I want to be in as a clinician is very important.

So for instance, I really enjoy working with people long term and talking about heavy issues. I talk about hospice on a regular basis.

Like what does death look like? And spent a lot of time in that space. I have colleagues that do exactly what I do who don't enjoy talking about that. But none of us are going in and removing a tumor, closing it up, and waving goodbye.

So you have to think about, what is my approach to taking care of patients?

So really, my first clinical experience was as an undergraduate, I was doing glioblastoma research, brain tumor research. And had an opportunity to go to the clinic and meet people with brain tumors. And I thought, oh, this is great. This is a bad disease. It's messy,

**Published** Jun 27, 2024

it's rough. There's ways that I can help these folks understand what's happening to their brain. There's treatments even though they were not great at the time. Survival was nine months.

And so that part was really interesting to me. And then I realized it was more oncology than neurology. And again, 12 year old me really loved the brain and what makes you move and tick and do.

And so neurology you know neuroscience as an undergraduate was more like what is dopamine? Very science based, not really clinical.

But as a medical student and thinking about this, I tried to keep an open mind, but I had a first love, you know, it was donezo for me.

And what I love about neurology really is that it's the bastion of clinical care. So everybody, not to beat on everybody else, but they ordered more tests than you would believe. Whereas I go in the room, I spend 45 minutes to an hour with a new patient. First of all, I know a lot about them at the end of that hour. That's a sacred space. But I can do some maneuvers with them and 95% of the time I can tell them what they have, what the rest of their life is going to look like. I mean, that's cool.
So inside of neurology, some of the subspecialties are more on that physical exam and versus um I'm ordering more MRIs or EEGs or what have you. And I really liked the magic of examining somebody, watching them move and figure out exactly how to describe that and figure out what's going on. There's an art to that.

And that was really cool for me. I could watch people walk all day. Don't sit me down in the food court at the mall because we'll never get up because we're watching everybody.

But the clinical care I'm doing, right? That's interesting. I'm teaching that. I'm really into teaching at the clinic but talking to somebody about things like what does it mean if you need end of life care and how do we work this out and you know your husband's getting chemo, how do we make sure that you need it while he's doing that.

And so that kind of dirty, messy space. And I'm very lucky. I have great social workers. We have a chaplain. Like I'm not doing this by myself. But I found a space where I love what I am doing.

I knew I could do it and I knew that not everybody could. And I think that's what a calling comes down to.

### *2.2.* ***[Laira] : Do you feel medicine should be less focused on finding a cure-all and move more towards early detection of diseases? Or does this mindset even apply to something like movement disorders where there are not currently cures for diseases like Parkinson's and Huntington's?***

**[Dr. Moore]:** It's interesting that you ask that because they are very tightly entwined with one another. You can't do one without the other. So although we don't have cures for anything yet, yet being the operative word. I do think that by detecting disease earlier, we will be able to better intervene with what we call disease modifying treatments.

So I think, you know, if I had a crystal ball and said, what is the world going to look like in 10, 20, 30 years with these diseases, I think what'll happen is we will be more focused on detecting it early because if we start a medication early, we can make it more of a chronic disease like diabetes or high blood pressure than something that is terminal.

And so a lot of the research going on now parallel to treatment options, looking at disease modifying therapy is for accurate and reliable ways to detect it early.

And so instead of relying on me doing an exam when it takes six to nine months to get an appointment with me, maybe the family doctor in your local community can do a blood test or a skin biopsy or an MRI with AI that does special measurements to detect that early.

So I think it's both. It has to be both.

### *2.3.* ***[Leyla]: I'm really interested in Parkinson's disease and was just wondering if there are any specific clinical trials or new research studies that you're excited about in that field.***

**[Dr. Moore]:** When you're talking to people about research in general, most people, like Laira was saying, are focused on cure and detection.

But I see a value in multiple areas of research. I'm excited for these disease modifying trials, but I gotta be honest, it's very hard to get really attached to them because so many do fail. That's the nature of research. My heart has been broken so many times. We're going to enroll people in these clinical trials, but I try not to get too attached to it.

As for some of the things that are really cool that are happening now in the treatment space. Just in the last year, we've had a new oral medication for Parkinson's, the approval of subcutaneous medication for Parkinson's, and something called adaptive DBS, which is where the deep brain stimulator responds to particular patterns in brain activity so that it's not constantly on, it adjusts to what the patients need. That was just approved within the last month.

So there's a lot of movement there in terms of treatment options.

I'm also very interested in how we best take care of patients and caregivers, right? And so that's something that has been part of why I chose medicine and why I chose some of these complicated diseases to take care of people when they're going through these really hard times.

There's really cool studies going on across the country about how we best support people in that journey. So to me, all of that is exciting. Even if you get the best early detection and the best disease modifying treatment, you're still going to have lessons that you learn from all of those things that are going to help people moving forward.

### *2.4.* ***[Adrija]: I'm really interested in deep brain stimulation particularly. I think it's absolutely fascinating. So what would you say are some of the most significant limitations of current deep brain stimulation techniques and what innovations or potential therapeutics do you think could possibly enhance those treatments?***

**[Dr. Moore]:** So I think the biggest limitation to people doing well is the selection of the correct patient for the procedure, which is paramount. I think where most missteps happen is when you're not picking the right patient to move forward with that procedure. And so if you look at the data around success rates of DBS, it is not necessarily indicative of an individual group, an individual surgeon and how they work together to select patients and make sure that they do well. I think information around choosing patients and techniques of those procedures. It is a treatment that requires a lot of interdisciplinary collaboration. I think that's really a big barrier.

The other is our understanding of who is going to do well and who isn't at a microcosm kind of level. And so we do know a lot about Parkinson's, although that field is growing in terms of who's going to respond well and not from a genetic marker perspective.

But there's a real opportunity for the use of DBS in something called dystonia. So dystonia is not a single diagnosis, but a large group of diagnoses involving excess pulling or posturing of the muscles coming from the deep brain regions.

And it can happen with Parkinson's, it can happen with Huntington's, but there are also many diagnoses that are just dystonia in some form or another. And so we're really getting a handle on what of those patients will do well, who won't, and how to expand DBS to other indications.
So it is being explored for ticks and Tourette's syndrome. It's being explored for OCD, Alzheimer's disease, and a number of other things. So I think understanding the target, what to expect and who is the right kind of patient for this is really important.

What's coming very quickly at us now is something called closed loop DBS.

And so right now with this adaptive DBS, I'm still doing the programming. I'm still setting up the machine to do what it needs to do, but then we're able to use these advancements in DBS to say, okay, within these measurements that I'm giving you, you can bounce between those if you're asleep or walking or what have you.

The dream is to put this in, we press a button and it programs itself. It does everything it needs by itself. But we're getting there.

*2.5.* ***[Navya]: Okay, so my question is also about neurodegenerative diseases. So I know that although there aren't specific causes to a lot of neurodegenerative diseases, there have been correlations between neurotransmitter levels and certain hormone levels to neurodegenerative diseases. Have you seen any promising research or clinical trials that specifically target neurotransmitter regulations in order to treat both motor and cognitive symptoms for neurodegenerative diseases?***

**[Dr. Moore]:** Yeah, absolutely. The dysregulation of neurotransmitters really is fundamentally what the disease is rather than a cause of it. The causes of neurodegenerative disease by and large are genetic and environmental.

Huntington's is all genetic with some environmental spring in. Parkinson's is mostly environmental with some genetics resulting in low dopamine. And so most of the treatment is in that space downstream of everything else. So treatments for Parkinson's disease are mostly dopamine, to supplement. And in Huntington's disease where people have too much dopamine, we're blocking the dopamine.

There is some research into this space with acetylcholine, which would be more of a cognitive chemical. You think about antidepressants. They help you keep your serotonin around. So all this is a very well-established area of modulation of these neurodegenerative diseases or chronic brain diseases.

*2.6.* ***[Laira]: I had one follow up to the question Adrija asked you. You mentioned genetic markers for deciding whether or not to treat with DBS. I was wondering how does your role typically interact with genetic pathologists or even like how is your data set of biomarkers increasing for Parkinson's? At least when I've looked into specific genetic markers for disease, it's often very small subgroups of people being tested and it's very hard to get a breadth and diversity of people and their genetic markers. How has this kind of been a factor in Parkinson's research moving forward?***

**[Dr. Moore]:** Yeah, so there's a lot to unpack there. I would say that clinically speaking for Parkinson's disease, genetics has little clinical implication right now.

I think it's helpful for some patients to say, I have this gene, but really that is in the research space. And that comes in two ways. One is when you find a genetic cause of a disease, right? So we're talking about a phenomenon like a phenotype here, right? So Parkinson's is many, many diseases.

It really is because there's different genes involved, there's different chemical exposures involved. And so there are small groups of people where in a family, they all get it in their 30s. Everybody has it. It has a particular flavor to it and it's caused by a specific gene, right?

And so we can use that information, use that gene to say, well, what does that gene affect at the cellular level? And how can that help us explain how Parkinson's is caused in everybody with this phenotype?

So there's that stuff. And that's where you see PARK2, PRKN, and some of these other smaller families and scientists get really excited when they find a family and they build a career off these people.

The other side is for us to understand at a population level what's happening with Parkinson's disease. I'm going to use Parkinson's here because it is different from Huntington's, where you have the gene, you have the disease. If you don't have the gene, you don't have the disease.

These are variable levels of penetrance, right? Which means I can have the gene and never get Parkinson's. And certainly you could have Parkinson's and not have any of these genes.

And so at the translational research point now, what they're typically looking at is the two most common genes involved in Parkinson's, which is GBA and LRRK2. LRRK2 research has been the most successful so far. And so I can see at some point saying, hey, we're going to test you for these genes because you might be able to participate in this clinical trial or have this medication accessible to you that's not accessible to other people. And that's certainly the way it is in a number of diseases.

Right now, the way genetic testing occurs is I can certainly order you a very expensive panel or series of panels, but the Parkinson Foundation is currently conducting a trial called PD generation. It's either a blood test or a swab to test for the seven most common genes involved in Parkinson's disease. They have genetic counselors both in English and Spanish, I believe some other languages. Their goal is to try to get a better sense of what's the genetic profile of people with Parkinson's across the globe, mostly in the United States. But you're right, most of the studies have been in the Ashkenazi Jewish population and various groups within the country where there are researchers already in that space and a genetically isolated people group. And so that's already ongoing and that work is there and can expand in Parkinson's pretty easily.

But it's very hard to get a genetic counselor. Like maybe a health system will have one.

They're mostly like in the pediatric side and understanding if you're at risk for having a baby with Tay-Sachs. What does that mean? Right. And so in the Huntington's disease space, ideally you have a genetic counselor that's part of your team. But it's not always the case. And we sort of play one on TV and try to do what we can. Fortunately, with Huntington's disease, it's one gene, one disease. So it doesn't get too terribly complicated, but I am often testing patients with an HD-like disease for other things if their HD test is negative.

*2.7.* ***[Leyla]: Going off of what you believe contributes to the cause of Parkinson's is environmental factors. I recently got really interested in the gut microbiome and how that plays a role. And from speaking to Mrs. Cummings, she mentioned how many patients have come in complaining of GI issues and constipation. How many of them might have some leaky gut or something penetrating their intestinal barrier?***

**[Dr. Moore]:**
Right. So the evidence is longstanding and very strong for both prodromal gut symptoms in patients with PD and disruption of the biosphere there as well as very longstanding evidence about environmental exposures.

Relating to environmental exposures is Camp Lejeune and Agent Orange. And there's a lot of work that's gone on that shows that in specific populations with specific exposures, as well as in specific regions of the country that there are much higher rates of Parkinson's that's not otherwise able to be explained.

So like Michael J. Fox, who was like the sort of public spokesperson for Parkinson's says, and I don't love this analogy, but he says this, that the genes load the gun and the environment fires the gun when you're talking about Parkinson's. I don't love gun analogies, but there you go.

Again, not like Huntington's, one gene, one disease. This is a conglomerate of things. And we see this often in our patients. So we'll have a number of them that present with a certain flavor and others that present in a different way.

The gut association was described many, many years ago by Brock thinking about Parkinson's. And so many people come in with decades of constipation. The current research in this space says, yeah, there's clearly a difference between people who have Parkinson's and those who don't with their gut flora, and you may have heard of fecal transplants, which thankfully you don't take it by mouth. It goes all the way down to the stomach and someone else's fecal material is put in you to help balance out your flora.

But where the space is right now is at some point we're going to be saying, take this probiotic, that prebiotic, what have you, but it's not quite there yet. So if patients are saying, should I take this? Well, if it helps your constipation, yeah.

But in terms of managing your Parkinson's, we can't say that. The world experts in this space say, we're not to the point to tell you which bacteria can be helpful. And in fact, a probiotic may be harmful if it somehow increases the other bacteria.
And in fact, if you say, all right, in someone with Parkinson's, this bacteria is low, this bacteria is high.So I need a supplement that does this. Well, that's like saying, you know, we need less lions in the Sahara and more giraffes. You're messing with a bigger system than you realize. And so you have to be really careful with that.

We can't go off like trends and feelings. We're scientists.

*2.8.* ***[Adrija]: I had another question about deep brain stimulation again. You were talking about how you had to look for certain patients that you think that the treatment would work the best in or ideal candidates. How exactly is it that you go about determining who would benefit the most?***

**[Dr. Moore]:** Yeah, so this has been very well described in the literature in terms of thinking about who we implant. So number one, you have to have the right diagnosis, right?

Number two, the goals have to be aligned. So if the person says, my left toe hurts, I want DBS, we may do DBS for other reasons, but that's not going to align with what you're trying to get here.

Right. And so I was saying before about how interdisciplinary teamwork is so important because I do DBS all the time. This is the person's one and only time they're going to do it. It's very complicated and overwhelming. And so you have to make sure that what you're hearing, what they want. Is it possible and aligned?

The other thing is you have to think about what are the potential harms I'm going to cause this patient. And that's true for anything you do as a physician, right? And so the things that I'm particularly looking at is, is this patient, number one, a surgical candidate?

This isn't major surgery, but it sort of is too, right? And so making sure that they're going to tolerate that, they're not on blood thinners that they can't come off. They don't have a horrible lung disease. They are able to be awake and laying flat for multiple hours with their head kind of stuck to the board, those things.

And then the other part is if they have cognitive issues, implanting this device may accelerate that. Less important, but part of what we think about is swallowing problems and balance problems that can be worsened by it.

I think the other thing too, for me, is that there has to be ethical reasons for putting this device into somebody's brain. Do I think their specific symptoms are going to improve or not? And is this too early, too late? And that's sort of the art of medicine

And thinking about candidacy for surgeries. I will say I think DBS is under offered for women and people of color and that's something that is being worked on certainly at our institution and at the global level from the Parkinson's Foundation. I think I want to just take a minute to emphasize that. It's certainly not about race or gender. We want to make sure that those people are getting offered those procedures.

Certainly walking them through if they'd be a candidate, it's frightening for many people of any background, but that's a huge part of it.

*2.9.* ***[Navya]: I know that you've led an international lecture series on movement disorders, and I thought that that was very, very impressive. What are the biggest gaps in current training for future neurologists that you've seen when it comes to understanding the basics of movement and cognitive disorders?***

**[Dr. Moore]:** Yeah. So good question. I think two things. Speaking first to someone going through their neurology residency in the United States. This is changing, but most programs are very inpatient heavy. And we won't get into the medical, legal, financial aspects of that, but the residents are not really in the outpatient setting that much. And so it's been well recognized that the outpatient exposure that residents have is not as strong as we would like it.

And someone in the hospital with Parkinson's looks very different from someone in the outpatient setting with Parkinson's and their care is very different.

So that's something that we as a group of movement disorder doctors around the country and the world have really worked on. From a national perspective, let's talk about North America. There are about 50 Movement Disorders fellows trained in North America every year. This varies. It depends on how many people are interested. So it's somewhere between 30 and 80. And you think about

And in this country, there's about 1.2 million people with Parkinson's in the United States. That's not enough neurologists for Parkinson's, ticks, Huntington's, dystonia, tremors, everything, right? So training people and increasing the number is important.

But the fellowship training is not regulated. Residency is, fellowship is not. There are clear pros and cons to that, right? So I'm able to offer at my center for my fellows extensive training in the operating room for DBS and ultrasound procedure, et cetera. And not every place is going to have that. And so if I say, well, only people that have DBS can train people, that's going to limit the number of trainees.

But how do we regulate that? There's some sort of like, let's call it a code of honor. And we have sort of recommendations that come to us from the movement disorder society, but they're at this point in time with the field of movement disorders being about 50 years old. So it's a baby field.

Internationally. In the continent of Africa there is about one neurologist for 2 million people. I've spoken to my African colleagues about this, they're dealing with cultural things like, if you have Parkinson's, some believe you've done some evil deed, you know, like all of this stuff that goes on and not to mention the resources that they have. So I've had patients that have moved from the United States back to Kenya or the Ivory Coast. And they maybe can buy something called Sinemet, but is it Sinemet? And it's all out of pocket. So the care is very, very different.

So one of the goals of the series is to you know with the North American trainees, you're going to get top world experts in every little field, whereas in your home institution, you may have five people you're working with if you're lucky and they're not going to, A, have time to give lectures, B, be good at lectures, or C, they have sub expertise in all these areas.

But on a global scale to say to our friends and colleagues around the world, whether that be Malaysia, Australia, Africa, what have you, this is what we're doing here are some fundamental things to consider.

We're keenly aware of the disparities that are there. But if I've got a lecture series that's going out to 100 North Americans, why not give everybody else the Zoom link? I think that's where we are.

It's a very complicated issue.

### *2.10.* ***[Leyla]: What do you think the greatest barrier within neurodegenerative care is?***

**[Dr. Moore]:** Yeah. Diagnosis. Diagnosis especially with atypical diseases takes years to get the diagnosis.

These are complex diseases, right? They can present in non-movement sort of ways, constipation, low blood pressure, sexual dysfunction, all different kinds of things. And so it takes number one, that somebody in the community goes, this is neurologic. You need to see a neurologist.

And then maybe you see a general neurologist who's like, this is in the movement family. We're going to treat it like Parkinson's. So then maybe I'm going to send you to a movement specialist.

The patient has been told eight different things by the time they come to see me and now this strange lady is telling him they have a terminal illness.

Two, and this is very fresh in my mind, we're trying to enroll patients in this progressive supernuclear palsy study. In order to enroll in the study, people have to be ambulatory. They have to be able to walk. Well, by the time they get to us, they're not walking.

Diagnosis, diagnosis. So this goes back to the whole early detection thing. If I can say, here's a blood test. Done, right? You get a brain scan and this program reads it and tells me if you should see a neurologist or not.

Done, right? So that would expedite things. And, you know, a lot of the referrals I get are not a movement disorder at all. And that's a space that could have been used by somebody else. So that access to care and getting the right diagnosis is a huge thing.

Because it affects not only that individual patient and family, but it has larger implications on research and how we move the field forward.

## 3. Discussion of Research Projects with Dr. Moore

**[Laira]:** Okay, so why don't we just kind of go in order and give a little synopsis of your research project and maybe Dr. Moore can ask you some questions or just have a conversation about your ideas.

**[Leyla]:** I wanted to see how introducing a probiotic treatment, a mixed probiotic treatment to be specific. I didn't isolate a strain or anything. How that would influence the motility, the lifespan, and the aggregation of alpha-synuclein within *C. elegans*. Which were my model organisms. It was a nice preliminary experiment because I could see how these aggregates diminished, if at all. And they were promising results in the sense that, yes, these probiotics did have some positive effect, although we can't make any definite conclusions with this research. We can say that it did overall have a more positive effect compared to the control whether that be reducing the alpha-synuclein aggregation, promoting vitality and reproduction, and also just increasing the thrashing behavior of the worms. My research ended up changing a lot because I did not want to go with the gut microbiome in the beginning but here I am, and I'm actually kind of glad because it shows that, you know, it's great to have accessible treatments as well for people who don't really have access to certain medications and surgeries.

**[Dr. Moore]:** Absolutely. How did you find it working with *C. elegans*? Did you enjoy it or was it gross or what?
What did you think?

**[Leyla]:** So Adrija and I both worked with them and we can say that they've been a hassle But there was definitely a learning curve working with them especially because you know, you have to work with so many, for the replicates in my experiment

But overall, I would definitely want to continue researching with *C. elegans* and then move on to mice because they actually have more complex digestive systems than *C. elegans*. *C. elegans* is just your intestine and then your anus. They don't even have stomachs.

**[Dr. Moore]:** And that brings up a great point about how we think about a model for disease.

Right. Versus a patient in the clinic with me. Like say you go home for the spring break and a cousin says, well, uncle so-and-so has Parkinson's.

Should he start a probiotic? What do you tell them?

**[Leyla]:** Honestly, I'd say that it wouldn't hurt but I was presenting my research at a science fair and one judge mentioned that one of their family members suffered from

Parkinson's. They were put on these probiotics as well as antibiotics. And then some infection ended up developing and they ended up potentially passing away from that infection, which was concerning but I guess it's just a matter of that balance because the antibiotics could have wiped out a bunch of good bacteria. And then it's a matter of whether probiotics actually contributed to actually helping restore that balance.

**[Dr. Moore]:** Yeah, I have to say that makes… That does not make clinical sense to me.

At all. But what I will tell you is… where I did my residency, we were not allowed to let patients continue their probiotics in the hospital. And I asked around to find out why. And this, I think, is very interesting, just a thought, you know, as we think about stuff that is not FDA regulated.

Supplements that we see in the store and how we counsel our patients about them, right?

So this is a bit of an extreme story, but there was a child getting a bone marrow transplant in this hospital. And so he had no immune system. He became septic. So he had bacteria in his blood. We couldn't figure out what it was. Unfortunately, the child passed and they were able to isolate the bacteria and discover that it's not something that's just roaming around in the world. That it was from one of these pills, one of these probiotics.

So natural, you know, cyanide and, um, arsenic are natural, so just be careful.

**[Leyla]:** That's good to know.

**[Dr. Moore]:** How do you think the research project and what you worked on is going to impact what you think about doing and are doing in the future? As you move forward to graduation.

**[Leyla]:** Yeah, so I was looking into some labs at Duke and there's this lab that has really interesting research with neuropsychology and gut microbiome I heard about on the Huberman Lab podcast.

I'm interested in looking into that and potentially deviating a bit from Parkinson's and looking into some of the other ways that our gut microbiome can influence our mental health and also behavior.

**[Dr. Moore]:** Yeah. And just the idea that there are more cells in your body that aren't you than cells that are you. That's weird. I'm sorry. That's just weird. Super. Well, I encourage you all as you think about moving to the next step, don't be afraid to cold call, cold email these labs.

They will have work for you to do, I promise, okay?
It's a tough time in research right now, as you may have seen on the news, but I think If you're waiting for somebody to call you, it's not going to happen. So call around. Don't be shy. The worst they can tell you is no. That's how I got my first lab job.

This is way off topic now, but I think you all are very well prepared just for being in the college environment. Everybody else is figuring out how to have a roommate and laundry and all that nonsense.

And so you can hit the ground running in a way that your classmates at college may not be able to.

Make sure you're doing okay in that environment and your grades before you start taking on a whole bunch of extra. That's just a pro tip.

**[Laira]:** Okay, Adrija, do you want to give your synopsis?

**[Adrija]:** Sure. So like Leyla said, I also worked with C. Elegans and I also researched Parkinson's disease specifically. I came across this article where some researchers took the structure of the alpha-synuclein protein and they did a computational study where they used an electric field to denature the protein. And so I wanted to know if this is a viable form of degradation of the protein in a model organism. So I used C. Elegans and I exposed them to an electric field and essentially tried to see if there was any decrease in the amount of protein in the worm. And also with that, in terms of motor dysfunction, seeing if there would be a benefit or I guess an increase in their neuromuscular function in terms of thrashing assays and velocity.

**[Dr. Moore]:** And you measure total protein or did you measure alpha-synuclein? Very good.

**[Adrija]:** Alpha-synuclein.

**[Dr. Moore]:** I'll be honest, I've not heard of that study, there are thousands of papers about Parkinson's released every day.

**[Adrija]:** Yeah, this is kind of why I kept asking questions about deep brain stimulation like. Right now, it's a relatively invasive technique. For potential applications of my research, some form of surgery I mean, obviously like *C. elegans* to humans is a huge jump that should not be made, but like in terms of, I guess the general idea of maybe more of like an outside exposure rather than like a direct, internal, invasive procedure.

**[Dr. Moore]:** Yeah. The questions that come to my mind, and I'm not expecting you to answer these, but the things that I think about hearing that is.

Well, how is it specific to alpha-synuclein is it? Is it specific to the different forms of alpha-synuclein versus its aggregated form, or phosphorylated form?

And… always thinking about down the road, and this is something that we in the last few have taken on, where patients and patient families are involved in research and research planning far earlier on rather than just like, here's this medicine we made. You may now take it.

And I think even if you said to me here's how this works. The branding around that would have to be really specific.

Because people are already spooked by EMF and all this other stuff. And there's no evidence that intense cell phone use makes you less likely to get Parkinson's.

One of the challenges in research is where you end up, right? Are you a basic researcher where I'm just learning how this process works? Versus translational, where my goal is to bring it from the basic lab, like this fact that we know about alpha-synucleins, and how do I bring it to patient care And so when you're in that translational space.

You have to be thinking about, is this something that is going to work? Like if you say, oh, I have a cure for left hand tremor is to take off your left hand. Great. It cures left hand tremor.

But no one, well nearly no one, is going to sign up for that.

So it's just something to think about as you're doing research. I think you shouldn't be afraid to try different things. But quite frankly, the funding agencies are going to help you with that by saying like, no, we don't think that's going to move anywhere. This is more where a whole bunch of brains in a room think and say, I think we need to move it in this direction.

Now, there are external procedures that are not medical. Are not pharmaceuticals. So there is high intensity focused ultrasound, it does cause a permanent change in the brain.

There's also TMS, right? And so there's been some, I think just this week, a release about a portable TMS device. And TMS is used for depression and all this. We're exploring it at our Center for Dystonia and a number of other things.

So it's not to discount external electromagnetic stuff, but I think we'd have to really think about how that works and what that does.

The other thing is when you're reading about Parkinson's, what you learn is alpha-synuclein, Lewy bodies, yada, yada. There's actually a really big argument going on for many years in space as to whether or not alpha-synuclein is the cause or the effect.

So we don't really know. They think it's the cause, but there are people with Parkinson's who have no alpha-synuclein.

And so it's really challenging to know where this is going to end up. And I think when you're thinking about research, whether it's basic, translational, pharmaceuticals, whatever, things happen in parallel and not everything pans out the way you hope it will.

But it's a really cool idea. I mean, I think there are plenty of my patients who would jump into a human-sized microwave to get rid of their Parkinson's for sure.

It sounds to me like Adrija, that you might be an engineer in the making.

What do you say?

**[Adrija]:** I think the interdisciplinariness of neuroscience is what really draws me to it. I don't necessarily think that I want to go the engineering route. That being said.

Especially this past year, doing research has made me really interested and more aware, I guess, of some of the relationships between biology and physics and the blend between the two of them. So I definitely want to study biophysics a lot more, but I think I'm also interested in more of the clinical side of medicine and applying some of the things that those engineers might end up making or doing.

**[Dr. Moore]:** Well, we definitely all work together, right? Some of these people overlap and so they have degrees in both and that's a very interesting place to be in. But I would at least make friends with some engineers. I certainly have over the years, more after college than during.

They're really cool people in helping us figure out how we do this adaptive DBS? How do we do a closed loop?

And then they come and teach us like, here are the buttons you press to make this happen. It's very collaborative in the neuromodulation space.

Very good. Well, when you get your Nobel Prize for microwaving Parkinson's, I will fly to Europe and wave my pom pom. I think it's a cool idea.

**[Adrija]:** Thank you.

**[Nayva]:** Okay, so my independent study isn't necessarily in the Parkinson's route, but it's about Alzheimer's. And what my group is doing is potato beetles produce a certain toxin called leptinotarsin and that toxin is associated with increasing your levels of acetylcholine in the body. So we're trying to see if we can take the leptinotarsin and turn off certain parts of the toxin so that we remove the toxic part of it.

Can we essentially mitigate the symptoms of Alzheimer's? And we're studying this using *C. elegans* with Alzheimer's. And my independent study is starting in the fall of this year, and I would really love your input on the direction I can go, the things I can keep in mind.

**[Dr. Moore]:** I will remind you all that I'm a clinician.

Let me see. So I definitely understand that you're talking about symptomatic management here and mitigating neurotransmitters after the fact.

And what I think about when I think about something like gene targeting or cellular targeting, and we're using a virus or a toxin or whatever, you have to be really careful about how am I taking out the toxin part?

And what am I adding in, you know. I think that's one of the big challenges with any of these gene therapies or what have you is making sure that you're targeting the right cell and the right and the right parts of the body. So I think that would be a big challenge which is way outside my scope of practice in terms of thinking about toxins.

But sometimes movement disorders share medicine with Alzheimer's. I'll say to my patients, look, here's the memory medicines that we borrow from Alzheimer's.

They don't really work all that great. So I think that would be an amazing space to be in.

Because unfortunately, like I was saying, everybody's goal is, how do we reverse this? How do we stop it?

But I think the reality is that if and when we can get disease modifying treatments for these there's still going to be some level of symptomatic management that's going to be needed.

**[Navya]:** That was very insightful. Thank you so much.

**[Dr. Moore]:** I'm happy you all are using *C. elegans*. When I was in school in Durham, my hall was sort of adjacent to the biology floor.

And you could always tell when it was like Drosophila season because they would escape. So I got really good at your age at killing fruit flies.

It's a special skill on my CV from Science and Math.

Killing fruit flies.

**[Leyla]:**
No, they still escape at our school. We find them everywhere.

**[Laira]:** Thank you. If anybody else has any lasting questions, feel free to.

**[Leyla]:** This is just one really quick question, but as an undergraduate student, like I know you mentioned earlier to get immersed in research early on, would you give any other advice for someone hoping to pursue that field of medicine?

**[Dr. Moore]:** I will tell you what I heard from a good friend of mine who's on the School of Medicine Admissions Committee.

And he's a lovely person. He lives on the freshman campus here. In his 60s with his wife, who's a geriatrician. It blows my mind, but there you go. He said you know your first year, put your head down, get the work done. It's those classes that are like, you just got to do basic bio, you got to do calculus, stuff that you have done for the past two years.

It's just in a different space. They may not be the most interested in your learning the way you're blessed to have right now. Right. And so that's it. It's challenging. It's not going to not be challenging, but focus on that.

Get your feet under you. Start to explore things in your sophomore year. By all means, call the lab in your freshman year, but like really getting into it and all of that in sophomore year, really exploring things.

Try new things. And then by the time you hit your junior year, it's really focusing on certain projects and the story that you're going to tell.
That can go on into senior year if you're going to take time apart from your education to do various things.

But the story that you're going to tell and a clear understanding of what career you want to pursue.

I know that this is changing in terms of shadowing, but I think now, this new show, The Pitt, is really good. But most doctor shows are not accurate. There's no real way of knowing what it's like without seeing it yourself. And if you were going to commit yourself to a lot of hard work. Cognitively, emotionally, physically hard work. I strongly encourage you to shadow in various areas. The undergraduates that come and shadow me, they're not there to learn medicine and science. They're there to see what Dr. Moore does on a Wednesday and what does that look like? So see that for yourself so that when you apply and they say, why do you want to be a doctor?

You have your reasons. And not just sort of, I think it's cool. I watched Grey's Anatomy. That's not going to work.

So anyway, those would be the things I would think about, but have fun, you know. Get out, get some sunshine. Play some pickleball, do something fun too.

Thank you to Dr. Moore for taking the time to speak with our authors. Additionally, thank you to Adrija, Leyla, and Navya for creating insightful questions for Dr. Moore and leading the conversation. A special thanks to Mr. Christopher Collins and Mrs. Jennifer Williams for making this opportunity possible.

# ESSAYS

Open Access | https://doi.org/10.62329/xgky2283

Morganton Scientific

*North Carolina School of Science and Mathematics*

Journal of Student STEM Research

# Designer Babies A Tale of Horrific Immoralities

**Ganga Nair**[1]

[1]NCSSM

**Keywords** Designer Babies, Ethics of genome engineering CRISPR, Human edited embryos

Over the years, the concept of a designer baby, otherwise known as a genetically engineered baby, has evolved from being science fiction to the prime topic of modern bioethical debate. A designer baby describes a child whose gene sequence has been intentionally selected to contain a specific preferred characteristic or eliminate genetic disease. While supporters say that this technology can help diminish inherited diseases and enhance human abilities, a variety of challenges develop a plethora of questions regarding the use of the technology. Some of the dangerous implications of bioengineered babies are considered concerning social inequity, less genetic diversity, biological damage, and morality regarding genetics. Ultimately, the practice of designer babies and human embryos raises ethical concerns and should be advocated against.

Discussing the ethical and social concerns of genome editing on embryos, a pressing problem that emerges is the potential for increased inequality. Genetic editing erodes the idea of equality and could form great divisions in the future and can accentuate immoral stratification. Suppose enhancement technologies begin to become widely available. In that case, there is a real and present danger that these technologies will only be available to richer families, further stratifying the privileged from the underprivileged. According to Harvard Law School, the average embryo-edited baby can cost up to $100,000 further amplifying the social gap that will be birthed if this practice continues. [1] Currently, medical care and quality therapies are distributed unfairly, therefore genetic engineering may tend to institutionalize these discrepancies. In communities where access to genes will turn to commercialization, there may emerge a divergence regarding aspects such as intelligence and physical health on account of children of rich families having the advantage over other “normal individuals”. Social stratification would accentuate and create a class of genetically superior individuals. In a world where traits such as high intelligence, physical attractiveness or athletic ability are selected for, individuals would be valued for their genes rather than their personhood.

Notably, another major concern with designer babies regards the loss of genetic diversity. Genetic diversity is critical in sustaining a species, as it offers protection against environmental changes, diseases, etc. A loss of genetic variance that confers resistance to a wide range of pathogens may occur if few genetic characteristics become preferred or emphasized. A narrow gene pool facilitated by the large-scale selection of traits considered desirable could make the human population more vulnerable to diseases or environmental stressors. Referencing a report conducted by The Guardian, this would make humans more vulnerable to diseases, which, up until recently, posed little threat. [2]

Beyond the risks of gene editing, genetic enhancement technologies could be utilized to enhance intelligence, physical ability, or resilience to conditions such as Leukemia or Hemophilia. Although the urge to improve human conditions is understandable, concern remains as much as the long-term biological influences of such enhancements remain unknown. There is a probability that in trying to enhance one characteristic, there might indeed be a corresponding decline in another, thus forming an offshoot effect of negative

**Published** Jun 27, 2024

**Correspondence to**
Ganga Nair
nair26g@ncssm.edu

implications for the person concerned. The pursuit of genetic enhancements could also bring together human characteristics consequently reducing natural diversity, an essential aspect of the well-being and survival of our species.

Another prevailing concern surrounding the ethics of baby design raises profound moral issues regarding parental control and the autonomy of the child. While many parents might view genetic modification as one sure way of making life for a child optimal, some others argue this intervention violates the child's autonomy and natural purpose. According to a survey conducted by the Pew Research Center, about 69% of American adults were hesitant to edit gene structures of their embryos, further indicating the prospect of genetic editing is still widely looked down upon by the general public. [3] Additionally, it raises questions surrounding the ethics involved in designing a baby before birth regarding individuality. Some claim it strips the child's right to self-definition and may push onto the child a specific set of expectations or desires not consciously decided upon by the individual. Who decides which traits are desirable? Is that a decision to be left to a few genetic engineers and their scientific peers: to decide which characteristics of human nature are superior or inferior? A world in which parents can select specific traits for their children risks diminishing diversity and encourages unrealistic standards of perfection.

This ideological shift first emanated from He Jiankui, a Chinese biophysicist, who gained international prominence in 2018 upon claiming to design the world's first genetically edited pair of twins. According to an article by Science, Jiankui had modified the embryos of the babies using CRISPR-Cas9, a gene-editing technique that provides resistance to HIV. CRISPR is extremely cost effective and was originally employed to diminish genetic diseases and strengthen the prevalence of desired traits. [4] Regardless of the lab extractions done in the interest of CRISPR, Jiankui's actions were widely condemned as unethical as they ignored established scientific guidelines and medical protocols. Eventually, through efforts of whistleblowing and media reports, it was revealed that Jiankui had not only acted without proper approval from administrators but had also misled patients regarding the risks of the procedure. According to Science Insider, after an international outcry and an investigation led by Chinese authorities, He Jiankui was found guilty of illegal medical practices, and sentenced to three years in prison. [5] Jiankui's actions have raised profound ethical questions concerning the limit of gene editing and the possibility of designer babies. If the creator of designer babies cannot conduct proper research with scientific approval, then what promises the safety of CRISPR and all its future practices? All of these controversies surrounding the development of designer babies contribute to the downfall of the concept and raise concerns regarding legibility.

Designer babies introduce a variety of complex questions that are difficult to resolve. While this technology may hold the potential to eradicate genetic disorders and contribute to an immense improvement in human condition, there is an extreme level of risk in applying it. Modifying genes could interfere with genetic diversity and produce unforeseen consequences, therefore proving once again that pursuing modified children is a far-reaching possibility placed into the hands of society. The moral jeopardies concerning control over the genes along with the potential reemergence of eugenics, demand raise a need for serious reflection and reconsideration. Since scientists will continue developing and researching new technologies for genetic engineering, long-term consequences should be reconsidered with adequate caution. Recognizing and weighing the downsides of such advances against their potential benefits will contribute to the realization that this field of technology has grown to become dangerously risky and contains the potential to diminish our social values. Ultimately, designer babies and

human embryo editing techniques are alarmingly immoral and fuel the rise of unfair prejudice in our thriving society.

## References

[1] "Silver Spoons and Golden Genes Designing Inequality?," 2018, [Online]. Available: https://blog.petrieflom.law.harvard.edu/2018/10/26/silver-spoons-and-golden-genes-designing-inequality/

[2] "Designer babies: an ethical horror waiting to happen?," 2017, [Online]. Available: https://www.theguardian.com/science/2017/jan/08/designer-babies-ethical-horror-waiting-to-happen

[3] "Americans are closely divided over editing a baby's genes to reduce serious health risk," 2022, [Online]. Available: https://www.pewresearch.org/internet/2022/03/17/americans-are-closely-divided-over-editing-a-babys-genes-to-reduce-serious-health-risk/

[4] "Chinese scientist who produced genetically altered babies sentenced to 3 years in jail," 2019, [Online]. Available: https://www.science.org/content/article/chinese-scientist-who-produced-genetically-altered-babies-sentenced-3-years-jail

[5] "Chinese scientist who produced genetically altered babies sentenced to 3 years in jail," 2024, [Online]. Available: https://www.technologyreview.com/2018/11/25/138962/exclusive-chinese-scientists-are-creating-crispr-babies/

Morganton Scientific

North Carolina School of Science and Mathematics

Journal of Student STEM Research

# Rewiring Eating Disorder Recovery: Neuroethical Implications of tDCS in ED Treatment

**Leyla Urmanova**[1]

[1]NCSSM

**Keywords** tDCS, eating disorders, neuromodulation, neuroethics, mental health, bioethics, non-invasive brain stimulation, anorexia nervosa, bulimia nervosa, binge-eating disorder

The term “fatal illness” can immediately strike fear. When we hear it, a few diseases often come to mind– cancer, heart disease, stroke, Alzheimer’s, depression, and more. However, we often overlook an illness that can devastate both the mind and body in a myriad of ways: eating disorders.

Eating disorders (ED) are psychiatric conditions that are associated with disturbances in eating behaviors as well as thoughts and emotions related to eating (K. Wu *et al.* [1]). Yielding the second highest mortality rate of any psychiatric illness, EDs harbor the potential to uproot individuals’ lives and detrimentally impact global society (J. Arcelus, A. J. Mitchell, J. Wales, and S. Nielsen [2]). Every 52 minutes, one person dies as a direct consequence to one ([3]), resulting in the annual loss of over 3.3 million healthy life years worldwide (D. Van Hoeken and H. W. Hoek [4]).

The symptoms of EDs vary depending on the condition, but this paper specifically focuses on anorexia nervosa (AN), bulimia nervosa (BN), and binge-eating disorder (BED). As a life-threatening illness, AN is characterized by an abnormally low body weight and intense fear of weight gain, resulting in the compulsive need to exercise and reduce food intake ([5]). BN differs from AN in that it includes episodes of binge eating (consuming a large amount of food in a short period of time), followed by purging, which may include vomiting, overexercising, or using laxatives ([5]). BED, on the other hand, involves binging without purging, which often results in individuals experiencing feelings of guilt, disgust, and shame after consuming large amounts of food ([5]). Despite their differences, all three EDs are serious health conditions that disrupt an individual’s relationship with food.

Unfortunately, the standard treatment for these disorders is far from ideal. Individuals suffering from them may undergo psychotherapy, take medications –often in the form of antidepressants and antipsychotics– and participate in nutritional counseling. In severe cases, particularly for AN patients with critically low BMI, hospitalization may be required ([6]). As of now, psychotherapies have significant limitations and often produce mixed results, with cognitive behavioral therapy sometimes yielding high dropout rates, inconsistent efficacy, and limited long-term success (H. Russell *et al.* [7]). Similarly, medications do not cure ED, as the majority of patients often experience minimal symptom improvement and adverse side effects with the existing options (D. L. Reas and C. M. Grilo [8]). Hence, due to its current inability to effectively reach and address the widespread population, ED treatment remains in its infancy. However, we are now on the precipice of a technological revolution, and within it may lie the key to revolutionizing ED treatment for the better: neuromodulation.

Neuromodulation refers to the technology that can alter neural signaling in the body. By sending electrical pulses to stimulate certain nerves, neuromodulatory devices can

**Published** Dec 09, 2024

**Correspondence to**
Leyla Urmanova
urmanova25l@ncssm.edu

profoundly influence the brain's activity, harboring the potential to save lives. Although this technology is primarily utilized to address conditions unrelated to mental health disorders, such as chronic neuropathic pain (K. Yu, X. Niu, and B. He [9]), researchers are currently testing its scope by exploring its application to EDs. With the goal of improving BMI and patients' mental health, neuromodulatory techniques serve as a promising alternative to the limitations of existing treatments (K. Wu *et al.* [1]).

There are numerous forms of neuromodulation– some invasive and others non-invasive. Deep brain stimulation (DBS) and vagus nerve stimulation (VNS) are invasive neuromodulatory techniques that require the insertion of a device into the body to provide mild electrical impulses. They are adjustable and reversible, allowing for flexibility in treatment and greater patient autonomy (Cleveland Clinic, 2022). Although these procedures exhibit potential in treating ED, both require a surgical procedure, which exposes individuals to a variety of medical risks and complications. In the case of DBS, these risks include internal bleeding, infection, stroke, and a coma, coupled with troubling side effects, such as issues with balancing, double vision, seizures, and depression (Cleveland Clinic, 2022). VNS can also yield risks and serious side effects, including difficulty swallowing, vocal paralysis, throat pain, shortness of breath, and sleep apnea ([10]).

On the other hand, with non-invasive neuromodulation, we can bypass these complications. Transcranial direct current stimulation (tDCS) is a modern method that can be applied by trained personnel– it acts to modulate the rate of naturally occurring neuronal firing within the stimulated tissue. In tDCS, a weak electrical current is delivered through two scalp electrodes –an anodal electrode, which increases the membrane potential, and a cathodal electrode, which decreases it– via a portable battery-powered stimulator (G. J. Elder and J.-P. Taylor [11]). With low purchase costs, mild adverse effects, and great therapeutic potential, this technology offers a promising answer for ED patients (S. Baumann *et al.* [12]). Unlike transcranial magnetic stimulation (TMS), tDCS is easier to administer, making it a viable option for widespread use.

However, before we consider the implementation of tDCS as a therapeutic tool for ED treatment, we must first evaluate its ethical implications. Given its low cost, portability, ability to target specific brain areas, potential unknown effects on the developing brain, and long-lasting impact, tDCS raises special ethical concerns. With the bioethical principles of autonomy, non-maleficence, beneficence, and justice in mind, how can we effectively implement this technology to treat ED? After all, how much autonomy do ED patients truly have in their decision-making? What are the general ethical considerations of neurotechnological treatment on mental health conditions? This paper seeks to explore the ethical controversies that can arise from tDCS, including its potential risks and implications for treatment. By considering possible misuse, safety concerns, and cognitive vulnerability, the ethical implications of applying tDCS in these specific circumstances can be thoroughly evaluated – offering a potential solution to this raging mental health crisis.

## 1. The Potential of tDCS for Treating ED

First, research suggests that tDCS can benefit AN patients by alleviating ED symptoms. Given that AN patients exhibit brain abnormalities, particularly in areas such as the dorsolateral prefrontal cortex (DLPFC), modulating these regions could help reduce ED symptoms (Z. Rząd, J. Rog, N. Kajka, P. Szewczyk, P. Krukow, and H. Karakuła-Juchnowicz [13]). Patients with AN also exhibit increased activity in the brain's right frontal hemisphere, indicating the potential need for excitatory tDCS to stimulate the left hemisphere and restore hemispheric balance (Z. Rząd, J. Rog, N. Kajka, P. Szewczyk, P. Krukow, and H. Karakuła-Juchnowicz [13]). Interestingly, three smaller open-label studies

evaluating the efficacy of left DLPFC anodal stimulation in AN have reported improvements in patients' BMI, eating patterns, and emotional well being (E. M. Khedr, N. A. Elfetoh, A. M. Ali, and M. Noamany [14]; F. Costanzo *et al.* [15]; R. Strumila *et al.* [16]). Although these studies differed in methodology, they all noted minimal adverse effects associated with tDCS treatment.

Similarly, BN patients are also characterized by changes in their DLPFC, a brain region involved in reward processing and self-regulatory control, which raises the need for neuromodulation (J. McClelland, N. Bozhilova, I. Campbell, and U. Schmidt [17]). In a double-blind randomized trial, thirty-nine participants received three sessions of targeted tDCS using different methods (M. Kekic *et al.* [18]). One approach, with the anode placed on the right and the cathode placed on the left, improved mood and reduced cognitive symptoms associated with ED (M. Kekic *et al.* [18]). This method assisted with suppressing the urge to binge-eat and increasing self-regulatory behavior, thus demonstrating the potential of tDCS in treating BN patients.

Patients with BED also experience abnormalities with self-regulatory processes. Hence, one experimental trial investigated the efficacy of at-home self-administered tDCS for this condition, recruiting 82 participants who were overweight and met the criteria for BED diagnosis ([19]). After undergoing tDCS treatment with attention bias modification training (ABMT), BED patients experienced significant weight loss, changes in eating behavior, and improvements in mood ([19]).

## 2. The Ethical Concerns Underlying tDCS

Despite the promising nature of tDCS, it holds certain drawbacks. Currently, tDCS remains unregulated by the U.S Food and Drug Administration (FDA) for over-the-counter and clinical use. Hence, as information regarding this technology has grown in accessibility over the years, users are increasingly utilizing it to conduct self-experimentation. They have formed an online tDCS community, "DIY-tDCS," which focuses on creating a self-stimulating mental health treatment by manufacturing a device based on basic tools and electronic parts (A. Wexler [20]). This, in turn, enables ED patients to avoid physicians in seeking treatment and thus circumvent the traditional process of informed consent. Since tDCS presents itself as a lightweight, low-risk, and inexpensive alternative, it holds a higher chance of being misused, such as for enhancement application, recreational using, and using without supervision (G. Tortella [21]). This misuse could worsen the challenges of managing ED since patients might prioritize self-directed, unsupervised interventions over evidence-based professional care.

Additionally, while tDCS may present minimal and benign side effects –mainly appearing as problems with the skin– in the short term, its long-term side effects remain unknown (H. Matsumoto and Y. Ugawa [22]). No studies of note have evaluated the long-term consequences of tDCS on ED patients, which raises the need for further evaluation to confirm its safety.

Anatomical differences may reduce the effectiveness of tDCS in treating ED patients compared to healthy individuals. After all, people with ED are characterized by altered cortical folding and lower levels of fat– factors that change the transfer of energy to the brain's surface (K. C. Widdows and N. J. Davis [23]). Thus, the efficacy of brain stimulation is dependent on the individual's nutritional state, which proves particularly significant when applying this technology to ED patients. If tDCS use is also extended to minors, it is also crucial to consider that, depending on the size of the head, a specific dose of stimulation will have a larger effect on the brain of a child or younger person compared to the brain of an adult (K. C. Widdows and N. J. Davis [23]). This calls for individualized

tDCS treatments to ensure maximal beneficence. Since studies have yet to evaluate all the ways in which nuances of an individual's brain morphology can impact the effect of neuromodulation, additional research in this field is needed.

Using neuromodulation for treating psychological disorders such as ED also begs the question of whether the treated patients' cognitive capacities are compromised. The technology tDCS grants individuals significant autonomy, which raises concerns regarding its use and consent to use by ED patients. Individuals with long-term ED often face significant neuropsychological impairments (A. Grau, E. Magallón-Neri, G. Faus, and G. Feixas [24]). These impairments, compounded by the cognitive effects of nutritional deficiencies, may impact their ability to make well-informed decisions about treatment and its potential risks (N. Scarmeas, C. A. Anastasiou, and M. Yannakoulia [25]).

This, in turn, raises the question of whether tDCS should be incorporated into ED treatment models. Due to the debilitating condition that ED patients are in, causing them to resist treatment, they often face coercion (J. A. Matusek and M. O. Wright [26]). Should coercion, in this case, be preserved? Would patients genuinely be consenting to tDCS administered by a physician, or would their agreement be influenced by the fear of facing involuntary commitment if they refused? Or, should tDCS be presented as a do-it-yourself (DIY) option to help avoid coercive treatment altogether? If the latter option is chosen, individuals with ED who are in denial about their condition and fearful of weight gain may be more likely to refuse treatment– potentially exacerbating their illness. Although the principle of autonomy involves respecting autonomous decisions despite believing in the wrongness of another's choice, it is also crucial to consider that autonomous decisions rely upon one's ability to use rational deliberation and whether or not one is competent enough to make a particular choice (J. A. Matusek and M. O. Wright [26]). Granting ED patients greater autonomy, in this case, may harm their health in the long term.

The question of distributive justice serves as another key concern surrounding the implementation of tDCS (O. M. Lapenta, C. A. Valasek, A. R. Brunoni, and P. S. Boggio [27]). Considering that individuals may continue to lack the financial means to provide themselves with tDCS treatment, they may face an unfair advantage. The aim of ED treatment is to be accessible and treat as many affected individuals as possible in an efficient manner, which may not be achieved on a global, national, or even regional basis with current healthcare inequities. In the case that tDCS may be utilized for purposes outside of mental health disorder treatment (e.g cognitive enhancement), the issue of justice becomes significantly more pressing, raising the question of how innovative technology could widen the gap between people of differing socioeconomic status (O. M. Lapenta, C. A. Valasek, A. R. Brunoni, and P. S. Boggio [27]).

## 3. Weighing The Benefits and Ethical Challenges

Despite the promising potential that tDCS holds for ED treatment, it holds significant ethical drawbacks. In the case of autonomy, tDCS is unique in that it offers users the opportunity to exercise their autonomy, which differs from most standard ED treatment plans. Unlike specialized treatment facilities or cognitive behavioral therapy, this neuro technology enables users to control the administration of their treatment. This can enable patients to feel empowered in their recovery and take ownership of their progress. However, greater autonomy can also prevent recovery, in some cases– considering that ED patients experience compromised cognitive capacity and are therefore more inclined to make choices that harm their well-being. They would be more likely to engage in maladaptive behaviors in their treatment.

While the misuse of tDCS (e.g incorrect placement of electrodes or excessive intensity) can put the individual at risk for skin problems, it has not inflicted severe harm to subjects. This technology thus far has exhibited non-maleficence, meaning it avoids causing harm to patients, as evidenced by the mild side effects thus far. However, its long term effects remain unknown.

Regarding beneficence, which refers to the efficacy of treatment, tDCS has shown promising preliminary results, signifying that it holds the potential to reduce ED symptoms. Its ability to stimulate certain regions of the brain enables it to promote self-regulation, improve mood, and reduce disordered eating behaviors. As a result, its application can address the gaps of other, less effective treatments.

Lastly, it remains crucial to promote widespread accessibility to affordable mental health care and emerging therapeutic technologies, which can help bridge the gap in treatment equity and ultimately uplift underserved populations. A lack of access to mental health treatment violates the ethical principle of justice. Thus, policymakers, healthcare providers, and researchers must collaborate to utilize tDCS in a manner that upholds ethical standards but also empowers marginalized communities.

## 4. Moving Toward Ethical Integration

Ultimately, tDCS presents concerns surrounding autonomy, treatment efficacy, safety, and health equity. These concerns emphasize the need for a thoughtful approach to integrate tDCS into clinical practice. By implementing comprehensive healthcare policies, many of these issues can be effectively addressed, thus paving the way for ethical and more equitable applications of this technology.

Presenting a new ethical-decision making model serves as the first step. This involves transparently explaining the rationale behind the client's treatment recommendation and actively inviting the client and other key stakeholders to participate in this decision process (J. A. Matusek and M. O. Wright [26]). To resolve conflicting viewpoints found in working with clients with severe ED, an interactive, process-oriented model is needed. Such a model is also crucial to ensure that innovative treatments such as tDCS are being implemented responsibly.

In addition to this model, tDCS should be incorporated into a comprehensive care plan that includes psychotherapy, nutritional counseling, and medical monitoring to maximize its benefits. This way, patients can be granted some autonomy while also being able to engage in a well-rounded and supported treatment approach.

Access to tDCS can be increased through the implementation of funding to subsidize tDCS treatments for low-income patients. For insurance coverage purposes, tDCS should be recognized as a reimbursable treatment option for eating disorders. The use of telehealth can also expand access by offering remote consultations and monitoring, particularly for patients in underserved areas.

Therefore, the administration of tDCS provides a promising method for ED treatment–one that is accessible, effective, and empowering for the patient and mental health society.

## References

[1] K. Wu *et al.*, "Neuromodulation of Eating Disorders: A Review of Underlying Neural Network Activity and Neuromodulatory Treatments," *Brain Sciences*, vol. 14, no. 3, p. 200, 2024, doi: 10.3390/brainsci14030200.

[2] J. Arcelus, A. J. Mitchell, J. Wales, and S. Nielsen, "Mortality Rates in Patients With Anorexia Nervosa and Other Eating Disorders: A Meta-analysis of 36 Studies," *Archives of General Psychiatry*, vol. 68, no. 7, p. 724, 2011, doi: 10.1001/archgenpsychiatry.2011.74.

[3] "Report: Economic Costs of Eating Disorders | Research Reports | Harvard T.H. Chan School of Public Health." [Online]. Available: https://hsph.harvard.edu/research/eating-disorders-striped/research-reports/economic-costs-eating-disorders/

[4] D. Van Hoeken and H. W. Hoek, "Review of the burden of eating disorders: mortality, disability, costs, quality of life, and family burden," *Current Opinion in Psychiatry*, vol. 33, no. 6, pp. 521–527, 2020, doi: 10.1097/YCO.0000000000000641.

[5] "Eating disorders - Symptoms and causes." [Online]. Available: https://www.mayoclinic.org/diseases-conditions/eating-disorders/symptoms-causes/syc-20353603

[6] "Eating Disorders - National Institute of Mental Health (NIMH)." [Online]. Available: https://www.nimh.nih.gov/health/topics/eating-disorders

[7] H. Russell *et al.*, "Psychotherapies for eating disorders: findings from a rapid review," *Journal of Eating Disorders*, vol. 11, no. 1, p. 175, 2023, doi: 10.1186/s40337-023-00886-w.

[8] D. L. Reas and C. M. Grilo, "Review and Metaanalysis of Pharmacotherapy for Bingeeating Disorder," *Obesity*, vol. 16, no. 9, pp. 2024–2038, 2008, doi: 10.1038/oby.2008.333.

[9] K. Yu, X. Niu, and B. He, "Neuromodulation Management of Chronic Neuropathic Pain in the Central Nervous System," *Advanced Functional Materials*, vol. 30, no. 37, p. 1908999, 2020, doi: 10.1002/adfm.201908999.

[10] "Vagus nerve stimulation." 2018.

[11] G. J. Elder and J.-P. Taylor, "Transcranial magnetic stimulation and transcranial direct current stimulation: treatments for cognitive and neuropsychiatric symptoms in the neurodegenerative dementias?," *Alzheimer's Research & Therapy*, vol. 6, no. 5–8, p. 74, 2014, doi: 10.1186/s13195-014-0074-1.

[12] S. Baumann *et al.*, "Effects of Transcranial Direct Current Stimulation Treatment for Anorexia Nervosa," *Frontiers in Psychiatry*, vol. 12, p. 717255, 2021, doi: 10.3389/fpsyt.2021.717255.

[13] Z. Rząd, J. Rog, N. Kajka, P. Szewczyk, P. Krukow, and H. Karakuła-Juchnowicz, "The efficacy of transcranial direct current stimulation in the treatment of anorexia nervosa: a randomized double-blind clinical trial," *Frontiers in Psychiatry*, vol. 15, p. 1284675, 2024, doi: 10.3389/fpsyt.2024.1284675.

[14] E. M. Khedr, N. A. Elfetoh, A. M. Ali, and M. Noamany, "Anodal transcranial direct current stimulation over the dorsolateral prefrontal cortex improves anorexia nervosa: A pilot study," *Restorative Neurology and Neuroscience*, vol. 32, no. 6, pp. 789–797, 2014, doi: 10.3233/RNN-140392.

[15] F. Costanzo *et al.*, "New Treatment Perspectives in Adolescents With Anorexia Nervosa: The Efficacy of Non-invasive Brain-Directed Treatment," *Frontiers in Behavioral Neuroscience*, vol. 12, p. 133, 2018, doi: 10.3389/fnbeh.2018.00133.

[16] R. Strumila *et al.*, "Safety and efficacy of transcranial direct current stimulation (tDCS) in the treatment of Anorexia Nervosa. The open-label STAR study," *Brain Stimulation*, vol. 12, no. 5, pp. 1325–1327, 2019, doi: 10.1016/j.brs.2019.06.017.

[17] J. McClelland, N. Bozhilova, I. Campbell, and U. Schmidt, "A Systematic Review of the Effects of Neuromodulation on Eating and Body Weight: Evidence from Human and Animal Studies," *European Eating Disorders Review*, vol. 21, no. 6, pp. 436–455, 2013, doi: 10.1002/erv.2256.

[18] M. Kekic *et al.*, "Single-Session Transcranial Direct Current Stimulation Temporarily Improves Symptoms, Mood, and Self-Regulatory Control in Bulimia Nervosa: A Randomised Controlled Trial," *PLOS ONE*, vol. 12, no. 1, p. e167606, 2017, doi: 10.1371/journal.pone.0167606.

[19] "New home-administered treatment for binge eating disorder shows promising results." [Online]. Available: https://www.sciencedaily.com/releases/2024/06/240606001349.htm

[20] A. Wexler, "The practices of do-it-yourself brain stimulation: implications for ethical considerations and regulatory proposals," *Journal of Medical Ethics*, vol. 42, no. 4, pp. 211–215, 2016, doi: 10.1136/medethics-2015-102704.

[21] G. Tortella, "Transcranial direct current stimulation in psychiatric disorders," *World Journal of Psychiatry*, vol. 5, no. 1, p. 88, 2015, doi: 10.5498/wjp.v5.i1.88.

[22] H. Matsumoto and Y. Ugawa, "Adverse events of tDCS and tACS: A review," *Clinical Neurophysiology Practice*, vol. 2, pp. 19–25, 2017, doi: 10.1016/j.cnp.2016.12.003.

[23] K. C. Widdows and N. J. Davis, "Ethical Considerations in Using Brain Stimulation to Treat Eating Disorders," *Frontiers in Behavioral Neuroscience*, vol. 8, 2014, doi: 10.3389/fnbeh.2014.00351.

[24] A. Grau, E. Magallón-Neri, G. Faus, and G. Feixas, "Cognitive impairment in eating disorder patients of short and long-term duration: a case–control study," *Neuropsychiatric Disease and Treatment*, vol. 15, 2019, doi: https://doi.org/10.2147/ndt.s199927.

[25] N. Scarmeas, C. A. Anastasiou, and M. Yannakoulia, "Nutrition and prevention of cognitive impairment," *The Lancet Neurology*, vol. 17, no. 11, pp. 1006–1015, 2018, doi: 10.1016/S1474-4422(18)30338-7.

[26] J. A. Matusek and M. O. Wright, "Ethical dilemmas in treating clients with eating disorders: A review and application of an integrative ethical decisionmaking model," *European Eating Disorders Review*, vol. 18, no. 6, pp. 434–452, 2010, doi: 10.1002/erv.1036.

[27] O. M. Lapenta, C. A. Valasek, A. R. Brunoni, and P. S. Boggio, "An ethical discussion of the use of transcranial direct current stimulation for cognitive enhancement in healthy individuals: A fictional case study.," *Psychology & Neuroscience*, vol. 7, no. 2, pp. 175–180, 2014, doi: 10.3922/j.psns.2014.010.

# PAPERS

Open Access | https://doi.org/10.62329/xmne7858

Morganton Scientific

*North Carolina School of Science and Mathematics*

Journal of Student STEM Research

# An Examination of the Enzymatic Degradation of PET Plastic via PETase and MHETase

**Ruby Allred**[1]

[1]North Carolina School of Science and Mathematics

## Abstract

Post-consumer plastic waste is a concerning issue in the world at large, and polyethylene terephthalate (PET) plastic is a key contributor of that waste. In 2016, Yoshida et al. discovered a system of enzymes, PETase and MHETase, in the bacteria *Ideonella sakaiensis*, which they claimed could degrade PET plastic. While true, this degradation only truly affects lower crystallinity PET (in the range of 2-3%), which is well below the crystallinity in which most PET plastic that is sold (a typical PET water bottle may be 31%). As such, while the surface of the plastic waste may be degraded, the core of the plastic tends to hold strong unless it is first melted into lower crystalline plastic. This study used a chimera of the two enzymes, developed by Knott et al., with the initial goal of testing various conditions for degradation. This work finds that these enzymes have a limited effect on the degradation of un-modified post-consumer PET plastic. While a minor increase in efficiency can be found in a solution which contains ethylene glycol, the rate of degradation is miniscule regardless.

**Keywords** Polyethylene terephthalate, Plastic degradation, Enzymatic degradation, MHETase, PETase

## 1. Introduction

Plastic has become a vital part of our global economy and society, and polyethylene terephthalate (PET) is one of the most common plastics in use, making up much of disposable packaging [1]. Of course, this causes massive amounts of waste, largely due to the fact that PET and other similar plastics are not easily broken down, and as such millions of tons of plastic waste are put into the ecosystem every year [2], [3], [4]. While the PET may be destroyed through intense heat and pressure or recycled through chemical processes, these are wasteful and often take up copious amounts of energy or use costly or hazardous chemicals [5], [6], [7]. Because of this the prospect of using enzymes to degrade the PET is appealing, both environmentally and economically, and a viable route toward this enzymatic degradation may involve the enzymatic system of PETase and MHETase. This system breaks down PET into terephthalic acid (TPA) and ethylene glycol (EG), which can be polymerized into PET, thus potentially creating a better closed loop. In addition, the EG could be sold for use in antifreeze or ballpoint pen ink, and the TPA can be utilized by bacteria such as *Rhodococcus sp* [8].

PETase and MHETase, discovered in *Ideonella sakaiensis* by Yoshida et al. in 2016, are notable because they are effective at 30 degrees celsius, as opposed to most other potential enzymes, which work best at PET's glass transition state (70 °C) [9]. Having a much lower temperature would mean less energy put into the process overall, which is environmentally preferable. Like with many other similar enzymes, the current main issue with PETase is that they require additional pretreatment for effective PET

**Published** Jun 27, 2024

**Correspondence to**
Ruby Allred
rubydiumallred@gmail.com

deconstruction, specifically they must be lowered in crystallinity, as PETase and MHETase are only truly effective at degrading PET at very low crystallinity (∼3%) [10]. Post-consumer plastics are often much higher in crystallinity, for instance a standard plastic water bottle may hold a crystallinity of 31% [11]. As such, ways to decrease the crystallinity of PET in a quick, efficient, and environmentally conscious manner is an important step in the development of infrastructure for the enzymatic recycling of PET plastic.

Many facets of PET degradation have been studied, for instance Falkenstein et al. researched the effects of UV light on PET degradation, and found that the UV light highly crystallizes the PET, making it much more difficult to degrade [12]. PETase has also been modified to become more effective, typically being modified to be more like a cutinase, which has been proven to make it much more efficient, so developments are being made in that regard [10], [13]. Other methods of degradation have also been investigated, such as the use of ethylene glycol as an agent of degradation, which has limited but present effects at room temperature [14].

Overall, more research is presently needed in the determination of stronger methods for PET degradation without the use of high temperatures or harmful chemicals. This paper sets out to examine the use of various reagents and conditions on the enzymatic degradation of PET plastic without first pushing the PET past the glass transition state, and optimally with as low a heat as possible.

## 2. Methods

### *2.1. Enzyme Broth Creation*

The enzymes were created and used as described in Knott et al's paper. The specific enzyme used was the chimeric enzyme PCJ190, a combination of PETase and MHETase which was shown to hold increased degradation over wild-type PETase and MHETase enzymes on low crystallinity plastic [10]. Four broths which contained the enzyme in equal measure were created, one at 7.5 pH, one at 7.0 pH, one at 8.0 pH, and one at 7.5 pH containing an added volume of ethylene glycol equivalent to 10% of the total volume.

### *2.2. Materials Preparation for Degradation*

The plastic which was degraded are small strips taken from various Sprite bottles bought at the same time from a local retailer. Specifically, areas of similar consistency, that being the area under the label but not affixed with the glue binding the label to the bottle itself, as that may cause inconsistencies in the samples. Samples of the plastic were cut out using a knife and scissors, with the intent that within a group of samples the sizes would be roughly the same. Some plastic was also ground using a combination of a coffee grinder and mortar and pestle, as a plastic grinder was unavailable.

### *2.3. Degradation Methods*

Twelve 50 mL beakers which were split into six categories were each filled with 20 mLs of the enzymatic broth. The categories are as follows: 7.5 pH with plastic strips, 7.5 pH with ground plastic, 7.0 pH with plastic strips, 8.0 pH with plastic strips, 7.5 pH containing ethylene glycol with plastic strips, and 7.5 pH containing ethylene glycol with ground plastic. The plastic samples were dried in an oven at sixty degrees celsius for one day and then weighed before being placed into the beakers. The beakers were placed into a water bath and then left for a week, with occasional observation. After seven days the beakers were extracted from the water bath, at which point vacuum filtration was used to isolate the plastic samples from the broth. The plastic was then dried under the same conditions as above, and weighed again. Two trials were recorded, one at room temperature and one at thirty degrees celsius.

### *2.4. The Detection of Ethylene Glycol*

Due to the low level of observed degradation on the plastic, CheMetrics Ethylene Glycol testing kits were obtained and used. The tests showed the presence of a glycol; however, it is possible that Sprite contains propylene glycol (a moderate sweetener used in certain soft drinks). Nevertheless, the presence of propylene glycol in Sprite is not disclosed [15]. In addition, the testing kits appear to be inconclusive in terms of exact concentrations, and as such the ethylene glycol testing kits are not a particularly viable method for determination of the extent of degradation.

## 3. Results and Discussion

Due to the ineffectiveness of the ethylene glycol testing kits, the only reliable value which could be collected from the tests performed was the weight loss of the plastic samples. Figure 1 and Figure 2 display the percent change in plastic mass before and after the samples of the two recorded runs. As can be seen, while the data for the room temperature experiment is largely consistent with some degree of degradation, the one which was run at 30 °C largely gained in mass to some extent. This was likely due to the buffer salinity being too high, however multiple assays of this were performed and all returned some level of salt precipitate. As such, the data from 30 °C is unreliable, although it is interesting to note that in both experiments the standard conditions do to some extent degrade the plastic. Figure 2's data is not presented to demonstrate the effectiveness of the degradation, but to warn of a potential flaw which can occur.

The unusually high peak of 7% mass loss seen in sample EGd-1 in Figure 1 (ground plastic degraded in the ethylene glycol broth) could either be due to a large amount of degradation, or could be due to the loss of some particulates of the ground plastic, which may have occurred in several different steps of the process. It should be noted that the ethylene glycol solution containing ground plastic does appear to be a better performer in comparison to the 7.5 pH samples, however more thorough testing would need to be performed to truly prove a correlation.

## 4. Conclusion

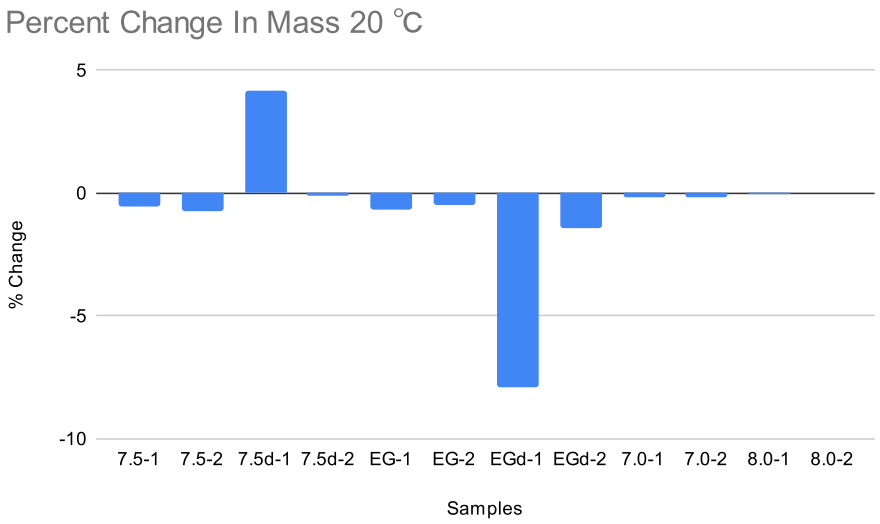


**Figure 1**. *Percent mass loss of PET at room temperature. "d" signifies ground plastic.*

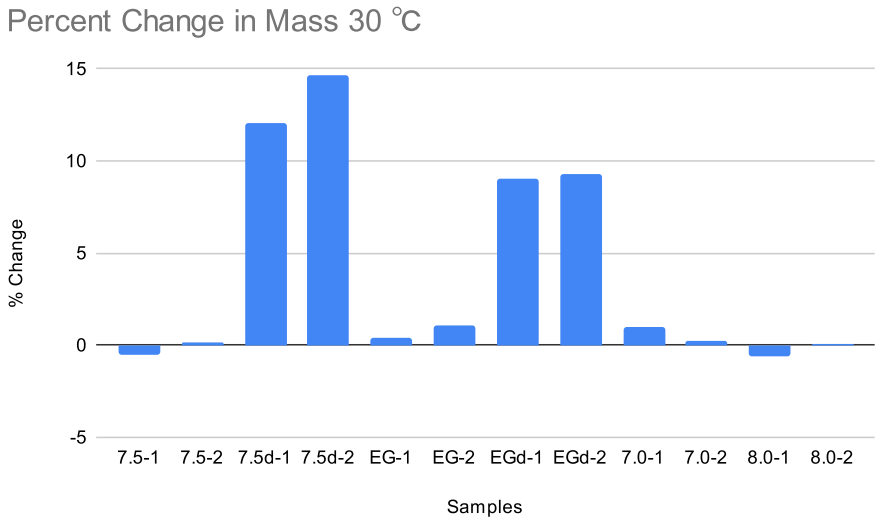


**Figure 2.** *Percent mass loss of PET at 30 ℃. "d" signifies ground plastic.*

This lack of greater degradation of the plastic samples seems to point to PETase's inability to degrade post-consumer goods such as a Sprite bottle, even with aided help. The average of the data collected at room temperature is 0.66% degradation of the bottle, which is an incredibly low value. This does assume that the enzyme functioned properly, however there was substantial enough degradation to imply the presence of enzyme to some degree. To corroborate this, more tests could be done on the presence of the enzyme in the broths before degradation is underway. One way which will likely increase degradation is decreasing the crystallinity of the plastic, as stated before, however doing so would typically require that said waste be brought to its glass transition state, which, in the case of PET, is 70 °C. This is also the temperature at which various other potentially valuable PET degrading enzymes function best, such as leaf-cutter cutinase or polyester hydrolases. As such, the use of other enzymes may still be viable under many circumstances, and further examination should be done in regards to the efficacy of these alternatives. PETase and MHETase should not necessarily be a guiding mark for other enzymes to be modeled around, the enzymatic system itself requires much more modification if it is to be significantly useful.

In addition, enzymatic recycling is not a perfect solution to plastic waste. Simply because a method of recycling which may eventually become a dominant force exists, does not mean that corporations and other groups may continue to produce mass amounts of plastic waste without being held accountable for said plastic. Methods such as pyrolysis are often supported by corporations as being reliable, even when they are not entirely faultless [16]. PETase and MHETase could become part of a larger trend where the most known method of potential recycling is picked up by plastic producers as a way to appear more environmentally conscious and thus more marketable to the masses. The scientific community must remain aware and conscious of the viability of the methods larger groups may claim to be infallible.

Thanks go to Dr. Tandy Grubbs of the Research in Chemistry program at NCSSM-Morganton for permitting this research and allowing for the use of his lab. Thanks also go to the other members of the Research in Chemistry program for being supportive in this endeavour. Finally, thanks go specifically to Ian Richards, for proof reading this document and allowing for further discussion of the topic.

## References


[1] R. Geyer, J. R. Jambeck, and K. L. Law, "Production, use, and fate of all plastics ever made," *Science Advances*, vol. 3, no. 7, 2017, doi: 10.1126/sciadv.1700782.

[2] J. R. Jambeck *et al.*, "Plastic waste inputs from land into the ocean," *Science*, vol. 347, no. 6223, pp. 768–771, 2015, doi: 10.1126/science.1260352.

[3] A. O. C. Iroegbu, S. S. Ray, V. Mbarane, J. C. Bordado, and J. P. Sardinha, "Plastic Pollution: A Perspective on Matters Arising: Challenges and Opportunities," *ACS Omega*, vol. 6, no. 30, pp. 19343–19355, 2021, doi: 10.1021/acsomega.1c02760.

[4] M. Bergmann *et al.*, "Plastic pollution in the Arctic," *Nature Reviews Earth & Environment*, vol. 3, no. 5, pp. 323–337, 2022, doi: 10.1038/s43017-022-00279-8.

[5] G. Pathak *et al.*, "Plastic pollution and the open burning of plastic wastes," *Global Environmental Change*, vol. 80, p. 102648, 2023, doi: 10.1016/j.gloenvcha.2023.102648.

[6] H. Jeswani *et al.*, "Life cycle environmental impacts of chemical recycling via pyrolysis of mixed plastic waste in comparison with mechanical recycling and energy recovery," *Science of The Total Environment*, vol. 769, p. 144483, 2021, doi: 10.1016/j.scitotenv.2020.144483.

[7] J.-P. Lange, "Managing Plastic WasteSorting, Recycling, Disposal, and Product Redesign," *ACS Sustainable Chemistry & Engineering*, vol. 9, no. 47, pp. 15722–15738, 2021, doi: 10.1021/acssuschemeng.1c05013.

[8] "Ethylene Glycol," 2022, [Online]. Available: https://www.chemicalsafetyfacts.org/chemicals/ethylene-glycol/

[9] S. Yoshida *et al.*, "A bacterium that degrades and assimilates poly(ethylene terephthalate)," *Science*, vol. 351, no. 6278, pp. 1196–1199, 2016, doi: 10.1126/science.aad6359.

[10] B. C. Knott *et al.*, "Characterization and engineering of a two-enzyme system for plastics depolymerization," *Proceedings of the National Academy of Sciences*, vol. 117, no. 41, pp. 25476–25485, 2020, doi: 10.1073/pnas.2006753117.

[11] N. E. Wallace, M. C. Adams, A. C. Chafin, D. D. Jones, C. L. Tsui, and T. D. Gruber, "The highly crystalline <scp>PET</scp> found in plastic water bottles does not support the growth of the <scp>PETase</scp>producing bacterium Ideonella sakaiensis," *Environmental Microbiology Reports*, vol. 12, no. 5, pp. 578–582, 2020, doi: 10.1111/1758-2229.12878.

[12] P. Falkenstein *et al.*, "UV Pretreatment Impairs the Enzymatic Degradation of Polyethylene Terephthalate," *Frontiers in Microbiology*, vol. 11, 2020, doi: 10.3389/fmicb.2020.00689.

[13] A. Barclay and K. R. Acharya, "Engineering Plastic Eating Enzymes Using Structural Biology," *Biomolecules*, vol. 13, no. 9, p. 1407, 2023, doi: 10.3390/biom13091407.

[14] J. Huang *et al.*, "Depolymerization of polyethylene terephthalate with glycol under comparatively mild conditions," *Polymer Degradation and Stability*, vol. 208, p. 110245, 2023, doi: 10.1016/j.polymdegradstab.2022.110245.

[15] Mauricio, "Carrier solvents in soft and energy drinks," 2022, [Online]. Available: https://magritek.com/2022/02/08/undeclared-carrier-solvents-in-soft-and-energy-drinks/

[16] A. H. Tullo, "Amid controversy, chemical companies bet on plastics pyrolysis. Retrieved from," 2022, [Online]. Available: https://cen.acs.org/environment/recycling/Amid-controversy-industry-goes-plastics-pyrolysis/100/i36

Open Access | https://doi.org/10.62329/xknn7875

**Morganton Scientific**

*North Carolina School of Science and Mathematics*

Journal of Student STEM Research

# The Psychological Profile of a Future Abuser

**Navya Bansal**[1]

[1]NCSSM

## Abstract

This research paper explores factors contributing to the psychology that makes up an abuser by analyzing two comprehensive studies: "Intergenerational Effects of Childhood Maltreatment: A Systematic Review of the Parenting Practices of Adult Survivors of Childhood Abuse, Neglect, and Violence" by C. A. Greene, L. Haisley, C. Wallace, and J. D. Ford [1] and "Psychophysiological Profiles of Batterers: Autonomic Emotional Reactivity as It Predicts the Antisocial Spectrum of Behavior Among Intimate Partner Abusers" by J. C. Babcock, C. E. Green, S. A. Webb, and T. P. Yerington [2]. These studies outline different aspects of what goes into making an abusive profile, as well as risk factors such as childhood maltreatment, emotional reactivity, mental disorders, and heart rhythms correlating with antisocial behaviors. The results of these studies can be further translated into improving society, rehabilitation, and psychological facilities for both the abusers and the abused. By recognizing the implications of abuse, this paper outlines the urgency of the matter and emphasizes the significance of further research to better understand and mitigate abusive relationships.

**Keywords** abuse, childhood maltreatment, emotional reactivity, relationships

## 1. Introduction

In the intricate workings of human tendencies, it is marveling to see how much of one's own behaviors science can not explain. This becomes especially concerning when it comes to behaviors that are abusive and potentially life-threatening. Society fears what it does not know. What it does not know, it can not fix. With domestic violence rates increasing by 25%-33% globally (L. Mineo [3]), abuse can not afford to continue being an issue that isn't understood. Whether it's in the form of physical, emotional, or sexual abuse, to a child, parent, or senior, the effects of perpetration can impact numerous generations in heavy-bearing cycles of trauma.

## 2. Significance

It is important to study abuse as abuse can be found anywhere. Out of the 7.2 million child abuse reports in the US ([4]), only 2.1 million children received care services, and one-third of childhood abuse victims go on to become abusers themselves (D. Goleman [5]). The cycle of abuse is complex, and the more understanding science has on this matter, the earlier an abusive case can receive adequate interventions to have its effects mitigated. It is only by understanding the workings of perpetrators, that one can hope to stop them. Although there is advancing research being conducted on abuse, this topic is so multifaceted that there is a great need for further studies to truly understand the psychology behind it, making it even more significant for one to study the psychology behind abusive profiles.

### *2.1. Study 1*

*Research Methods:*

**Published** Jun 27, 2024

**Correspondence to**
Navya Bansal
bansal26n@ncssm.edu

In the study titled “Intergenerational Effects of Childhood Maltreatment: A Systematic Review of the Parenting Practices of Adult Survivors of Childhood Abuse, Neglect, and Violence” by C. A. Greene, L. Haisley, C. Wallace, and J. D. Ford [1], the authors used a comprehensive literature review to study the effects of childhood maltreatment. This systematic review identified relevant studies using the online databases *PsycInfo* and *PubMed* and selected fit studies using a set criteria. This included solely empirical studies that (i) demonstrated an association between childhood maltreatment and parenting, (ii) assessed at least one positive/negative parenting behavior, (iii) were published in a peer-reviewed journal. The exclusion criteria were any non-empirical studies that didn’t include perpetration as an outcome variable or did not include parental figures as their primary population. Using the inclusion and exclusion criteria, 97 final manuscripts were used in the review. These articles were drawn with an 88% consensus from all authors and were further quality-checked by software. The finalized studies had significant variety in terms of how childhood maltreatment was operationally defined (single vs cumulative victimization), the assessment method (questionnaire, survey), the included population (mother vs father), the parenting outcomes (behavioral implications), and the research design (cross-sectional, longitudinal, or prospective), inducing heterogeneity in the review. (C. A. Greene, L. Haisley, C. Wallace, and J. D. Ford [1]).

#### 2.1.1. *Limitations:*

The relevancy of a literature review relies heavily on the sources chosen for the review. Any apparent biases in the studies and the selection of the studies must be avoided, thus, extensive quality analysis and selection are required for a literature review to maintain its value. With this study, the most apparent limitation is that the majority of the included research relies solely on adult participants to recall their childhood experiences. Retrospective interference, current circumstances, self-serving bias, and cognitive functioning could have affected the accuracy of the participant’s responses, hence affecting the accuracy of the studies. Confounding and third variables that failed to be accounted for in numerous studies include the effects of children’s behavior on parents, socioeconomic status of the family, and cultural factors. Confounding variables affect the relationship between the independent and dependent variables and, therefore, can call into question the true value and validity of the study. Lastly, the literature review acknowledged that over half of the studies examining the intergenerational transmission of abuse only included mothers. The lack of a representative and random sample induces sampling bias, hence, not allowing for the generalizability of that section. Consequently, this leaves the question of whether the results focusing on intergenerational transmission can be applied to fathers as well, or if this could be another potential confounding variable (C. A. Greene, L. Haisley, C. Wallace, and J. D. Ford [1]).

#### 2.1.2. *Results:*

The empirical studies analyzed in this literature review yielded significant insight into understanding the role of child maltreatment in intergenerational parenting outcomes. Nearly all of the studies identified an association between experiencing childhood physical abuse or witnessing violence and an increased risk of engaging in abusive or neglectful parenting with a rate of 75% or higher. There was additional support for the association between childhood sexual abuse (CSA) and the use of physical punishment among mothers. The greatest risk for perpetrating child abuse was found amongst adults experiencing a cumulative effect of maltreatment; the more of a victim somebody is, the more of a perpetrator they will become. Even mothers who experienced both physical abuse and intimate partner violence automatically became twice as likely to abuse physically as opposed to mothers who only experienced one. The research identified that explanations (mediators) for this direct relationship include poor education, stress levels,

substance use disorders, depression, and post-traumatic stress disorder (PTSD) symptoms that contribute to abusive parenting. Furthermore, victims of child maltreatment have an even greater chance of engaging in a variety of poor parenting behaviors such as hostile, inconsistent, authoritarian, controlling, permissive, and role-reversal parenting. Parents experiencing CSA can also be associated with withdrawal from their children's needs and a flattened affect. Social support and the presence of an adult intimate relationship have been proven effective in moderating physical abuse and emotional over-involvement (C. A. Greene, L. Haisley, C. Wallace, and J. D. Ford [1]).

### *2.2. Study 2*

#### 2.2.1. *Research Methods:*

In the study titled "Psychophysiological Profiles of Batterers: Autonomic Emotional Reactivity as It Predicts the Antisocial Spectrum of Behavior Among Intimate Partner Abusers" by J. C. Babcock, C. E. Green, S. A. Webb, and T. P. Yerington [2], the researchers conducted an extensive questionnaire screening followed by a conflict discussion to understand the results of battering amongst couples. Using flyers, 101 couples were recruited, all of whom needed to have been married and living together for at least 6 months. These couples were further divided into domestic violence (DV) or nonviolence (NV) groups using the Conflict Tactics Scales (CTS2). To be eligible for the DV group, any one partner had to report at least one incident of aggression (beaten up, threatened) in the past year. To be eligible for the NV group, both partners had to report no violence in the entirety of the relationship. Couples were paid $40 to 50 for participation. After the participants were finalized, they completed a three-hour-long questionnaire individually. This questionnaire assessed factors such as intimate partner violence, psychopathy, antisocial personality, and anger levels using standardized scales such as the CTS2, The Self-Report of Psychopathy-II, the Millon Clinical Multiaxial Inventory-III, the State-Trait Anger Expression Inventory, and more. One part of the questionnaire included using the Articulated Thoughts in Simulated Situations test (ATSS), which involves using two audiotaped scenarios designed to induce anger with maritally violent men. These men listened to these audiotapes for four minutes and were asked to imagine their wife in the role of the protagonist, as the protagonist engages in behaviors of complaining about the husband and subtly flirting with other males. In the collective conflict discussion afterward, couples sat quietly for four minutes to get a baseline heart rate before the discussion began, and heart rate and skin conductance levels were both constantly monitored. Debriefing was conducted and the participants' identities were kept confidential. (J. C. Babcock, C. E. Green, S. A. Webb, and T. P. Yerington [2])

#### 2.2.2. *Limitations:*

The limitations of using a questionnaire include incorrect feedback and social influences impacting the responses. Discussions can be long and tedious, resulting in a longer duration of data collection in order to yield adequate results. For this study specifically, the research included a relatively small sample of couples. Additionally, the flyers to recruit participants for the study were only posted in low-income African American and Hispanic communities and were placed specifically near the employment section of the newspapers in order to attract the unemployed. Due to the sampling bias, the participants were not representative of the population, hence limiting the scope for the generalizability of this study. Although it was intentional, choosing low-income minorities can also skew the results of the study as it can interfere with the measurements of heart rate and anger reactivity.

#### 2.2.3. *Results:*

The study mentioned numerous mediators contributing to antisocial behaviors in intimate significant relationships, with a strong emphasis on psychophysiological factors. These factors included extreme cardiac hyporeactivity and hyperreactivity, Type A/B personalities, and temperaments. Low temperaments and cardiac reactivity can demonstrate how the batterer can become desensitized to interpersonal conflict, which is more commonly found in low-level violence abusers (LLV). The study stated that the lack of expressed emotions from the avid abuser stems from poor operant conditioning which had impaired the development of affection and behavioral responses, hence allowing for the expression of more aggressive and criminal behavior. High temperaments and cardiac reactivity stem from poor anger and emotional control, commonly characterized among severely violent (SV) men. The study also acknowledged correlations between income and culture in battering behaviors (J. C. Babcock, C. E. Green, S. A. Webb, and T. P. Yerington [2]).

## 3. Comparison

The studies in this paper explored unique aspects of abuse and studied using different ways and participant populations. C. A. Greene, L. Haisley, C. Wallace, and J. D. Ford [1]'s study focused on the effects of various types of childhood maltreatment, including sexual abuse, physical abuse, and negligence, and the various ways it can resurface as poor parenting techniques in adulthood. Hence, C. A. Greene, L. Haisley, C. Wallace, and J. D. Ford [1]'s study required studies focusing on a participant population of parental figures. This study made effective use of a systematic literature review and had highly selective criteria for the studies to abide by (C. A. Greene, L. Haisley, C. Wallace, and J. D. Ford [1]). Whereas, J. C. Babcock, C. E. Green, S. A. Webb, and T. P. Yerington [2]'s study used a questionnaire followed by a discussion to test the association between psychophysiology and battering. Unlike the results of C. A. Greene, L. Haisley, C. Wallace, and J. D. Ford [1]'s study, this one focused on mediators regarding emotional reactivity, jealousy, and antisocial behaviors in a participant population of couples living together (J. C. Babcock, C. E. Green, S. A. Webb, and T. P. Yerington [2]).

Despite their differences, both studies contribute to the field of psychology and abuse research. Both studies have shown the negative impacts of heightened anger, as they demonstrate it as a common significant mediator. Lastly, both studies consistently reference the work of Gottman and aim to further his numerous studies of abuse. (C. A. Greene, L. Haisley, C. Wallace, and J. D. Ford [1]) (J. C. Babcock, C. E. Green, S. A. Webb, and T. P. Yerington [2]).

## 4. Application

Abusive studies have proven that certain traditional practices, such as spanking and negligence, easily instill fear and resentment in children which can often maliciously resurface in adulthood. These findings can be applied to improve parenting methods from an early stage by informing the public of healthy behavior-shaping techniques. Whether it's by implementing positive reinforcement instead of physical punishment, or by hiring babysitters to avoid leaving infants alone for prolonged periods of time, new societal improvements can foster healthier and stronger relationships. In doing so, one is informed of and implements the evidence-based methods to reduce the likelihood of distress in family and future relationships henceforth.

Shedding light on abusive mediators such as emotional reactivity and hostility informs the public of triggers, signs, and common behaviors exhibited by abusers. Such educational awareness empowers individuals to reach out and report cases that one witnesses or even suspects. The results of abuse studies can be put towards reducing the

stigma attached to speaking up by encouraging individuals to prioritize individual well-being over traditional societal thinking. This especially applies to rural or conservative regions where such multiple taboo topics may not have been addressed, and many are still forced to stay silent in the face of abusive relationships and acts.

Additionally, understanding the biopsychosocial aspects behind abusers encourages community engagement by pushing for collective efforts. Whether these stem from support groups, rehabilitation and outreach programs, or the creation of public awareness campaigns, such community interventions can allow for a holistic approach to effective aid against all forms of abuse. Such efforts can even be translated into improved workplace policies and alert hotlines.

Ultimately, by embracing evidence-based practices in society, both collective and individualistic changes can be made to respond to instances of abuse proactively. The more understanding the world has about the dynamics of abuse, the better-equipped individuals can be to make safe and resilient changes for all members. In doing so, society can work together to finally end the endless cycles of abuse and provide prompt intervention and care to those who need it.

## 5. Relevance

Emotional intelligence (EI) refers to the ability to appropriately interpret and respond to both external and internal emotional stimuli. Abusive actions generally stem from a low level of emotional management and are reinforced by the sensations of superiority. These low EI levels can be linked to the way that abusers have been operantly conditioned to view violence and manipulation as acceptable responses, and thus, continue with the expression of aggressive behaviors with other relations.

Poor parenting techniques and anxious-ambivalent attachments are prominent benchmarks for future abusive tendencies. Experiencing negligence or deceitful behaviors during childhood can serve as early trauma for a future abuser. Authoritarian parents are very stringent and more likely to resort to physical punishment. Children of authoritarian parents often grow up to be troubled and likely continue using physical punishment on their own children in the future as well.

Abuse is multifaceted, incorporating numerous mediators such as temperament, anger, and hostility, and furthered by aggression and personal dehumanization. This multifaceted nature also relates to the biopsychosocial approach. Whether it is due to substance abuse (biological), mental health (psychological), or past abusive relationships (social), it is evident that concepts relating to abuse are heavily engraved into psychology's teachings and interests.

## 6. Conclusion

The two studies by (C. A. Greene, L. Haisley, C. Wallace, and J. D. Ford [1]) and J. C. Babcock, C. E. Green, S. A. Webb, and T. P. Yerington [2] collectively provide valuable insight into the topic of abuse. Abusive tendencies stem from a variety

of factors, including economic health, childhood maltreatment, mental health (C. A. Greene, L. Haisley, C. Wallace, and J. D. Ford [1]) emotional reactivity, and antisocial behaviors (J. C. Babcock, C. E. Green, S. A. Webb, and T. P. Yerington [2]). This only emphasizes the complexities left to unfold the puzzling workings of human behavior. From understanding the multifaceted mediators to applying the moderators of abuse, science has come a long way in its efforts to mitigate its effects. By continuing efforts to research abusive actions and relations, society can work to prioritize this urgent manner

so that it can be a prominent topic addressed in public forums and gain the recognition and priority it requires.

## References

[1] C. A. Greene, L. Haisley, C. Wallace, and J. D. Ford, "Intergenerational effects of childhood maltreatment: A systematic review of the parenting practices of adult survivors of childhood abuse, neglect, and violence," *Clinical Psychology Review*, vol. 80, p. 101891, 2020, doi: 10.1016/j.cpr.2020.101891.

[2] J. C. Babcock, C. E. Green, S. A. Webb, and T. P. Yerington, "Psychophysiological Profiles of Batterers: Autonomic Emotional Reactivity as It Predicts the Antisocial Spectrum of Behavior Among Intimate Partner Abusers.," *Journal of Abnormal Psychology*, vol. 114, no. 3, pp. 444–455, 2005, doi: 10.1037/0021-843X.114.3.444.

[3] L. Mineo, "'Shadow pandemic' of domestic violence." [Online]. Available: https://news.harvard.edu/gazette/story/2022/06/shadow-pandemic-of-domestic-violence/

[4] "Child Maltreatment Statistics." [Online]. Available: https://americanspcc.org/child-maltreatment-statistics/

[5] D. Goleman, "Sad Legacy of Abuse: The Search for Remedies." 1989.

Open Access | https://doi.org/10.62329/rujg3592

**Morganton Scientific**

*North Carolina School of Science and Mathematics*

Journal of Student STEM Research

# Risk Factors of Frequent Poor Mental Health Days Among Adults in the United States (2022)

**Anil Chintapalli**[1]

[1]North Carolina School of Science and Mathematics

## Abstract

Mental health has become a prominent public health issue in the United States. As such, understanding the risk factors for any condition affecting mental well-being is an important undertaking. This study analyzed the 2022 Behavioral Risk Factor Surveillance System (BRFSS) survey to determine the relationship between frequent poor mental health (FPMH) and several demographic, behavior, and quality of life factors among adults in the United States. The Centers for Disease Control and Prevention (CDC) defines FPMH as 14 or more poor mental health days in the past 30 days. Weighted cross-tabulation and multivariate logistic regression were used to find the factors associated most strongly with FPMH. Overall, about 15% of American adults had FPMH. There were significant disparities in the prevalence of FPMH based on demographics, notably among adults with annual incomes below $15,000 (29.43%) and adults unable to work (38.12%). Additionally, current smokers were 1.55 times more likely to report FPMH than non-smokers; this number rose to 4.20 when adults managing 6-8 chronic conditions were compared to adults managing 0 conditions. These findings highlight the importance of targeted mental health interventions, providing a blueprint for future support.

**Keywords** Mental Health, Health Disparities, Behavioral Risk Factors

## 1. Introduction

Mental health has become an increasingly prominent public health issue in the United States. Frequent poor mental health (FPMH), which the Centers for Disease Control and Prevention (CDC) defines as 14 or more days of poor mental health in the past month [1], affects a significant portion of the adult population, resulting in significant disturbances to an individual's quality of life. Previous research has identified links between demographic factors and mental health outcomes [2], but there is little comprehensive analysis that incorporates behavioral risk factors and quality of life indicators for the broader patient population that is adults in the United States [3]. This paper intends to fill this gap by implementing three categories (levels) of potential risk in relation to FPMH: demographic, behavioral, and quality of life.

A demographic factor is a widely accepted characteristic used to classify or analyze specific patient populations. Some common examples include age, gender, and income bracket. Analysis through this lens is useful because it provides a measure of the inherent societal imbalances (in relation to mental health) within the United States. However, these characteristics are relatively static in the short term. Results can guide targeted intervention but do not offer the patient a solution. As such, behavioral factors are also important.

**Published** Jun 27, 2024

**Correspondence to**
Anil Chintapalli
chintapalli25a@ncssm.edu

A behavioral factor refers to the effect of a patient's actions on their health. Some lifestyle choices, such as smoking or binge drinking, negatively impact a patient's overall well-being. Others, such as daily physical exercise, have a positive effect. In contrast to demographic factors, one has a greater degree of control over these characteristics of one's life. This section of analysis provides more actionable results for the individual patient.

Finally, some factors do not refer to specific patient populations or behaviors. Generally, these refer to a patient's "quality of life". For example, if a patient manages multiple chronic conditions, this reduced quality of life may have effects that extend beyond physical well-being. Accounting for this type of factor allows for a model more sensitive to the connection between physical and mental health.

Every year, the CDC performs the Behavior Risk Factor Surveillance System (BRFSS). This is a nationwide telephone survey intended to gather information about the United States adult population for public health purposes. The survey records the respondent's demographics, screens for risky behaviors, and asks quality of life questions. Through the CDC's extensive outreach and weighting strategies, the results of this survey can be generalized to the greater United States adult population [4]. As such, this paper refers to the respondent pool when referencing raw (unweighted) data, and to the United States adult population when discussing the weighted data.

This paper utilizes 2022 BRFSS data (the latest year available at the time of analysis) to determine the prevalence of demographic, risk, and quality of life factors among adults aged 18 or older in the United States in relation to FPMH. The survey, using both landline and cellphone outreach, garnered 445,132 responses from all 50 states, the District of Columbia, Guam, Puerto Rico, and the US Virgin Islands [4]. For the remainder of this paper, "states" will be used as a blanket term for any region that participates in the BRFSS.

The BRFSS includes 3 parts: a core component, optional modules, and state-added questions [1]. All states use the core component, which allows for a standardized view of public health in the United States. The optional modules ask about more specific topics. A state particularly worried about one of these topics may elect to include the necessary module in its BRFSS. If a state desires more targeted information not asked by the CDC, it may develop the required questions individually and add them solely to its state-specific section of BRFSS [4].

## 2. Methods

### *2.1. Enviroment and Packages*

This analysis was performed with the R programming language (version 4.4.1) and run in the RStudio environment. The following libraries were used:

- survey (version 4.4-2): This package provides the tools necessary to handle weighted survey data, stratified sampling, and clustering sampling.
- dplyr (version 1.1.4): This package allows for data manipulation through recoding and filtering nonresponse values.
- openxlsx (version 4.2.7.1): This package reads, writes, and manipulates an Excel workbook to better format the analysis results.

### *2.2. Weighting, Stratification, and Clustering*

The CDC performs extensive stratification, weighting, and clustering to ensure that the results from the survey can be generalized to the greater population [5]. Weighting corrects for biases due to unequal coverage or nonrandom high nonresponse rates. By selectively altering the significance of each datapoint, the BRFSS results better reflect the

demographics of the United States population. Stratification also improves representativeness by dividing the population into subgroups (strata) based on geographic area and density of phone numbers [5]. Each stratum is sampled from separately, ensuring that each region is represented correctly. Finally, clustering simplifies the sampling process by dividing the population into primary sampling units (PSUs). These sampling units are then chosen at random for data collection [5].

This study considers the core-only section of the 2022 BRFSS. Optional or state-specific modules were not included. Responses to those modules cannot represent the condition of the greater United States population, as there are inherent differences in the information gleaned from each question. To weight the variables in solely the core section, the CDC includes the _LLCPWT variable. Similarly, _STSTR is used for stratification, and _PSU applies the necessary clustering. These methods are passed through the survey design object in R.

### *2.3. Recording and Nonresponse Filtration*

When someone participates in the survey, they can provide one of two response types for a given question. The first is an uninformative response: they elect not to respond or don't know the answer. The second is informative. It can be an affirmative or negative, the option that matches their behavior or demographic, or the number of days or diseases that best fit their condition. All these potential responses are coded as a different number, which is indicated by the corresponding BRFSS Codebook for 2022 [1].

If a question elicits an affirmative or negative response, as is the case with "During the past month, other than your regular job, did you participate in any physical activities or exercises such as running, calisthenics, golf, gardening, or walking for exercise?", it is simple to code the potential responses:

- Yes = 1
- No = 2
- Don't know / Not sure = 7
- Refusal to answer = 9

For questions where respondents select the best matching option from multiple choices (like behavioral tendencies or demographics), the coding varies by question due to the range of possible responses. For example, consider the question which determines current employment:

#### 2.3.1. *"Are you currently… ?":*

- Employed for wages = 1
- Self-employed = 2
- Out of work for 1 year or more = 3
- Out of work for less than 1 year = 4
- A Homemaker = 5
- A Student = 6
- Retired = 7
- Unable to work = 8
- Refused = 9

Finally, questions for which responses are provided by selecting a number of days or conditions are coded based on the number provided by the respondent. Further distinctions can be manually recoded once the data is downloaded from the CDC. Consider the following question:

2.3.2. *"Now thinking about your mental health, which includes stress, depression, and problems with emotions, for how many days during the past 30 days was your mental health not good?":*

- Number of days = _ _ (01-30)
- None = 88
- Don't know / Not sure = 77
- Refused = 99

Note that the "catch-all" (None, Don't know / Not sure, Refused) codes have been multiplied by 11 because it is possible for the respondent to report 7, 8, or 9 days of poor mental health in the past month. This removes ambiguity regarding the significance of a particular code. This is done any time there is a possibility of an overlap between an informative response and a catch-all code [1].

The CDC recodes responses to make analysis more straightforward. For yes/no and categorical questions, it simplifies the levels and groups all missing responses under code 9 [6]. For numerical responses (like number of days or conditions), it creates standardized levels. These recoding procedures help streamline data analysis. Variables recoded by the CDC are preceded with an underscore (_).

All responses containing 7/9 and 77/99 codes in the analyzed variables were removed to prevent these non-substantive responses from artificially skewing the statistical calculations.

The following were used as predictor (independent) variables for this analysis. Manual recodes are noted where applied. If a variable was renamed for this analysis, this is indicated by an arrow next to the original variable name.

**_SEX**

- Male = 1
- Female = 2

**_AGE_G**

- Age 18 to 24 = 1
- Age 25 to 34 = 2
- Age 35 to 44 = 3
- Age 45 to 54 = 4
- Age 55 to 64 = 5
- Age 65 or older = 6

**_RACEPR1**

- White only, non-Hispanic = 1
- Black only, non-Hispanic = 2
- American Indian or Alaskan Native only, non-Hispanic = 3
- Asian only, non-Hispanic = 4
- Native Hawaiian or other Pacific Islander only, non-Hispanic = 5
- Multiracial, non-Hispanic = 6
- Hispanic = 7

**_EDUCAG → _educag_**

- Did not graduate High School = 1
- Graduated High School = 2
- Attended College or Technical School = 3

- Graduated from College or Technical School = 4

**MARITAL → _marital_**

- Married = 1
- Divorced = 2
- Widowed = 3
- Separated = 4
- Never married = 5
- A member of an unmarried couple = 6

**EMPLOY1 → _employ1_**

- Employed for wages = 1
- Self-employed = 2
- Out of work for 1 year or more = 3
- Out of work for less than 1 year = 4
- A Homemaker = 5
- A Student = 6
- Retired = 7
- Unable to work = 8

**_INCOMG1 → _income3_**

- Less than $15,000 = 1
- $15,000 to <$25,000 = 2
- $25,000 to <$35,000 = 3
- $35,000 to <$50,000 = 4
- $50,000 to <$100,000 = 5
- $100,000 to <$200,000 = 6
- $200,000 or more = 7

**VETERAN3 → _veteran3_**

- Yes = 1
- No = 2

**_CHLDCNT → _CHLDCNT_**

- No children in household = 1
- One child in household = 2
- Two children in household = 3
- Three children in household = 4
- Four children in household = 5
- Five or more children in household = 6

**_TOTINDA → _TOTINDA_**

- Had physical activity or exercise = 1
- No physical activity or exercise in the last 30 days = 2

**_RFSMOK3 → _RFSMOK3_**

- No = 1
- Yes = 2

**_RFBING6 → _RFBING6_**

- No = 1
- Yes = 2

**DIABETES4, _MICHD, CVDSTRK3, _LTASTH1, _DRDXAR2, CHCSCNC1, CHCOCNC1, CHCCOPD3, CHCKDNY2 → chronic_disease**

- Manages no chronic conditions = 1
- Manages 1-2 chronic conditions = 2
- Manages 3-5 chronic conditions = 3
- Manages 6-8 chronic conditions = 4

This variable was recoded. First, the existence of each chronic condition (diabetes, cancer, asthma, arthritis, chronic kidney disease, stroke, coronary heart disease, or chronic obstructive pulmonary disease) was recorded. Respondents were then grouped by the number of conditions they managed, as indicated above.

The following was used as the outcome (dependent) variable. The 14-day cutoff is based on the CDC's recommendation for classifying a respondent's mental health as frequently poor [1].

**_MENT14D → _ment14_**

- Less than 14 days of poor mental health in the last 30 days ("satisfactory") = 0
- 14 or more poor mental health days in the last 30 days ("frequent, poor") = 1

This variable was manually recoded to create a binary outcome, which is necessary to perform logistic regression analysis.

### *2.4. Cross-tabulation for Column Percentages*

Once the variables were recoded, original frequency counts were found for each cross tabulation between all predictor variable levels and the two outcome variable levels. Then, a weighted count for each cross-tabulation was generated (based on the CDC's survey design weighting, stratification, and clustering). This allows the number to more accurately represent the true number of United States adults who fit a given cross-tabulation (give or take the standard error upon weighting, which is also included). Column percentages were calculated by taking the weighted number of people with FPMH in each level and dividing by the weighted total number of people in the same level. For example, the column percentage for adult women in the United States with frequent poor mental health was found by dividing that weighted frequency by the estimated total number of adult women in the United States (also a weighted frequency count). 95% confidence intervals were then found for each column percentage based on the standard errors of the respective weighted frequencies.

Rao-Scott chi-squared tests were performed on weighted frequency counts for each cross tabulation. This allows one to determine whether the distribution of adults reporting FPMH differed by cross-tabulation. The Rao-Scott chi-squared test was chosen because these frequency counts are weighted. A standard Pearson chi-squared test cannot account for the effect of weighting, stratification, and clustering [7]. Significance was set at a p-value $< 0.01$.

### *2.5. Multivariate Logistic Regression Analysis*

A multivariate logistic regression model was built based on the recoded variables. This was used to assess the variation each factor had on FPHM. The logistic regression provides the multiplicative change in odds that _ment14_ = 1 for each one-unit increase in a given predictor variable, while holding all other variables constant [8].

For each variable, one level was chosen as the reference category. For a clearer comparison, the level expected to have the lowest prevalence of FPMH was set for reference. These are indicated below for each predictor variable:

- _SEX: Male (1)
- _AGE_G: Age 18 to 24 (1)
- _RACEPR1: White only, non-Hispanic (1)
- _educag_: Graduated from College or Technical School (4)
- _marital_: Married (1)
- _employ1_: Employed for wages (1)
- _income3_: $200,000 or more (7)
- _veteran3_: No (2)
- _CHLDCNT_: No children in household (1)
- _TOTINDA_: Had physical activity or exercise (1)
- _RFSMOK3_: No (1)
- _RFBING6_: No (1)
- chronic_disease: Manages no chronic conditions (1)

The desired logistic regression returns coefficients ($\beta$) which represent the log odds for each predictor variable level compared to its reference level (both in relation to an individual's likelihood of developing FPMH). Each log odd is then transformed into an odds ratio by calculating $e^{\beta}$ (raising e to the power of each log odd) [8]. A significant odds ratio is a valuable tool to compare the effects of each level on the outcome variable. This value indicates how much more or less likely an individual in a specific level is to report FPMH compared to the reference level, while holding the other predictor variables constant. The significance of each odds ratio was determined by the 95% confidence interval. If the interval included 1, the odds ratio was deemed insignificant [8].

## 3. Results

The following tables provide the cross-tabulation results from the most significant predictor variables.

| RS 2 $p < .0001$ | Did not graduate High School | Graduated High School | Attended College/Technical School | Graduated College/ Technical School |
|---|---|---|---|---|
| **<14 days of FPMH** | | | | |
| Column Percentage | 80.04% | 82.29% | 82.67% | 89.04% |
| Column Percentage 95% CI | 79.06% -80.99% | 81.82% - 82.75% | 82.24% - 83.09% | 88.75% - 89.33% |
| **≥14 days of FPMH** | | | | |
| Column Percentage | 19.96% | 17.71% | 17.33% | 10.96% |
| Column Percentage 95% CI | 19.01% - 20.94% | 17.25% - 18.18% | 16.91% - 17.76% | 10.67% - 11.25% |
| **Total** | | | | |
| Weighted Frequency | 29266273 | 70592764 | 77912720 | 79203973 |

**Table 1: FPMH by Education**

| RS 2 $p < .0001$ | Employed for wages | Self - employed | Out of work ≥ 1 yr | Out of work < 1 yr | Home - maker | Student | Retired | Unable to work |
|---|---|---|---|---|---|---|---|---|
| **<14 days of FPMH** | | | | | | | | |
| Column Percentage | 85.55% | 87.88% | 72.97% | 70.46% | 86.04% | 75.56% | 90.96% | 61.88% |
| Column Percentage 95% CI | 85.23% - 85.86% | 87.16% - 88.57% | 71.08% - 74.79% | 68.46% - 72.39% | 84.84% - 87.16% | 74.07% - 76.99% | 90.59% - 91.33% | 60.66% - 63.08% |
| **≥14 days of FPMH** | | | | | | | | |
| Column Percentage | 14.45% | 12.12% | 27.03% | 29.54% | 13.96% | 24.44% | 9.03% | 38.12% |

| RS 2 *p* < .0001 | Employed for wages | Self - employed | Out of work ≥ 1 yr | Out of work < 1 yr | Home - maker | Student | Retired | Unable to work |
|---|---|---|---|---|---|---|---|---|
| Column Percentage 95% CI | 14.14% - 14.77% | 11.43% - 12.84% | 25.21% - 28.92% | 27.61% - 31.54% | 12.84% - 15.16% | 23.01% - 25.93% | 8.67% - 9.41% | 36.92% - 39.34% |
| **Total** | | | | | | | | |
| Weighted Frequency | 120779738 | 24004358 | 6394978 | 6501600 | 12513220 | 12168959 | 51715285 | 15868736 |

## Table 2: FPMH by Employment Status

| RS 2 *p*<.0001 | <$15,000 | $15,000 - <$25,000 | $25,000 - <$35,000 | $35,000 - <$50,000 | $50,000 - <$100,000 | $100,000 - <$200,000 | ≥$200,000 |
|---|---|---|---|---|---|---|---|
| **<14 days of FPMH** | | | | | | | |
| Column Percentage | 70.57% | 77.50% | 79.70% | 82.94% | 85.75% | 89.44% | 92.06% |
| Column Percentage 95% CI | 69.27% - 71.83% | 76.58% - 78.39% | 78.85% - 80.52% | 82.20% - 83.66% | 85.30% - 86.20% | 88.93% - 89.92% | 91.35% - 92.72% |
| **≥14 days of FPMH** | | | | | | | |
| Column Percentage | 29.43% | 22.50% | 20.30% | 17.06% | 14.25% | 10.56% | 7.94% |
| Column Percentage 95% CI | 28.17% - 30.73% | 21.61% - 23.42% | 19.48% - 21.15% | 16.34% - 17.80% | 13.80% - 14.70% | 10.08% - 11.07% | 7.28% - 8.65% |
| **Total** | | | | | | | |
| Weighted Frequency | 13236673 | 20217159 | 24663916 | 25475921 | 57235233 | 41762275 | 15434731 |

## Table 3: FPMH by Income Level

| RS 2 *p* = .0002 | A Veteran | Not a Veteran |
|---|---|---|
| **<14 days of FPMH** | | |
| Column Percentage | 85.56% | 84.08% |
| Column Percentage 95% CI | 84.85% - 86.25% | 83.84% - 84.33% |
| **≥14 days of FPMH** | | |
| Column Percentage | 14.44% | 15.92% |
| Column Percentage 95% CI | 13.75% - 15.15% | 15.67% - 16.16% |
| **Total** | | |
| Weighted Frequency | 25351175 | 228681952 |

## Table 4: FPMH by Veteran Status

| RS 2 *p* < .0001 | Had physical activity | Did not have physical activity |
|---|---|---|
| **<14 days of FPMH** | | |
| Column Percentage | 85.99% | 78.66% |
| Column Percentage 95% CI | 85.73% - 86.24% | 78.14% - 79.18% |
| **≥14 days of FPMH** | | |
| Column Percentage | 14.01% | 21.34% |
| Column Percentage 95% CI | 13.76% - 14.27% | 20.82% - 21.86% |
| **Total** | | |
| Weighted Frequency | 196628045 | 61155165 |

## Table 5: FPMH by Participation in Physical Activity

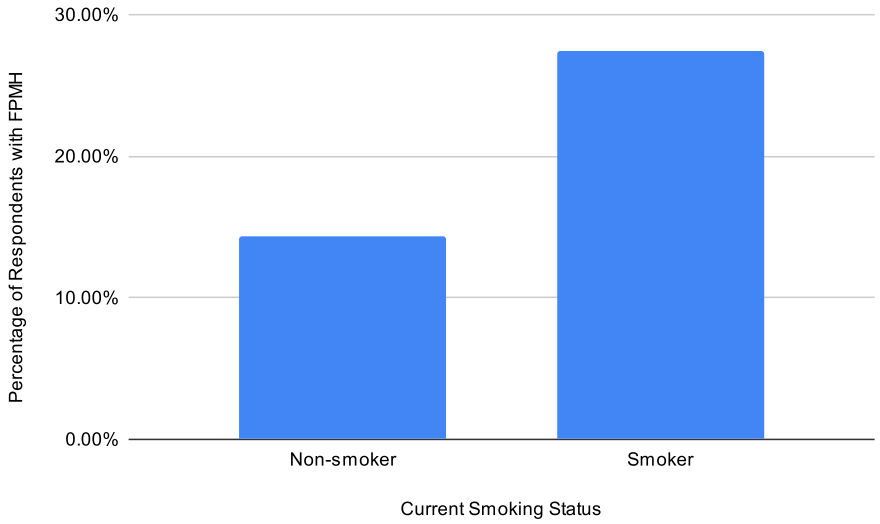


**Figure 1**. *FPMH by Smoking Status*

| RS 2 $p < .0001$ | Current Smoker | Not a Current Smoker |
|---|---|---|
| **<14 days of FPMH** | | |
| Column Percentage | 72.59% | 85.70% |
| Column Percentage 95% CI | 84.62% - 85.15% | 79.57% - 80.84% |
| **≥14 days of FPMH** | | |
| Column Percentage | 27.41% | 14.30% |
| Column Percentage 95% CI | 14.85% - 15.38% | 19.16% - 20.43% |
| **Total** | | |
| Weighted Frequency | 29959928 | 204459603 |

**Table 6: FPMH by Current Smoking Status**

27.41% of smokers had FPMH while 14.30% of non-smokers had FPMH. The national average was 15%.

| RS 2 $p < .0001$ | 0 Chronic Conditions | 1-2 Chronic Conditions | 3-5 Chronic Conditions | 6-8 Chronic Conditions |
|---|---|---|---|---|
| **<14 days of FPMH** | | | | |
| Column Percentage | 87.15% | 82.93% | 74.57% | 59.48% |
| Column Percentage 95% CI | 86.84% - 87.45% | 82.56% - 83.29% | 73.68% - 75.44% | 53.66% - 65.04% |
| **≥14 days of FPMH** | | | | |
| Column Percentage | 12.85% | 17.07% | 25.43% | 40.52% |
| Column Percentage 95% CI | 12.55% - 13.16% | 16.71% - 17.44% | 24.56% - 26.32% | 34.96% - 46.34% |
| **Total** | | | | |
| Weighted Frequency | 132091777 | 102192756 | 22955304 | 1056305 |

**Table 7: FPMH by Number of Chronic Conditions**

40.52% of people with 6-8 chronic conditions had FPMH while 12.85% of people with 0 chronic conditions, 17.07% of people with 1-2 chronic conditions, and 25.43% of people with 3-5 chronic conditions had FPMH. The national average was 15%.

The following figure highlights the most significant odds ratios and their 95% confidence intervals.

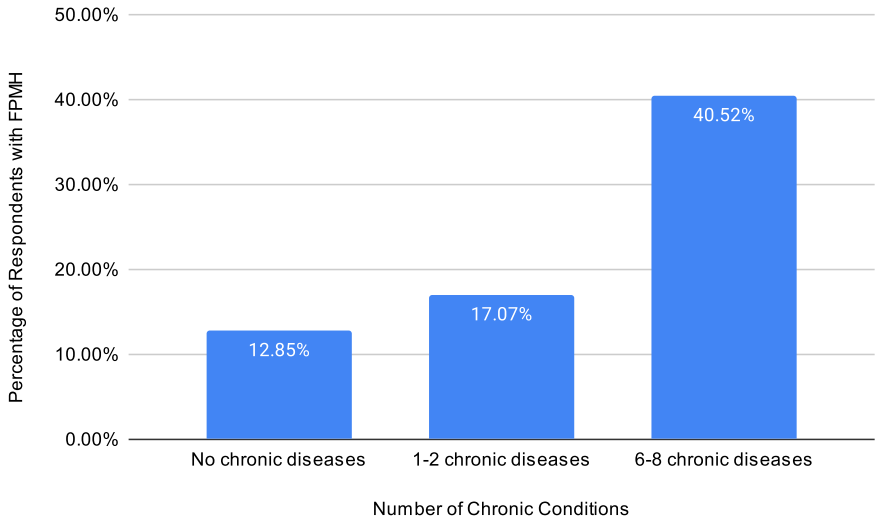


**Figure 2.** *FPMH by Number of Chronic Conditions*

### *3.1. Most Significant Results*

This analysis supports the characterization of poor mental health as a prominent public health issue, as 15% of American adults met the criteria to be considered as having FPMH. Based on the demographic factors, females (18.33%), those aged 18 to 24 (25.11%), multiracial non-Hispanics (24.44%), those unable to work (38.12%), and those making less than $15,000 annually (29.43%) had the highest prevalence of FPMH (p-value < .0001 for all).

Behavioral and quality of life factors also significantly affected an individual's likelihood of having FPMH, as those who completed no physical activity in the last 30 days (21.34%), current smokers (27.41%), those who engaged in binge drinking in the last 30 days (19.78%), and those who managed chronic diseases (17.07% - 40.52%) also experienced a higher prevalence of FPMH than the national average (p-value <.0001 for all).

The multivariate model revealed more about the demographic, behavioral, and quality of life factors associated most strongly with FPMH. Notably, adults unable to work were 2.49

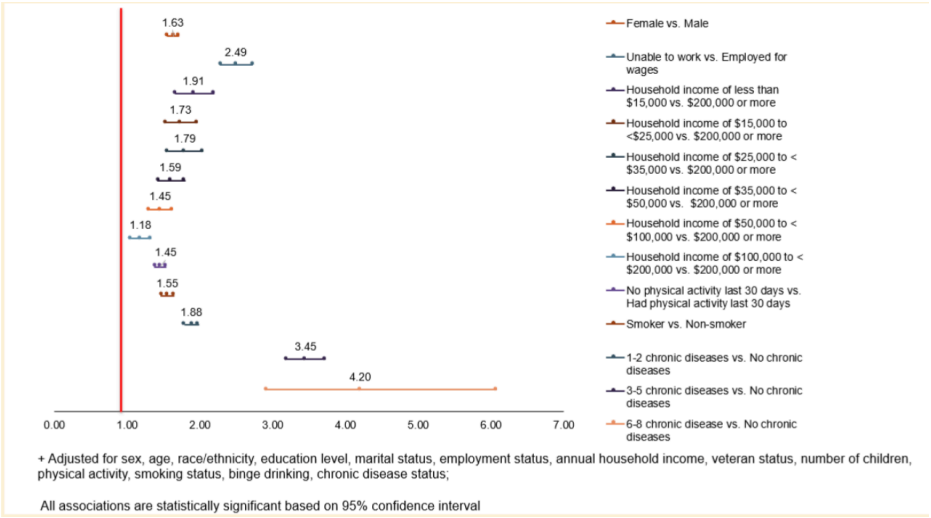


**Figure 3.** *Significant odds ratios and 95% confidence intervals*

(95% CI: 2.28 – 2.72) times more likely to report FPMH than adults employed for wages. FPMH prevalence increased as the income bracket decreased: FPMH was 1.91 (95% CI: 1.66 – 2.19) times more likely for adults in households earning less than $15,000 than those in households earning $200,000 or more. Smoking posed the highest behavioral risk of FPMH, as current smokers were 1.55 (95% CI: 1.46 - 1.64) times more likely to have FPMH than non-smokers. Similarly, those who lacked physical activity were 1.45 (95% CI: 1.38 – 1.53) times more likely to have FPMH than those who exercised in the last month. Finally, the prevalence of FPMH increased with an individual's number of chronic diseases. Adults managing 6-8 chronic diseases were 4.20 (95% CI: 2.91 – 6.06) times more likely to meet criteria for FPMH than those managing no chronic diseases.

### *3.2. Implications*

These results suggest that there is a significant income-based disparity among adults affected by FPMH in the United States. Many treatments such as therapy and medication are not readily accessible to lower-income households. This finding highlights the need for expanded support programs that provide mental health resources for those struggling financially, such as increased funding for community mental health centers and more flexible payment options. Physical activity, an accessible method of managing mental health, also requires enhanced promotion. Finally, work is needed to integrate the mental health needs of physically vulnerable patients into their care strategies. These patients require support for both managing chronic conditions and the associated mental stress.

### *3.3. Limitations*

There are a few primary limitations of this study. Most significantly, this is a cross-sectional analysis, meaning that it is taken from a single point in time. As such, the findings indicate significant correlation between the predictor variables and FPMH but cannot establish causation. As the analysis was performed on survey data, one cannot determine the direction of effect for the predictor variables and an individual's likelihood of having FPMH. For example, if a respondent who was a current smoker reported FPMH, one cannot know if smoking caused FPMH, or if FPMH resulted in smoking as a coping strategy. Additionally, while the multivariate logistic regression analysis controls for each demographic, behavior, and quality of life factor in the study, it cannot account for any confounding variables not captured by the BRFSS. Some examples include family history of mental health conditions and existence of social support networks.

Furthermore, while not an arbitrary categorization, respondents who experienced some poor mental health days but not 14 or more still need support. Further splitting of the outcome variable levels is necessary for a more nuanced analysis. Similarly, grouping effect of chronic conditions solely by number (disregarding which each condition is) muddies the conclusions that can be drawn about quality of life factors. A more specific categorization would result in a more actionable analysis.

Finally, the only other reference to mental health in the 2022 BRFSS questionnaire was: "Do you have a depressive disorder (including depression, major depression, dysthymia, or minor depression)?" However, existence of depression was not chosen as a predictor variable because of its inherent strong association with FPMH. Existence of depression would predict FPMH very well, causing inflated standard errors and unreliable coefficient estimates. Thus, the model becomes unstable, making it difficult to assess the correlation between the other predictor variables and FPMH.

## 4. Future Direction

A future direction for this project is to run another analysis in which existence of depression is the outcome variable and compare the difference in results. This

illuminates the disparity among which patients can obtain a diagnosis of depression out of those who experience FPMH, guiding future supplemental mental health support.

## 5. Data Availability Statement

The deidentified data and code that support the findings of this study are openly available in the following GitHub repository: https://github.com/anilchintapalli/BRFSS_study.git

## References

[1] Centers for Disease Control and Prevention, "LLCP 2022 Codebook Report." [Online]. Available: https://www.cdc.gov/brfss/annual_data/2022/zip/codebook22_llcp-v2-508.zip

[2] H. Miyakado-Steger and S. Seidel, "Using the Behavioral Risk Factor Surveillance System to Assess Mental Health, Travis County, Texas, 2011–2016," *Preventing Chronic Disease*, vol. 16, p. 180449, 2019, doi: 10.5888/pcd16.180449.

[3] C. Pierannunzi, S. S. Hu, and L. Balluz, "A systematic review of publications assessing reliability and validity of the Behavioral Risk Factor Surveillance System (BRFSS), 2004–2011," *BMC Medical Research Methodology*, vol. 13, no. 1, p. 49, 2013, doi: 10.1186/1471-2288-13-49.

[4] J. Liu, N. Jiang, A. Z. Fan, and R. Weissman, "Alternatives in Assessing Mental Healthcare Disparities Using the Behavioral Risk Factor Surveillance System," *Health Equity*, vol. 2, no. 1, pp. 199–206, 2018, doi: 10.1089/heq.2017.0056.

[5] Centers for Disease Control and Prevention, "Weighting the Data." [Online]. Available: https://www.cdc.gov/brfss/annual_data/2022/pdf/2022-Weighting-Description-508.pdf

[6] Centers for Disease Control and Prevention, "Calculated Variables in the 2022 Data File of the Behavioral Risk Factor Surveillance System." [Online]. Available: https://www.cdc.gov/brfss/annual_data/2022/pdf/2022-calculated-variables-version4-508.pdf

[7] J. N. K. Rao and A. J. Scott, "The Analysis of Categorical Data from Complex Sample Surveys: Chi-Squared Tests for Goodness of Fit and Independence in Two-Way Tables," *Journal of the American Statistical Association*, vol. 76, no. 374, pp. 221–230, 1981, doi: 10.1080/01621459.1981.10477633.

[8] S. Sperandei, "Understanding logistic regression analysis," *Biochemia Medica*, pp. 12–18, 2014, doi: 10.11613/BM.2014.003.

Open Access | https://doi.org/10.62329/dhuu7748

# Exploring the Use of Immunotherapy Techniques in Lymphocytic Leukemia

**Enoch Edwin**[1]

[1]North Carolina School of Science and Mathematics

**Morganton Scientific**

*North Carolina School of Science and Mathematics*

Journal of Student STEM Research

## Abstract

Lymphocytic leukemia is a cancer that affects the white blood cells. It occurs when the cancerous, abnormal cells outcompete and reproduce more efficiently than the healthy cells in the body. Although there are therapies like chemotherapy and radiation, these therapies often lead to relapse or are simply not effective. Emerging Immunotherapy techniques like immune checkpoint inhibitors and chimeric antigen receptor (CAR T-cell) therapy offer a new gaze into what can be done to use the body's own immune system to apoptotic cancer cells. This research review paper monitors advancements made in immunotherapy, highlighting clinical trials and research done in Seoul, Munich, and New England that investigate drugs like Blinatumomab and CART19 therapies. Despite great progress, there still need to be more consistent results in trials, costs need to be lowered, and the efficiency of immunotherapy needs to be muchswifter. For future research, trials on other diseases using the same techniques need to be underway, and the applications of this miracle drug need to be fully explored and pioneered.

**Keywords** Lymphocytic Leukemia, Immunotherapy, CAR T-Cell Therapy, Blinatumomab

## 1. Introduction and Background of Lymphocytic Leukemia

Lymphocytic leukemia is a type of cancer that affects white blood cells, and these white blood cells cause blockages and can crowd out healthy blood cells, choking the bloodstream. Although the exact cause of leukemia is unknown, scientists believe that it may result from factors like genetics, lifestyle, and environmental exposures [1]. There are two different types of lymphocytic leukemia: acute lymphocytic leukemia and chronic lymphocytic leukemia. Acute lymphocytic leukemia affects mostly children and younger adults, while chronic lymphocytic leukemia affects primarily older adults, though exceptions exist [2].

Like most cancers, lymphocytic Leukemia manifests more in the developed parts of the world, mainly in North America and Europe [3]. There are many underlying mutations to lymphocytic leukemia, such as the Philadelphia chromosome, a translocation between chromosomes 9 and 22; the BCR-ABL1 fusion gene, which causes cancerous cells to exhibit abnormal tyrosine kinase activity; TP53 mutations, which confer resistance to therapy; and NOTCH1 mutations, which enable cell proliferation and differentiation [4].

Acute lymphocytic leukemia requires expedited treatment, often leading to a lower life expectancy, while individuals with chronic lymphocytic leukemia may live for decades with sporadic and controlled treatment [5]. Treatments for lymphocytic leukemia include chemotherapy, radiation, immunotherapy, and stem cell transplantation [6]. The likelihood of developing chronic lymphocytic leukemia is about 0.57%, or 1 in every 175 people in the United States, with men having a slightly higher risk [1]. For acute lymphocytic leukemia, the incidence is less than 1% of all cancer cases in the United

**Published** Jun 27, 2024

**Correspondence to**
Enoch Edwin
edwin26e@ncssm.edu

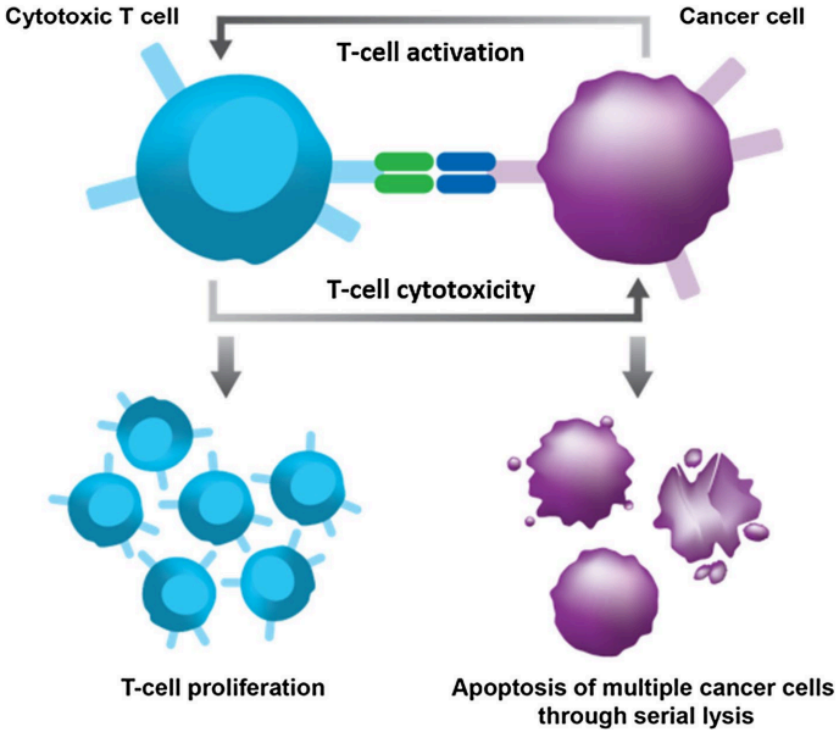


**Figure 1**. *How Blinatumomab affects T-cells and apoptotic cancer cells*

States [7]. Although acute lymphocytic leukemia primarily affects children, most deaths occur among adults, with 4 out of 5 deaths involving adult patients [2]. The purpose of this paper is to highlight what research is being done to cure these ailments and ultimately make these statistics much more powerful with a deeper emphasis on the clinical trials and their criteria.

## 2. Immunology Methods to Prevent and Hinder Lymphocytic Leukemia

Scientists use immune checkpoint inhibitors and chimeric antigen receptor (CAR) T-cell therapy to treat lymphocytic leukemia [8]. Immune checkpoint inhibitors target pathways like PD-1/PD-L1 and CTLA-4 to enhance and utilize T-cell responses against leukemia cells [3]. CAR T-cell therapy involves genetically modifying the patient's T cells to recognize and destroy cancer cells [6].

A common method for leukemia cells to evade T-cell recognition is over-expressing PD-L1, which hinders T-cell function. When PD-L1 on a somatic cell binds to PD-1 on a T cell, it deactivates the T cell and leads to apoptosis [8]. Immunotherapy techniques aim to block this interaction, enabling T cells to function and destroy leukemia cells [7].

In CAR T-cell therapy, scientists extract blood from patients, isolate the T cells, genetically modify them to target specific proteins on leukemia cells, and then reinfuse them into the patient [6]. Although this therapy shows remarkable success, it is costly and highly individualized [2].

Success rates for CAR T-cell therapy range between 30% and 40% depending on the modifications made [8]. However, limitations include the high costs, unintended destruction of healthy blood cells, relapse risks, and side effects such as cytokine release

syndrome (symptoms like coughing, low blood pressure, and organ dysfunction) and neurotoxicity (confusion, delirium, and nausea) [8]. CAR T-cell therapy is ineffective against solid tumors [5].

The FDA has approved CAR T-cell therapy for treating B-cell acute lymphoblastic leukemia using drugs such as blinatumomab, nelarabine, and inotuzumab ozogamicin [2]. Similarly, immune checkpoint inhibitors include drugs such as nivolumab, pembrolizumab, and cemiplimab [6].

## 3. Research and Studies on Immunology Treatments for Leukemia

*Seoul Trial*

There was a study in 2019 in Seoul, South Korea, for lymphocytic leukemia, particularly referencing the recurrence around the marrow. The drug Idarubicin was used for the reinduction stage with the drug, Blincyto used for the study. This study is in stage 2, meaning that there are human trials and with people more at risk for any more cancer progression. A criteria for the patients for age was they must be at least more than one years old and at most 22 years old. The patients could not have received Blinatumomab before this study either. The study focused on many exclusion factors: patients should have adequate renal function, could not have the Philadelphia chromosome, could not have any mixed phenotypes for leukemia, and could not have had HIV either. Patients would be tested with Blinatumomab, and then the efficacy rate, disease-free survival rate, and death rate related to treatment would be tested. The patients would be tested for an average of 9 years.

*Munich Trial*

A recent Phase II clinical trial by Amgen Research (Munich) GmbH investigated the use of Blinatumomab (MT103) in targeting minimal residual disease of B-precursor acute lymphoblastic leukemia (ALL). The scientists used Blinatumomab to treat patients with Philadelphia chromosome-positive acute lymphoblastic leukemia (ALL). Blinatumomab doesn't directly repair the Philadelphia Chromosome, but it can help eliminate leukemia cells that carry this abnormality. The inclusion criteria they used were that the patients must have B-precursor ALL and complete hematological remission with molecular failure, and must also be able to sign their informed consent to do so. Some of the exclusion criteria are that they do not have a history or have a current autoimmune disease, cannot have any anti-murine antibodies, cannot be pregnant or nursing either, and cannot have any current extramedullary involvement.

*New England Trial*

Another study in New England did a Phase 1 clinical trial that started with a patient diagnosed with chronic lymphocytic leukemia (CLL) in 1996. The patient had treatment started in 2002, which was Rituximab plus fludarabine treatment (Chemotherapy and Targeted Therapy Combination). The clinical treatment started in July of 2010. The purpose of the treatment was to test the safety and feasibility of CART19 in relapsed/refractory B-cell neoplasms. Autologous T-cells were genetically modified using a lentiviral vector to express CD19-specific CAR. Some of the inclusion criteria were that patients had to be of sound body and health, express previous treatment failure, have autologous T-Cell availability to harvest the patients T-Cells, have adequate organ function, and the patient must have signed informed consent.

## 4. Conclusion

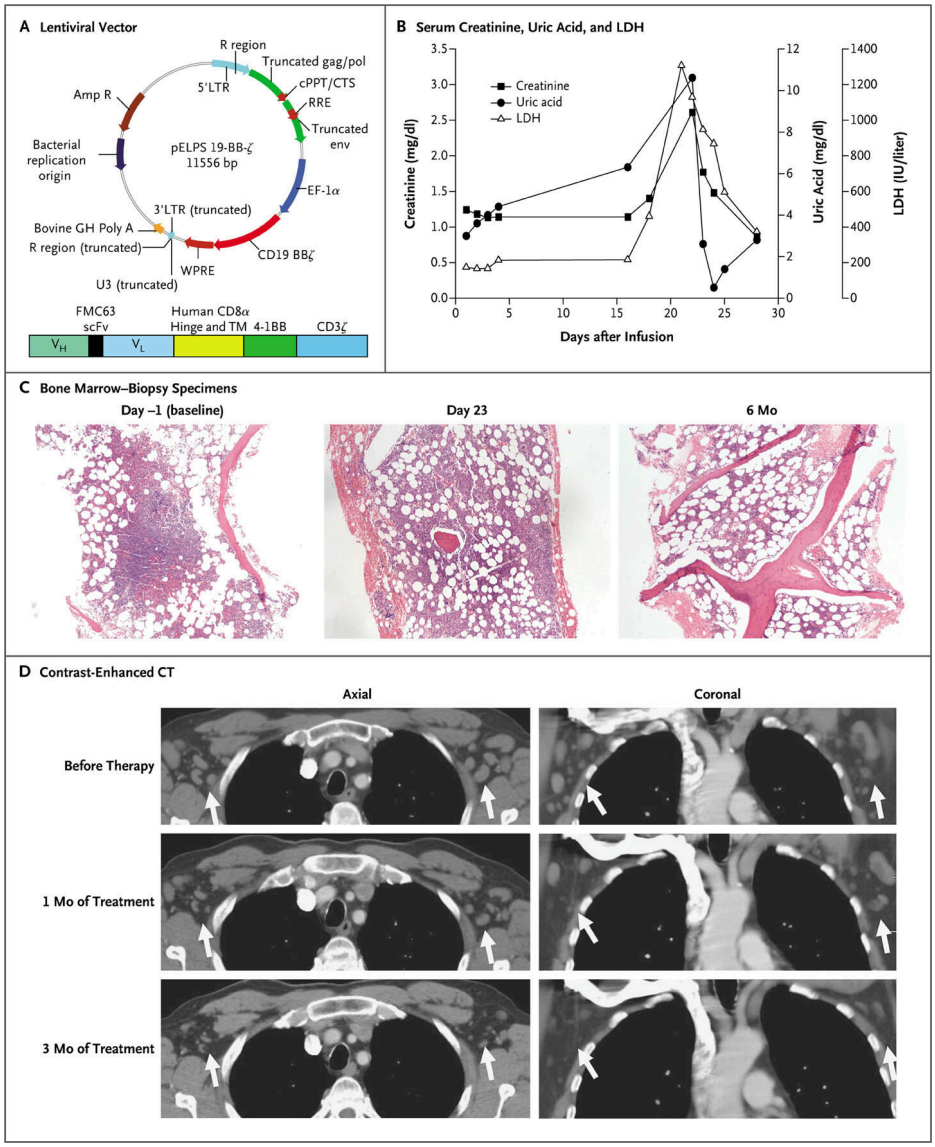


**Figure 2.** *Panel A illustrates the lentiviral vector used to modify T cells for CART19 therapy, containing key functional elements for targeting CD19, while Panels B, C, and D show clinical data and imaging, including serum markers, bone marrow biopsies, and CT scans before and after treatment, highlighting tumor response and recovery.*

The exploration of immunotherapy techniques, particularly through the use of Blinatumomab has shown great potential in treating patients with lymphocytic leukemia and can be another venue scientists and research approach how to address cancer. These trials not only state the efficacy of Immunotherapy techniques, they also underscore the importance of patient criteria in trials to get the most consistent data that correlates to the general human population. As these trials get to later phases and advance, the follow-up research will be a key to our understanding of this novice therapy that has the potential to cure most cancers. More research in different types of cancers and different strands of leukemia can be predicted for the near future as Blinatumomab is reaching greater strides in the battle against cancer.

## References

[1] C. Pérez-Carretero *et al.*, "The Evolving Landscape of Chronic Lymphocytic Leukemia on Diagnosis, Prognosis and Treatment," *Diagnostics*, vol. 11, no. 5, p. 853, 2021, doi: 10.3390/diagnostics11050853.

[2] S. Sharma and K. R. Rai, "Chronic lymphocytic leukemia (CLL) treatment: So many choices, such great options," *Cancer*, vol. 125, no. 9, pp. 1432–1440, 2019, doi: 10.1002/cncr.31931.

[3] E. Carballido, M. Veliz, R. Komrokji, and J. Pinilla-Ibarz, "Immunomodulatory Drugs and Active Immunotherapy for Chronic Lymphocytic Leukemia," *Cancer Control*, vol. 19, no. 1, pp. 54–67, 2012, doi: 10.1177/107327481201900106.

[4] Z. Wang *et al.*, "Preclinical efficacy against acute myeloid leukaemia of SH1573, a novel mutant IDH2 inhibitor approved for clinical trials in China," *Acta Pharmaceutica Sinica B*, vol. 11, no. 6, pp. 1526–1540, 2021, doi: 10.1016/j.apsb.2021.03.005.

[5] B. Eichhorst, P. Cramer, and M. Hallek, "Initial therapy of chronic lymphocytic leukemia," *Seminars in Oncology*, vol. 43, no. 2, pp. 241–250, 2016, doi: 10.1053/j.seminoncol.2016.02.005.

[6] D. L. Porter, B. L. Levine, M. Kalos, A. Bagg, and C. H. June, "Chimeric Antigen Receptor–Modified T Cells in Chronic Lymphoid Leukemia," *New England Journal of Medicine*, vol. 365, no. 8, pp. 725–733, 2011, doi: 10.1056/NEJMoa1103849.

[7] K. Vincent, D.-C. Roy, and C. Perreault, "Next-generation leukemia immunotherapy," *Blood*, vol. 118, no. 11, pp. 2951–2959, 2011, doi: 10.1182/blood-2011-04-350868.

[8] A. Major *et al.*, "Efficacy of checkpoint inhibition after CAR-T failure in aggressive B-cell lymphomas: outcomes from 15 US institutions," *Blood Advances*, vol. 7, no. 16, pp. 4528–4538, 2023, doi: 10.1182/bloodadvances.2023010016.

Open Access | https://doi.org/10.62329/vwrx3559

Morganton Scientific

*North Carolina School of Science and Mathematics*

Journal of Student STEM Research

# In Silico Exploration of L-Valine Ester Prodrug Designs for Enhanced Pharmacokinetics in BCS Class IV Nucleoside Antivirals

**Kevin Gencel**[1]

[1]North Carolina School of Science and Mathematics

## Abstract

Nucleoside derivatives are among the few families of molecules with antiviral properties. However, pharmacokinetic limitations have historically limited their capabilities for oral administration, the preferred administration mechanism with historically improved outcomes, versatility, and ability for at-home administrations. In recent years, Valacyclovir and Valganciclovir have demonstrated how the addition of a valine promoiety to nucleoside antivirals allow the drugs to overcome oral pharmacokinetic boundaries through the usage of the PepT1 pathways as prodrugs. Torcitabine is a highly potent hepatitis B virus inhibitor, but faced limited usage in countries with prevalent HBV cases due to requirements for intravenous administration. Cyclopropavir is a cytomegalovirus inhibitor like Ganciclovir, but has pre-clinically exhibited multiple advantages, including 10-fold increases in potency, half-life, and reduced complications. Using Gaussian 16, B3LYP, and a 6-31g basis set, we conducted molecular orbital, natural bond orbital, and bond order calculations to predict key indicators of bioavailability, including dissociation rates, electrostatic binding affinity, and bond stability. Then, key quantitative structure activity relationship (QSAR) properties and molecular docking affinities were obtained from Optibrium's StarDrop Software to predict effectiveness when binding to important target proteins, including the PepT1 receptor and Valacyclovir Hydrolase enzyme. Valtorcitabine and Valcyclopropavir both exhibited high pharmacokinetic potential for use as oral medications, with similar properties to Valacyclovir and Valganciclovir. The results of this study support future in vivo experimentation for both drugs as drug candidates for hepatitis B virus and cytomegalovirus, respectively.

**Keywords** Valine, Valtorcitabine, Valcyclopropavir, PepT1, Valacyclovir Hydrolase

**Published** Jun 27, 2024

**Correspondence to**
Kevin Gencel
gencel25k@ncssm.edu



## 1. Introduction

Nucleoside-derived molecules are the most prominent group of antiviral drug candidates, chosen for their rare ability to mimic DNA material to attract viral enzymes [1]. However, most nucleoside derivatives are classified by the Biopharmaceutics Classification System (BCS) as class IV drugs. Class IV drugs exhibit numerous unfavorable characteristics (low solubility and permeability, high presystemic metabolism, efflux transport) that impede safe oral delivery with an effective bioavailability, limiting much of their historical clinical usage to intravenous administration in hospital settings. Due to the significant financial and health advantages of oral medications, more studies have emerged on the development of prodrugs, modified drugs made to achieve high oral bioavailability, of many existing Class IV drugs that require intravenous administration. Prodrugs are defined as biologically inactive drug molecules that undergo an enzymatic and/or chemical transformation in vivo to release an active parent drug [2]. Prodrugs are created by attaching a promoiety, a chemical group that enhances the molecule's absorption,

distribution, or stability. Prodrugs allow for oral distribution by enabling absorption into the bloodstream, then using enzymatic cleavage to remove the promoiety and release the parent drug, which can freely move through the bloodstream into the target site. Quantitative measures of a prodrug's effectiveness come from its ability to improve the parent drug's absorption proportion. They must also be highly stable to prevent unwanted metabolism but be able to rapidly convert into the parent drug after reaching the bloodstream.

Nucleoside-derivatives are incredibly promising for prodrug studies due to their compatibility with promoieties and the need for orally-administered antivirals. This interest and compatibility have led to multiple prodrug forms of nucleoside-derived antivirals being clinically approved and incredibly successful in the pharmaceutical markets. Acyclovir and Ganciclovir, for example, were among the first successful antiviral drugs, and are highly potent against Herpes Simplex Virus and Cytomegalovirus, respectively. While both had essentially no function as oral drugs and had to be administered intravenously, the prodrug variants of both these molecules, Valacyclovir and Valganciclovir, have bioavailabilities greater than 50%, and receive millions of prescriptions annually due to their improved convenience and effectiveness.

The selection of a prodrug's promoiety is based on the parent drug's needs and available functional groups. In this regard, amino acid promoieties have proven to be highly advantageous and compatible with the nucleoside derivative family of drugs, and Valacyclovir and Valganciclovir both utilize a valine promoiety. Research by [3] has revealed that, despite the improved yet still suboptimal ADME parameters, the addition of an amino acid promoiety allows the prodrugs to bind to the intestinal PepT1 and PepT2 receptors, which are used for active transport of oligopeptides from the intestines into the bloodstream. Through these L-valine ester prodrug designs, Beutner observed that Valacyclovir can achieve an approximate oral bioavailability of 54.5%, 3-5 times greater than its parent. Similarly, Valganciclovir has an oral bioavailability of 60%, as compared to Ganciclovir's 5-8% (PubChem [4], N. S. Umapathy, V. Ganapathy, and M. E. Ganapathy [5]).

Cytomegalovirus (CMV) is among the most prevalent viral agents in the world. A leading cause of mortality in immunocompromised patients, CMV infects one in every 100-150 newborns, making it the most common congenital infection in most countries [6]. Hepatitis B Virus (HBV) is similarly prevalent, as approximately 296 million people are currently living with a chronic HBV infection, and 820,000 deaths annually are attributed to HBV-related complications [7]. With that said, Torcitabine has been preclinically found to be a potent nucleoside inhibitor against HBV and Cyclopropavir possesses high antiviral properties against CMV (J. Ahmad, S. Ikram, A. B. Hafeez, and S. Durdagi [7], Z. Wu *et al.* [8]). Both are BCS class IV drugs that, despite their in vitro antiviral properties, weren't studied extensively as oral drug candidates, largely due to their poor pharmacokinetic properties as an oral medication. However, both drugs showed promise for high compatibility with the valine ester promoiety, having hydroxyl groups that could be masked by forming an ester bond with valine that could be broken by esterase enzymes like Valacyclovir Hydrolase in the blood.

The absorption, distribution, metabolism, and excretion (ADME) properties of the prodrug derivatives, including LogP, polar surface area, pKa, etc. to predict the stability and solubility of the molecule as it travels through the gastrointestinal tract. We also conducted a molecular docking study of the prodrugs to quantify their ability to bind to the external PepT1 and PepT2 proteins, which is the primary mechanism for transmitting valine-based prodrugs into the bloodstream. Quantum calculations were run through Gaussian 16 to predict the stability and reactivity of the prodrugs as they are absorbed in

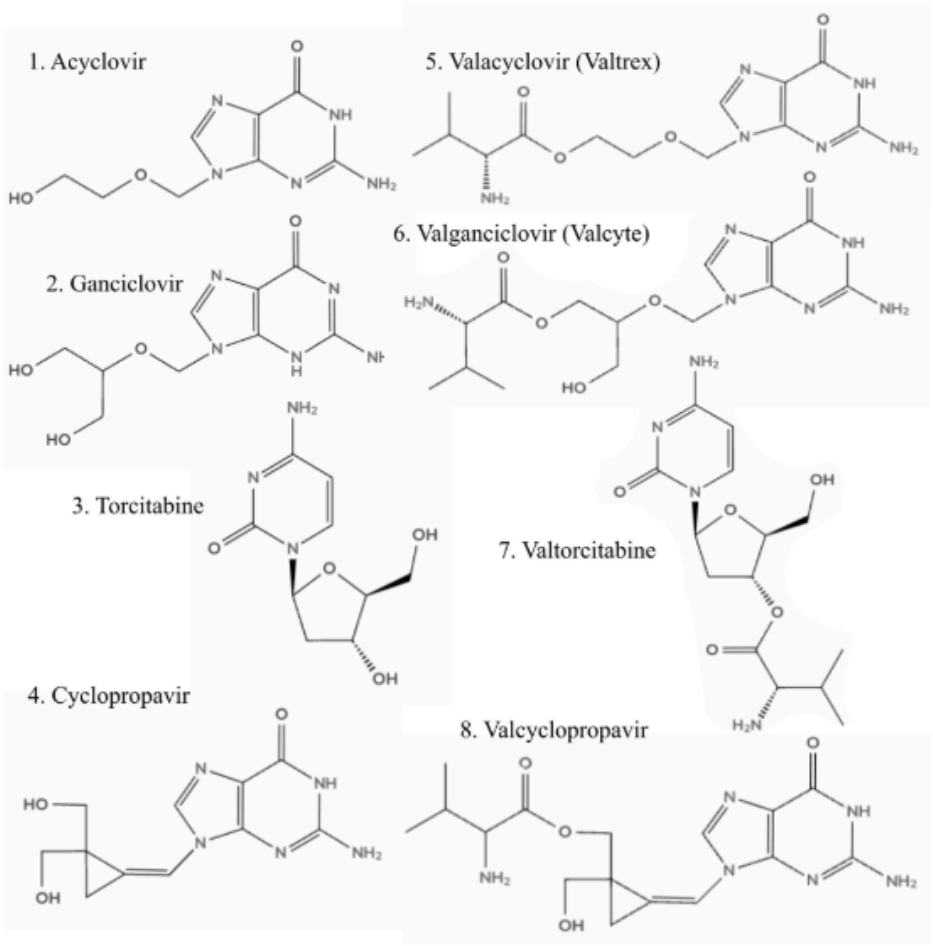


**Figure 1**. *Molecules 1-8, 4 parent drugs and 4 prodrugs*

the gastrointestinal tract, which were assessed qualitatively using a variety of electronic and orbital properties including HOMO-LUMO gaps, electrostatic potential models, bond order calculations, and natural population analysis. This study aimed to determine the effectiveness of Valtorcitabine and Valcyclopropavir as prodrugs relative to successful prodrugs like Valacyclovir and Valganciclovir, using this data to inform further in vivo research as oral drug candidates for HBV and CMV.

## 2. Computational Approach

*Quantum Calculations*

Density functional theory (DFT) with the Lee-Yang-Parr correlation functional, denoted B3LYP, was used to execute the theoretical calculations [9]. All quantum chemistry was calculated using the quantum chemical package Gaussian 16 [10]. Each calculation was run at the B3LYP/6-31G(d,p) level of theory to allow for timely calculation times given the number and size of the molecules included in this study (8 molecules each up to 26 heavy atoms). The North Carolina High School Computational Chemistry Server was used to organize and manage all jobs [11]. The starting geometries of all calculated molecules 1-8 in Figure 1 were designed in WebMO and then optimized. Vibrational frequency calculations were then run to confirm that the geometry optimizations were at the lowest energy states. With the confirmed geometry optimizations, molecular orbital calculations

and natural bond order calculations were run for each molecule. Bond order calculations were run for prodrug molecules 5-8.

*Molecular Orbital Calculation*

First, a molecular orbital calculation was run to ascertain the magnitude of each molecule's HOMO-LUMO gap. These values are obtained by measuring the difference in orbital energy between the highest-energy molecular orbital occupied by electrons (HOMO) and the lowest-energy molecular orbital unoccupied by electrons (LUMO). The HOMO and LUMO were visualized to predict the behavior of electrons in excited states, and their values were compared with literature values for Valacyclovir's HOMO-LUMO gap [12]. Using the same calculation, we visualized and interpreted the electrostatic potential maps of prodrug molecules 5-8 to predict the regional reactivities in specific biochemical reactions as molecules travel through the body. Specifically, the valine group was analyzed to make predictions of their efficacy for two key interactions: electrophilic sites for affinity to enzymatic nucleophilic attacks, and negatively charged regions that are likely to bind to positively charged PepT1 transporter residues.

*Natural Bond Orbital (NBO)*

A natural bond orbital calculation was run to predict how the addition of a valine promoiety affected the molecule's ADME properties. Specifically, we used a natural population analysis to measure the extent to which the valine group masks the charges of the parent drug's OH group. This reduction of charge was studied as it can help the molecule resist rapid excretion and increase absorption proportions.

*Bond Order Calculation*

A bond order calculation was run to measure the relative strengths and bond order of the prodrug's ester linkage to make predictions of the inherent strength of the bond and its ability to resist dissociation prior to esterase enzyme exposure in the bloodstream. If the prodrug were to dissociate early, the drug's total bioavailability would decrease because the parent drug could not enter the bloodstream without the valine promoiety.

*QSAR and pKa Calculations*

The second round of calculations used specialized medicinal chemistry software instead of quantum calculations. All calculations were run using Optibrium's StarDrop software [13]. To do so, Molecules 1-8 were coded into SMILES notation and uploaded into StarDrop software to calculate quantitative data of the pharmacokinetic properties of the molecules. Stardrop's modeling tool ran calculations for LogP, TPSA, and various pKa values for molecules 1-8. The valine group does not enable the prodrugs to permeate cell membranes passively or effectively dissolve into solvents they otherwise couldn't, but it does enable their active diffusion into the bloodstream. Knowing how the promoiety alters the parent drug's ADME properties allows us to gauge the prodrug's bioavailability, which is dependent on its stability and resistance to degradation. Because the gastrointestinal tract has multiple regions with varying pH environments, we calculated various pKa values, including the most acidic and basic values of each prodrug, to predict their behaviors in different pH environments.

*Molecular Docking Calculations*

To assess the ability of Valcyclopropavir and Valtorcitabine to bind to key proteins involved in the absorption of valine prodrugs, Stardrop's SEESAR tool was used to calculate their binding affinity to PepT1, PepT2, and Valacyclovir Hydrolase. The binding sites of these three proteins were represented using the Protein Data Bank codes 7PMW, 9BIS, and 20CI (L. Lai, Z. Xu, J. Zhou, K.-D. Lee, and G. L. Amidon [14], J. L. Parker *et al.* [15],

| Parent Drug | Parent Drug HOMO-LUMO Gap (eV) | Prodrug HOMO-LUMO Gap (eV) | Percent Reduction (%) |
|---|---|---|---|
| Acyclovir | 5.44 | 5.44 | 0 |
| Ganciclovir | 5.42 | 5.14 | 5.17 |
| Torcitabine | 5.28 | 5.25 | 0.57 |
| Cyclopropavir | 4.87 | 4.75 | 2.46 |

**Table 1**. *HOMO-LUMO gap values*

Y. Ural-Blimke *et al.* [16]). Valine-based prodrugs must interact with PepT1 and PepT2 proteins to be actively transported from the intestines into the bloodstream. Thus, to enter the bloodstream, it is imperative for Valtorcitabine and Valcyclopropavir to successfully bind to the receptors with similar magnitudes to Valacyclovir and Valganciclovir to use those pathways. Additionally, the enzyme primarily responsible for metabolizing Valacyclovir into Acyclovir is Valacyclovir Hydrolase; this enzyme is the primary esterase responsible for removing the valine group from the parent drug. The number of conformers each molecule had within the binding pocket and their respective binding affinities was calculated for each protein, measured in pKi.

## 3. Results and Discussion

*Molecular Orbitals Analysis*

The molecular orbital calculations were run using a 6-31G(d,p) basis set, and the results could be verified to a <5% margin of error compared to literature values of Valacyclovir's HOMO-LUMO gap [12].

Table 1 shows the HOMO-LUMO gap values for each molecule. A decrease in the magnitude of the HOMO-LUMO gap indicates increased reactivity in the prodrug structure, which can relate to reduced stability. In addition to gap magnitude, the location of a molecule's HOMO and LUMO can indicate reactive tendencies. Acyclovir and Torcitabine had essentially no change in their HOMO and LUMO's location when converting into their prodrug forms, centering directly around the pyrimidine structures. By contrast, Ganciclovir and Cyclopropavir's conversion to prodrug form causes their LUMO to move toward the valine ester, as can be seen in Figure 2. Valganciclovir's possession of this property causes electrophilic attacks to the valine ester bond, which results in a favorable cleavage of the bond and release of the parent drug. Valcyclopropavir sharing this characteristic with Valganciclovir suggests it would also be able to cleave the valine group when in acidic environments.

*Electrostatic Potential Mapping*

Figure 3 shows the electronic charge density maps for prodrugs 5-8. The blue regions of the molecules represent areas with positive charge density, where hydrogens have high affinity for enzymatic binding and are more susceptible to electrophilic attacks. The

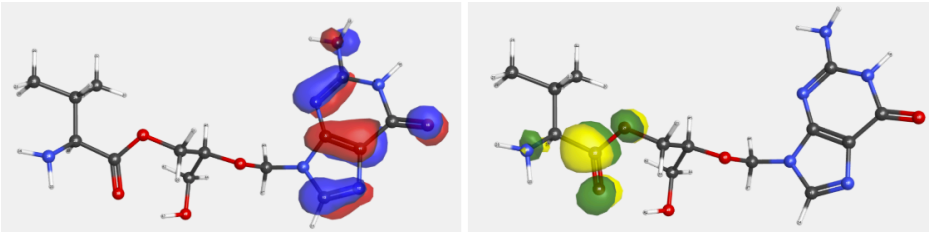

**Figure 2**. *Valgancyclovir's HOMO (red/blue) and LUMO (yellow/green)*

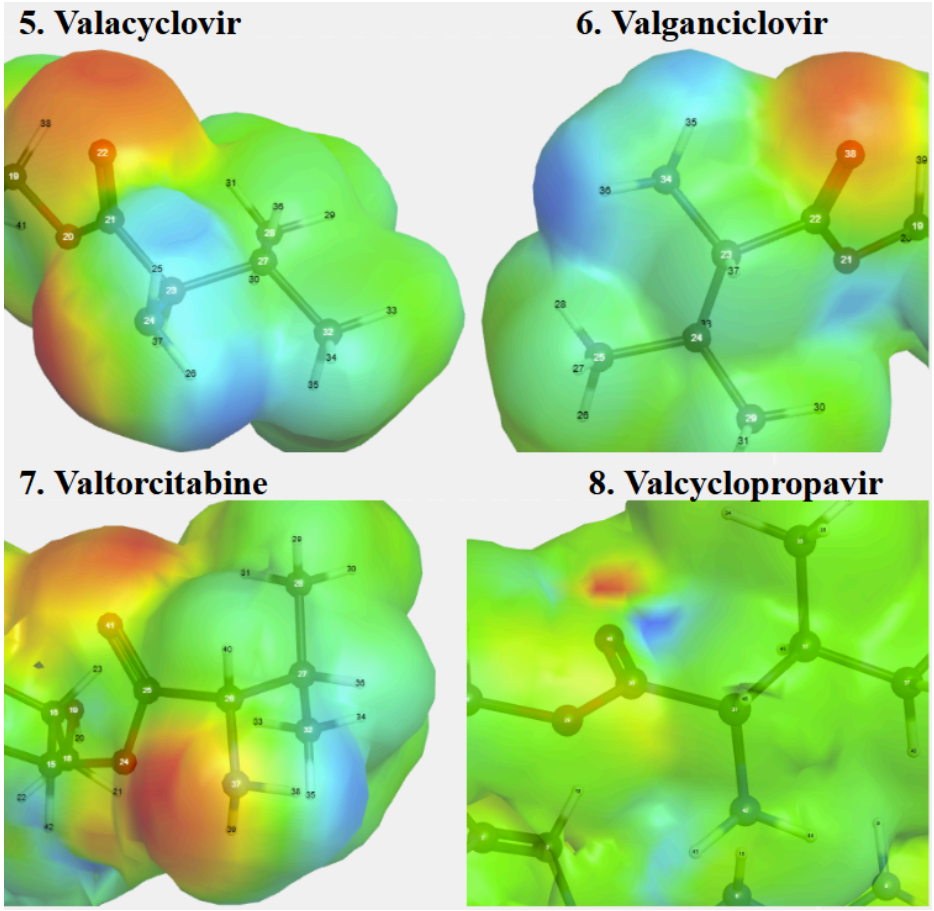


**Figure 3.** *Electrostatic potential visual representation for prodrugs 5-8*

valine promoiety's amine group on Valacyclovir, Valganciclovir, and Valtorcitabine have a clear area of high positive charge density, which suggests that they would willingly bind to esterase enzymes. A strong localized negative charge, represented by red regions, around the ester carbonyl carbon is required for binding to the positively charged PepT1 transporter residue. Valtorcitabine having this property indicates it will be able to use this pathway effectively. By contrast, Valcyclopropavir exhibited minimal polarity in its valine charge distribution, likely due to the molecule's inherently high steric bulk and electrostatic density. This lack of necessary polarity on the valine's functional groups can prevent necessary protein binding.

*ADME Property Calculations*

A large contributor to the significant polarity in the parent drugs is their common hanging hydroxyl group, and an effective prodrug would mask some of this polarity to

| Parent Drug | Parent Drug OH Charge | Prodrug OH Charge | Percent Charge Reduction (%) |
|---|---|---|---|
| Acyclovir | -0.758 | -0.556 | 26.65 |
| Ganciclovir | -0.766 | -0.542 | 29.24 |
| Torcitabine | -0.760 | -0.549 | 27.76 |
| Cyclopropavir | -0.730 | -0.570 | 21.92 |

**Table 2.** *Relative charge-masking effect of valine group addition on parent drug hydroxyl group*

| Parent Drug | Percent Change LogS at pH 7.4 | Percent Change LogP | Percent Change Flexibility |
|---|---|---|---|
| Acyclovir | +9.92% | -60.58% | +41.65% |
| Ganciclovir | +7.45% | -42.40% | +31.53% |
| Torcitabine | +17.77% | -63.96% | +112.59% |
| Cyclopropavir | +14.41% | -58.81% | +74.95% |

**Table 3**. *Relative change of LogS (at pH 7.4), LogP, and flexibility from the addition of a valine group to parent drugs 1-4*

improve pharmacokinetics. In all four prodrug derivatives, the valine group successfully masked 20-30% of the OH group's polarity (Table 2). The reduction of this charge should increase LogP value and reduce the effective topological polar surface area. However, due to the high polarity of the carbonyl & amine substituents, the valine group did not have this desired effect in a calculation of the entire molecule.

Many drug designers prefer their oral drug candidates to have a LogS in the range of -1 to -3 to optimize water solubility while allowing the drug to permeate intestinal lipid-based membranes. The high LogS of the experimental prodrugs does not hinder absorption due to its distinctive ability to use the PepT1 transport mechanism, but masking the OH group to reduce molecular polarity is still of interest (Table 3). Additionally, an increased number of flexible bonds in a drug improves their ability to conform and bind to key proteins, such as the PepT1 residue and esterase enzymes in this study.

The addition of the valine promoiety had a drastic effect on LogP and molecular flexibility in the prodrug derivatives relative to their parent drug. As can be seen in Table 3, each parent drug experienced an average LogP change of approximately 60%, which correlates to the molecules exhibiting approximately 400% greater nonpolar character. These changes to LogP and LogS could alleviate some of the challenges the parent drug experiences in being absorbed. For example, the extreme polarity of the parent drug can trigger rapid excretion through urination before it can be absorbed into the intestines, and the change in LogP helps slightly with this challenge. Additionally, the change in flexibility should allow the prodrugs to more readily conform and bind to important proteins like the PepT1 protein residue or esterase enzymes.

*Structural Stability Predictions*

Valtorcitabine and Valcyclopropavir had similarly strong ester bonds to Valacyclovir and Valganciclovir, all having a bond order from 1.020-1.075. This indicates similar resistance to dissociating into the parent drug before the molecule enters the bloodstream. In vivo studies of Valacyclovir conducted by [3] revealed that it does not experience pre-absorption dissociation, and the results of the bond order calculation suggests that this will be the case for Valtorcitabine and Valcyclopropavir as well.

The results of the pKa calculations were largely consistent with the control prodrugs, with the most basic pKa values being almost identical between prodrugs 5-8 at ~7-8. However, while Valacyclovir, Valganciclovir, and Valtorcitabine all had minimum pKa values of 7.5-8.5, Valcyclopropavir's most acidic pKa value was 3.9. This suggests that in an environment like the intestines, which have a pH of ~6-8, the molecule will completely deprotonate, decreasing its stability and increasing the chance it will undergo base-catalyzed hydrolysis as it passes through.

*Protein-Ligand Docking Study*

| Prodrug | PepT1 Binding Affinity | PepT2 Binding Affinity | Valacyclovir Hydrolase |
|---|---|---|---|
| PDB | 7PMW | 9BIS | 2OCI |
| Valacyclovir | 3.5 | 5.4 | 1.7 |
| Valganciclovir | 4.2 | 0.7 | 2.8 |
| Valtorcitabine | 4.1 | 1.5 | 5.1 |
| Valcyclopropavir | 4.7 | 2.0 | 3.0 |

**Table 4**. *Prodrug binding affinities (pKi) to PepT1, PepT2, and Valacyclovir Hydrolase protein residues*

Finally, we conducted a docking study binding Valtorcitabine and Valcyclopropavir to three major protein systems that influence bioavailability: the PepT1/PepT2 solute transporter and the Valacyclovir hydrolase enzyme. Optimally, the experimental prodrugs would have a very high binding affinity to the PepT1/PepT2 proteins, allowing almost all of the drug to enter the bloodstream, but a moderate binding affinity to the Valacyclovir Hydrolase enzyme to allow for moderate release of the parent drug without rapid release from esterase enzymes in the gastrointestinal tract.

Table 4 contains the binding affinities of prodrugs 5-8 to each binding receptor, expressed as pKi. Valacyclovir was the only molecule capable of effectively binding to the PepT2 transporter protein, with a pKi of 5.4. However, both Valcyclopropavir and Valtorcitabine exhibited favorable binding affinity to the PepT1 transporter at a similar magnitude to Valganciclovir. Valtorcitabine's docking to PepT1 can be seen in Figure 4, where the valine promoiety's constituents contribute significantly to the binding interaction. The results suggest that Valtorcitabine and Valcyclopropavir should have a similar ability to Valganciclovir to use the PepT1 active transport mechanism to enter the bloodstream.

Valacyclovir, Valganciclovir, and Valcyclopropavir all had low to moderate binding affinity to Valacyclovir Hydrolase, having pKi values less than 3. However, Valtorcitabine had a binding affinity of 5.1. Because Valacyclovir Hydrolase is found in small concentrations in the intestines, Valtorcitabine's binding affinity to the enzyme being 100 times greater than Valganciclovir may cause a large proportion of Valtorcitabine to lose its promoiety before bypassing intestinal membranes, decreasing the concentration of Torcitabine available in the bloodstream. If Valtorcitabine does have high bioavailability, however, it will be a very fast-acting drug due to the increased binding affinity.

## 4. Conclusion

Relative to Valacyclovir and Valganciclovir, both proven to use the valine prodrug mechanism to reach bioavailabilities greater than 60%, Valcyclopropavir and Valtorcitabine indicated similar capabilities in key measurements of prodrugs, such as stability, reactivity, and ability to penetrate intestinal membranes using a valine promoiety. There were, however, a handful of characteristics that may hold them back from exhibiting similar bioavailabilities in vivo. Valcyclopropavir had a highly distributed LUMO, which could potentially make it more reactive and unstable. Its electrostatic potentials were also very neutral around the valine group, possibly preventing favorable polar enzyme/protein binding. Valcyclopropavir also had a very low minimum pKa value, potentially causing rapid dissociation or excretion in high-pH environments such as the intestines. Valtorcitabine had an abnormally high binding affinity to Valacyclovir Hydrolase, potentially causing premature release of the parent drug before entering the bloodstream. Despite these suboptimal properties, overall our results suggest that the addition of a valine promoiety to Torcitabine and Cyclopropavir will allow the drugs to

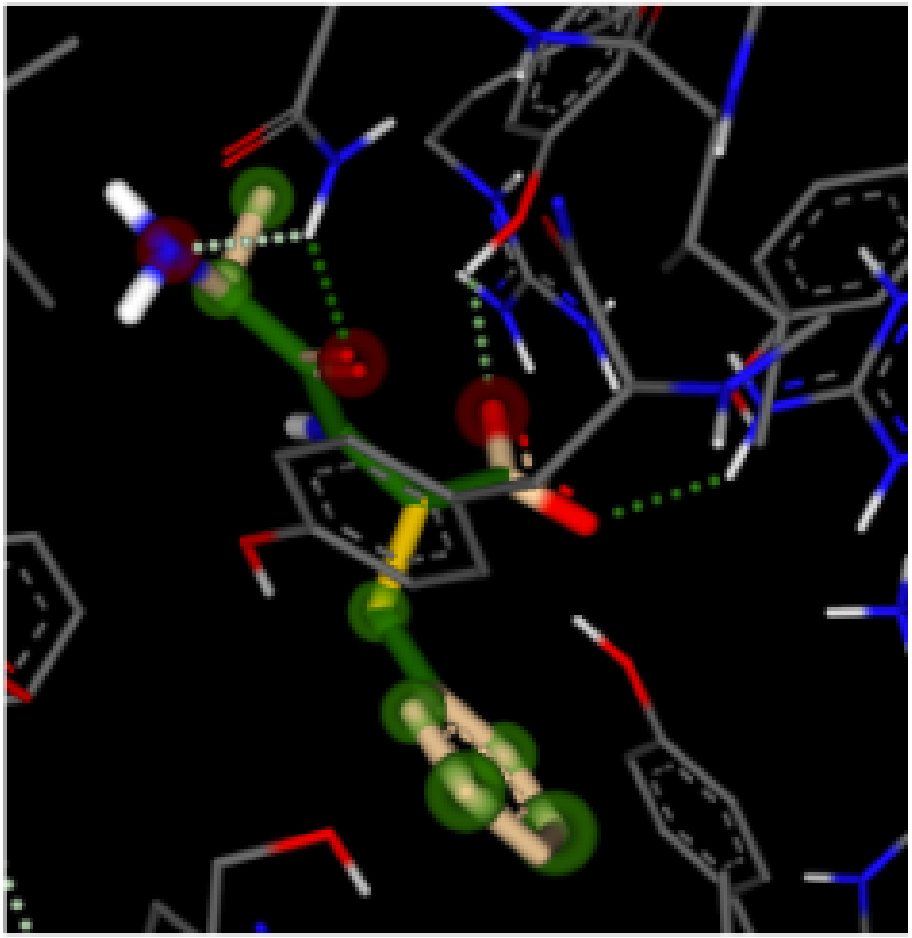

**Figure 4.** *Valtorcitabine docked to PepT1 transporter protein*

achieve very high oral bioavailabilities. Valcyclopropavir's LUMO location will allow for increased stability and effective parent drug release, and Valtorcitabine's polar electrostatic potentials around the valine group will allow for favorable PepT1 binding. Both prodrugs had stark improvements to their ADME properties, bond strength, stability/acid resistance, and binding affinities, enabling effective usage of the PepT1 oligopeptide transporter mechanism and esterase parent drug release mechanism in similar or improved ranges to Valacyclovir and Valganciclovir. Given their established antiviral potency in vitro against cytomegalovirus and hepatitis B virus, two viruses with highly limited oral treatment options, we believe it would be worthwhile to conduct future in vivo studies of Valtorcitabine and Valcyclopropavir. In doing so, we would hope to verify our prediction that their numerous favorable pharmacokinetic qualities will allow them to reach high oral bioavailability in humans and contribute to the sparse roster of oral antiviral medication.

## Acknowledgements

The author thanks Mr. Robert Gotwals for assistance with this work. Appreciation is also extended to the Burroughs Wellcome Fund and the North Carolina Science, Mathematics and Technology Center for their funding support for the North Carolina High School Computational Chemistry Server.

## References

[1] M. Markovic, M. Zur, I. Ragatsky, S. Cvijić, and A. Dahan, "BCS Class IV Oral Drugs and Absorption Windows: Regional-Dependent Intestinal Permeability of Furosemide," *Pharmaceutics*, vol. 12, no. 12, p. 1175, 2020, doi: 10.3390/pharmaceutics12121175.

[2] B. Vig and J. Rautio, "Amino Acid Prodrugs for Oral Delivery: Challenges and Opportunities," *Therapeutic Delivery*, vol. 2, no. 8, pp. 959–962, 2011, doi: 10.4155/tde.11.75.

[3] K. R. Beutner, "Valacyclovir: a review of its antiviral activity, pharmacokinetic properties, and clinical efficacy," *Antiviral Research*, vol. 28, no. 4, pp. 281–290, 1995, doi: 10.1016/0166-3542(95)00066-6.

[4] PubChem, "Ganciclovir." [Online]. Available: https://pubchem.ncbi.nlm.nih.gov/substance/46507294

[5] N. S. Umapathy, V. Ganapathy, and M. E. Ganapathy, "Transport of Amino Acid Esters and the Amino-Acid-Based Prodrug Valganciclovir by the Amino Acid Transporter ATB\textsuperscript{0,+}," *Pharmaceutical Research*, vol. 21, no. 7, pp. 1303–1310, 2004, doi: 10.1023/B:PHAM.0000033019.49737.28.

[6] G. J. Demmler-Harrison, "Congenital cytomegalovirus: Public health action towards awareness, prevention, and treatment," *Journal of Clinical Virology*, vol. 46, pp. S1–S5, 2009, doi: 10.1016/j.jcv.2009.10.007.

[7] J. Ahmad, S. Ikram, A. B. Hafeez, and S. Durdagi, "Physics-driven identification of clinically approved and investigation drugs against human neutrophil serine protease 4 (NSP4): A virtual drug repurposing study," *Journal of Molecular Graphics and Modelling*, vol. 101, p. 107744, 2020, doi: 10.1016/j.jmgm.2020.107744.

[8] Z. Wu *et al.*, "L-Valine Ester of Cyclopropavir: A New Antiviral Prodrug," *Antiviral Chemistry and Chemotherapy*, vol. 20, no. 1, pp. 37–46, 2009, doi: 10.3851/IMP782.

[9] R. G. Parr, S. R. Gadre, and L. J. Bartolotti, "Local density functional theory of atoms and molecules," *Proceedings of the National Academy of Sciences*, vol. 76, no. 6, pp. 2522–2526, 1979, doi: 10.1073/pnas.76.6.2522.

[10] M. J. Frisch *et al.*, "Gaussian}16 Revision C.01." 2016.

[11] "North Carolina High School Computational Chemistry Server." [Online]. Available: http://chemistry.ncssm.edu/

[12] F. R. B., J. C. Prasana, S. Muthu, and C. S. Abraham, "Molecular docking studies, charge transfer excitation and wave function analyses (ESP, ELF, LOL) on valacyclovir : A potential antiviral drug," *Computational Biology and Chemistry*, vol. 78, pp. 9–17, 2019, doi: 10.1016/j.compbiolchem.2018.11.014.

[13] J. Besnard *et al.*, "Automated design of ligands to polypharmacological profiles," *Nature*, vol. 492, no. 7428, pp. 215–220, 2012, doi: 10.1038/nature11691.

[14] L. Lai, Z. Xu, J. Zhou, K.-D. Lee, and G. L. Amidon, "Molecular Basis of Prodrug Activation by Human Valacyclovirase, an \alpha-Amino Acid Ester Hydrolase", *Journal of Biological Chemistry*, vol. 283, no. 14, pp. 9318–9327, 2008, doi: 10.1074/jbc.M709530200.

[15] J. L. Parker *et al.*, "Structural basis for antibiotic transport and inhibition in PepT2," *Nature Communications*, vol. 15, no. 1, p. 8755, 2024, doi: 10.1038/s41467-024-53096-6.

[16] Y. Ural-Blimke *et al.*, "Structure of Prototypic Peptide Transporter DtpA from \textit{E. coli} in Complex with Valganciclovir Provides Insights into Drug Binding of Human PepT1," *Journal of the American Chemical Society*, vol. 141, no. 6, pp. 2404–2412, 2019, doi: 10.1021/jacs.8b11343.

Open Access | https://doi.org/10.62329/xhfp5742

# Modeling Shifts in Reversible Chemical Reactions and Economic Markets

**Radhika Goel**[1]

[1]North Carolina School of Science and Mathematics

**Morganton Scientific**

*North Carolina School of Science and Mathematics*

Journal of Student STEM Research

## Abstract

The purpose of this paper was to investigate how economic principles of supply and demand can model reversible reaction's equilibrium, using computational approaches. This study primarily utilized the WebMO server, Gaussian software, and Mathematica-based modeling to simulate two key reversible reactions: $NH_3 + H_2O \rightleftharpoons NH_4^+ + OH^-$ and $2NO_2 \rightleftharpoons N_2O_4$. By adjusting different components of these reactions, such as their reactant and product concentrations, temperatures, and perturbations, the behavior of each system was cross-applied to analyze effects on economic markets. The results suggest that increases in reactant concentrations resulted in proportional increases in product formation, which mirror market responses to supply boosts in a given situation. Additionally, perturbations, such as sudden changes in reactant concentrations, caused the system to shift dynamically and restored balance within the chemistry and economics-based models. Ultimately, integrating economic and chemical models through interdisciplinary pathways allowed for the opportunity to further refine the computational analogies through more complex reactions.

**Keywords** Le Chatelier's Principle, Reversible Reactions, Perturbations, Price Elasticity, Supply-Chain Shocks

## 1. Introduction

Establishing an equilibrium in various disciplines, such as chemistry and economics, is important to create a balanced system. In chemistry, equilibrium refers to a reversible reaction where the products react to form the original reactants at equal rates [1]. Essentially, this means that the rate of the forward reaction equals the rate of the reverse reaction. The equilibrium constant, $K$, describes the balance between reactants and products at equilibrium. This constant is extremely important when determining how a system at equilibrium will adjust if it is disturbed, disequilibrium. Additionally, the Gibbs free energy of a reaction is imperative in accurately determining whether a system is at equilibrium. Gibbs free energy measures the available energy in a system (or the change in energy of a system) using enthalpy, entropy, and temperature. Gibbs free energy helps determine whether a reaction will proceed spontaneously under the given conditions [2].

Another key principle this paper hinges on is Le Chatelier's principle. Le Chatelier's principle is incredibly important in predicting how a system will respond and restore equilibrium. Essentially, Le Chatelier's principle states that if an external change affects the equilibrium, the position of equilibrium must shift to counteract and re-establish an equilibrium [3]. The products and reactants have reached equilibrium where the concentration stays relatively constant Figure 1. Although the minuscule shifts between products to reactants are not visible in most graphs, reversible reactions' dynamic nature assumes the products and reactants are always reacting with each other to re-establish equilibrium Figure 1. When the equilibrium shifts and responds to the stress, it must shift in the direction that will minimize the stress applied to a system. Different stresses, such

**Published** Jun 27, 2024

**Correspondence to**
Radhika Goel
goel25r@ncssm.edu

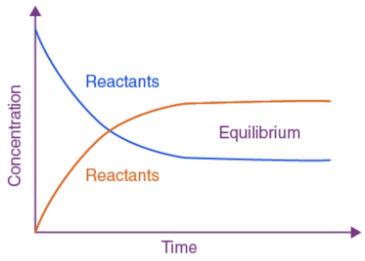


**Figure 1**. *Chemical Equilibrium*

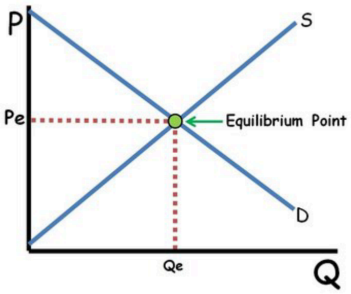


**Figure 2**. *Supply and Demand Graph*

as shifts in temperature, concentration, or pressure, may force an equilibrium to shift either in the opposite direction, to offset the change, or in the same direction, to reduce the added stress. Ultimately, Le Chatelier's principle explains how a reaction will dynamically adjust to external changes.

In economics, equilibrium is also established in a similar manner. Within a simplified market of supply and demand, the price of a good and its quantity must be balanced when an exchange takes place.

The intersection of an upward-sloping supply curve and a downward-sloping demand curve is called the equilibrium, which is a point specified at a certain price and quantity Figure 2. The supply and demand curves can be shifted due to a multitude of factors [4]. Supply can shift due to a change in the price of resources, the number of producers, improvements in technology, fluctuations in taxes or subsidies, and influences on consumer expectations. On the other hand, demand can shift due to differences in tastes and preferences, the number of consumers, changes in the price of related goods, fluctuations in income, and influences on consumers' future expectations.

Similar to chemistry, equilibrium in economics follows a dynamic nature, constantly adjusting to different external factors such as resource costs, subsidies, and government regulations [5]. The price of a certain good is what drives markets towards balance, similar to how Gibbs free energy establishes equilibrium in chemical systems.

Although the connections between chemistry and economics may not be immediately apparent, this paper aims to research possible and existing parallels at a deeper level. Both, chemistry and economics, involve systems that seek balance through opposing forces. For instance, in a chemical reaction, the concentrations of reactants and products adjust based on external factors to re-establish equilibrium. On the other hand, in an economic market, prices adjust to shifts in supply or demand to efficiently reallocate resources.

To further analyze overlapping trends between chemistry and economics, a few key assumptions were made. First, the reactants are compared to the supply curve. In a practical chemistry context, this means that an increase in reactants pushes the reaction towards producing more products. In a practical economics context, this means that increasing the supply pushes the market towards lowering the equilibrium price. Second, in a similar manner, the products are compared to the demand curve. Third, the equilibrium constant, $K$, is compared to price elasticity of demand. Price elasticity measures the change in the demand for a product as a result of a change in its price [5].

If the demand for a product is elastic, a small change in price leads to a significant change in quantity demanded. Conversely, if the demand for a product is inelastic, a change in price leads to a small change in quantity demanded [5]. Essentially, the elasticity of demand measures the sensitivity or responsiveness of the quantity demanded to changes in a product's price. This economic principle corresponds with the equilibrium constant because they both compare smaller changes to evaluate larger systems. Finally, perturbations in chemical systems can be compared to shocks in economic conditions [6]. As explained previously, external influences can shift the balance and automatically adjust a system. In context, altering temperatures in a chemical system will be compared to the effects of increasing tax rates in a market.

These four assumptions set up the basis of this paper's purpose, which is to answer the following question: How can shifts in reactant or product concentration (in a reversible reaction) be modeled similarly to market supply and demand shifts?

## 2. Computational Approach

To maximize the result's validity, two unique models were created for two specific reactions. The first reaction is the following acid-base reaction: $\mathrm{NH_3 + H_2O \rightleftharpoons NH_4^+ + OH^-}$. This reversible reaction's properties accurately align with the concept of market equilibrium in economics. This reaction sets up the model's key components so that they can be cross-applied to additional reactions. The second reaction is the dimerization of nitrogen dioxide: $\mathrm{2NO_2 \rightleftharpoons N_2O_4}$. This was chosen because the equilibrium constant $(K)$ of this reaction is solely dependent on the concentrations of the reactants and has a corresponding influence on economic equilibrium calculations [7].

These two reactions were run through a WebMO [8], [9], a computational chemistry platform that specializes in outputting molecular properties using quantum chemistry software, such as MOPAC and Gaussian.

In order for these reactions to be accurately run in WebMO, a "Geometry Optimization" job must be run. This enables WebMO to find the most stable arrangement of atoms in a given molecule, which means minimizing the molecule's total energy. To run this job, in the WebMO Job Manager page, a "New Job" is created. Then, the molecule is built using the "Build" tool, and the geometry is optimized using the Gaussian computational engine. Gaussian [10] was used for all the molecules chosen because this paper only focuses on smaller molecules and Gaussian is more suitable for precisely calculating smaller molecules' geometries and energetics. Then, the B3LYP theory is chosen (under the DFT umbrella) with a basis set of 6-31G(d) for all molecules except for $\mathrm{OH^-}$ and $\mathrm{NH_4^+}$. This is because $\mathrm{OH^-}$ and $\mathrm{NH_4^+}$ have a more complex atomic arrangement, so an accurate basis set of 6-311+G(2d,p) will produce more precise results. A total of six "Geometry Optimization" jobs were run.

Because $\mathrm{NH_3 + H_2O \rightleftharpoons NH_4^+ + OH^-}$ is a water based reaction, a solvent model calculation is included. This allows the calculation to simulate the effect of water as a solvent, which allows WebMO to calculate the energetics of the reaction system more accurately.

To calculate the actual data in each of these molecules, a “Vibrational Frequency” calculation is run for each of the six molecules. This allows for thermodynamic properties to be calculated for each molecule, which provide further insight into a molecule’s properties. Specifically, the Gibbs Free Energy and Enthalpy values are used for each molecule to create a reaction-specific model.

After all the data was collected, two models were built in Wolfram Mathematica. Mathematica is a powerful computing software that is most commonly used to solve and model complex problems from various disciplines. For the purposes of this paper, Mathematica was used to create a model that demonstrates chemical shifts in economic contexts.

In a new Mathematica notebook, the gas constant, the Gibbs free energy constant, and the Hartrees to Joules per mole conversion are established at the beginning of each model. It is also important to note that most of the code for both models is the same, except for the specific data (in constants) different between both reactions. The gas constant, in Joules per mole per Kelvin, was defined, and will be used in thermodynamic calculations. The conversion from Hartrees to Joules is also established to keep all calculations in the same unit. Then, the Gibbs free energy for each molecule is calculated by converting the Gibbs free energy from Hartrees to Joules per mole. To calculate the change in Gibbs free energy, based on the changes in temperature, a function for each molecule is defined. Then, to convert the change Gibbs free energy to the equilibrium constant $(K)$, “theDeltaGtoK” function is created that expresses the following equation: $K = e^{-\frac{\Delta G}{RT}}$.

Next, the “RateConstants” function is created to calculate the forward rate constant, $k_f$, and the reverse rate constant, $k_r$, for a reaction based on the equilibrium constant, $K$. This sets up a formula for the differential equations that will be calculated. Then, to establish a reaction’s equilibrium, the “ReactionEquilibrium” function is defined, which models the time evolution of the reactants and products. This function also initializes a few local variables for the differentials equations. The inputs for the differential equation are written concisely (before their calculation) with the “dReactants” and “dProducts” variables, which define the rate of change for the reactants and products, respectively. Finally, a system of differential equations is created, where r[t] and p[t] represent the concentrations of the reactants and products at a specific time, t.

After establishing the basic chemistry, the model focuses on the economics approach. First, an “EconomicDynamics” function is defined, which models an economic market’s supply and demand dynamics in context. The local variables, including “Supply”, “Demand”, “Elasticity”, and “EquilibriumPrice” are also initialized. Afterwards, each of the four assumptions are coded into the model. The equation for elasticity is scaled by a factor of 10 to see its influence on the model when compared with the reversible reactions.

Next, the interactive model is created with the “Manipulate” command, which initializes the different plots that will be created and the variables required to create them. Then, the equilibrium constant is calculated based on the current temperature, defined as “Temp”, using the previously coded function “DeltaGtoK”.

Afterwards, the perturbations that would influence an economic market in a chemistry context are established with the current concentrations of the reactants and products and the calculated rate constants. In the way that the chemistry results were portrayed, the economic dynamics with perturbations included are also calculated with the “EconomicDynamics” function.

Then, a plot for the concentration of reactants and products over time, called “ChemPlot”, is generated based off of the current products and reactants calculated. Similarly, a plot

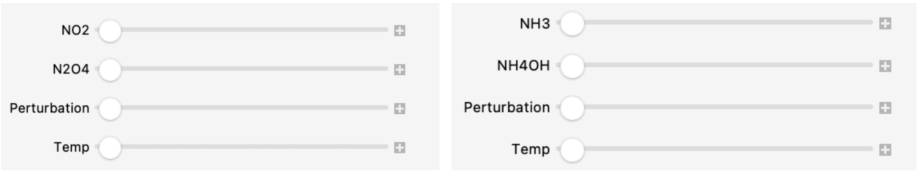


**Figure 3**. *Sliders for Chemistry Aspects in Both Interactive Models*

for the supply and demand curves, as a function of price, is generated based off of the economic results. Finally, different ranges of values are established for the reactants, products, perturbations, and temperature (in Kelvin).

Ultimately, the two models created accurately portray the dynamic equilibrium between $NH_3 + H_2O \rightleftharpoons NH_4^+ + OH^-$ and $2NO_2 \rightleftharpoons N_2O_4$ and compare them to their associated economic-based supply and demand system. Because of the equilibrium constant, the chemical and economic dynamics are modeled in a manner that creates an interactive simulation. Using the "Manipulate" command, it is possible to change the concentrations, perturbations, or temperature each reaction takes place at, and see the respective influence on the supply and demand curves.

## 3. Results

At its pre-condition representation, the model for $NH_3 + H_2O \rightleftharpoons NH_4^+ + OH^-$ and for $2NO_2 \rightleftharpoons N_2O_4$ outputs a simple economics graph. First, the sliders representing the model in a chemistry context are demonstrated below Figure 3. Second, the basic chemistry model demonstrates the reactants' concentration, products' concentration, and equilibrium point Figure 4. Third, the basic economics model with a supply curve, demand curve, and equilibrium point (if an intersection occurs in the defined range) is shown.

Essentially, base_models shows how the model would output an economic graph with quantities of 0 for the reactants and products. The economic graph measures prices vs. quantity, which will be the same format followed for all additional economic graphs in this paper.

To explain the validity of the results, different economic scenarios will also be discussed and explained alongside the chemistry systems. First, when reactant $NO_2$ was introduced into the system with no initial products, over time, $NO_2$ began converting into $N_2O_4$. This can be seen in Figure 5, specifically at the chemical equilibrium. Although the forward reaction seemed to dominate the reaction initially, as the system approached equilibrium,

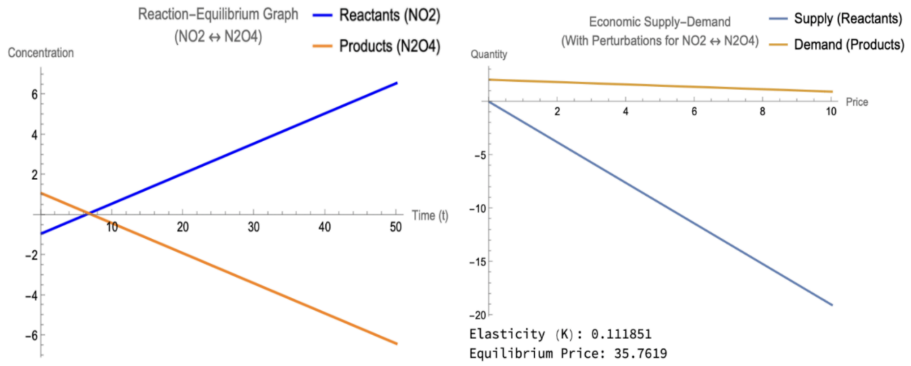


**Figure 4**. *Base Chemistry and Economics Models*

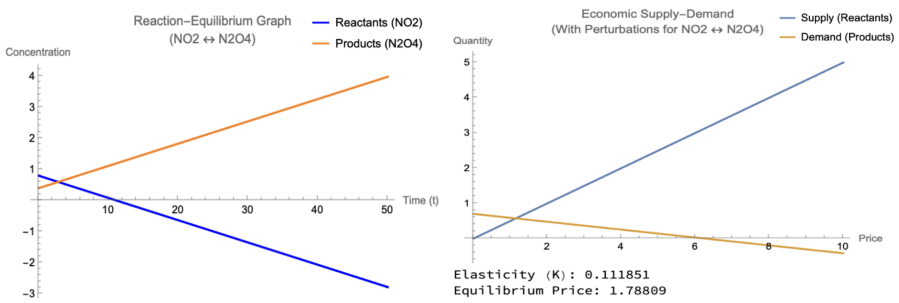


**Figure 5**. *Reactants Introduced in Chemistry and Economics Models*

the rate of the reverse reaction also increased, which stabilized the concentrations. From an economics standpoint, these results correspond to a market with a sudden influx of supply. The supply curve shifted to the right substantially, which lead to a decrease in the equilibrium price in the short-term. In the long-term, the market adjusted as the demand rose to counteract the supply influx.

Next, with the $NO_2$ reactant present in the system, a negative perturbation was applied to the concentration of $NO_2$ Figure 6. This reduced the available reactants mid-reaction. The $NO_2$ concentrations dropped sharply and the forward reaction slowed. This difference can be seen between the equilibrium constant, $K$, in the addition of reactants to the addition of a negative perturbation. In an economic context, this market can represent the impacts of a supply chain shock. A sudden decrease in the supply curve may have been caused by external factors, such as resource shortages or logical disruptions. The leftward shift of the supply curve increased the equilibrium price in the short-term, which would decrease the quantity demanded at the specific equilibrium point. However, the demand curve itself remains unaffected, which shows that the elasticity of this market is relatively inelastic, as consumer interest continues despite a lower supply and higher market price.

In Figure 7, the products, $N_2O_4$, were artificially introduced mid-reaction to create a response in the economic market. This demonstrates the chemical system's response, where $N_2O_4$ concentrations significantly increased temporarily. This caused the reverse reaction to accelerate, as seen with the $K$ value, and converted some of the $N_2O_4$ back into $NO_2$. From an economic standpoint, this situation represents a substantial surge in demand. In the real world, this can be seen during the holiday shopping season, where consumers significantly increase their spending. This resulted in the demand curve shifting to the right, which increased the equilibrium price and simultaneously simulated supply-side responses.

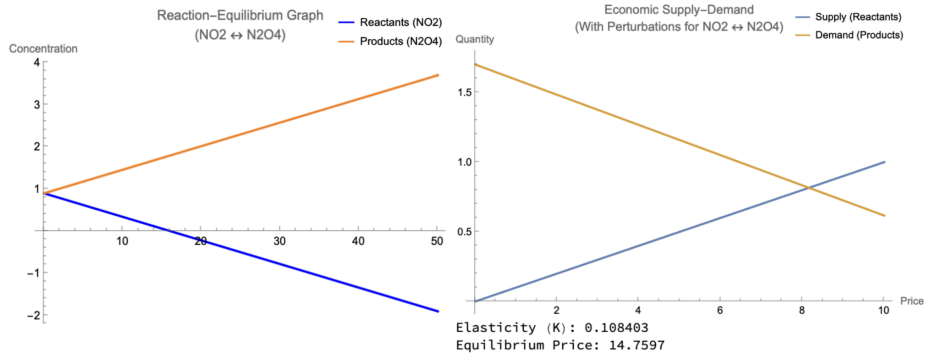


**Figure 6**. *Reactants and Negative Perturbations on Chemistry and Economics Models*

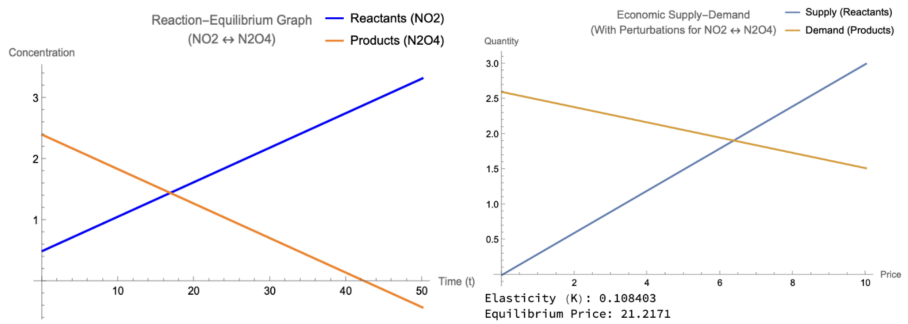


**Figure 7**. *Reactants, Products, & Negative Perturbation on Chemistry and Economics Models*

Finally, Figure 8 demonstrates that although equal concentrations of $N_2O_4$ and $NO_2$ were inputted into the model, these were not remotely close to the correct concentrations for this system to attain the equilibrium. Within this system, the equilibrium constant indicates that product formation is incredibly limited because the reactants were not given substantial concentrations or time frames to convert into products. However, in an economic context, a clear equilibrium point exists, with the demand curve following more elastic properties than the supply curve Figure 8. This means that the supply curve continues to decrease as resources be used and eventually deplete; contrastingly, the rising demand curve reflects a continuous increase in product consumption. Specifically, the low elasticity and relatively high equilibrium price demonstrate a constrained market that functions with a high demand and relatively limited adaptability. In the real world, this could be seen where $NO_2$ would represent the supply of a raw material, while $N_2O_4$ would represent the demand of a processed good. This model's economic implications are unique, as they demonstrate that due to the equilibrium price's elevated level, the scarcity of raw materials and increasing production costs are directly seen.

## 4. Discussion

The results of this study demonstrate how the fundamental principles of chemical equilibrium and economic supply-demand systems can intersect to model dynamic shifts. Their shifts' implications were seen in both physical and market environments, adjusting to perturbations and imbalance between reactants and products. When the system began without any products, $NO_2$ concentrations steadily decreased while $N_2O_4$ concentrations rose until the equilibrium was reached. This dynamic mirrors real-world markets, as portrayed through the economic markets in the results section. When raw materials are consumed to produce goods, the supply and demand forces successfully stabilize process over time. Additionally, lower elasticities coinciding with higher equilibrium prices tend to occur in resource-dependent markets where the supply is limited, as seen in Figure 7.

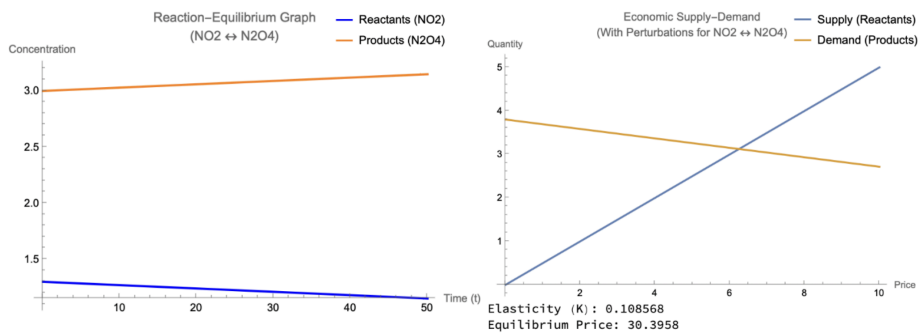


**Figure 8**. *Artificial Equilibrium Compared Between Chemical and Economic Systems*

Beyond the changes in reactants and products, the models created reveal the significant impact of external perturbations over time. When the reactant concentration was significantly increased (artificially), the reaction shifted to favor the formation of the products, as explained through Le Chatelier's principle. Similarly, in an economics scenario, this can be compared to a surge in resource availability, where increases and supply can decrease the equilibrium prices. When the opposite occurred in Figure 7, products were artificially manipulated instead of reactants, the system rebalanced to restore equilibrium. This scenario may resemble how excess goods in a market lower demand and alter unique equilibrium conditions.

For future research, extending the model to include temperature and pressure effects on chemical equilibrium may provide deeper insights into additional thermodynamic factors influence on market dynamics. For instance, by directly incorporating temperature as a variable, larger-scale external shocks, such as global events or policy changes, could be simulated to alter certain market conditions. Additionally, an improved model could include real-world data that would adjust for factors such as fluctuating raw material costs or supply chain disruptions, which can enhance the practicality of the model. Lastly, from a chemistry standpoint, more complex reversible reactions may be used to improve certain specifics in the chemistry-economics analogy.

## 5. Significance and Implications

By nature, the economics and chemistry fields revolve around systems that are constantly fluctuating. Through cross-discipline exploration, uniting these two fields further highlights the similarities and patterns that can be found in seemingly "random" changes. Many real-world challenges with multifaceted backgrounds align with this background and require a solution that surpasses disciplinary boundaries. For instance, in fields such as environmental economics, a pure economic lens falls short in understanding the balance that must be achieved between natural resources and economic demand—a conclusion that can easily be reached through the integration of chemistry and economics. While chemistry plays a crucial role in managing the use and conservation of resources, economics proposes strategies to allocate these resources efficiently. By combining these fields, researchers can pave the way towards sustainable economic practices, spearheading better strategies for resource management.

Beyond environmental economics, overlaps between economics and chemistry can be seen in upcoming fields, such as energy economics and pharmaceutical industries. By analyzing changes in certain chemical processes —such as carbon emissions— and their influence on economic markets, insights regarding climate change policy and sustainability strategies may also be explored. From an economics lens, because scarcity drives innovation in goods and services, scientists can further contextualize the impacts of chemical innovation on various economic sectors. This may lead to breakthroughs in energy sources and methods of chemical production, creating efficient technologies to maintain and sustain energy-dependent industries.

The heightened focus on the field of green chemistry also holds great promise for economic modeling. Understanding the economic impacts of adopting sustainable technologies may promote and encourage faster acceptance and implementation of sustainable development, such as renewable energy resources. Ultimately, by prioritizing both chemistry and economics perspectives, scientists can drive the transition towards environmentally responsible and economically friendly solutions.

## 6. Conclusion

Ultimately, the results of this paper strengthen the interconnectedness between chemical and economic systems. As seen in the models generated, equilibrium, elasticity, and stability have the ability to describe and predict molecular behavior and market dynamics. The low elasticity in various scenarios created in the $2NO_2 \rightleftharpoons N_2O_4$ reaction implies the limited responsiveness to changes in both, chemical models and economic models. As seen in larger industries with higher fixed costs or inflexible supply chains, adapting to attain equilibrium from all viewpoints may prove difficult at certain times. Regardless, this study has explored how abstract science concepts can apply to real-world scenarios, and opens doors for additional interdisciplinary approaches to further strengthen the relation between modeling economic systems using chemical analogies.

The author thanks Mr. Robert Gotwals for assistance with this work. Appreciation is also extended to the Burroughs Wellcome Fund and the North Carolina Science, Mathematics and Technology Center for their funding support for the North Carolina High School Computational Chemistry Server.

## References

[1] Z. Shaymardanov *et al.*, "Approach for the Description of Chemical Equilibrium Shifts in the Systems with Free and Connected Chemical Reactions," *Processes*, vol. 10, no. 12, p. 2493, 2022, doi: 10.3390/pr10122493.

[2] J. J. Middelburg, "The Gibbs Free Energy," in *Thermodynamics and Equilibria in Earth System Sciences: An Introduction*, Springer Nature Switzerland, 2024, pp. 35–46. doi: 10.1007/978-3-031-53407-2_4.

[3] M. Peris, "Understanding Le Châtelier's principle fundamentals: five key questions," *Chemistry Teacher International*, vol. 4, no. 3, pp. 203–205, 2021, doi: 10.1515/cti-2020-0030.

[4] D. F. Perkis, "The Science of Supply and Demand," 2021, [Online]. Available: https://www.stlouisfed.org/publications/page-one-economics/2021/03/01/the-science-of-supply-and-demand

[5] S. Jordan-Wood, "Price Elasticity (Demand) Explained," 2024, [Online]. Available: https://www.stlouisfed.org/open-vault/2024/june/price-elasticity-demand-explained

[6] B. F. Farrell and P. J. Ioannou, "Perturbation dynamics in atmospheric chemistry," *Journal of Geophysical Research: Atmospheres*, vol. 105, no. D7, pp. 9303–9320, 2000, doi: 10.1029/1999jd901021.

[7] M. F. Romero and A. J. Rossano, "Acid-Base Basics," *Seminars in Nephrology*, vol. 39, no. 4, pp. 316–327, 2019, doi: 10.1016/j.semnephrol.2019.04.002.

[8] J. P. W. Schmidt, "WebMo Pro, version 7.0," 2007, [Online]. Available: http://www.webmo.net/

[9] "The North Carolina High School Computational Chemistry Server," 2024, [Online]. Available: http://chemistry.ncssm.edu/

[10] "Gaussian," 2024, [Online]. Available: http://www.gaussian.com/

Open Access | https://doi.org/10.62329/acjn2734

**Morganton Scientific**

*North Carolina School of Science and Mathematics*

Journal of Student STEM Research

# Evaluating the Effects of Lactic Acid Fermented Foods on Type 2 Diabetes Mellitus using Bombyx Mori Silkworms

**Vivek Gottumukkala**[1]

[1]NCSSM

## Abstract

Type 2 diabetes mellitus (T2D) continues to rise globally, highlighting an urgent need for effective and accessible interventions. In this study, *Bombyx mori* silkworms were employed as a novel, cost-effective model to evaluate the impact of lactic acid fermented foods on hyperglycemia. Thirty silkworms were randomly divided into three groups: Group 1 (control diet), Group 2 (10% glucose diet), and Group 3 (10% glucose diet plus probiotic supplementation). Following a period of induced hyperglycemia in Groups 2 and 3, hemolymph samples were collected and assessed for relative glucose levels using a colorimetric quantitation assay.

Results indicated that while both Groups 2 and 3 exhibited higher hemolymph glucose levels than controls, silkworms receiving the probiotic supplement (Group 3) generally showed lower glucose concentrations compared to those fed only the high-glucose diet (Group 2). These observations, although modest, support the hypothesis that lactic acid bacteria (LAB) in fermented foods can reduce hyperglycemia in silkworms, likely through mechanisms such as improved insulin sensitivity or enhanced metabolic regulation.

Despite the promising findings, a key limitation of this pilot study was the small sample size, which restricted statistical power. Future research should include larger experimental groups, investigate strain-specific probiotic effects, and explore mechanistic pathways such as insulin receptor gene expression and gut microbiota shifts. Nonetheless, this work highlights the value of *Bombyx mori* as a physiologically relevant model for T2D and suggests that LAB-rich fermented foods may offer an accessible dietary strategy to help manage hyperglycemia.

**Keywords** Type 2 Diabetes Mellitus (T2D), Lactic Acid, Hyperglycemia, Glucose, Silkworms

**Published** Jun 27, 2024

**Correspondence to**
Vivek Gottumukkala
gottumukkala25v@ncssm.edu



## 1. Introduction

Diabetes is a global health crisis, affecting an estimated 463 million people worldwide as of 2019, with projections suggesting this number will rise to 700 million by 2045 ([1]). The disease not only imposes a significant burden on individuals but also on healthcare systems and economies. In 2019, diabetes-related health expenditure reached $760 billion globally ([1]). The most common form of diabetes, Type 2 diabetes (T2D), is characterized by insulin resistance and chronic hyperglycemia. As the prevalence of T2D continues to rise, there is an urgent need for effective, accessible, and affordable treatment options.

Current research indicates that the development of T2D involves a complex interplay of genetic, environmental, and lifestyle factors. Insulin resistance, a potential indication of T2D, occurs when cells in the body become less responsive to insulin, leading to elevated blood glucose levels. Persistent hyperglycemia over time can lead to severe complications, including cardiovascular disease, kidney failure, and nerve damage ([2]). The urgent need

for new therapeutic strategies drives ongoing research into alternative treatments for T2D.

*Bombyx mori* silkworms have recently emerged as a promising model organism for studying T2D due to their unique physiological characteristics. Silkworm larvae progress through multiple instars, which are the developmental larval stages between molts, during which their metabolism and growth rates fluctuate significantly. Their prolegs, the fleshy, stub-like appendages on their abdomen, play a role in locomotion and feeding behaviors, which may influence glucose metabolism. These silkworms can develop hyperglycemia within 1-2 days when fed a high-glucose diet and exhibit insulin sensitivity similar to that of mammals (J. Hou *et al.* [3]). This makes them an attractive model for large-scale studies due to their cost-effectiveness and ease of rearing.

Previous studies have demonstrated the potential of certain strains of lactic acid bacteria (LAB) in managing blood glucose levels. For instance, *Lactococcus lactis* has been shown to suppress glucose levels in silkworms, exhibiting immunoreactive properties that may contribute to its therapeutic effects (Y. Matsumoto, M. Ishii, and K. Sekimizu [4]). Moreover, LAB strains from fermented foods, such as those isolated from dairy products and vegetables, have been highlighted for their probiotic potential, which could be leveraged in managing T2D (Y. Ismail, C. Yulvizar, and B. Mazhitov [5]; P. Sethi, R. Maharana, S. Ameeruddin, and S. Das [6]; S.-Y. Yang and K.-S. Yoon [7]).

Fermented foods, which are rich in LAB, have long been recognized for their health benefits. For example, kefir and Greek yogurt contain LAB strains that enhance gut health and may influence glucose metabolism (Y. Ismail, C. Yulvizar, and B. Mazhitov [5]; S.-Y. Yang and K.-S. Yoon [7]). Similarly, fermented beverages like kombucha are being explored for their ability to enhance biological activities due to their LAB content (N. K. Nguyen, N. T. N. Dong, H. T. Nguyen, and P. H. Le [8]). These findings suggest that the probiotic potential of LAB strains in fermented foods could play a role in T2D management.

This study aims to investigate the effects of LAB strains from various fermented foods on blood glucose levels in *Bombyx mori* silkworms, with the hypothesis that some LAB strains will significantly reduce hemolymph glucose levels compared to controls and other strains.

## 2. Methods

### 2.0.1. *Silkworm Preparation:*

To investigate the effect LAB strains have on hemolymph glucose levels, a batch of 30 small *Bombyx mori* silkworms was purchased from Coastal Silkworms. Upon arrival, these silkworms were randomly sorted into three experimental groups (Groups 1, 2, and 3) without discriminating between size and length. Each group was housed in a separate container and maintained under identical conditions to ensure consistency. These containers and group assignments were used throughout the experiment.

### 2.0.2. *Habitat Preparation:*

To maintain a controlled environment conducive to optimal silkworm growth and development, a specialized habitat was prepared using a HovaBator incubator. The silkworms were placed in the incubator at 26–28°C and 75–85% relative humidity. These conditions were kept constant until silkworms reached the 5th instar, at which point the temperature was decreased to 16–18°C and relative humidity to 65–75% to prolong the 5th

instar period. A digital thermometer and hygrometer were placed inside the incubator (under the transparent lid) to continuously monitor temperature and humidity levels.

#### 2.0.3. *Diet Preparation:*

All three groups were initially reared on the same normal, artificial “Silkworm Chow” mulberry diet (Carolina Biological), with fresh food provided every other day or when moisture loss became excessive. After 1–2 weeks, only Groups 2 and 3 were switched to a 10% w/v glucose mulberry diet, consisting of 90% normal diet mixed with 10% dextrose, and fed this for 24–30 hours to induce hyperglycemia. Following this, only Group 3 was given an additional diet containing 9 mL of probiotic supplementation mixed into the original glucose diet for another 24–30 hours, after which the trials were conducted.

#### 2.0.4. *Probiotic Dilutions:*

For the probiotic supplement, Spring Valley’s Extra Strength Probiotic Dietary Supplement was used. 1 capsule was opened and its contents were poured and mixed into 1 mL of molecular biology grade water to create a 1010 CFU stock solution which was centrifuged at 6000 rpm for 3 minutes. A 1:10 serial dilution was performed to create additional concentrations of 109, 108, 107, and 106 CFU by taking 1 mL of the previous dilution mixed into 9 mL of molecular biology grade water. This study proceeded to only use the 108 CFU solution as the probiotic treatment, as it had a suitable clarity that was not too transparent or too opaque, and was administered on the same day all the dilutions were made.

#### 2.0.5. *Weight Assay:*

To ensure consistency in size and health, only silkworms weighing at least 0.9 g were selected for trials. Silkworms under this threshold were considered to be underfed or otherwise suboptimal, which could compromise the accuracy of the data. No maximum weight limit was established, as the focus was on excluding individuals that appeared to be growing poorly. Each silkworm was weighed individually on an analytical balance every day to monitor growth and confirm normal feeding behavior.

#### 2.0.6. *Hemolymph Dilutions:*

Six different 5th instar silkworms were selected: two from Group 1 (control diet), two from Group 2 (glucose diet), and two from Group 3 (glucose + probiotic diet). To collect hemolymph, a small hole was created under the first proleg, and gentle pressure was applied to allow hemolymph to flow out. Exactly 4 $\mu$L of hemolymph was collected from each worm using a micropipette.

Each original 4 $\mu$L sample was then diluted in a 1:5 ratio by mixing it with 16 $\mu$L of assay buffer. From this dilution, 4 $\mu$L was taken and mixed with another 16 $\mu$L of assay buffer to create the next dilution. Repeating this process allowed the creation of sequential dilutions at 1/5, 1/25, 1/125, and 1/625 for every hemolymph sample collected.

### *2.1. Glucose Quantitation Assay*

#### 2.1.1. *Kit and Stock Preparation:*

Relative glucose concentrations in hemolymph were measured using AAT Bioquest’s Amplite Colorimetric Glucose Quantitation Kit. Seven glucose standards (GS1 – GS7) were prepared via a 1:2 serial dilution of a 100 $\mu$M stock, producing 50, 25, 12.5, 6.3, 3.1, and 1.6 $\mu$M standards. All kit stock solutions were prepared according to the manufacturer’s instructions, then divided into 20 aliquots each to reduce freeze-thaw cycles and stored at –20°C when not in use. Working solution was freshly prepared on the day of testing.

#### 2.1.2. *Microplate Layout:*

A clear-bottom, 96-well microplate (12 columns × 8 rows) was used:

- Columns 1–2: Glucose standards (and blank) in duplicate.
- Columns 3–4: Hemolymph samples from two Group 1 silkworms.
- Columns 5–6: Hemolymph samples from two Group 2 silkworms.
- Columns 7–8: Hemolymph samples from two Group 3 silkworms.

#### 2.1.3. *Standard Curve Wells:*

- Wells A1–A2 served as blank controls (50 $\mu$L assay buffer + 50 $\mu$L working solution).
- Wells B1–H2 contained 50 $\mu$L of the appropriate glucose standard plus 50 $\mu$L working solution (in duplicate, down the columns).

#### 2.1.4. *Hemolymph Sample Wells:*

For each diet group, rows A–D contained 45 $\mu$L assay buffer plus 5 $\mu$L of hemolymph dilution (1/5, 1/25, 1/125, or 1/625), topped off with 50 $\mu$L working solution (total 100 $\mu$L). Rows E–H contained 95 $\mu$L assay buffer plus 5 $\mu$L of the same hemolymph dilutions but no working solution; this helped account for any cloudiness or background absorbance caused by proteins, oxidation, or other sample components.

#### 2.1.5. *Assay Protocols:*

After loading all wells, the microplate was incubated at 37°C in three 10-minute intervals (10, 20, and 30 minutes). At each time point, the plate was transferred to a microplate reader, and absorbance was measured at 570 nm. Data from blank wells and standards were used to create a standard curve for determining relative glucose concentrations in each hemolymph sample.

## 3. Results

#### 3.0.1. *Glucose Quantitative Assay:*

For each of the 10 minute intervals, using the absorbance data from columns 1 and 2, the values in each row were averaged and the blank standard in row A was subtracted out from the standards in the remaining rows. Using these new values, a standard curve was created with the glucose standards and regression line plotted, as well as the regression line equation.

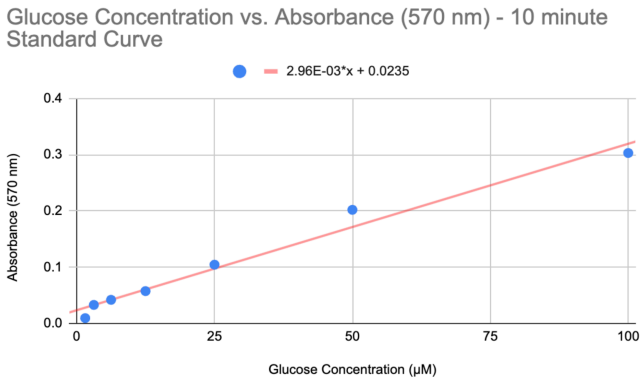


**Figure 1**. *Standard Curve of Absorbances of Glucose Standards after 10 minutes of incubation at 37°C.*

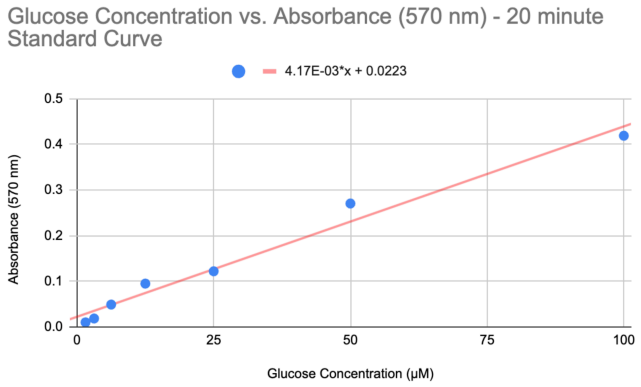


**Figure 2.** *Standard Curve of Absorbances of Glucose Standards after 20 minutes of incubation at 37°C.*

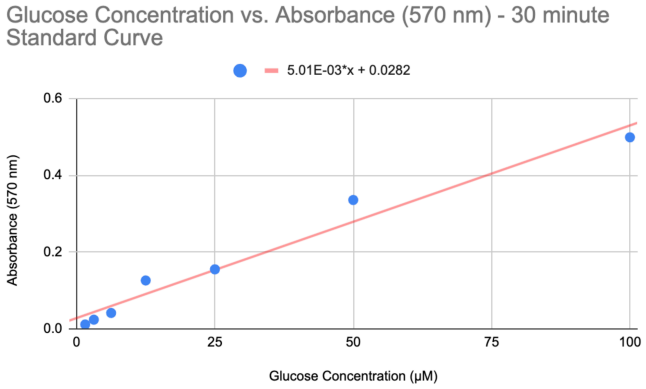


**Figure 3.** *Standard Curve of Absorbances of Glucose Standards after 30 minutes of incubation at 37°C.*

The same was done with the test sample columns, where the blanks were subtracted, the 2 replicates for each group were averaged, and absorbance values were converted into the "relative" glucose concentration values, which are not the same as the absolute glucose concentration values. Below are the concentration and absorbance graphs for each dilution from each 10 minute interval of incubation:

Below are the raw data from all three time intervals, which served as the basis for data processing and the calculation of absorbance and glucose concentrations:

## 4. Discussion

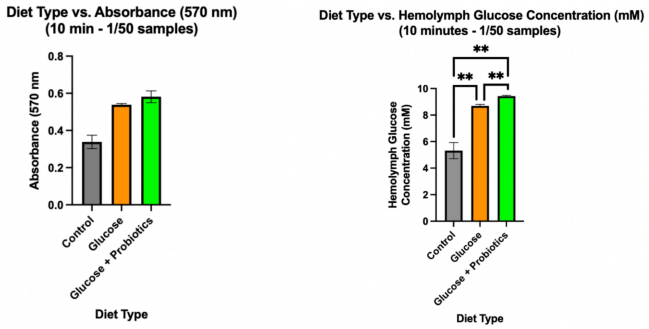


**Figure 4.** *Absorbance and Glucose Concentration Data for the 1/50 dilution samples incubated for 10 minutes. In both graphs, the values for the Group 2 and Group 3 worms are higher than the control, confirming that glucose concentration increased after having a diet that consisted of glucose. Very slight statistical difference between Group 2 and Group 3, if any.*

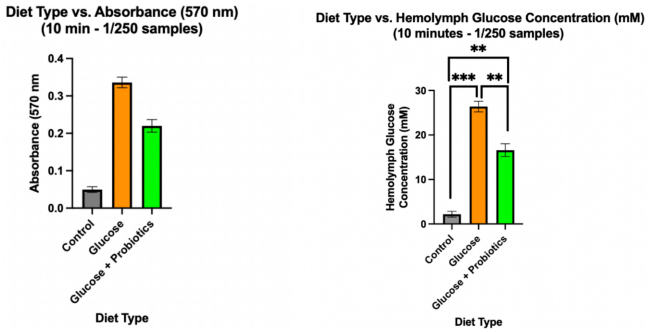


**Figure 5**. *Absorbance and Glucose Concentration Data for the 1/250 dilution samples incubated for 10 minutes. In both graphs, the values for the Group 2 and Group 3 worms are higher than the control, confirming that glucose concentration increased after having a diet that consisted of glucose. Strong statistical difference between Group 2 and Group 3, indicating glucose concentration dropped in Group 3 worms after adding probiotics to their diet.*

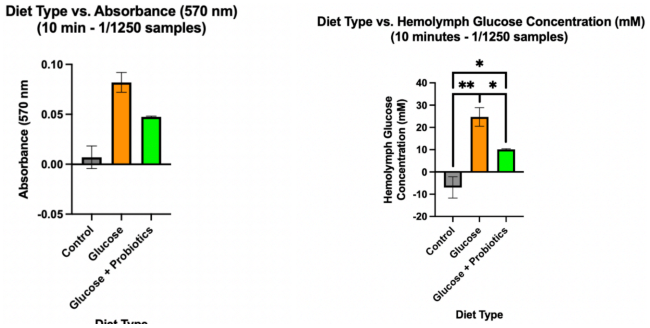


**Figure 6**. *Absorbance and Glucose Concentration Data for the 1/1250 dilution samples incubated for 10 minutes. In both graphs, the values for the Group 2 and Group 3 worms are higher than the control, confirming that glucose concentration increased after having a diet that consisted of glucose. Statistical difference between Group 2 and Group 3 is present, indicating glucose concentration dropped in Group 3 worms after adding probiotics to their diet.*

The findings of this study suggest that probiotic supplementation that contains a majority of lactic acid bacteria (LAB) may help mitigate hyperglycemia in *Bombyx mori* silkworms induced by a high-glucose diet. Compared to silkworms receiving only the glucose diet, those administered the glucose + probiotic diet generally demonstrated lower relative hemolymph glucose levels across multiple incubation time points and dilutions. While the differences varied in magnitude and were limited by the small sample size, the overall

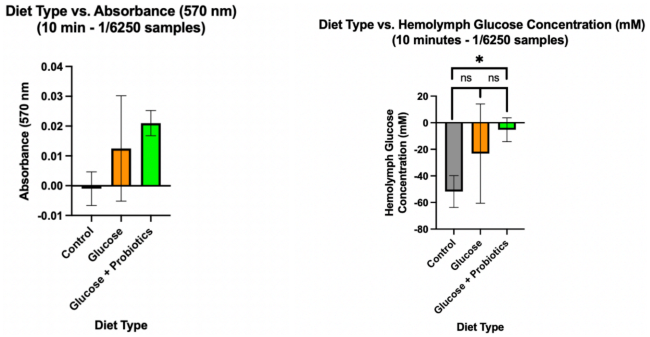


**Figure 7**. *Absorbance and Glucose Concentration Data for the 1/6250 dilution samples incubated for 10 minutes. In both graphs, the values for the Group 2 and Group 3 worms are higher than the control, confirming that glucose concentration increased after having a diet that consisted of glucose. However, after data analysis, it appears that there is no difference that is statistically significant between the three groups.*

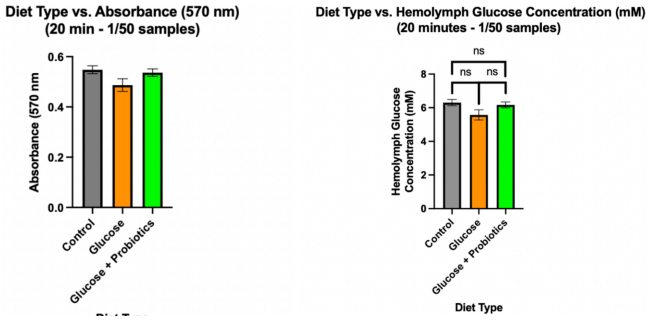


**Figure 8**. *Absorbance and Glucose Concentration Data for the 1/50 dilution samples incubated for 20 minutes. In both graphs, the values for the Group 2 and Group 3 worms seem to be around the same value as the control, indicating that there is no difference present that is statistically significant between the three groups.*

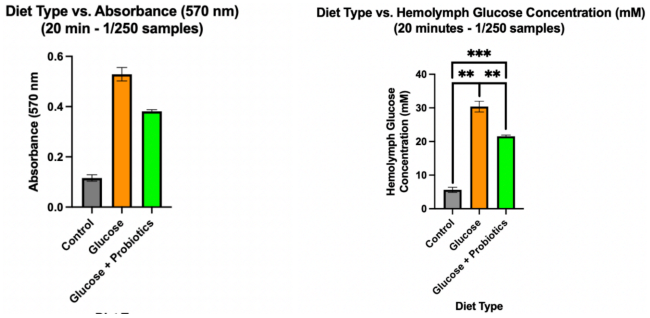


**Figure 9**. *Absorbance and Glucose Concentration Data for the 1/250 dilution samples incubated for 20 minutes. In both graphs, the values for the Group 2 and Group 3 worms are higher than the control, confirming that glucose concentration increased after having a diet that consisted of glucose. Statistical difference between Group 2 and Group 3 is present, indicating glucose concentration dropped in Group 3 worms after adding probiotics to their diet.*

trend supports the hypothesis that introducing LAB strains can offer glycemic benefits in this novel insect model of Type 2 diabetes mellitus (T2D).

These observations are in line with previous reports that specific LAB strains, such as *Lactococcus lactis*, can reduce elevated glucose levels in silkworms (Y. Matsumoto, M. Ishii, and K. Sekimizu [4]). Various mechanisms have been proposed for these glucose-lowering effects, including enhanced insulin signaling, improved gut barrier function, and beneficial shifts in microbial composition (N. K. Nguyen, N. T. N. Dong, H. T. Nguyen,

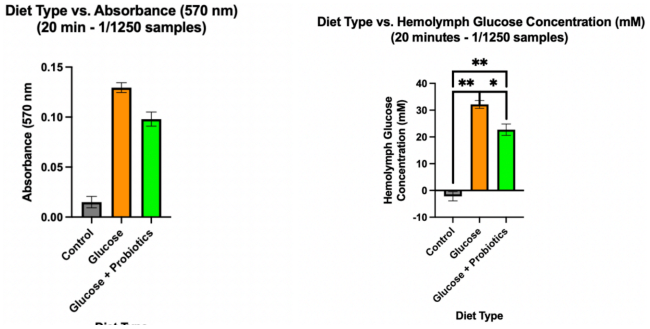


**Figure 10**. *Absorbance and Glucose Concentration Data for the 1/1250 dilution samples incubated for 20 minutes. In both graphs, the values for the Group 2 and Group 3 worms are higher than the control, confirming that glucose concentration increased after having a diet that consisted of glucose. Statistical difference between Group 2 and Group 3 is present, indicating glucose concentration dropped in Group 3 worms after adding probiotics to their diet.*

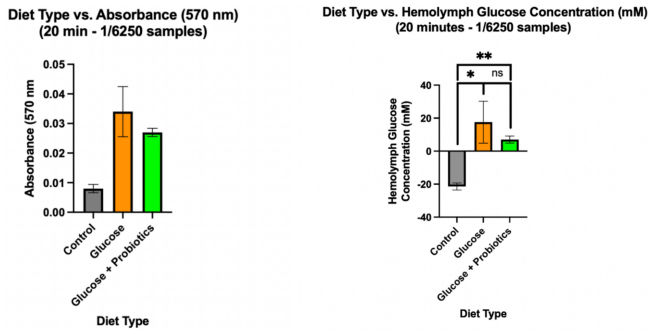


**Figure 11**. *Absorbance and Glucose Concentration Data for the 1/6250 dilution samples incubated for 20 minutes. In both graphs, the values for the Group 2 and Group 3 worms are higher than the control, confirming that glucose concentration increased after having a diet that consisted of glucose. No difference that is statistically significant is present between Group 2 and Group 3.*

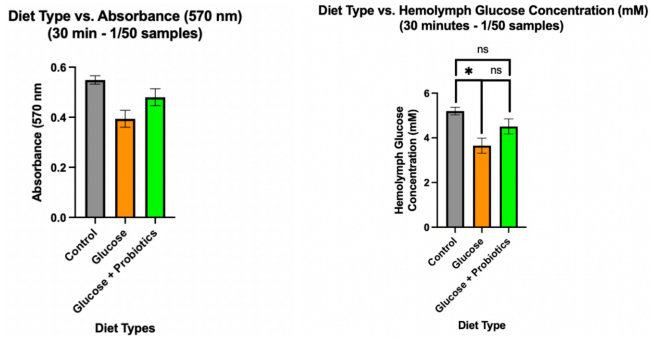


**Figure 12**. *Absorbance and Glucose Concentration Data for the 1/50 dilution samples incubated for 30 minutes. In both graphs, the values for the Group 2 and Group 3 worms seem to be slightly lower than the control, indicating that there is no difference present that is statistically significant between the three groups.*

and P. H. Le [8]; S.-Y. Yang and K.-S. Yoon [7]). Given that silkworms share certain physiological parallels with mammals, such as the ability to rapidly develop hyperglycemia and respond to insulin-like peptides, these findings hold promise for extrapolation to more complex organisms (J. Hou *et al.* [3]).

Nevertheless, interpreting these results requires caution. One of the primary limitations of this study is the small sample size, as each dietary group was represented by only two silkworms in the glucose quantitation assay. Because the data are limited, its makes it much more difficult to reliably spot important differences and to be confident in any

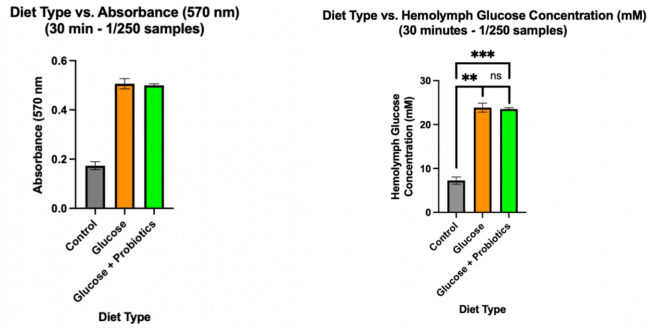


**Figure 13**. *Absorbance and Glucose Concentration Data for the 1/250 dilution samples incubated for 30 minutes. In both graphs, the values for the Group 2 and Group 3 worms are higher than the control, confirming that glucose concentration increased after having a diet that consisted of glucose. No difference that is statistically significant is present between Group 2 and Group 3.*

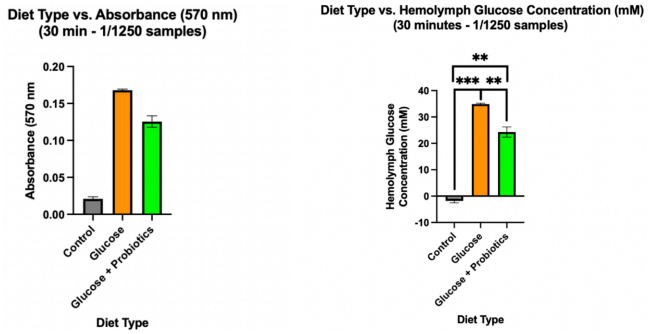


**Figure 14**. *Absorbance and Glucose Concentration Data for the 1/1250 dilution samples incubated for 30 minutes. In both graphs, the values for the Group 2 and Group 3 worms are higher than the control, confirming that glucose concentration increased after having a diet that consisted of glucose. Statistical difference between Group 2 and Group 3 is present, indicating glucose concentration dropped in Group 3 worms after adding probiotics to their diet.*

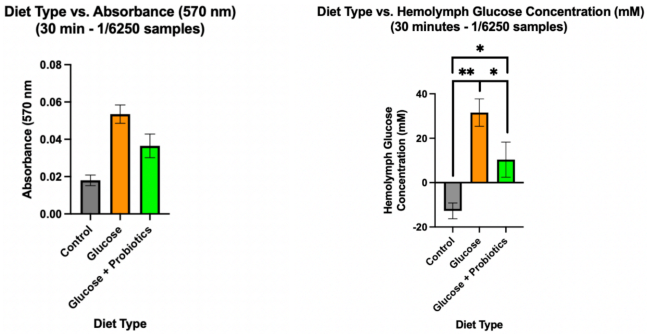


**Figure 15**. *Absorbance and Glucose Concentration Data for the 1/6250 dilution samples incubated for 30 minutes. In both graphs, the values for the Group 2 and Group 3 worms are higher than the control, confirming that glucose concentration increased after having a diet that consisted of glucose. Statistical difference between Group 2 and Group 3 is present, indicating glucose concentration dropped in Group 3 worms after adding probiotics to their diet.*

conclusions drawn. Additionally, the probiotic supplement used in this experiment was administered at a single concentration (108 CFU), and it is possible that different strains or dosages could yield varying effects on hemolymph glucose levels. Another consideration is the short exposure period to the probiotic diet: more extended feeding regimens or investigations over multiple instars might be necessary to observe sustained or more pronounced glycemic changes.

Future studies should prioritize increasing the number of silkworms in each group to bolster statistical confidence. Investigating strain-specific effects could also illuminate which LAB strains are most effective at reducing glucose levels. Moreover, studies aimed at elucidating mechanistic pathways, such as quantifying changes in key metabolic enzymes, insulin receptor gene expression, or gut microbiota composition, would provide

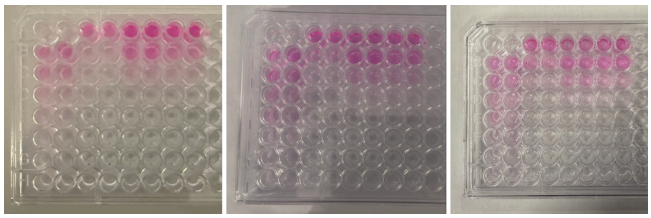

**Figure 16**. *From left to right: 10 minutes, 20 minutes, and 30 minutes after incubating hemolymph samples. Overall, the concentrations of the working assay are increasing over time among the samples. A clear difference is observable between the Group 1 and Groups 2/3 column concentrations.*

deeper insights into how LAB supplementation exerts glycemic control. Long-term research examining whether LAB-induced glycemic improvements persist throughout the silkworm life cycle or across multiple generations could further clarify the potential of fermented foods as a strategy for T2D management.

In conclusion, this pilot study highlights the value of *Bombyx mori* silkworms as a low-cost, physiologically relevant model to explore interventions for T2D. The apparent efficacy of lactic acid bacteria in lowering hemolymph glucose levels in this model aligns with growing evidence that fermented foods rich in LAB may offer therapeutic benefits for glycemic control (Y. Ismail, C. Yulvizar, and B. Mazhitov [5]; P. Sethi, R. Maharana, S. Ameeruddin, and S. Das [6]). With larger-scale confirmatory studies and mechanistic research, especially ones that directly test with samples of lactic acid fermented food items, LAB supplementation may emerge as a simple yet effective dietary approach to complement existing T2D therapies.

I would like to sincerely thank Mrs. Jennifer Williams and Dr. Mareca Lodge for assisting with the experimental procedures and data analysis during the study.

## References

[1] "Home." [Online]. Available: https://diabetesatlas.org/

[2] "Standards of Medical Care in Diabetes," *Diabetes Care*, vol. 44, no. Supplement_1, pp. S1–S2, 2021, doi: 10.2337/dc21-Sint.

[3] J. Hou *et al.*, "Establishment of diabetes mellitus model using \textit{Bombyx mori} silkworms in a lowtemperature environment," *Archives of Insect Biochemistry and Physiology*, vol. 115, no. 1, p. e22083, 2024, doi: 10.1002/arch.22083.

[4] Y. Matsumoto, M. Ishii, and K. Sekimizu, "An in vivo invertebrate evaluation system for identifying substances that suppress sucrose-induced postprandial hyperglycemia," *Scientific Reports*, vol. 6, no. 1, p. 26354, 2016, doi: 10.1038/srep26354.

[5] Y. Ismail, C. Yulvizar, and B. Mazhitov, "Characterization of lactic acid bacteria from local cow}s milk kefir," *IOP Conference Series: Earth and Environmental Science*, vol. 130, p. 12019, 2018, doi: 10.1088/1755-1315/130/1/012019.

[6] P. Sethi, R. Maharana, S. Ameeruddin, and S. Das, *Isolation of probiotics and scientific validation of using curd and salad vegetables for health benefits*. Research Journal of Berhampur University, 2023. [Online]. Available: https://www.researchgate.net/publication/376190174_Isolation_of_probiotics_and_scientific_validation_of_using_curd_and_salad_vegetables_for_health_benefits

[7] S.-Y. Yang and K.-S. Yoon, "Effect of Probiotic Lactic Acid Bacteria (LAB) on the Quality and Safety of Greek Yogurt," *Foods*, vol. 11, no. 23, p. 3799, 2022, doi: 10.3390/foods11233799.

[8] N. K. Nguyen, N. T. N. Dong, H. T. Nguyen, and P. H. Le, "Lactic acid bacteria: promising supplements for enhancing the biological activities of kombucha," *SpringerPlus*, vol. 4, no. 1, p. 91, 2015, doi: 10.1186/s40064-015-0872-3.

Open Access | https://doi.org/10.62329/upur9568

# Utilizing Alkaline Hydrolysis to Recover Terephthalic Acid Monomer From PET-Based Textile Waste

**Sarrah Kitchell**[1]

[1]North Carolina School of Science and Mathematics

**Morganton Scientific**

*North Carolina School of Science and Mathematics*

Journal of Student STEM Research

## Abstract

Over 85% of textile waste in the U.S. ends up in landfills, primarily because most textiles are difficult to recycle in an economically feasible manner if they consist of a blend of natural and synthetic fibers (United States Environmental Protection Agency, 2018). Mechanically separating natural and synthetic fibers is a labor-intensive and inefficient process. However, alkaline hydrolysis is a prospective method to chemically recycle blended textiles by recovering the monomer terephthalic acid (TPA) from fibers of its polymer, polyethylene terephthalate (PET). Applied industrially, this process could contribute to a circular economy by recycling textile waste into virgin-quality PET.

Alkaline hydrolysis was performed on 9 textiles varying in color, density, and composition, each containing between 25% and 84% polyester blended with a variety of other fibers. 2 control samples composed of 100% cotton and 100% polyester were hydrolyzed as well. In each case, the yield of TPA from hydrolysis was measured using three experimental approaches with the goal of determining whether any one of the methods might lead to error when assessing TPA recovery. The mass of the TPA was determined from each sample by stoichiometrically calculating the expected yield, performing UV-Visible spectrophotometry, and weighing the solid TPA that precipitated after acidification. All 9 textiles produced solid TPA flakes in yields exceeding 60% and as high as 96%. Analysis of the recovered TPA via infrared spectroscopy presented strong evidence that it was identical to lab-grade TPA. Further research into alkaline hydrolysis will be needed to determine which properties of a textile affect its TPA yield, develop methods of optimizing the hydrolysis process for different types of textiles, and polymerize the recovered TPA into PET.

**Keywords** PET Recycling, Textile Waste, Waste Management

**Published** Jun 27, 2024

**Correspondence to**
Sarrah Kitchell
kitchell25s@ncssm.edu



## 1. Background

Each year, the US throws out over 34 billion pounds of textiles [1]. Of these discarded textiles, at most 15% are recycled, but many of these “recycled” textiles are simply shipped abroad to international landfills [1]. Textiles are rarely recycled due to the inefficiency with which the fibers can be separated; a single scrap of fabric often contains multiple types of fibers blended together. For instance, fabric in a sweatshirt could be made of 75% cotton and 25% polyester, and fabric to make athletic wear could be a proprietary mixture of synthetic fibers [2]. In order to recycle these fabrics, the fibers that make up the textile must be separated, which is extremely difficult due to their microscopic scale [3].

Polyethylene terephthalate (PET), commonly known as polyester, is a highly recyclable plastic commonly used for food packaging and other consumer products. The monomers of PET, terephthalic acid (TPA) and ethylene glycol, can be obtained via alkaline

hydrolysis, a type of chemical recycling. Rather than trying to mechanically separate polyester fibers from other materials, chemical recycling can employ many types of chemical reactions to isolate raw materials more efficiently. Of the 3 types of hydrolysis (acid hydrolysis, alkaline hydrolysis, and neutral hydrolysis), alkaline hydrolysis was chosen for this study because it can occur under mild reaction conditions and does not require specialized equipment or chemicals [4].

The alkaline hydrolysis reaction (Figure 1) involves heating PET with aqueous sodium hydroxide, which cleaves the PET chain along the ester bond and produces disodium terephthalate and ethylene glycol. Adding sulfuric acid to these products will trigger a precipitation reaction that produces solid terephthalic acid and aqueous sodium sulfate. Bengtsson et al. (2022) utilized alkaline hydrolysis to break down PET in the 100% polyester fabric tricot while investigating which fabric preparation methods would produce the highest yields of TPA. They converted nearly 100% of PET in the sample into TPA and dissolved all of the fabric in the process, leaving behind no solid waste in trials hydrolyzed for 24 hours [5]. Bengtsson et al.'s research established a method for performing alkaline hydrolysis on textiles and assessing the products that this research builds on.

This study explores whether alkaline hydrolysis could break down blended textiles and generate high yields of TPA. Additionally, the TPA was assessed qualitatively to determine its applicability to be reintroduced in the manufacturing process. If alkaline hydrolysis can efficiently recycle blended textiles on an industrial scale, it would eliminate the need to identify and sort fabric samples by composition. Consequently, textile recycling could generate "virgin-quality" TPA used to manufacture new products, in a closed-loop manufacturing system instead of relying on petroleum and natural gas to create more plastics destined for the landfill [7].

## 2. Materials and Methods

9 blended fabric samples of varying compositions, colors, and densities were provided by Hanesbrands Inc. Control samples of 100% cotton and 100% polyester were purchased at

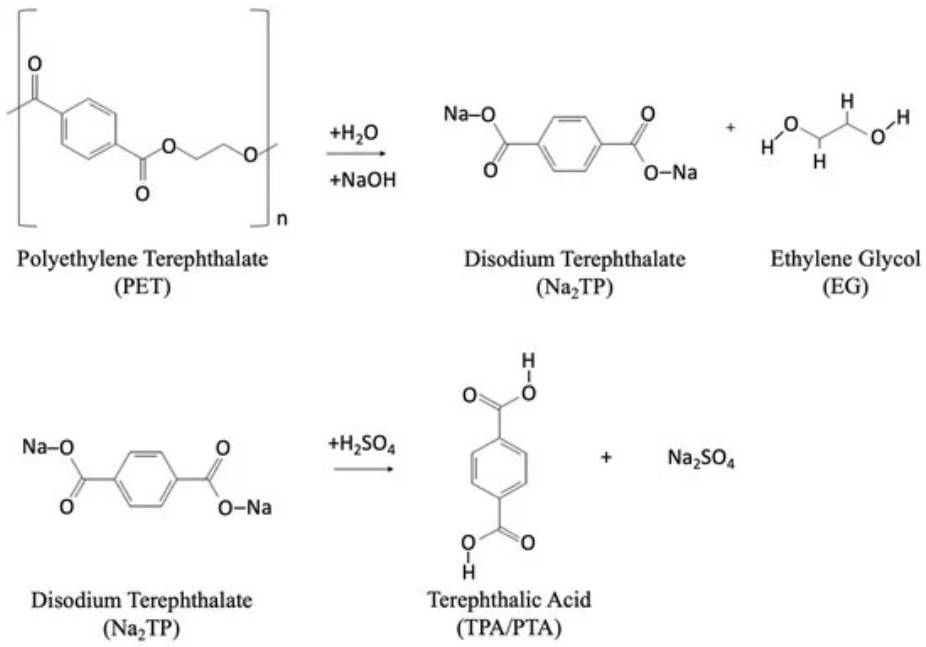


**Figure 1**. *Alkaline Hydrolysis and Acidification Reactions to Yield TPA from PET [6]*

| Sample | % Polyester | % Cotton | % Elastane | % Rayon | Density (GSM) | Color | Vendor |
|---|---|---|---|---|---|---|---|
| 1 | 0 | 100 | 0 | 0 | 141 | White | Walmart |
| 2 | 25 | 75 | 0 | 0 | 430 | “Ash Heather” | Liztex |
| 3 | 26 | 70 | 4 | 0 | 155 | Navy Blue | Best Pacific |
| 4 | 26 | 70 | 4 | 0 | 185 | White | Best Pacific |
| 5 | 48 | 48 | 4 | 0 | 280 | “Utility Brown” | Liztex |
| 6 | 48 | 48 | 4 | 0 | 390 | “Utility Brown” | Liztex |
| 7 | 50 | 50 | 0 | 0 | 210 | “Utility Brown” | Liztex |
| 8 | 50 | 50 | 0 | 0 | 300 | “Utility Brown” | Liztex |
| 9 | 78 | 0 | 22 | 0 | 245 | Black | TexRay |
| 10 | 84 | 0 | 4 | 12 | 160 | Black | Best Pacific |
| 11 | 100 | 0 | 0 | 0 | 106 | White | Walmart |

**Table 1**. *Summary of Textiles Used for Hydrolysis*

Walmart. Table 1 shows a summary of the textiles in order of increasing polyester content.

Guided by the Swedish Institute for Standards’ proprietary instructions, all textile samples were washed together on warm in a laundromat-style front-loading washing machine and tumble dried on high in a front-loading dryer. Afterwards, all samples were cut into 1 cm squares. Immediately before hydrolysis, each sample was oven dried for at least 105 minutes to remove moisture.

The alkaline hydrolysis reaction was carried out in a standard reflux setup Figure 2. A 500 mL single neck round bottom flask connected to a condenser column was used as the reaction vessel. The flask was suspended in an oil bath over a stirring hotplate to heat the reaction evenly, with a thermometer in the oil to monitor the temperature.

In the flask , 250 mL of 5% NaOH solution was heated to approximately 90°C. Then, 2.50 g of dried textile was added to the solution. The temperature and stirring rate were maintained for 18 hours, after which the hot plate was turned off and the flask was raised out of the oil to cool. Any remaining solids were separated using vacuum filtration with a Buchner funnel and Whatman 1 filter paper. Both the filtrate and the retentate were retained for analysis. Three methods were used to calculate the TPA yield from each sample.

### *2.1.* Stoichiometric Yield

The first way TPA yield was calculated was by determining the mass change of the sample before and after hydrolysis. The remaining textile in the flask was first neutralized in 2M acetic acid, using phenolphthalein as a pH indicator. Then, the sample was dried in the

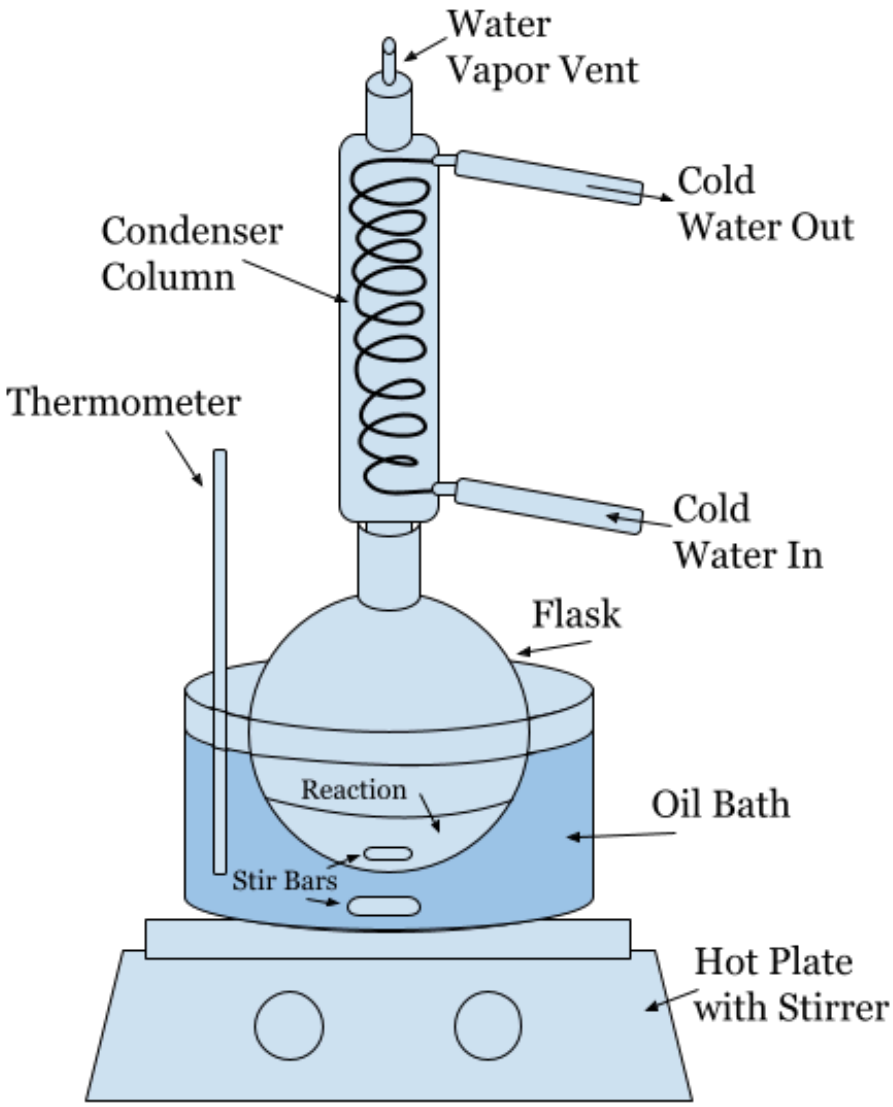


**Figure 2.** *Hydrolysis Reaction Setup*

oven at 105°C until no mass change was detected. Once the sample was dry, its mass was used to calculate the mass of the TPA recovered.

### *2.2.* Absorbance Yield

To find the yield of TPA from the post-hydrolysis filtrate, a Thermo Scientific Evolution Pro UV-Vis spectrophotometer was used to find the absorbance of the sample at 242 nm [5]. First, a standard curve was created using 7 concentrations of TPA dissolved in 5% NaOH, diluted in water 1600 times Figure 3. After each hydrolysis reaction, 100 $\mu$L of post-hydrolysis filtrate was added to 160 mL of water to create a 1:1600 dilution. Then the absorbance value was found via UV-Vis spectrophotometry and mapped to the standard curve to find the concentration of TPA dissolved in the reaction solution Figure 3.

### *2.3.* Gravimetric Yield

The gravimetric yield of solid TPA was determined by acidifying the reaction solution. 18M H2SO4 was added to the filtrate until the pH reached roughly 2.5 and TPA formed as

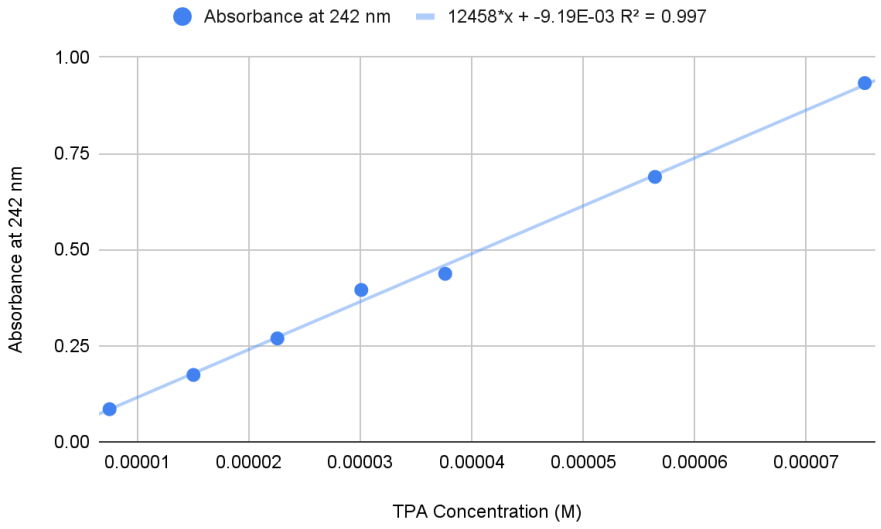


**Figure 3**. *TPA Absorbance Standard Curve at 242 nm*

a precipitate. The resulting mixture was allowed to sit until the TPA settled to the bottom. As much of the aqueous layer as possible was decanted and vacuum filtered in a Buchner funnel using Whatman 1 filter paper. The remaining mixture was centrifuged for 10 minutes at 6000 rpm. The new aqueous layer was decanted and vacuum filtered to separate any TPA particles. Excess liquid retained in the TPA was drawn out using vacuum filtration. Afterwards, the TPA and filter papers were dried in the oven at 105°C for at least 2 hours. Once dry, all TPA was scraped off of the filter paper and massed.

The purity of the solid TPA recovered was assessed using FTIR spectroscopy. Ten KBr samples made with recovered TPA from each of 9 hydrolyses and an additional control sample with lab grade TPA were prepared in a 1:1000 ratio of TPA to potassium bromide. These samples were then analyzed using a Shimadzu IRSpirit FTIR spectrophotometer.

## 3. Results and Discussion

The TPA recovered from each trial had few to no impurities revealed by FTIR spectroscopy. An FTIR spectrum was collected from each sample and compared to a spectrum collected from lab-grade TPA (Thermo Scientific 99+%). Figure 4 shows the FTIR spectrum of TPA from sample 6 (Table 1) overlaid onto the lab-grade TPA spectrum. For every trial, each peak on the synthesized TPA spectrum corresponded to a peak found on the control TPA spectrum at the same wave number. Any impurities, which would have likely caused extraneous peaks, did not appear to be present, indicating that the TPA recovered from the samples did not contain any contaminants.

Each of the 3 methods for finding the yield of TPA from a textile sample were plotted together in order of increasing polyester content Figure 5. Overall, there is a direct relationship between the amount of polyester in a sample and the mass of TPA extracted from that sample. The blue circles represent the yield of TPA by subtracting the mass of the solid waste after hydrolysis from the mass of the initial textile sample and calculating the stoichiometric mass of TPA recovered:

$$(x\,\text{grams of product}) \times (166.13\,\text{g} \,\backslash/\, \text{mol TPA} + 62.07\,\text{g} \,\backslash/\, \text{mol EG}) = \text{grams of TPA}$$

For nearly every sample with a polyester content less than or equal to 50%, this metric of measuring TPA yield was practically identical to the other two, indicating that all 3

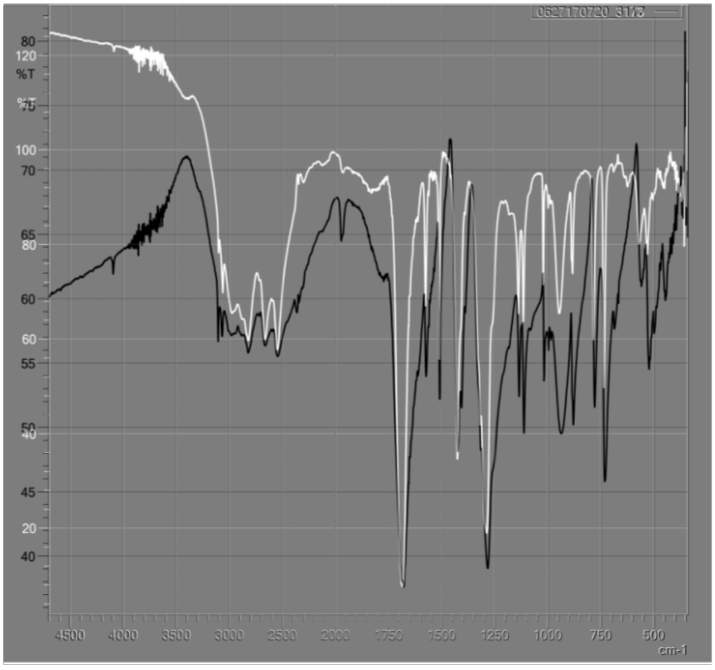


**Figure 4**. *Overlaid FTIR Spectra of TPA Recovered from Textile Sample 6 and Lab-Grade TPA*

methods of finding TPA yield are equally accurate. In the case of the 100% cotton sample, not all fibers could be recovered after hydrolysis, as some remained suspended in the aqueous product or stuck to the filter paper. This accounts for a higher than expected mass loss and subsequent higher calculated TPA mass.

The red squares Figure 5 represent the TPA yield calculated from running the aqueous hydrolysis product in the UV-Visible spectrophotometer. After obtaining the concentration of TPA in sodium hydroxide using the standard curve Figure 3, the following conversion was used to obtain the mass of TPA in the original 250 mL reaction:

$$(250\,\text{mL solution}) \cdot \left(x\ \frac{\text{mol TPA}}{\text{L water}}\right) \cdot \left(\frac{1\,\text{L}}{1000\,\text{mL}}\right) \cdot \left(\frac{160\,\text{mL water}}{100\,\text{L TPA}}\right) \cdot \left(\frac{105\,\text{L}}{1\,\text{L}}\right) \cdot \left(\frac{1\,\text{L}}{1000\,\text{mL}}\right) \cdot \left(\frac{166.13\,\text{g TPA}}{1\,\text{mol TPA}}\right) = \text{grams TPA}$$

The yellow triangles Figure 5 represent the yield of TPA obtained via precipitation out of the reaction solution. With the exception of samples 10 and 11 (Table 1), the gravimetric mass of TPA matched the absorbance mass of TPA.

3 pairs of samples contained the same composition of fibers, either differing in fabric density, type of knit, or color Figure 6. According to the labels provided by Hanesbrands, the only difference between the samples 5 and 6 (Table 1) was the fabric density listed. According to [bengtsson_chemical_2022], textiles with a greater “accessible area” for hydrolysis, such as textiles with a lower density, fibers that have been texturized to improve breathability, or samples that are finely cut or shredded, are more responsive to alkaline hydrolysis. This statement is consistent with samples 5 and 6, where the medium weight textile demonstrated a higher TPA yield than the heavy weight sample Figure 6.

Samples 7 and 8 (Table 1) were constructed using different knits, with sample 7 made of a lower density jersey knit and sample 8 made of a higher density fleece knit Figure 6. Contrary to the findings of Bengtsson et al. (2022), sample 8 had a higher yield, indicating the knit or weave of a sample may affect its TPA yield more than a sample’s density. However, since the density was not controlled for, a definite conclusion cannot be reached.

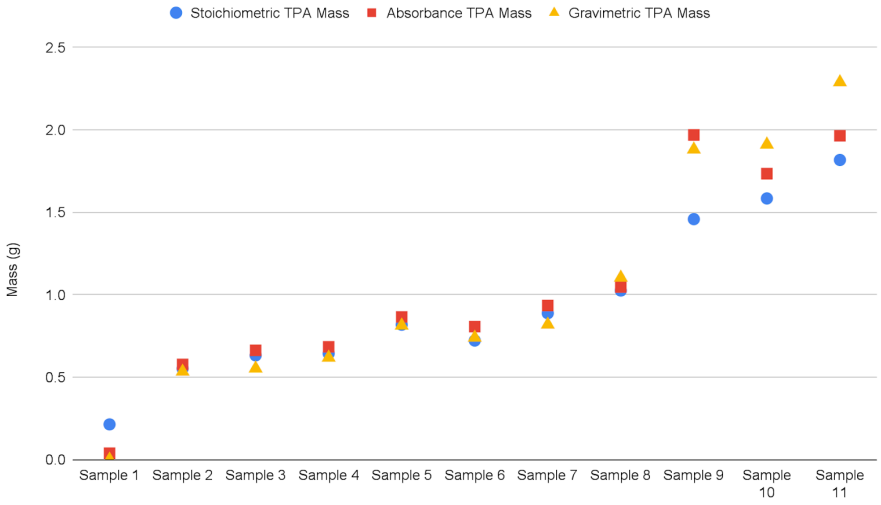


**Figure 5.** *Three Methods for Collecting TPA Yields Per Sample*

Samples 3 and 4 had comparable densities but were different colors. The yields of TPA for each sample were similar, indicating that different dyes used did not affect the yield Figure 6.

The theoretical mass of TPA obtained from hydrolysis was found by multiplying the initial mass of the sample by the percentage of polyester in the sample. Some samples included multiple types of polyester such as “recycled polyester” or “bulk polyester” listed separately. For this purpose, all types of polyester were combined into a single percentage. A total experimental yield of TPA for each sample was found by averaging the three methods for collecting TPA yield Figure 7. While the theoretical TPA mass was proportional to the amount of polyester in the sample, the experimental mass was not, indicating that some properties of the textile affected the TPA.

The percent yield from each sample containing polyester was visualized in 2 ways: with data organized by increasing sample density Figure 8 and by increasing percent polyester Figure 7. Percent yield of TPA was calculated by dividing the average experimental TPA yield by the theoretical TPA yield and multiplying by 100. Every sample had a yield of TPA over 60%, but neither the percent composition of polyester nor the fabric density correlated with the percent yield. Bengtsson, et al. (2022) indicated that higher density textiles may hinder TPA yields because alkaline hydrolysis proceeds from the ends of the polymer, but this trend was not detected. Additionally, the amount of polyester in the textile had no bearing on TPA yields, indicating that the reaction doesn’t cease after a certain amount of PET has been hydrolyzed. Additional experimentation separately

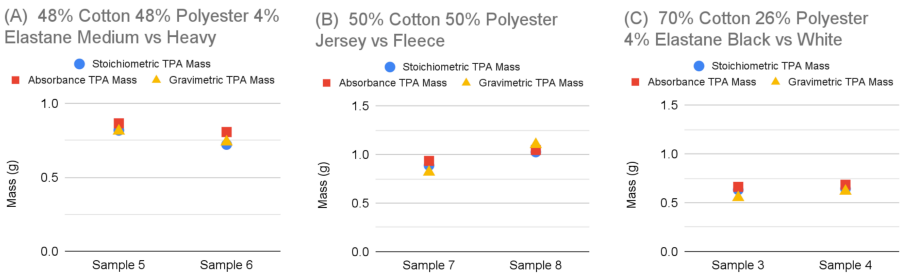


**Figure 6.** *Comparison of TPA Yields of Textiles With Identical Composition*

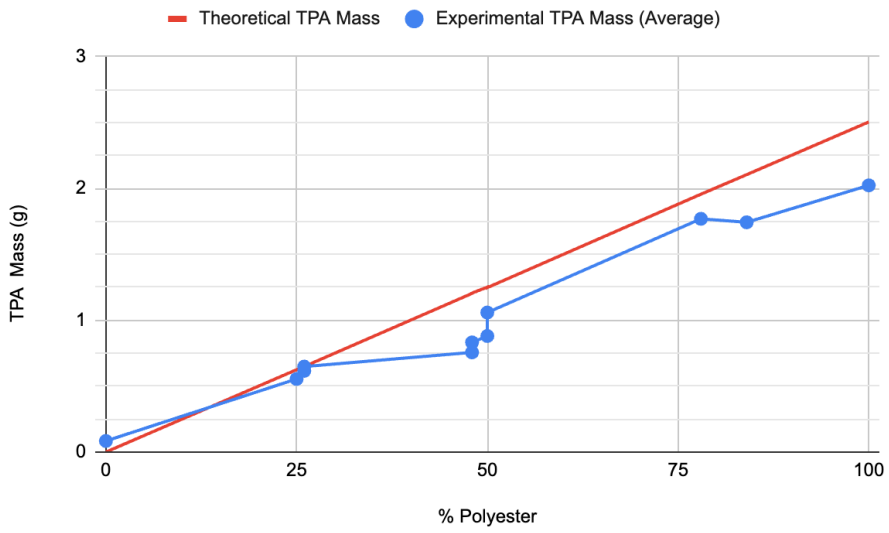


**Figure 7.** *Theoretical vs Experimental Yields of TPA Per Sample*

controlling for variables such as fiber composition, color, and density would need to be performed to determine which factors affect a fabric's percent TPA yield.

## 4. Conclusions

High quality TPA was successfully recovered via alkaline hydrolysis from every blended textile sample tested, indicating alkaline hydrolysis could be a type of chemical recycling utilized commercially and applied to the closed-loop manufacturing model. The TPA recovered from all samples contained few to no impurities as revealed by FTIR spectroscopy, although the color of the recovered TPA varied slightly depending on the color of the fabric sample hydrolyzed. Of the three ways that TPA yield was estimated, TPA yields based on UV-Visible spectrophotometry provided accurate yield estimates and proved to be an efficient method for estimating the yield of TPA in a sample before it was precipitated. In future experimentation, finding the TPA yield via absorbance could be

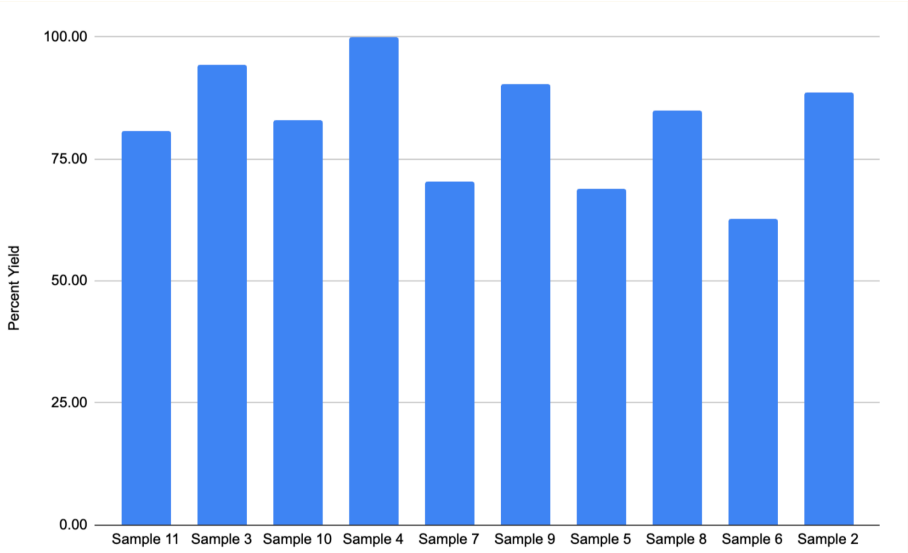


**Figure 8.** *Percent Yield of TPA Per Sample Organized by Increasing Sample Density*

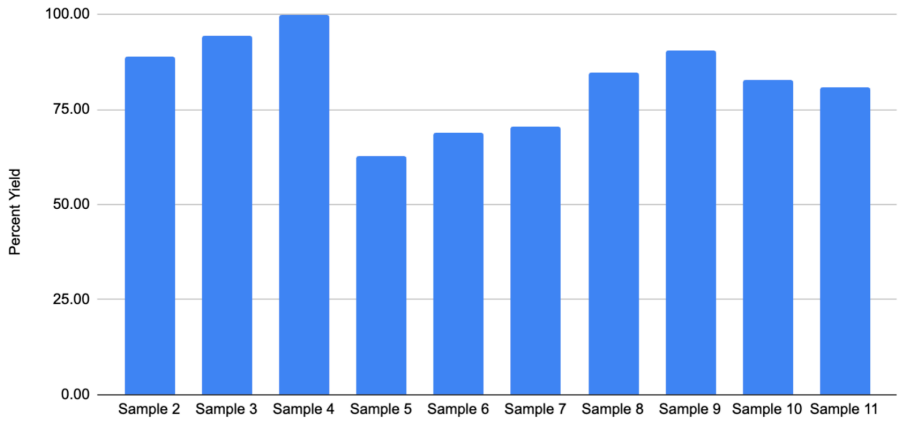


**Figure 9**. *Percent Yield of TPA Per Sample Organized by Increasing Polyester Content*

used alone to estimate the yield of TPA from hydrolysis. All 9 samples produced an average TPA yield over 60% of the theoretical yield, but identifying which characteristics of a fabric sample affect TPA yield as well as modifying the hydrolysis process to optimize TPA yield for any given sample are areas of further study. Moreover, testing whether the produced TPA can be polymerized into usable PET is a crucial next step to determining whether alkaline hydrolysis is a feasible and effective method for recycling blended textiles on an industrial scale.

The North Carolina School of Science and Mathematics is acknowledged for providing funding, equipment, and lab space to complete this research. Furthermore, Dr. Tandy Grubbs is acknowledged for his mentorship and guidance during this project.

## References

[1] United States Environmental Protection Agency, "Textiles: Material-Specific Data." [Online]. Available: https://www.epa.gov/facts-and-figures-about-materials-waste-and-recycling/textiles-material-specific-data

[2] W. Ng, "Proprietary Weaving Technology and Fabric Material Meant That Clothing Companies Are Monopolistic in Their Individual Market Segment." [Online]. Available: https://ssrn.com/abstract=4266519

[3] S. Bianchi *et al.*, "Opportunities and Limitations in Recycling Fossil Polymers from Textiles," *Macromol*, vol. 3, no. 2, pp. 120–148, 2023, doi: 10.3390/macromol3020009.

[4] H. Abedsoltan, "A focused review on recycling and hydrolysis techniques of polyethylene terephthalate," *Polymer Engineering & Science*, vol. 63, no. 9, pp. 2651–2674, 2023, doi: 10.1002/pen.26406.

[5] J. Bengtsson, A. Peterson, A. Idström, H. De La Motte, and K. Jedvert, "Chemical Recycling of a Textile Blend from Polyester and Viscose, Part II: Mechanism and Reactivity during Alkaline Hydrolysis of Textile Polyester," *Sustainability*, vol. 14, no. 11, p. 6911, 2022, doi: 10.3390/su14116911.

[6] P. Benyathiar, P. Kumar, G. Carpenter, J. Brace, and D. K. Mishra, "Polyethylene Terephthalate (PET) Bottle-to-Bottle Recycling for the Beverage Industry: A Review," *Polymers*, vol. 14, no. 12, p. 2366, 2022, doi: 10.3390/polym14122366.

[7] E. I. M. Bardoquillo, J. M. B. Firman, D. B. Montecastro, and A. M. Basilio, "Chemical recycling of waste polyethylene terephthalate (PET) bottles via recovery and polymerization of terephthalic acid (TPA) and ethylene glycol (EG)," *Materials Today: Proceedings*, p. S2214785323020564, 2023, doi: 10.1016/j.matpr.2023.04.160.

Open Access | https://doi.org/10.62329/yjme9696

Morganton Scientific

*North Carolina School of Science and Mathematics*

Journal of Student STEM Research

# Utilizing Enzymatic and Chemical Delignification Methods on Fibrous Plants for Decentralized Production of Absorbent Materials for Menstrual Pads in Semi-Arid Regions

**Prerana Kulla**[1]

[1]NCSSM

## Abstract

Over 500 million women suffer from period poverty from around the world. These women lack adequate menstrual pads that are both affordable and efficient and instead resort to unsanitary solutions, such as rags and goat skin. Currently, traditional sanitary pads are primarily composed of cotton. Though they have exceptional absorbency, cotton-based pads are less sustainable in regions that do not traditionally grow cotton, leading to higher costs and scarcity. Previously, sisal fibers were tested to find an alternative material for cotton. The findings showed that sisal fibers had a higher absorbency than cotton. This study explores the viability of using biodegradable materials—pineapple and sisal fibers— that are found in locations that do not locally grow cotton. These fibers are used as sustainable alternatives for making menstrual hygiene products. By also going through experimental methods with sisal, the results were compared. These fibers were modified through the processes of decortication followed by enzymatic and chemical delignification to enhance their absorbent properties. Fourier Transform Infrared (FTIR) spectroscopy and ABTS assays were conducted to assess changes in chemical composition. Absorbency tests were designed to compare the absorbency of treated sisal and pineapple fibers against conventional cotton. The results show that pineapple and sisal fibers achieve absorbency levels nearing cotton with appropriate processing. This research supports the development of eco-friendly menstrual products composed of pineapple and sisal fibers that are accessible and effective, contributing to a sustainable solution for managing menstrual health in resource-limited settings.

**Keywords** Enzymatic, Delignification, Fibrous plants

**Published** Jun 27, 2024

**Correspondence to**
Prerana Kulla
kulla25p@ncssm.edu



## 1. Introduction

Women comprise half of the world's population and undergo the menstrual cycle, which they must properly manage. Sanitary products help accomplish this management by absorbing menstrual blood. When it comes to monthly bleeding, women select from a variety of menstruation products based on criteria like affordability, accessibility, and safety. Unfortunately, not all women worldwide have unconditional access to menstrual products. It is estimated that 500 million women have difficulty obtaining menstrual products [1]. Period poverty refers to the lack of any negative consequences that come with inadequate management of the menstrual cycle, which includes women turning to makeshift remedies, which pose critical health concerns [2]. These materials include old garments, paper, cotton, wool scraps, goat skin, mattress fragments, and leaves, which do not have reliable absorbency and will often leave stains on outer clothing. This can

discourage girls and women from going to school and work, which may endanger the financial security of their families [3]. Given this, it is particularly challenging for women to maintain good menstrual hygiene in low and even middle-income countries where period poverty is prominent. A common product is cotton-based pads, which present problems regarding cost and environmental impact. Although cotton is a versatile plant growing in various regions, some countries lack industrial areas to produce cotton menstrual pads commercially. This causes a high cost for cotton-based pads in these regions as they import them from other countries. Considering that women use 6–8 menstrual pads on average per cycle— which adds up to about 125 kg of menstrual waste — it is essential to remember that most disposable menstrual pads have a breakdown time of 500–800 years for each pad [4]. Additionally, due to the limited private changing facilities, inadequate sanitation infrastructure, and a lack of disposal options, hygiene products are also disposed of in open spaces or latrines to avoid shame [5]. All of these factors contribute to environmental pollution. To overcome these challenges, this research project explored a natural, biodegradable process for the production of menstrual pads. Fibers from pineapple and sisal grown in rural areas can be used as an alternative material for menstrual pads. These fibers are hydrophilic since hydroxyl and other oxygen-containing groups in the cell wall promote moisture absorption through hydrogen bonding and are responsible for their high absorption capacity [6]. Furthermore, the diameters of these fibers vary in response to changes in moisture content; when moisture content rises, the fibers expand until they saturate, at which point they stop growing further [4]. These plants are chosen not just for their superior absorbing qualities but also for their resilience and the comparatively low environmental effect of their processing and cultivation. In addition, because these plants are frequently found and grown in rural regions, the production of the menstrual pads can be localized, which lowers expenses compared to commercial menstruation pads, which are produced and imported from foreign countries [7]. This research seeks to innovate in the field of biodegradable materials and aims to significantly improve accessibility to menstrual hygiene products, thereby addressing both environmental concerns and social inequalities. This work will contribute to a sustainable and equitable world where menstrual health is managed with dignity and without detriment to the environment.

## 2. Materials and Methods

### *2.1. Decortication*

Decortication pertains to the process of removing the outer layer or covering of a structure. The sisal fibers used in the experiment were already decorticated; however, the pineapple fibers had to be manually decorticated when conducting preliminary tests Figure 1. These fibers were then processed by being soaked in a sodium hydroxide (NaOH) and distilled water bath Figure 2. After soaking for five hours, the leaf's outer layer was stripped with a knife, leaving the fibers behind. These fibers were then sun-dried and saved for later use.

### *2.2. Fourier Transform Infrared (FTIR) spectroscopy*

**Figure 1**. *Pineapple leaf in the process of being decorticated*


**Figure 2.** *Sodium Hydroxide bath to prepare for decortication*

FTIR spectroscopy was used to analyze the chemical structure of the fibers throughout the delignification process. This technique is crucial in verifying lignin removal by detecting changes in the functional groups present in the fibers. For the FTIR to properly analyze fibers, they must first be in a powder form. To achieve this, liquid nitrogen was used to freeze the fibers, making them brittle and more accessible to break down in a mortar and pestle. Next, the fibers were ground in a blender to be broken down even further. This powder was then transferred to an oven, which was left at 60 degrees Celsius to eliminate all residual moisture. This step is crucial so there is no chance of hindering the FTIR readings. FTIR spectra analysis occurred after the different delignification methods to see how efficient each method was in removing lignin while preserving the cellulose for absorbency.

### *2.3. Leica ICC50 W*

To continue reinforcing the findings of delignification, a Leica ICC50 W microscope was used to observe the structural changes of the fibers throughout the experiment. The untreated fibers had a generally larger diameter with rougher surfaces due to debris from parenchymal cells. After usage of PFA, the macrofibers began to unbundle into smaller constituents.

### *2.4. Delignification Preparation*

Delignification is crucial when working with sisal and pineapple fibers, which are often very stubborn and rigid. Lignin, a natural phenolic polymer with high molecular weight, has a complex composition and structure in the plant cell wall [8]. It consists primarily of three different monolignols: p-coumaric alcohol, coniferyl alcohol, and sinapyl alcohol, which are linked by various types of ether and carbon-carbon bonds [6]. This intricate network contributes to plant cell walls' rigidity and water resistance. Removing as much lignin as possible is essential when working with these fibers since lignin is hydrophobic and red and uses the fiber's ability to absorb water. By removing lignin, the cellulose content becomes more accessible, which is crucial for improving the fibers' mechanical properties. This process also increases the fiber's porosity and surface area, improving its functionality in various products. Taking FTIR spectrums verified delignification since the results reflected what chemical bonds were present in the fiber throughout time. To prepare for delignification, the sun-dried pineapple and sisal fibers were cut into short segments of around 10mm. These fibers were pretreated with a high-pressure autoclave with distilled water at 180 °C for 30 minutes. Two enzymatic and one chemical methods were used to undergo the delignification process. The chemical method required a peroxyformic acid (PFA) stock solution. 88% formic acid, 30% hydrogen peroxide, and 3M sulfuric acid were obtained for this. To work with 0.5g of fiber, 50 mL of volume is needed to fully submerge the fibers. For this, 86 mL of peroxyformic stock solution was made by mixing 50 mL of 30% $H_2O_2$, 21 mL of 88% formic acid, and 15 mL of $H_2SO_4$ in an amber

bottle. This mixture was left to rest and react for about 90 minutes [9]. Additionally, to prepare the enzymatic delignification, four flasks, two laccase-producing mushrooms, Pleurotus djamor (P. djamor) and Trametes versicolor (T. versicolor), were obtained from Mushroom Mountain. First, potato-dextrose agar (PDA) was poured onto culture plates to ensure laccase is consistently produced and its reliability is optimized. As the PDA hardened, clusters of mushroom fungi were picked up using a 1000mL pipette tip and placed face down on the PDA plates. This way, over time, there is certainty that laccase from the T. versicolor and P. djamor is always accessible regardless of the condition of the initial culture slant.

### *2.5. Delignification Process*

The delignification process was carried out in two distinct ways: chemically and enzymatically. The chemical route utilized PFA and followed up with a sodium hydroxide solution. The enzymatic route utilized laccase, an enzyme meant to break down the lignin within the plant fibers, initially from both T. versicolor and P. djamor; however, for the second enzymatic method, only a powder form of T. versicolor was used. Two Pyrex media glasses were utilized; one was for pineapple fibers, and the other was for sisal fibers. Each glass was filled with 50 mL of diluted PFA acid. To do this, 45mL of deionized water is first put into the glassware, then 5 mL of PFA acid is added. This order minimized the risk of splashing during the addition process, ensuring that any potential splash would involve water rather than the more hazardous PFA. Then, 0.5 g of each fiber was placed into its respective glass. These glasses were incubated at 50 degrees Celsius for approximately 48 hours. After two days, the flasks were removed from the incubator, and the fibers were decanted so that the PFA waste could be appropriately disposed of in an amber bottle. Next, the fibers' pH was neutralized by washing them with deionized water thoroughly, followed by neutralization checks using pH strips. Following this, the fibers went through a sodium hydroxide bath. The NaOH bath is created by diluting 50 mL of 2M NaOH with 50 mL of DI water. 100 mL of 1M NaOH may also be used. The neutralized pineapple and sisal fibers are transferred into two new glassware, each with 50 mL NaOH solution. These two glasses are left to incubate at 50 degrees Celsius for 4 hours. The fibers were gathered after this process, and their pH was neutralized. To let them dry, the fibers were left on a weight tray in an incubator at room temperature for three days [9]. These protocols are appropriate for two samples of fibers, but when more than two are necessary, the chemical ratios must increase proportionally. It is important to note that the chemical methods, while effective, often require harsh reagents and elevated temperatures, which can have adverse environmental impacts and may degrade the fibers' structural integrity. An enzymatic method was also employed to address these challenges and explore a more sustainable approach. Enzymatic delignification offers several advantages, such as operating under milder conditions and being more environmentally friendly, as it uses natural catalysts, like laccase, to selectively break down lignin without the need for aggressive chemicals. Furthermore, enzymatic methods preserve more cellulose fibers, critical for maintaining the absorbent properties essential for menstrual pads. The first enzymatic delignification process used four flasks. Each flask was filled with 45 mL of miracle grow, adding a 1000 mL pipette tip worth of both P. djamor and T. versicolor fungi. The miracle growth serves as a nutrient solution that promotes the growth and activity of the fungi, ensuring optimal production of laccase enzymes. This is crucial for breaking down the lignin in the fibers. Next, 60mg of pineapple and sisal fibers were added to each flask. This ensured that the experimental setup covered both fibers so that they could be degraded by both fungi. These flasks were incubated at 40 degrees Celsius [10]. For the next three days of this assay, qualitative analysis was conducted, and it was found that the laccase enzyme's degradability was decreasing. To overcome this, Luria broth was added to the flasks to provide additional nutrients and support the sustained growth of the fungi. Luria broth, commonly used in

microbial culture, contains essential nutrients like peptides and vitamins that promote robust cell growth.

### *2.6. 2,2-azinobis (3-ethylbenzothiazoline-6-sulfonic acid) (ABTS) method*

The 2,2-azinobis (3-ethylbenzothiazoline-6-sulfonic acid) (ABTS) method was used to measure the activity of laccase enzymes in breaking down lignin in the fibers. ABTS acts as a substrate for laccase, and its oxidation by the enzyme leads to a color change, which can be quantitatively measured through spectrophotometry. First, the sodium acetate buffer was diluted from 1.7 mM to 1.0 mM by mixing 2.8 µL of sodium acetate buffer with 5 mL of distilled water. Next, a stock solution of ABTS was prepared by dissolving 1.37 mg of ABTS in the diluted sodium acetate buffer, achieving a final concentration of 0.5 mM. This method used a UV spectrometer for which three cuvettes were prepared. The first cuvette served as a blank control, containing only 1 mL of the sodium acetate buffer without any enzyme to ensure no reaction occurred. The second cuvette was designated for the experimental condition involving Trametes versicolor (TV), containing 1 mL of the fungal culture medium, sodium acetate buffer, and ABTS stock solution.Similarly, the third cuvette was prepared for Pleurotus djamor (PD), using 1 mL of the PD culture medium alongside the buffer and ABTS solution. The volume of the culture medium was adjusted based on initial results to optimize enzyme concentration in each cuvette. After preparing the cuvettes, the spectrophotometer was set to 420 nm to measure absorbance, and readings were taken at 5-minute intervals to track changes in absorbance, which correlate with the activity of the laccase enzyme [11].

### *2.7. Test Squares*

The fibers were first made into test squares to prepare the fibers for the absorbency test. A template measuring 1.25″ x 1.25″ x 0.25″ was 3D printed Figure 3. After delignification, the wet pulp was decanted and left to air dry for three days. After drying, the resulting fluff was dry blended. Once the fluff pulp was fully processed, it was molded into the template to create uniform absorbent pads per the study's specifications [9].

A gelatine solution was prepared to test the absorbency of different fabrics. 2g of gelatine was added to 60 mL of water. The mixture was heated to 60°C while stirring continuously until all gelatine particles had fully dissolved. The solution was then divided into three 20 mL volumes, each allocated for testing cotton, pineapple fiber, and sisal fiber. Before testing, the temperature of each 20 mL volume was checked to ensure it had cooled to room temperature (21°C) to maintain consistent viscosity representative of menstrual fluid. These protocols are appropriate for 3 test fibers. Each fabric sample was weighed using a precision lab scale. The weighted fabrics were placed into containers of the same size. Then, 20 mL of the gelatine solution was poured onto each fabric sample. After 60 seconds, the fabrics were removed from their containers and weighed again to determine

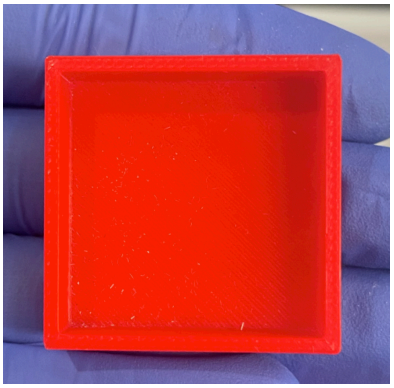

**Figure 3**. *3-D printed template*

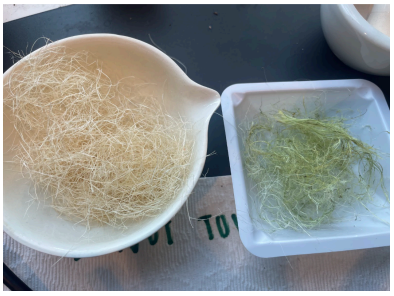

**Figure 4**. *Decorticated fibers (sisal, left; pineapple, right)*

the amount of liquid absorbed. The absorption index for each fabric was calculated by taking the ratio of the absorbed mass to the fabric's dry weight. [7].

## 3. Results

### *3.1. Decortication*

After soaking fibers in a sodium hydroxide and water bath and following it up with scraping with a spoon, if necessary, the fibers came to be separated and softened. Both fibers were prepared for enzymatic and chemical delignification.

An FTIR spectra was taken immediately after decortication. It is known that there is a high level of lignin in both the sisal and pineapple fibers. However, after the lignin is degraded, the fiber could be mainly composed of cellulose, leading to absorbency similar to cotton.

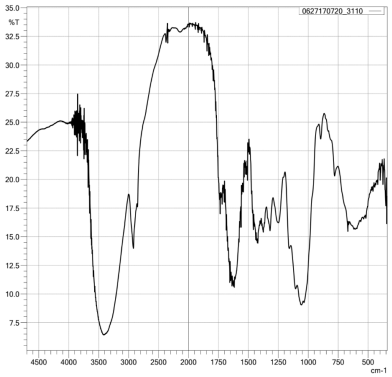


**Figure 5**. *Pineapple fibers pre-treatment FTIR spectra*

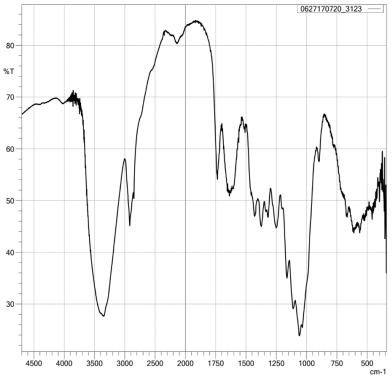


**Figure 6**. *Sisal Fibers pre-treatment FTIR spectra*

**Figure 7**. *Delignified fibers*

Above, the FTIR spectra of both fibers prior to delignification are shown. Key absorbance peaks around 1600 cm-1 and 1500 cm-1 show characteristics of aromatic skeletal vibrations typically associated with lignin. These initial observations confirm a significant presence of lignin within the fibers, setting a baseline for assessing the efficacy of subsequent delignification processes.

### *3.2. Delignification & ABTS*

The fibers went through both the chemical and enzymatic delignification processes and had varying results Figure 7. When chemically delignified, pineapple fibers (left) seemed to have a higher rate as the consistency of the fibers was much more similar to one of cotton. Sisal (right) on the other hand was not as soft since it had small, rigid fibers undelginified.

The enzymatic delignification, on the other hand, seemed to have a much slower process when breaking down lignin. The enzymatic delignification was completed by using T.versicolor and P.djamor from a culture. Below are the fibers' status at their optimal stage of degradation according to the ABTS assay Figure 8 & Figure 9.

An FTIR spectra was taken of these fibers to better understand the degradation of lignin shown in these fibers. The analysis of the spectra indicates that there are differences in lignin within the fibers. In the pineapple fiber spectrum, there is a noticeable reduction in

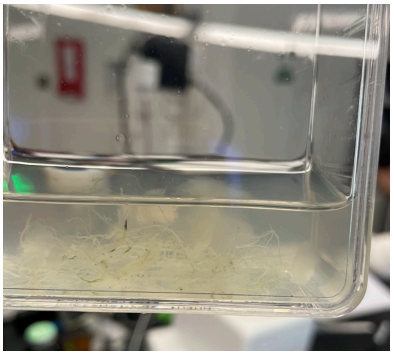

**Figure 8**. *Pineapple fibers day 6 of assay*

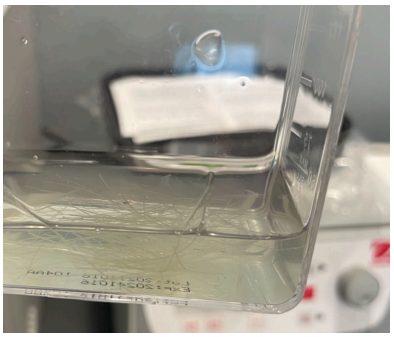

**Figure 9**. *Sisal fibers day 6 of assay*

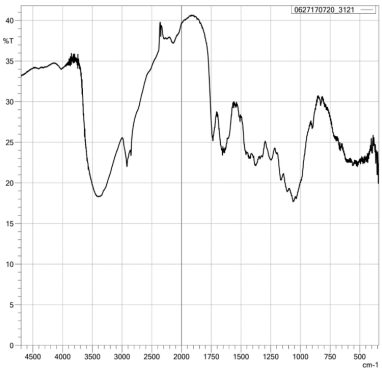


**Figure 10**. *FTIR spectra of pineapple*

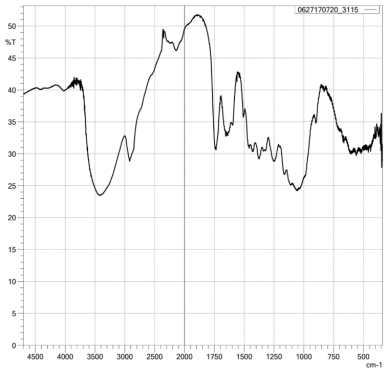


**Figure 11**. *FTIR spectra of sisal*

the intensity of peaks around 1600 cm-1 and 1500 cm-1, typically associated with the aromatic skeletal vibrations of lignin. The sisal fiber shows similar reductions, though less pronounced, suggesting varying efficiency in lignin degradation between the two fibers or inherent differences in their lignin composition. Additionally, the sisal fiber exhibits slight enhancement of peaks around 1100 cm-1, indicative of C-O stretching in cellulose and hemicellulose, suggesting that the cellulose structure remains intact and functional. The broadening and shifts in the OH stretch region around 3400 cm-1 in both fibers suggest increased hydroxyl group accessibility, likely due to lignin removal, which enhances fiber absorbency. These observations confirm using laccase to selectively degrade lignin without adversely affecting cellulose is crucial for developing biodegradable and absorbent materials suitable for sanitary products. The ABTS assay showed significant enzymatic activity in both T. versicolor and P. djamor cultures. There was a colorimetric change indicating a solid presence of laccase activity. This activity facilitated a noticeable degradation of lignin, particularly in the pineapple fibers, which demonstrated a higher delignification rate than the sisal fibers.

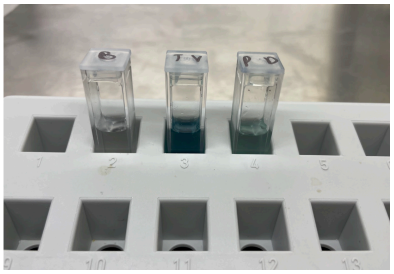

**Figure 12**. *ABTS assay indicator intensity*

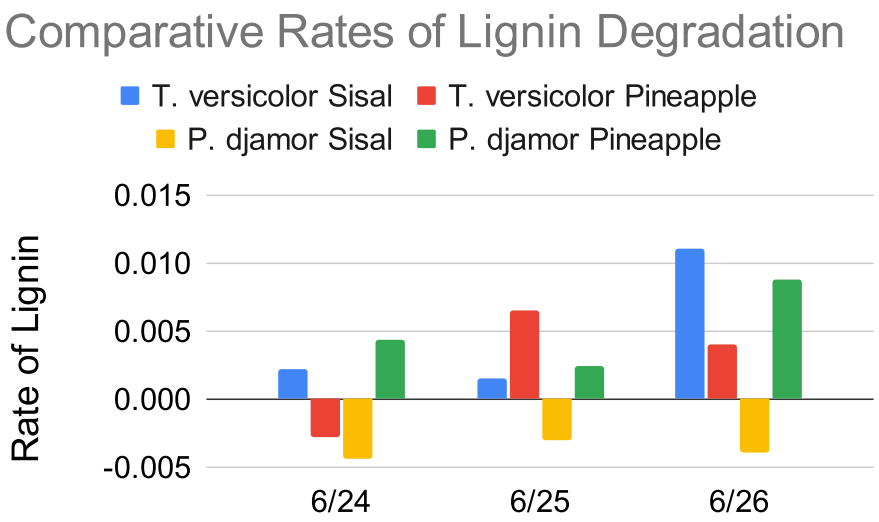


**Figure 13**. *Rates of Lignin Degradation in Pineapple and Sisal Fibers with T. versicolor vs. P. djamor*

Additionally, when focusing solely on the activity of the enzyme, the T. versicolor had a darker color change from the indicator than P. djamor Figure 12. The quantitative measurements confirmed that the laccase enzymes from both fungi effectively reduced the lignin content, enhancing the fibers' potential absorbency for use in menstrual pads.

The graph above represents the enzymatic delignification effects of T. versicolor and P. djamor on two types of fibers over three consecutive days. T. versicolor exhibits a more pronounced impact on sisal fibers, particularly on the assay's final day, where the lignin degradation rate peaks significantly compared to other treatments. This suggests a strong adaptability of T. versicolor enzymes towards the cellulose structure of Pineapple fibers, possibly due to better enzyme-fiber interaction or enzyme specificity towards the lignin components of Pineapple fibers. Conversely, P. djamor, while showing consistent activity across both types of fibers, does not reach the degradation rate exhibited by T. versicolor on either fiber. To further understand the significance of this conclusion, p-value tests were conducted. Though both were statistically insignificant as p-values were more significant than 0.05, by conducting more trials, there is potential for a lower p-value would likely be found to prove the differences between the two fungi. This could indicate a different mode of enzymatic action or lower efficiency of P. djamor enzymes in breaking down lignin under experimental conditions. To modify the enzymatic technique in hopes of getting higher rates of delignification, the powder T. versicolor was used rather than the culture. Only T. versicolor was used since it showed more significant delignification than P. Djamor in the ABTS assay. To prepare the enzyme solution for lignin degradation, 10 mg of laccase was dissolved in 10 mL of sodium acetate buffer (pH 4-5) to achieve a stock concentration of 1 mg/mL. The buffer was prepared by mixing 1.443 g of sodium acetate and 0.445 g of acetic acid in 160 mL of distilled water, adjusting the pH to approximately 5.0 with 10N hydrochloric acid (HCl), and then bringing the final volume to 200 mL with additional distilled water. This preparation resulted in a sodium acetate concentration of approximately 1.8 M and an acetic acid concentration of about 0.95 M, based on the provided weight percentages and molar masses. Following buffer preparation, 0.2 g of cut-up fibers from pineapple and sisal were placed into two flasks and labeled accordingly. Each flask then received 10 mL of the enzyme solution. The flasks were incubated at 40-50 degrees Celsius for 36 hours on a shaker or stirrer to facilitate the enzymatic degradation of lignin in the fibers. This method aims to optimize

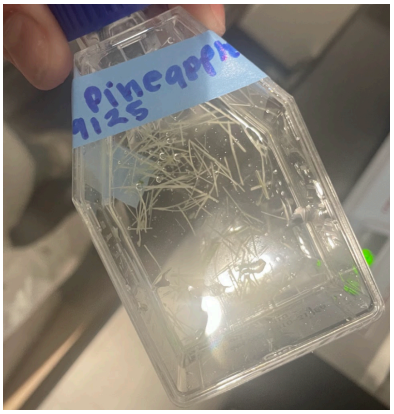

**Figure 14**. *Second enzymatic delignification assay pineapple*

**Figure 15.** *Second enzymatic delignification assay sisal*

the conditions for effective lignin removal, enhancing the fibers' potential absorbency [12].

Result analysis with the ABTS method and FTIR spectra aided in evaluating the practical implications of the delignification process on the fibers' usability in real-world applications. Due to lignin removal, the chemically softened fibers displayed enhanced malleability and surface area. This simulated the absorbency characteristics that are essential for high-quality menstrual pads. This step validated the delignification treatment's effectiveness in mimicking the desirable properties of cotton and provided a benchmark for comparing the functional performance of pineapple and sisal fibers post-treatment. Ultimately, absorbency was performed using the delignified fibers. For this, the softened fibers from chemical degradation were utilized.

### *3.3. Absorbancy Testing*

Absorption was assessed through the weight of the fibers. The initial dry weight, Wi, and a final wet weight, Wf, to define absolute absorption. By subtracting the initial weight from the final weight, then dividing the difference by the initial weight, the absorption, in grams fluid/grams fiber, can be found.

$$\text{Fluid Absorbed per Square} = \frac{\text{Final Weight} - \text{Initial Weight}}{\text{Area (Squares)}} \tag{1}$$

Absorption tests conducted over four trials revealed distinct behaviors among pineapple, sisal, and cotton fibers. Throughout all trials, cotton fibers consistently showed high absorbency. They maintained an average absorbency ratio of approximately 95.4 grams

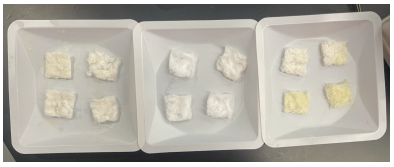

**Figure 16**. *Pad samples pre Absorption test*

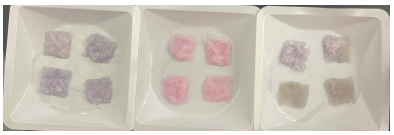

**Figure 17**. *Pad samples post absorption test*

fluid/grams square. This high performance is typical of cotton due to its natural properties, including a high degree of crystallinity and a porous structure, which are ideal for absorbing and retaining large amounts of liquid. In comparison, after treatment, pineapple and sisal fibers reached absorbency levels nearing those of cotton, with average ratios of 63.9 and 112.5 grams fluid/grams square, respectively. This performance is significant, demonstrating that with appropriate processing, such as enzymatic treatment, natural fibers like pineapple and sisal can be enhanced to perform at levels competitive with cotton for applications that require high fluid absorption. After conducting a t-test and following up with p-values for the four trials between pineapple and sisal, a p-value of 0.02 was found for cotton and pineapple, 0.381 for cotton and sisal, and 0.054 for sisal and pineapple were found. This is not significant, which means that both pineapple and sisal fibers, after treatment, have comparable levels of fluid absorption, making them similarly effective for applications requiring high absorbency. This convergence in performance underscores the efficacy of the enzymatic treatments used. It suggests that pineapple and sisal fibers could be viable alternatives to cotton in producing eco-friendly, absorbent materials. These findings open potential avenues for using pineapple and sisal fibers in sanitary products.

Evaluation of each individual fibers diameter, before and after the delignification process can show the extent of change the fibers have gone through. The swelling of the fiber is indicative of the degree of structural breakdown and increased porosity. Below, Figure 19 & Figure 20 compare a 28 gauge wire with the two fibers, pineapple and sisal, prior to delignification. The 28 gauge wire, on the right, is 0.321 mm in diameter and through using ImageJ's measurements and cross-sectional area analysis, the pineapple fiber came out to be 0.136 mm while the sisal fiber came out to be 0.145 mm. After delignification Figure 21 & Figure 22 the pineapple fiber came out to be 0.00834 mm while the sisal fiber came to be 0.01468 mm showing a significant reduction in diameter due to the removal of lignin components.

The overall reduction in diameter is 93.87% for the pineapple fiber and 89.87% for the sisal fiber.

| Trial | Pineapple | Sisal | Cotton |
|---|---|---|---|
| Trial 1 | 46.5 | 72.8 | 94.5 |
| Trial 2 | 57.3 | 102.3 | 100.0 |
| Trial 3 | 73.4 | 123.2 | 90.2 |
| Trial 4 | 78.5 | 151.7 | 96.7 |
| Average | 63.9 | 112.5 | 95.4 |

**Table 1**. *Sisal, cotton, pineapple absorption test grams fluid/grams square*

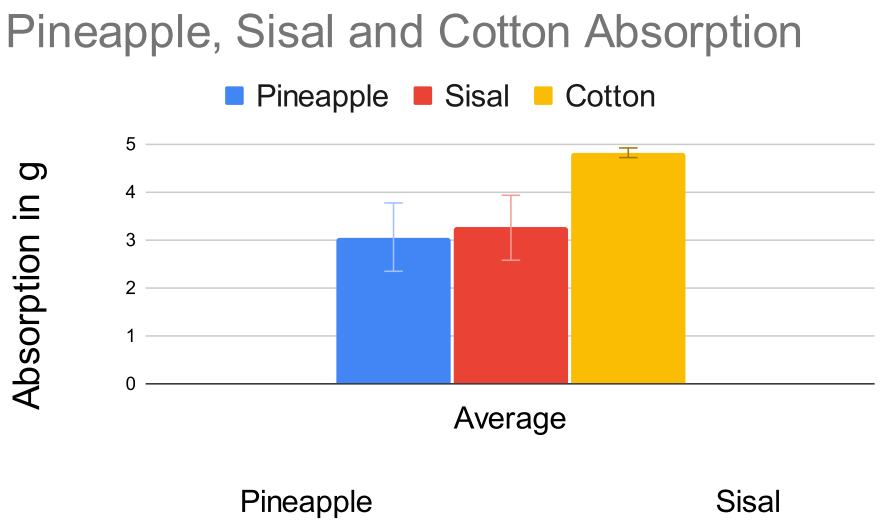


**Figure 18**. *Sisal, pineapple, cotton absorption test*

## 4. Conclusions

Delignifying fibers and testing for absorbance from plants found in semi-arid regions is one of the first steps in addressing the crucial issues of period poverty. Using locally sourced, biodegradable materials reduces dependency on non-renewable resources like high-maintenance crops like cotton and offers a cost-effective solution for communities in resource-limited settings. Throughout these experiments, cotton, a commonly used material in menstrual pads, was used as a benchmark. By conducting the ABTS assay, T. versicolor seemed to be a suitable source of laccase, specifically for the fibers used for this project. Although enzymatic delignification was not as successful as chemical

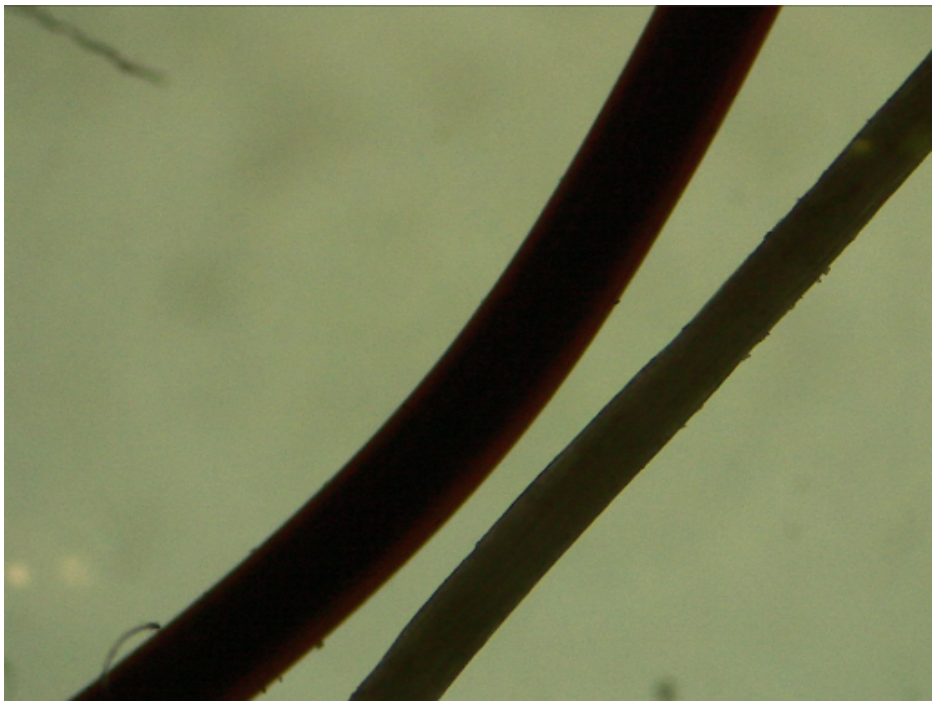

**Figure 19**. *Pre-delignified Pineapple Fiber Compared to 28 Gauge Wire*

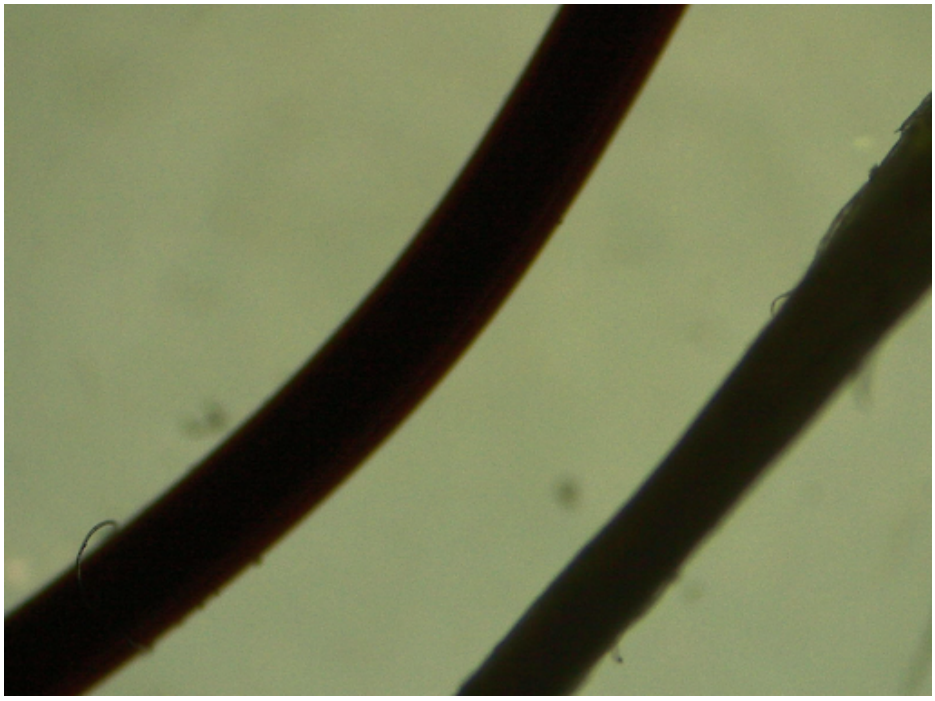

**Figure 20**. *Pre-delignified Pineapple Fiber Compared to 28 Gauge Wire*

delignification, lignin content was still decreased based on the FTIR. Combining laccase activity and decreased lignin concentrations promises improved fiber absorbency and functionality. Additionally, from absorption testing, it was found that both pineapple and sisal fibers reached absorbency levels nearing those of cotton. This implies that the fibers can be competitive with cotton as menstrual pads with enhancement. The diameter comparison through ImageJ allowed for further confirmation of lignin component

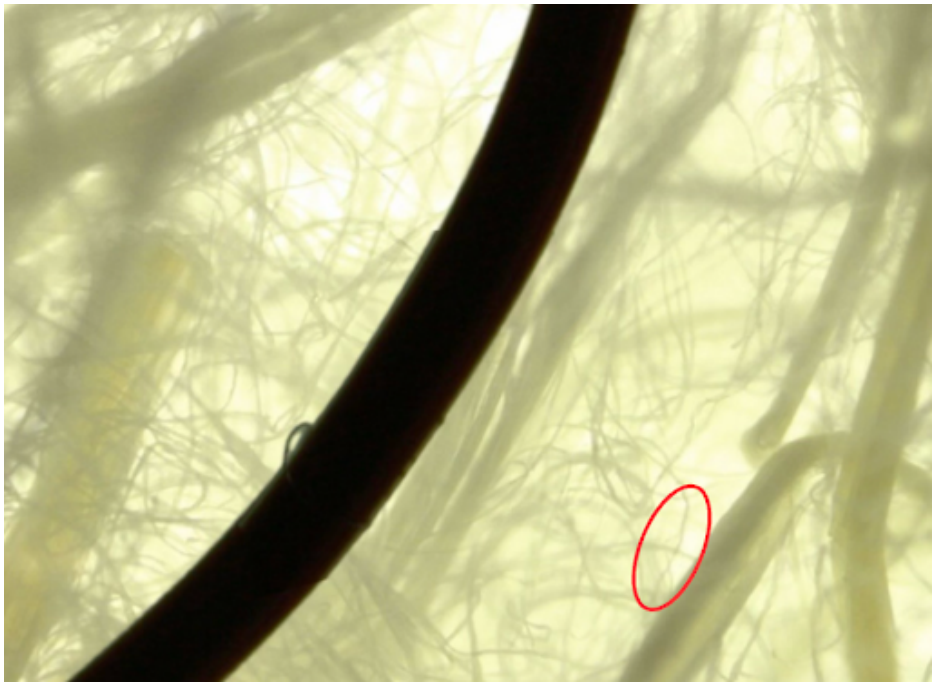

**Figure 21**. *Delignified Pineapple Fiber Compared to 28 Gauge Wire. The red circle is indicative of the exact fiber that was measured.*

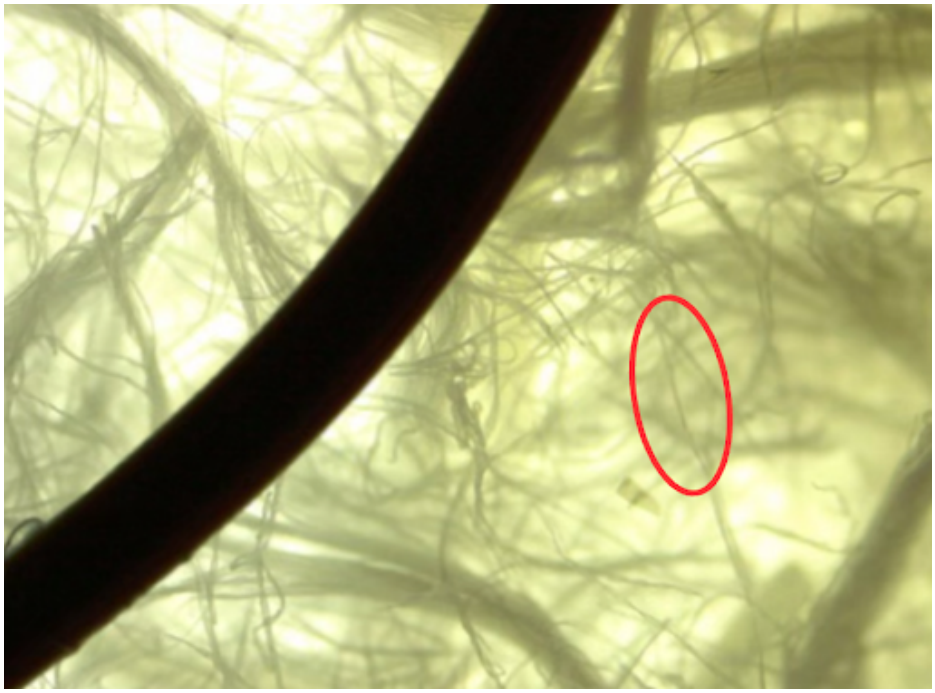

**Figure 22**. *Delignified Sisal Fiber Compared to 28 Gauge Wire. The red circle is indicative of the exact fiber that was measured.*

removal as there was a 93.87% reduction in the pineapple fiber and 89.87% for the sisal fiber.

## 5. Discussion

The visual examination throughout lignin degradation yielded importance on how the fiber samples react to the varying delignification treatments. For instance, when completing the chemical delignification, the fibers began to look similar to cotton. The comparison to cotton was a visual basis for determining lignin degradation. When the enzymatic delignification occurred, the fibers visually did not look similar to cotton, even after day three passed when the laccase activity peaked. These visual results indicated that a change was necessary. Still, we did not realize that T. versicolor seemed to be the suitable enzyme for these fibers until the ABTS assay was performed. Though quantitative data is crucial, qualitative data yields just as much information. After realizing the sudden shortfall in laccase activity after day three of performing the ABTS method on the initial enzymatic delignification with T. versicolor and P. djmor fungi, it was realized that the laccase enzyme's degradability was decreasing. To supplement the nutritional deficiency, luria broth was obtained to revive laccase activity; unfortunately, positive results were not shown. Throughout this experiment, FTIR spectra were often taken. Taking these spectra includes crushing up the samples, in this case, the fibers, to the point where it was nearly perfectly homogenized with the KBr used as a matrix for the film within the machine. Unfortunately, these fibers are very stubborn, especially before delignifying. Therefore, despite the pre-FTIR treatment of crushing with mortar and pestle or freezing to make the fibers brittle with dry ice, there may still have been minor errors with the output spectra. Fortunately, the deficit of lignin was still apparent, so perhaps if the reading was more precise, the loss of lignin would have been more drastic. Initially, the intensity of red was to be a determinant of absorbency. Qualitatively, however, after the first trial, a violet shade was observed on the pineapple and sisal fibers post-absorption. This could indicate residual coloration from the test solution, suggesting

differences in how these fibers interact with and retain fluid-based substances. So, instead, the difference in weights over the initial weights is the sole factor of absorption efficacy. Additionally, the initial weights of the sisal, pineapple and cotton fibers had disparities given the nature of each pad. Sisal is usually denser and stronger therefore, it has a very high initial weight compared to pineapple and cotton fibers. Pineapple fibers are less dense compared to sisal. Cotton is the least dense therefore it has the lowest initial weight. Substantial room exists for future work. The research findings from the results can be used as a baseline to enhance enzymatic delignification. This will open an environmentally sustainable avenue for developing biodegradable and high-performance menstrual products. Further investigations could focus on optimizing enzyme concentrations and reaction conditions to maximize lignin removal while preserving fiber integrity by conducting mass trials. Additionally, exploring the combination of different types of enzymes, potentially through a synergistic approach, might improve efficiency and cost-effectiveness, making these natural fibers a viable alternative to traditional materials in various consumer products beyond just sanitary pads. Exploring surface tensiometry is also critical as it provides insights into the wettability and spreadability of fluids on fiber surfaces, which is essential for assessing their potential in absorbent applications. Future studies might also explore the scalability of these processes for industrial application, evaluate the long-term environmental impacts of widespread adoption of such fibers, and assess the carbon footprint. Moreover, researching additional natural fibers native to third-world countries could tailor solutions to specific local needs, further expanding the global impact of this sustainable technology.

My sincere gratitude goes to the Research in Biology program at the North Carolina School of Science and Mathematics at Morganton as well as Mrs. Jennifer Williams and Dr. Mareca Lodge.

## References

[1] R. Kaur, K. Kaur, and R. Kaur, “Menstrual Hygiene, Management, and Waste Disposal: Practices and Challenges Faced by Girls/Women of Developing Countries,” *Journal of Environmental and Public Health*, vol. 2018, pp. 1–9, 2018, doi: 10.1155/2018/1730964.

[2] M. E. Harrison and N. Tyson, “Menstruation: Environmental impact and need for global health equity,” *International Journal of Gynecology & Obstetrics*, vol. 160, no. 2, pp. 378–382, 2022, doi: 10.1002/ijgo.14311.

[3] “Progress on household drinking water, sanitation and hygiene 2000-2022: Special focus on gender.,” 2023, [Online]. Available: https://data.unicef.org/resources/jmp-report-2023/

[4] F. Angeli, A. K. Jaiswal, and S. Shrivastava, “Integrating poverty alleviation and environmental protection efforts: A socio-ecological perspective on menstrual health management,” *Social Science & Medicine*, vol. 314, p. 115427, 2022, doi: 10.1016/j.socscimed.2022.115427.

[5] M. Elledge *et al.*, “Menstrual Hygiene Management and Waste Disposal in Low and Middle Income Countries—A Review of the Literature,” *International Journal of Environmental Research and Public Health*, vol. 15, no. 11, p. 2562, 2018, doi: 10.3390/ijerph15112562.

[6] A. Etale, A. J. Onyianta, S. R. Turner, and S. J. Eichhorn, “Cellulose: A Review of Water Interactions, Applications in Composites, and Water Treatment,” *Chemical Reviews*, vol. 123, no. 5, pp. 2016–2048, 2023, doi: 10.1021/acs.chemrev.2c00477.

[7] J. Foster and P. Montgomery, “A Study of Environmentally Friendly Menstrual Absorbents in the Context of Social Change for Adolescent Girls in Low- and Middle-Income Countries,” *International Journal of Environmental Research and Public Health*, vol. 18, no. 18, p. 9766, 2021, doi: 10.3390/ijerph18189766.

[8] Q. Liu, L. Luo, and L. Zheng, “Lignins: Biosynthesis and Biological Functions in Plants,” *International Journal of Molecular Sciences*, vol. 19, no. 2, p. 335, 2018, doi: 10.3390/ijms19020335.

[9] A. Molina, A. Kothari, A. Odundo, and M. Prakash, “Agave sisalana: towards distributed manufacturing of absorbent media for menstrual pads in semi-arid regions,” *Communications Engineering*, vol. 2, no. 1, 2023, doi: 10.1038/s44172-023-00130-y.

[10] R. Banerjee, A. D. Chintagunta, and S. Ray, “Laccase mediated delignification of pineapple leaf waste: an ecofriendly sustainable attempt towards valorization,” *BMC Chemistry*, vol. 13, no. 1, 2019, doi: 10.1186/s13065-019-0576-9.

[11] "Comparative study on the determination of assay for laccase of Trametes sp," 2008, [Online]. Available: https://www.researchgate.net/publication/228345841_Comparative_study_on_the_determination_of_assay_for_laccase_of_Trametes_sp

[12] M. M. Atalla, H. K. Zeinab, R. H. Eman, A. Y. Amani, and A. A. E. A. Abeer, "Characterization and kinetic properties of the purified Trematosphaeria mangrovei laccase enzyme," *Saudi Journal of Biological Sciences*, vol. 20, no. 4, pp. 373–381, 2013, doi: 10.1016/j.sjbs.2013.04.001.

Open Access | https://doi.org/10.62329/khkv4846

# Binding Affinity and Selectivity of Peptide Ligands for G-Protein-Coupled Receptors

**Lily Li**[1]

[1]NCSSM

**Morganton Scientific**

*North Carolina School of Science and Mathematics*

Journal of Student STEM Research

## Abstract

Chemokine receptors like CXCR4 play critical roles in cellular signaling, influencing processes such as cancer metastasis and immune regulation. Understanding CXCR4's interaction with its natural ligand, CXCL12, is key for targeted drug design. In this study, we used SwissDock to probe the binding interactions of CXCL12 with CXCR4, comparing them to CXCR3 to evaluate specificity. The docking analysis showed several binding clusters for CXCR4, out of which Cluster 6 was the most promising with a highly favorable SwissParam Score of -13.3878 and interaction patterns such as many hydrogen bonds and hydrophobic contacts. Critical residues, including Asp262 and Glu288, were found to stabilize ligand binding. In contrast, CXCR3 showed reduced binding affinity with the highest score of -10.6949, likely due to the absence of key residues like Arg167 and Glu288, which diminished hydrogen bonding and hydrophobic interactions. These findings highlight the structural basis for CXCL12's specificity toward CXCR4, guiding the development of CXCR4-targeted therapeutics. Future work should validate these results experimentally and assess dynamic conformational changes through molecular dynamics simulations.

**Keywords** Binding Affinity, Selectivity, Peptide Ligands, CXCL12

## 1. Introduction

G-Protein-Coupled Receptors (GPCRs) represent a vital family of integral membrane proteins, pivotal in mediating cellular signaling across a broad spectrum of physiological systems. In man, more than 800 genes in the human genome encode GPCRs, which regulate critical biological processes, including neurotransmission, immune response, hormonal signaling, and sensory perception [1]. Structurally, these receptors all possess a conserved architecture of seven transmembrane $\alpha$-helices, an extracellular ligand-binding domain, and an intracellular domain responsible for interacting with G-proteins or other signaling molecules. Their central role in maintaining physiological homeostasis makes GPCRs a major focus in pharmacology, with approximately 34 percent of all FDA-approved drugs targeting this receptor family [2]. Within this family, the chemokine receptor CXCR4 has emerged as an important therapeutic target because it plays a critical role in the development of several pathological conditions, such as cancer, HIV infection, and inflammatory diseases.

CXCR4 is widely expressed on the surface of various cells and is primarily activated by its natural ligand, CXCL12 (also known as stromal-derived factor-1 or SDF-1). The CXCR4-CXCL12 signaling axis sets up fundamental physiological processes, such as hematopoiesis, immune surveillance, and embryonic development. However, the dysregulation of this axis contributes to cancer metastasis, which accounts for the high mortality rates related to the disease [3]. CXCR4 allows for tumor cell migration to organs outside of their native sites, while activation encourages angiogenesis, immune avoidance, and anti-apoptotic properties to enhance tumor development. Characteristics

**Published** Jun 27, 2024

**Correspondence to**
Lily Li
li25lily@ncssm.edu

include making CXCR4 a target of interest in therapeutic intervention, particularly for metastatic cancers. Among new treatment methods, peptide-based ligands have gained attention for their specific advantages over traditional small molecules. Peptides show high receptor specificity, reduced off-target effects, improved tissue penetration, and lower immunogenicity, although challenges remain in achieving optimal binding affinity and selectivity [4].

The CXCL12 signaling network primarily operates through two receptors: CXCR4 and CXCR7, each with distinct functional roles. CXCR4 triggers G-protein-coupled pathways, activating downstream effectors such as phosphatidylinositide 3-kinase (PI3K), protein kinase B (AKT), and mitogen-activated protein kinase (MAPK). These pathways are critical for regulating cell survival, proliferation, and migration (Figure 1). In contrast, CXCR7 signals mainly via $\beta$-arrestin-mediated pathways, which influence receptor internalization, recycling, and cellular responses such as adhesion and migration [5]. Interestingly, CXCR4 and CXCR7 can form heterodimers, modulating their signaling outputs and affecting the fate of CXCL12. The interaction dynamics of CXCR4 with other ligands, such as macrophage migration inhibitory factor (MIF), further underscore its functional versatility.

Upon binding of CXCL12, intracellular signal transduction via the heterotrimeric G-protein complex coupled to CXCR4 is mediated by G$\alpha$, G$\beta$, and G$\gamma$ subunits. Several cascades are activated, such as the PI3K-AKT pathway for survival and the MAPK pathway for proliferation. These pathways are important in normal physiological functions but are often in control of cancer, toward the promotion of disease progression [6].

Peptide-based therapies that target the CXCR4-CXCL12 interaction are a promising strategy in efforts to combat cancer metastasis. By disrupting this axis, peptide inhibitors can prevent tumor cell migration to distant tissues, reducing metastatic potential. However, in order to develop these therapeutics, understanding the structural and sequence of the peptide-receptor interaction is important. High specificity and selectivity are very important to minimize off-target effects and enhance therapeutic efficacy.

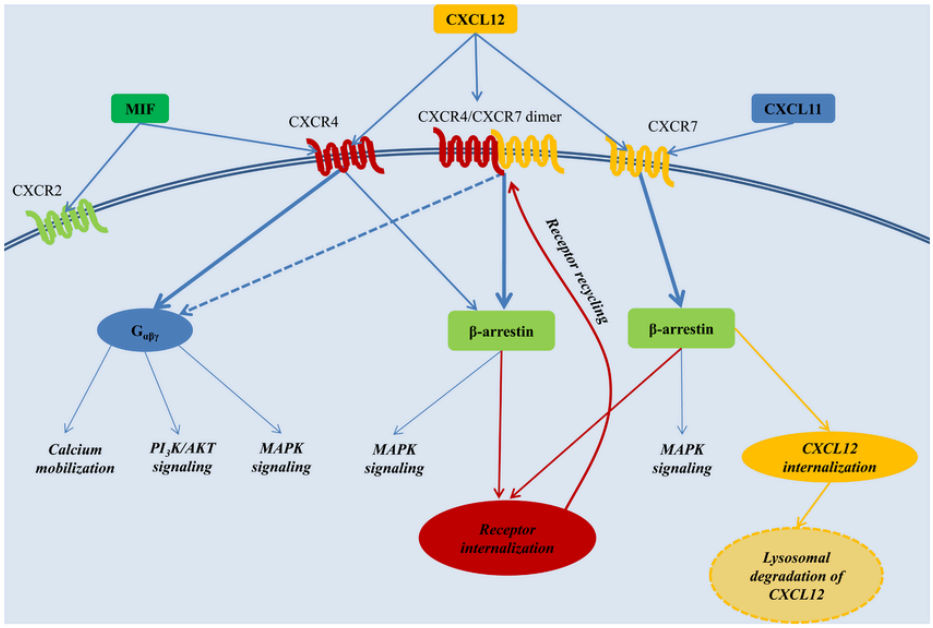


**Figure 1**. *The CXCL12 signaling network. From the network, the simulation of CXCR4 triggers G-protein-coupled signaling.*

Computational tools such as molecular docking, molecular dynamics simulations, and QSAR modeling enable researchers to predict ligand binding orientation, estimate binding affinity, and study structural features for receptor specificity.

The present study aims to explain the structural and sequence-specific factors that influence peptide binding to CXCR4. Using structural data from the Protein Data Bank (PDB ID: 3OE6 for CXCR4 and PDB ID: 2KEC for CXCL12), we employ molecular docking to predict binding poses and estimate binding free energies. Molecular dynamics simulations were used to further explore the stability of ligand-receptor interactions and reveal any conformational changes upon ligand binding.

This integrated approach is expected to provide a comprehensive understanding of peptide-GPCR interactions, paving the way for the development of peptide inhibitors with therapeutic potential. Targeting the CXCR4-CXCL12 axis, this study will further the area of GPCR-targeting drug discovery and provide new therapeutic options in combating metastasis and other CXCR4-related diseases. Ultimately, the insights gained from this study could significantly contribute to the design of peptide-based therapeutics, addressing current challenges in binding affinity and selectivity while improving patient outcomes.

## 2. Computational Approach

This study explored the binding interactions between CXCR4 chemokine receptor and its ligand, CXCL12, investigating its selectivity with respect to CXCR3 through a systematic computational approach. Combining receptor and ligand preparation, molecular docking, and interaction analyses, through this study, the aim is to identify the most promising binding poses and their biological validation. This section details the methodology and tools used throughout the research.

The receptor of choice for this study was the CXCR4 chemokine receptor, the PDB ID is 3OE6. This receptor was selected due to its high-resolution crystal structure at 3.20 Å, providing a reliable framework for the analysis of interactions with CXCL12. The receptor structure was prepared using PyMOL (Schrödinger, LLC) by downloading the 3OE6.pdb file from the RCSB Protein Data Bank. After loading the structure into PyMOL, the non-essential components such as water molecules and co-crystallized ligands were removed using remove solvent and remove organic (Figure 2). This will ensure a clean environment around the receptor to be used for docking.

Hydrogen atoms were added to the receptor structure using the h-add command to facilitate appropriate bonding interactions. The protonation states of the receptor were then checked and adjusted with PDB2PQR to match physiological conditions at pH 7.4. Following a visual inspection to ensure the integrity of the binding pocket structure, the processed receptor was saved as receptor-prepared.pdb for subsequent docking simulations.

Ligand preparation focused on CXCL12, a peptide optimized to include only its first 17 residues, CXCL12, 1-17, with the emphasis of maintaining the active binding region. The peptide was modeled and minimized using Avogadro 2 for proper geometry and generation of the SMILES representation of input for docking. The final structure was saved in PDB format, as requested for docking.

For docking studies, SwissDock was selected because it carries out the EADock DSS algorithm that has been widely used for efficient prediction of receptor-ligand interactions. The prepared receptor structure (3OE6) and the optimized ligand were uploaded to SwissDock, with docking settings applied in order to allow conformational

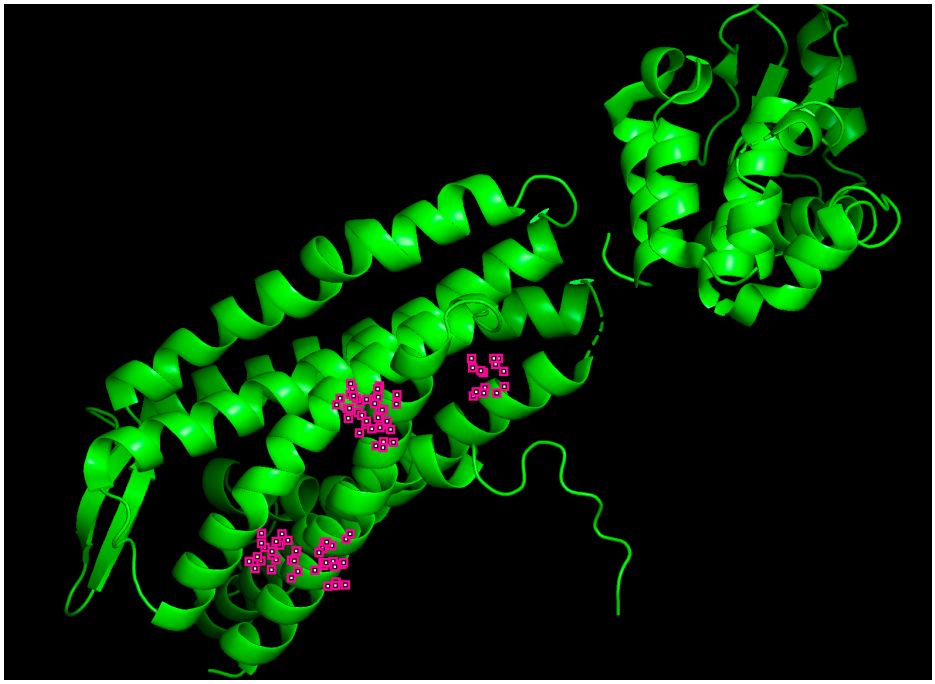

**Figure 2.** *3OE6 PyMOL Structure Visualization*

adjustments in the ligand. To assess the selectivity of the ligands, the process was repeated for CXCR3 (PDB ID: 4RAU), a receptor that is closely related to CXCR4. CXCR3 was prepared using the same protocol as before to make sure consistency is maintained for the various docking experiments.

Docking results from SwissDock were then obtained in detail with key scores, including AC Score (Atomic Contact Energy) and SwissParam Score, used to rank clusters. For CXCR4, the most negative SwissParam Score was for Cluster 6, with a value of -13.3878, indicating the highest binding affinity; Cluster 0 was also identified as a promising candidate with a SwissParam Score of -13.2294 and a lower AC Score of 66.855750.

After the docking results were obtained from SwissDock, data were visualized in UCSF Chimera for detailed analysis of the interactions with the receptor. Both complexes, CXCR4 and CXCR3, were loaded into Chimera's FindHBond and Find Clashes/Contacts were used to identify H-bonds, hydrophobic contacts, and salt bridges. This allowed more insights into molecular mechanisms that show the stability of the complex. Hydrogen bonds, for example, were visualized and measured to confirm their contribution to stability, while hydrophobic interactions were highlighted by coloring the receptor surface based on hydrophobicity.

The selectivity was analyzed by comparing the binding scores and interaction patterns of CXCR4 with CXCR3. From the SwissDock results, CXCL12 had higher affinity toward CXCR4, as depicted by more negative SwissParam Scores and stronger interaction profiles in Cluster 6. This is further supported at Chimera, where the distinct binding poses revealed unique interaction patterns that distinguish the binding behavior of the ligand between the two receptors.

Overall, CXCR4 demonstrates higher binding affinity for CXCL12 (1-17) than CXCR3, with Cluster 6 of CXCR4 appearing as the most promising binding pose. This matched with the biological function of the receptor and with the hypothesis of selective ligand binding. Experimental validation is also used, such as SPR/ITC, to validate these predicted affinities

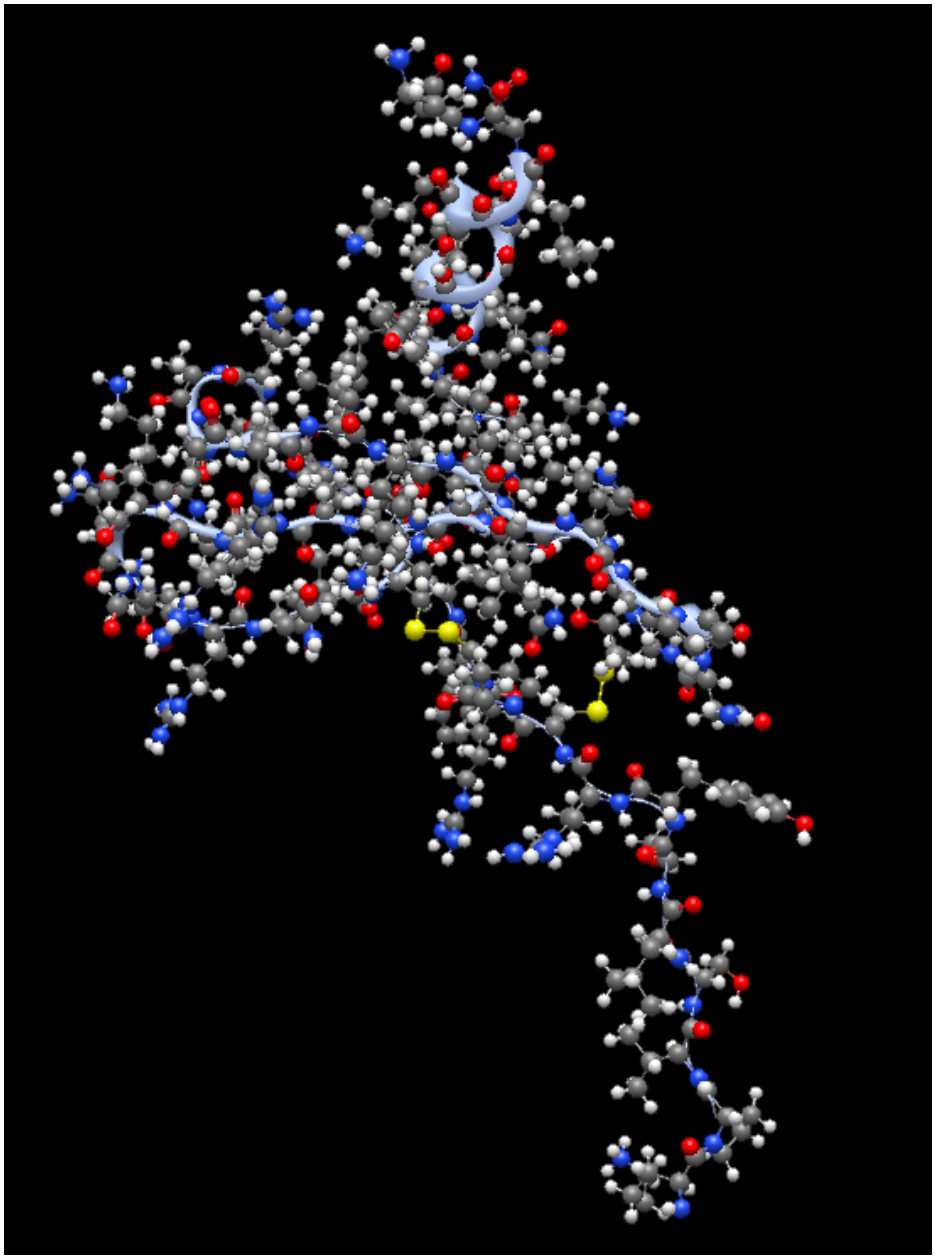

**Figure 3.** *Optimized CXCL12 using Avogadro 2 Visualization*

and interactions. This computational approach shows the utility of combining computational docking and visualization to show receptor-ligand interactions.

## 3. Results and Discussion

The results were analyzed to assess the strength and specificity of receptor-ligand interactions and to explore selectivity against the closely related CXCR3 receptor. By examining docking scores, visualizing binding poses, and examining interaction patterns, providing more depth into receptor-ligand dynamics.

The docking results of CXCR4 showed some clusters of binding poses with variable interaction energies. Cluster 6 was the most promising cluster based on its SwissParam Score of -13.3878, indicating the highest binding affinity among all the clusters. This was

| Cluster Number | AC Score | SwissParam Score |
|---|---|---|
| 0 | 66.8557 | -13.2294 |
| 1 | 84.0352 | -11.7598 |
| 2 | 86.30812 | -11.6143 |
| 3 | 90.8880 | -12.0000 |
| 4 | 110.5392 | -10.9333 |
| 5 | 113.4679 | -12.1289 |
| 6 | 121.9372 | -13.3878 |
| 7 | 153.4154 | -9.2210 |
| 8 | 160.9903 | -12.2709 |
| 9 | 256.7092 | -5.5639 |

**Table 1**. *Cluster number, AC Score, and SwissParam Score for the CXCR4 and CXCL12 interaction docking*

further supported by the presence of numerous stabilizing hydrogen bonds and hydrophobic contacts. Visual inspection using UCSF Chimera highlighted key residues within the CXCR4 binding pocket that interacted with CXCL12, such as Asp262 and Glu288, which formed hydrogen bonds with the ligand's polar groups. These interactions align with the receptor's known binding mechanism and suggest a biologically plausible binding pose.

Cluster 0, though slightly less favorable regarding binding affinity (SwissParam Score: -13.2294), showed the lowest AC Score of 66.855750, which indicates strong atomic-level interactions (Table 1). The binding poses of Cluster 0 showed a different orientation of CXCL12 inside the pocket, with key interactions involving residues such as Arg167 and His281. These are implicated in the stabilization of the hydrophobic core of the ligand, further underlining the relevance of the cluster. Although having a slightly higher SwissParam Score, Cluster 0 is still significant due to its unique interaction profile, which may be important for alternate binding modes under physiological conditions.

From the analysis of interaction patterns, Cluster 6 showed a higher number of hydrogen bonds and hydrophobic contacts than Cluster 0. For example, five hydrogen bonds were observed in Cluster 6, while three were seen in Cluster 0. This indicates that the binding pose of Cluster 6 is more stable. Moreover, in Cluster 6, hydrophobic interactions were highly focused around aromatic residues like Trp94 and Phe292, contributing to a more stable hydrophobic environment for CXCL12. These indicated that Cluster 6 represents an optimal binding configuration since the appropriate balance of polar and non-polar interactions enhances its affinity. Changes in AC Score and SwissParam Score for the different cluster numbers were graphed, showing cluster number 0 has the lowest AC score, and Cluster 6 has the lowest SwissParam Score (Figure 4).

Ligand selectivity was further tested by the docking of CXCL12 with CXCR3, its related receptor. The results showed that CXCL12 binds less effectively to CXCR3, as evidenced by its higher (less negative) SwissParam Scores across all clusters. For example, Cluster 0 of CXCR3, which had the best binding affinity, still had a SwissParam Score of -10.6949, considerably less favorable than those for CXCR4. Similarly, for CXCR3, Cluster 0 showed a better binding profile compared to Cluster 3, as it had more favorable scores (Table 2). And from the graph showing the AC score and SwissParam Score for CXCR3, we can see a pattern where cluster 3 has the lowest AC Score and SwissParam Score (Figure 5).

A detailed comparison of the binding poses between CXCR4 and CXCR3 revealed notable differences. In CXCR3, the binding pocket lacked critical residues that contributed to

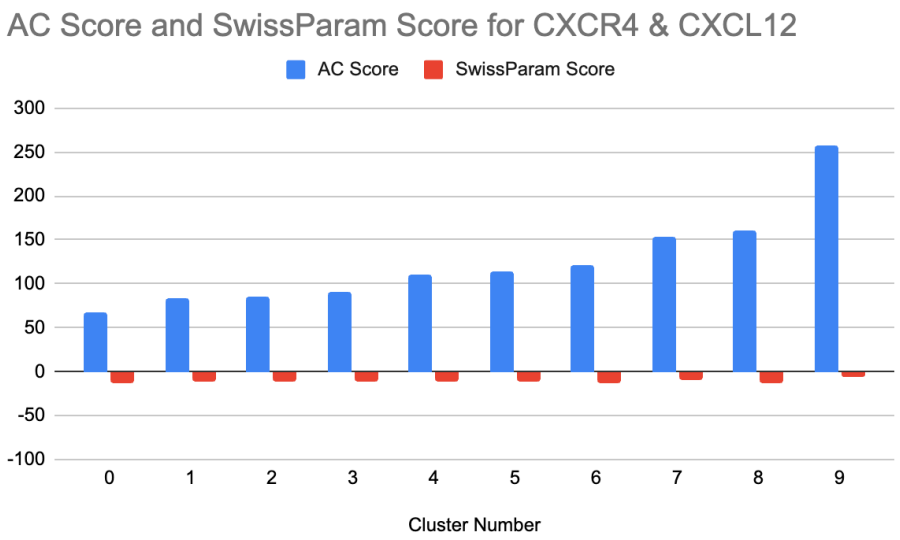


**Figure 4.** *Graph showing the cluster number vs. AC Score and SwissParam Score for the CXCR4 and CXCL12 interaction docking.*

CXCL12's stabilization in CXCR4. For example, while Arg167 and Glu288 in CXCR4 formed strong hydrogen bonds with the ligand, the corresponding residues in CXCR3 were either missing or could not establish similar interactions. This difference in residue composition, along with the spatial configuration, underlines the selectivity of CXCL12 to CXCR4. Secondly, the hydrophobic contact in CXCR3 was less deep and involved mainly aliphatic residues. This resulted in lower binding stability.

Visual inspection of the binding poses in Chimera gave further insight into the orientation and interaction pattern of the ligand. In the case of CXCR4, Cluster 6 showed a more compact ligand conformation, allowing for maximum interaction with the receptor pocket, while Cluster 0 adopted a slightly extended conformation. This indicates that CXCL12 may adopt multiple binding modes, depending on the conformational flexibility of the receptor. The binding poses obtained for CXCR3 seemed less well fitted, as the ligand was partially exposed outside the binding pocket of the receptor, indicating suboptimal geometry of interaction. In the case of CXCR4 and CXCL12 interaction, Cluster 6 was analyzed to show the hydrogen bonding (Figure 6).

| Cluster Number | AC Score | SwissParam Score |
|---|---|---|
| 0 | 91.9419 | -10.6949 |
| 1 | 104.9577 | -10.105 |
| 2 | 105.3274 | -10.8275 |
| 3 | 109.2432 | -9.4856 |
| 4 | 116.0195 | -9.023 |
| 5 | 123.229 | -9.1946 |
| 6 | 130.2115 | -8.8027 |
| 7 | 154.4236 | -9.8637 |
| 8 | 224.8291 | -7.8741 |
| 9 | 267.3134 | 3.9274 |

**Table 2.** *Cluster number, AC Score, and SwissParam Score for the CXCR3 and CXCL12 interaction docking.*

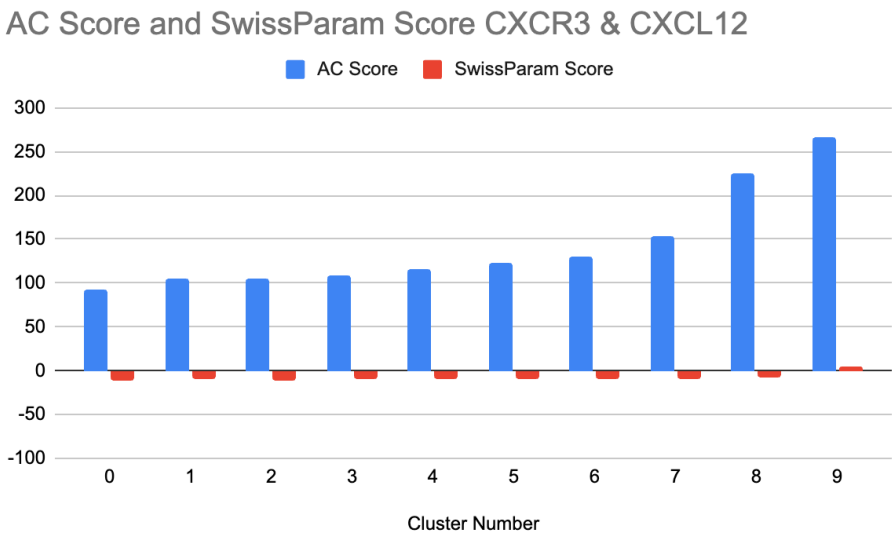


**Figure 5.** *Graph showing the cluster number vs. AC Score and SwissParam Score for the CXCR3 and CXCL12 interaction docking.*

The results are in good agreement with the experimental data deposited in the BindingDB database, as it had shown the binding of CXCR4 against ligands, like CXCL12, with nanomolar affinity. SwissParam Scores and interaction pattern of CXCR4 computational approach accurately reproduced the experimentally obtained receptor binding properties. Similarly, as compared to CXCR4, lower binding affinity obtained in case of CXCR3 indicates that the role and structural make-up of this receptor diverged with its cognate receptor CXCR4.

Overall, the results point toward the specificity of CXCL12 for CXCR4, and Cluster 6 represents the most favorable binding pose. This specificity is likely driven by the unique composition and arrangement of residues within the CXCR4 binding pocket that allow for strong polar and hydrophobic interactions. Lower affinity for CXCR3 further reinforces the selectivity of CXCL12 and underlines the structural determinants of this specificity.

These findings have important implications for the design of drugs targeting CXCR4. The identification of key residues involved in ligand stabilization provides the basis for designing high-affinity inhibitors or modulators. Moreover, the insight into selectivity could underpin the development of compounds designed to minimize off-target effects against related receptors such as CXCR3. Further studies should be performed to experimentally validate the affinities and interactions predicted using techniques such as SPR or ITC. Further molecular dynamics simulation could be used to investigate conformational flexibility of the receptor-ligand complex and its implications for binding stability.

In summary, this study illustrates the power of computational docking and visualization in analyzing the nature of receptor-ligand interactions. The results highlight the selective affinity of CXCL12 for CXCR4 and provide a detailed characterization of the binding poses and interaction patterns driving this specificity. These findings add to our knowledge of chemokine receptor biology and provide a basis for the rational design of therapeutics targeting CXCR4.

## 4. Conclusions

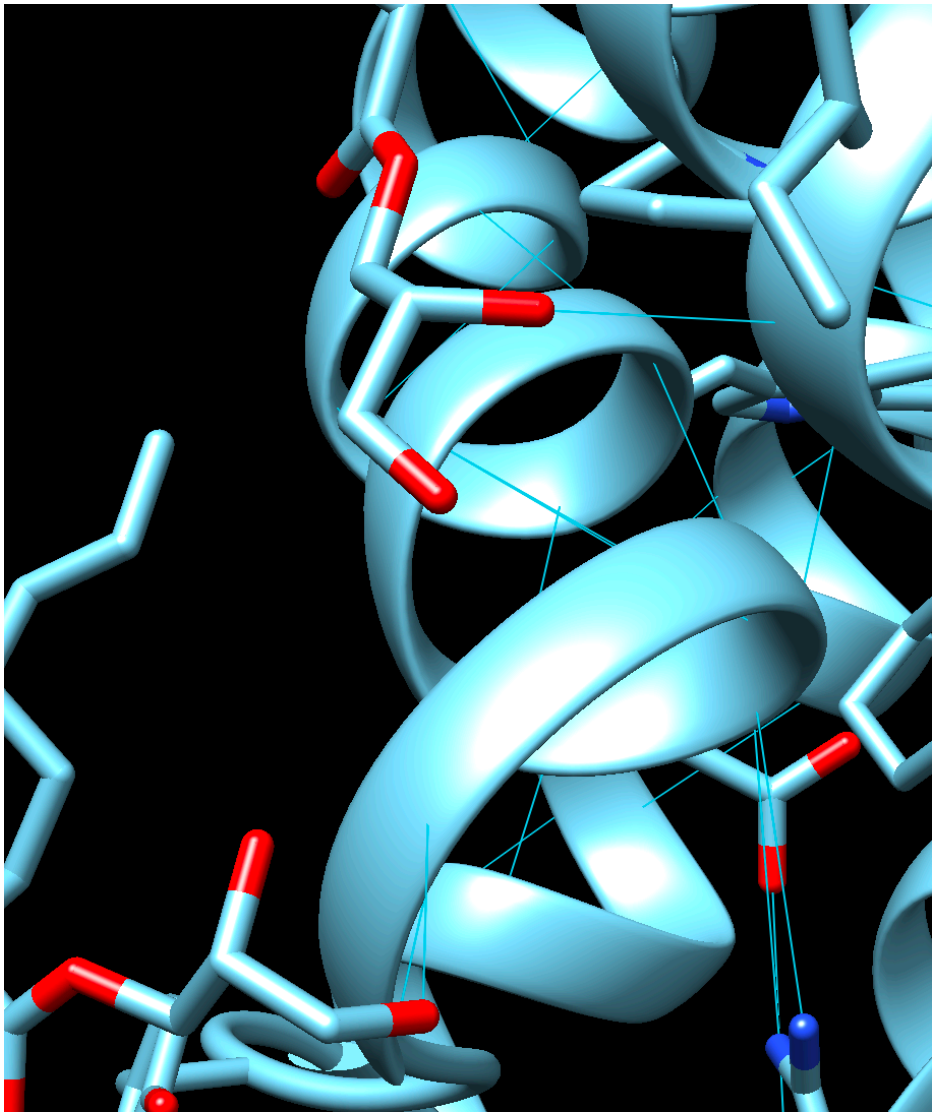

**Figure 6**. *Visualization of Cluster 6 in CXCR4 and CXCL12 hydrogen bonding interaction in Chimera.*

In conclusion, this study successfully demonstrates the selective binding of CXCL12 to CXCR4 over CXCR3, providing valuable insights into the molecular mechanisms behind this specificity. By using computational docking and visualization tools like Chimera, key interaction patterns such as hydrogen bonds and hydrophobic contacts were identified, showing that CXCR4 exhibits a higher binding affinity for CXCL12. The distinct binding poses, and interaction profiles further emphasize the structural determinants responsible for this selectivity. This computational approach, supported by experimental validation, underlines the potential for designing targeted therapeutics for CXCR4 while minimizing off-target effects. Further studies, including molecular dynamics simulations and experimental techniques like SPR or ITC, will be essential to validate and refine these findings, offering a deeper understanding of receptor-ligand interactions for drug development.

## Acknowledgements

The author thanks Mr. Robert Gotwals for assistance with this work. Appreciation is also extended to the Burroughs Wellcome Fund and the North Carolina Science, Mathematics

and Technology Center for their funding support for the North Carolina High School Computational Server.

## References

[1] M. C. Lagerström and H. B. Schiöth, “Structural diversity of G protein-coupled receptors and significance for drug discovery,” *Nature Reviews Drug Discovery*, vol. 7, no. 4, pp. 339–357, 2008, doi: 10.1038/nrd2518.

[2] A. S. Hauser, M. M. Attwood, M. Rask-Andersen, H. B. Schiöth, and D. E. Gloriam, “Trends in GPCR drug discovery: new agents, targets and indications,” *Nature Reviews Drug Discovery*, vol. 16, no. 12, pp. 829–842, 2017, doi: 10.1038/nrd.2017.178.

[3] A. Zlotnik, A. M. Burkhardt, and B. Homey, “Homeostatic chemokine receptors and organ-specific metastasis,” *Nature Reviews Immunology*, vol. 11, no. 9, pp. 597–606, 2011, doi: 10.1038/nri3049.

[4] L. Otvos and J. D. Wade, “Current challenges in peptide-based drug discovery,” *Frontiers in Chemistry*, vol. 2, 2014, doi: 10.3389/fchem.2014.00062.

[5] S. Rajagopal *et al.*, “$b\eta$-arrestin- but not G protein-mediated signaling by the ``decoy'' receptor CXCR7”, *Proceedings of the National Academy of Sciences*, vol. 107, no. 2, pp. 628–632, 2010, doi: 10.1073/pnas.0912852107.

[6] Y. DÃ¶ring, L. Pawig, C. Weber, and H. Noels, “The CXCL12/CXCR4 chemokine ligand/receptor axis in cardiovascular disease,” *Frontiers in Physiology*, vol. 5, 2014, doi: 10.3389/fphys.2014.00212.

Open Access | https://doi.org/10.62329/cvjn4247

Morganton Scientific

*North Carolina School of Science and Mathematics*

Journal of Student STEM Research

# Green synthesis of decomposing rubber; comparing processing using carboxymethyl cellulose and Ipomoea pes-caprae

**Zuzanna A. Mikolajec**[1]

[1]NCSSM

## Abstract

In recent years effort has been made to innovate alternative sustainable options to classic materials. Rubber is one of those materials that poses a major problem worldwide as it fills landfills, infiltrates ecosystems, and poses a threat to wildlife. Previous research that sought out to develop compostable or biodegradable plastics had found that CMC increases mechanical properties and decomposition in the production of biodegradable films, while CSG improves swelling and decomposition. In another study Ipomoea alba was used to cure LNR and it increased the material's malleability and elasticity. The goal of this research was to develop a method of green synthesis of a latex natural rubber (LNR) material specific to the purpose of rubber band production with increased decomposability and a decreased negative impact on the ecosystem as well as minimized cost. To accomplish this, the LNR was combined with a solution of cassava starch and glycerol (CSG). The study also compared the qualities of LNR/CSG material processed using Carboxymethyl cellulose (CMC) with LNR processed using an extract from the Ipomoea pes-caprae vine (IPC), native to North Carolina. Additionally, it examined how different ratios and concentrations of Cassava Starch Glycerol (CSG) solution affected the properties of LNR samples.This study confirmed that processing a CSG and LNR material with CMC increases its solubility and it additionally discovered that it also increases its uniformity. It also found that levels of CMC are directly proportional to percent mass loss, and CMC enhances elastic properties of the CSG/LNR material due to its high interfacial crosslinking capacity with starch. Additionally, increasing [CSG] (from 10 to 15) did not show positive solubility patterns between samples of the same ratios, and increasing the viscosity of the solution decreased mechanical properties immensely. Notably, the IPC extract had effects on the LNR material similar to those caused by processing using Ipomoea alba vine extract in a previous study. It greatly improved the mechanical elastic properties of the CSG/LNR material and the material cohered more when twisted and was malleable when heated. Processing utilizing a combination of IPC and CMC resulted in a rigid material with low flexibility. Consequently, the most optimal ratio for a rubber band material that balances decomposition and mechanical properties was found to be 60:40:15 of CSG (10%):LNR:CMC.

**Keywords** green chemistry, biodegradability, synthesis of latex natural rubber, carboxymethyl cellulose, ipomoea alba

**Published** Jun 27, 2024

**Correspondence to**
Zuzanna A. Mikolajec
mikolajec25z@ncssm.edu



Published by Curvenote

## 1. Introduction

In 2018 the U.S. produced 9.2 million tons of rubber waste (H. Chittella, L. W. Yoon, S. Ramarad, and Z.-W. Lai [1]), and the rates are only increasing with the rise in population and production. This rubber waste poses a huge threat to native wildlife and ecosystems. On an isolated UK island, huge amounts of rubber bands and fishing nets have been found in the undigested pellets of sea birds who mistake them for worms (R. Prior [2]). Due to the vulcanization process that it undergoes, recycling rubber is extremely

demanding. Vulcanized rubber also displays great resistance to decomposition due to the presence of highly hydrophobic cross-linked structures, provided by certain additives and the vulcanization process itself.

Vulcanization is the process through which latex natural rubber (LNR) is mixed with curing agents (which induce crosslinking of the polymer chains creating a tight molecular network) and then heated to solidify the overall polymer structure. Vulcanized products have greater retractile properties – increased elasticity and decreased plasticity under a greater range of changes in temperature and wear. Most common-day materials are only mildly vulcanized. Sulfur is the most commonly used crosslinking agent but its downside is that it requires toxic and expensive activators and accelerators (Freudenrich [3]) and it combusts into the highly toxic sulfur dioxide.

A previous study set out to increase biodegradability, reduce cost, and improve the mechanical properties of Polylactic acid using a mixture of pineapple stem starch and modified natural rubber (W. Tessanan, P. Phinyocheep, and T. Amornsakchai [4]). Starch is a low-cost, renewable, biodegradable, and highly-available substance. It increases the swelling of the material in moist conditions and has been proven to lead to weight loss during degradation. Starch also has a high amylose content which drives the growth of beneficial microbes that feed on it ([5]), metabolizing the material, consequently breaking it down and promoting biodegradability. Simultaneously, using starch in rubber materials unfortunately reduces the tensile strength and water-resistant properties of the polymer, therefore glycerol can be used as a plasticizer to improve the flexibility and processing ability of the starch (N. Leksawasdi *et al.* [6]).

Another study, by N. Leksawasdi *et al.* [6], developed biopolymer films using reactive blending of corn starch and glycerol (CSG), latex natural rubber (LNR), and carboxymethyl cellulose (CMC). CMC is a cellulose derivative obtained from alkali cellulose and sodium salt reactions. CMC can be prepared using a wide variety of organic products and industrial waste (W. Wongvitvichot, S. Pithakratanayothin, S. Wongkasemjit, and T. Chaisuwan [7]), and it is non-toxic. CMC was used as a crosslinking agent because it is highly compatible with starch, carboxylic groups, and sodium ions – therefore structurally similar to CSG. It increases interactions between hydroxide groups, connecting the CSG (hard phase) and LNR (elastic phase) which improves the mechanical properties of the blend and increases elongation at the break, max tensile strength, and Young's modulus.

Additionally, due to swellable content and effective interfacial crosslink density of CSG/LNR through the reaction mechanism of CMC, CMC can increase the solubility of the CSG/LNR/CMC blend. Yet, at too high of a concentration, the CMC forms a dense interfacial crosslinking with LNR, so it is crucial to find the right balance.

This study developed a tough, transparent, water-resistant, biodegradable material with high tensile properties. In this case, the purpose of the material was packaging, hence, it was thin and film-like. My study will work on discovering an optimal ratio of starch to glycerol to CMC for a thicker material that can be used for rubber bands; it will also utilize cassava starch instead of cornstarch, because of its high purity and chemical modification abilities.

Although the process of rubber making can involve much chemical refinement, the craft originates from ancient Mesoamericans, who created it using the Castilla elastica and the Ipomoea alba plants. I.alba vine extract purifies the natural rubber latex by phase separation. It concentrates and removes proteins (plasticizing agents), and its oil content induces latex coagulation (behaves better with the whole vine extract). Natural Latex Emulsion consists of three phases: a cis-1,4-polyisoprene phase, an aqueous phase, and

insoluble components, such as plasticizers, which reduce viscosity by disrupting interactions between polymer chains. Treatment of suspension with I. alba vine extract destabilizes the emulsion, separates the polymer and aqueous phases (a process called coagulation), and solubilizes plasticizing agents, allowing chain entanglement and interchain interactions. The resulting coagulated solid is amorphous except for some crystalline material which improves the mechanical properties as a non-covalent crosslinker.

Multiple spectroscopy tests identified aliphatic methyl and methylene groups and indicated the presence of sulfonyl chloride and sulfonic acid moieties in the I.alba vine extract. These sulfur-containing organic groups are capable of reacting with the alkenes in the polymer chain, and a bifunctional molecule could act as a cross-link. Sulfonyl chlorides and sulfonic acids are also known to induce cyclization of 1,4-polyisoprene, which introduces rigid segments into the polymer chain. A small number of these segments would have the same effect on elastic behavior as cross-links and would consequently increase elasticity. Overall the plant increased stiffness and the degree of interchain interactions in the processed rubber, which could have been introduced by covalent cross-linking or by noncovalent interactions (D. Hosler, S. L. Burkett, and M. J. Tarkanian [8]).

My study aims to determine whether other plants from this genus, such as the Ipomoea pes-caprae have the same coagulating, elastic, and flexibility-increasing properties.

In the past, the investigations towards a more sustainable future in rubber production were centered around two main groups of study: (1) improving performance while ensuring sustainability, or (2) improving properties of biodegradability. Most studies do not discuss both factors in relation to each other, but that is the challenge this project undertook.

## 2. Methods of Preparation

### *2.1. Derivation of Vine Extract from Ipomoea pes-caprae*

Within a few minutes of cutting, strip the plant of leaves and flowers, leaving only the vine. Crush the vine using a mortar and pestle to squeeze as much juice out as possible. After the most possible amount has been extracted, add silicon sand to aid with grinding. Centrifuge at 10000 rpm for 5 min.

### *2.2. Preparation of Rubber Samples*

To synthesize the rubber samples, latex natural rubber (LNR), cassava starch glycerol solution (CSG), along with the processing agent of either carboxymethyl cellulose (CMC), extract from the Ipomoea pes-caprae vine (IPC), or both were combined utilizing the method of melt blending. The 10% CSG solution was prepared by combining 7 g of cassava starch (CS) with 3 g of 99% glycerol in 100 ml of deionized water in a capped 125 ml Erlenmeyer flask and heated in a water bath at a temperature of 50 °C for 30 minutes, utilizing a magnetic stir bar to keep solution agitated evenly. The 15% CSG solution was prepared via the same method but with 10.5 g of CS and 4.5 g of glycerol. To make a CSG solution of a viscous homogeneous consistency the parameters change to heating at 80 °C. The CSG solution was then drawn using a plastic cuvette and transferred to 25–50 ml beakers to be combined with LNR at the given ratio. A CMC gel was prepared by heating a ratio of 1 g/ 10 ml DI water at 80 °C for 10 minutes in a 25 ml Erlenmeyer flask and stirring periodically. For samples utilizing CMC as a processing agent, the gel was drawn using a plastic cuvette and squeezed into the individual beaker samples of LNR/CSG. The same action was performed for samples utilizing IPC vine extract, which was previously centrifuged at 10000 rpm, as a processing agent. In both cases, the beaker was placed over

a simmering water bath and all of the components were stirred together till evenly combined and warm.

### 2.3. Heat Processing

The CSG/LNR/CMC and CSG/LNR/IPC and CSG/LNR/CMC/IPC solutions were poured into previously prepared and dried metal forms (4.80 cm x 3.60 cm x 1.70 cm) glued to a baking sheet using leftover CMC solution. The samples were then heat processed in the muffle furnace at their respective temperatures. The researcher created samples at various ratios of component ingredients. They are demonstrated in Table 2- Table 5. The concentration ratios were narrowed down to the most optimal ones through the testing of samples with modified variables.

### 2.4. Debubbling

Two methods of debubbling were attempted. The first used a small heat gun on the unbaked form-poured samples. The second consisted of putting the form-poured samples into a sealed bell jar connected to a vacuum for 2-5 minutes, or till the amount of apparent bubbles in the sample was minimized and the surface was glossy and smooth, without the sample boiling over due to the excessive decrease in pressure.

## 3. Methods of Testing

### 3.1. Solubility

The solubility of the samples was used as a guiding factor to help indicate the possible biodegradability of a given sample of rubber. The researcher prepared samples of equal dimensions (4.50 cm x 0.875 cm x ~0.10 cm) and measured their initial mass. They were submerged in 50 ml of DI water and shaken at 35 rpm for 24 hours. After the samples had dried completely, their mass was recorded again. Percent mass loss, or solubility, was calculated using the following formula:

$$\frac{M_i - M_f}{M_i} * 100 = \%M_L \quad (1)$$

Where %ML is the percent mass loss, $M_i$, is the initial mass, and $M_f$ is the final mass.

### 3.2. Mechanical Properties

A modified Vernier Structures and Materials tester was utilized to observe patterns of elasticity. Values for displacement and force were recorded as coordinate pairs for every turn of the wheel. Although this machine is not as accurate as industrial lab-grade tensile testing machines, it was possible to create a stress-strain curve and point out the regions of elasticity, strain hardening, and necking (Figure 1). By applying a linear curve fit on the elastic range, it was possible to find a Young's modulus value that could be compared between experimental samples to aid in the analysis of their elasticity. Qualitative analysis was the primary method used to determine the mechanical merits of the material. Factors that the researcher considered included the formation of rips and cracks, elongation at break, brittleness, holes in the material, surface regularity, and how well the species retained its original length.

### 3.3. Melting

Rectangular samples of rubber were placed between two pieces of aluminum foil on a hot plate for 10 minutes at each of the following temperatures: 100 °C, 160 °C, 200 °C. Their qualitative properties of malleability, cohesiveness, and melting point were observed and recorded.

## 4. Discussion and Analysis

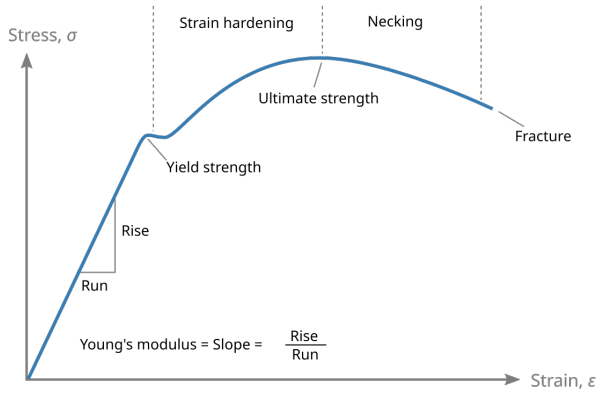


**Figure 1.** *([9]): Example of Stress-Strain Curve*

Percentages of solubility of all samples are displayed in Table 1 - Table 5 below.

| CSG Concentration | CSG % | LNR % | CMC pph | Initial Mass (g) | Mass After Dissolving (g) | Percent Loss % |
|---|---|---|---|---|---|---|
| | 90 | 10 | 10 | 0.16 | 0.12 | 25 |
| 10 | 80 | 20 | 10 | 0.12 | 0.1 | 16.66666667 |
| 10 | 70 | 30 | 10 | 0.17 | 0.16 | 5.882352941 |
| 10 | 60 | 40 | 10 | 0.24 | 0.22 | 8.333333333 |
| 10 | 50 | 50 | 10 | 0.27 | 0.25 | 7.407407407 |
| 10 | 40 | 60 | 10 | 0.2 | 0.18 | 10 |
| 10 | 30 | 70 | 10 | 0.34 | 0.32 | 5.882352941 |
| 10 | 20 | 80 | 10 | 0.4 | 0.38 | 5 |
| 10 | 0 | 100 | 10 | | | |
| 10 | 70 | 30 | 15 | 0.27 | 0.22 | 18.51851852 |
| 10 | 60 | 40 | 15 | 0.45 | 0.31 | 31.11111111 |
| 10 | 50 | 50 | 15 | 0.41 | 0.38 | 7.317073171 |
| 15 | 60 | 40 | 15 | 0.32 | 0.27 | 15.625 |
| 15 | 40 | 60 | 15 | 0.4 | 0.37 | 7.5 |
| 15 | 40 | 60 | 0 | | | |

**Table 1.** *CMC processed rubbed at 80 ℃ for 18 h*

| CSG Concentration | CSG % | LNR % | IPC pph | Initial Mass (g) | Mass After Dissolving (g) | Percent Loss % |
|---|---|---|---|---|---|---|
| 10 | 60 | 40 | 10 | 0.184 | 0.16 | 13.04347826 |
| 10 | 60 | 40 | 10 | 0.255 | 0.226 | 11.37254902 |
| 10 | 60 | 40 | 0 | 0.306 | 0.2782 | 9.08496732 |
| 10 | 60 | 40 | 0 | 0.258 | 0.2326 | 9.84496124 |

**Table 2.** *IPC processed rubber at 80 ℃ for 18 h*

| CSG Concentration | CSG % | LNR % | CMC pph | Initial Mass (g) | Mass After Dissolving (g) | Percent Loss % |
|---|---|---|---|---|---|---|
| 10 | 60 | 40 | 15 | 0.251 | 0.2175 | 13.34661355 |
| 10 | 60 | 40 | 15 | 0.35 | 0.3017 | 13.8 |
| 10 | 60 | 40 | 10 | 0.315 | 0.2712 | 13.9047619 |
| 10 | 60 | 40 | 10 | 0.212 | 0.1825 | 13.91509434 |
| 10 | 60 | 40 | 0 | 0.306 | 0.2782 | 9.08496732 |
| 10 | 60 | 40 | 0 | 0.258 | 0.2326 | 9.84496124 |

**Table 3**. *CMC processed rubber 150 °C 15 min*

| CSG Concentration | CSG % | LNR % | IPC pph | Initial Mass (g) | Mass After Dissolving (g) | Percent Loss % |
|---|---|---|---|---|---|---|
| 10 | 60 | 40 | 10 | 0.189 | 0.1629 | 13.80952381 |
| 10 | 60 | 40 | 10 | 0.219 | 0.1927 | 12.00913242 |

**Table 4**. *IPC processed rubber 150 °C 15 min*

| CSG Concentration | CSG % | LNR % | CMC pph | IPC pph | Initial Mass (g) | Mass After Dissolving (g) | Percent Loss % |
|---|---|---|---|---|---|---|---|
| 10 | 60 | 40 | 10 | 10 | 0.325 | 0.2829 | 12.95384615 |
| 10 | 60 | 40 | 10 | 10 | 0.379 | 0.3247 | 14.32717678 |

**Table 5**. *ICMC and IPC processed rubber 150 °C 15 min*

Tensile strength testing found that increasing the concentration of LNR –simultaneously decreasing the watery CSG– leads to a denser, stiffer material and decreases solubility because more polymer molecules and less starch and moisture intercepting the web creates a denser polymer structure. Experiments have also shown that the material samples processed with the agitated watery consistency CSG displayed far better mechanical properties than those processed with the viscous, homogenous CSG. The watery CSG created smooth, elastic, and more tear-resistant material, while the viscous CSG created a highly brittle, leather-like material that tore easily (Figure 2). Although the solubility was increased in the viscous CSG sample, the improvement was insignificant considering the tremendous compromise to the quality of mechanical properties. Further increase of the concentration of CSG from 10% to 15% did not show a positive behavior pattern concerning solubility and mechanics between samples of otherwise identical ratios. This may be due to the decreased interfacial interaction between the LNR and CSG.

It was also discovered that materials processed using I. pes-caprae vine extract displayed similar behaviors to those processed with I.alba vine extract. When processed at a low heat of 80 °C for 18 hours, the rubber samples displayed patterns of improved elasticity and adhered to themselves minimally when twisted – a behavior caused by the lack of a fully crosslinked network. When heated during melt testing, the material was somewhat malleable at temperatures between 100 °C - 200 °C. When samples of the same ratios were processed at an increased heat of 160 – 200 °C for 20 min, their mechanical properties decreased tremendously to a low elongation at break. This may be due to the organic

**Figure 2.** *LNR sample processed using viscous CSG*

matter from the plant extract burning within and creating microscopic holes in the process.

The data collected during testing, displayed in Figure 3, demonstrates that increasing pph of CMC from 10 to 15 displayed trends of either largely improved solubility or minimal change in solubility between samples of the same ratio. Samples of CSG/LNR processed with CMC displayed increased solubility and swelling due to the increase in the interfacial crosslink density of CSG/LNR through the CMC reaction mechanism (N. Leksawasdi *et al.* [6]). Although normally a higher density would prevent the penetration of water and decrease solubility, in this case, because CSG and the CMC gel are both hydrophilic, their interference in the polymer network draws water in making it swell and creating gaps in the structure, which helps it break down. By this crosslinking mechanism, CMC also makes the material more elastic and uniform. There is also crosslinking within the CMC phase itself. Its Na+ ions, from its synthesis process, form physical crosslinks with the carboxylic acid groups (Figure 4).

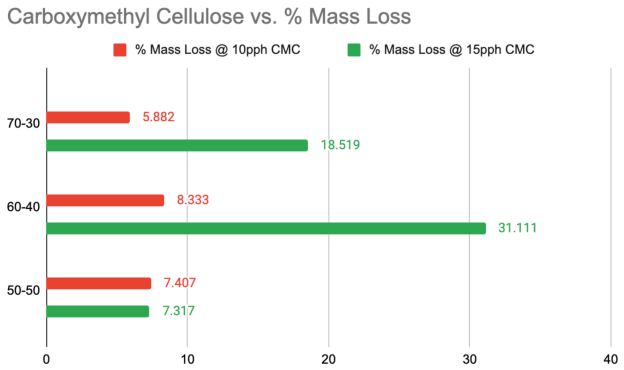


**Figure 3.** *Comparison of mass loss between LNR samples processed with a higher and a lower concentration of CMC*

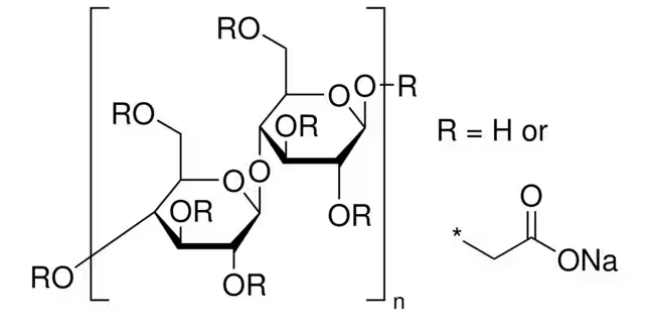


**Figure 4**. *([10]): Lewis Structure of carboxymethyl cellulose*

Changing the heat processing conditions from 18 h at 80 °C to 15 min at 150 °C, and afterward leaving them to dry, improved the mechanical properties of the samples processed with CMC. The reason for this pattern could be that the higher temperature allows more bonds to form as the bond enthalpy is reached. Higher temperatures also catalyze reactions allowing for more reactions to occur. This finding is significant as this method would expedite the process and lower energy consumption, making the process greener.

The results of CSG/LNR material processed with a combination of CMC and IPC were largely negative. The material was very hard and brittle, with minimal elasticity, and an almost minimal elongation at break (Figure 5). It is important to note that this is largely the result of the high temperature that the sample was baked at (which in the IPC-only sample also resulted in negative results), but additionally, the inclusion of both processing agents might have created too dense of a crystalline structure between the polymers of polyisoprene, resulting in the rigidity of the material.

In the 60:40:CMC sample of CSG:LNR:CMC where the concentration of CSG was 10%, it was observed that increasing the concentration of CMC from 10 pph to 15 pph was correlated with a minimally decreased solubility (Table 3), but a positively increased Young's Modulus, yield strength, and superior mechanical properties. The stretching behaviors of two samples of each of the two ratios are displayed in Figure 6- Figure 9. Young's Modulus increased from an average of 0.07841 N/mm to an average of 0.1513 N/mm, and yield strength increased from 1.3 N to an average of 2.45 N between the CSG:LNR:CMC samples of 60:40:10 and 60:40:15 accordingly. Although both of the samples, 60:40:10 and 60:40:15 baked on an aluminum surface at 150 °C for 15 min and previously debubbled possessed excellent mechanical properties, the latter sample had a significantly greater elongation at break and did not develop any tears or holes (Figure 10).

The experiments also showed that objectively minor adjustments in methodology provide significantly improved results. Debubbling using a bell jar proved to be an efficient way of getting rid of bubbles in the liquid samples before heat-processing them, which resulted in a baked and dried material with minimal holes/gaps, which in turn improved the

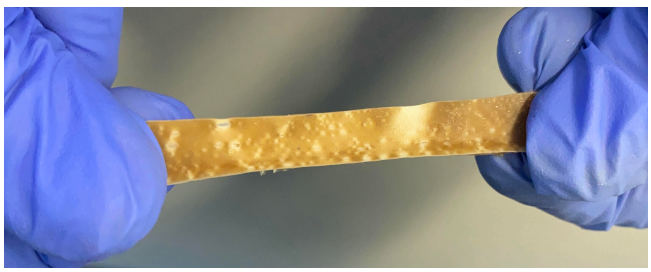

**Figure 5**. *LNR processed with a combination of CMC and CSG*

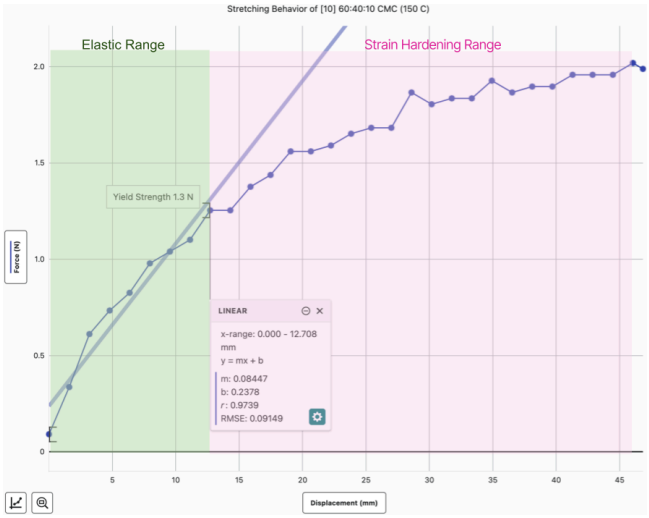


**Figure 6**. *Stress-strain curve of [10]60:40:10 (150℃) sample*

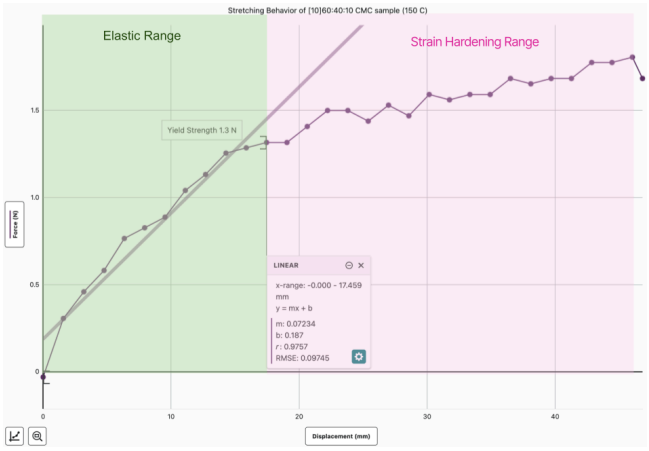


**Figure 7**. *Stress-strain curve of [10]60:40:10 (150℃) sample*

mechanical properties of the material, namely elongation at break and tear resistance.

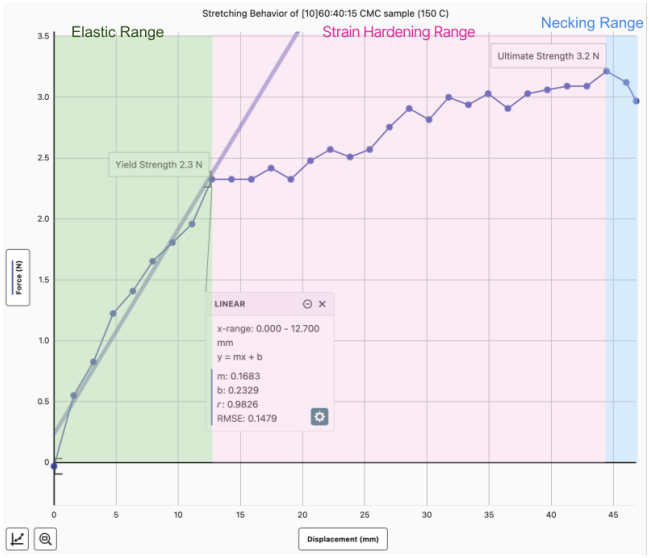


**Figure 8**. *Stress-strain curve of [10]60:40:15 (150℃) sample*

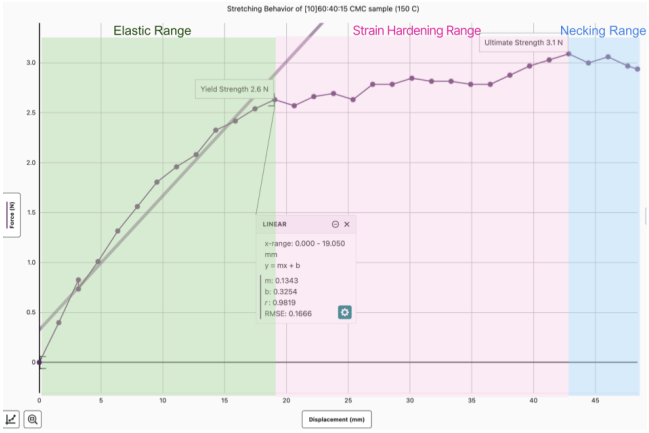


**Figure 9**. *Stress-strain curve of [10]60:40:15 (150℃) sample*

**Figure 10**. *Lack of noticeable tears and holes in [10]60:40:15 (150℃) sample*

Meanwhile, baking samples on a surface of aluminium resulted in samples with a smooth and even surface (Figure 11), which also improved their mechanical properties significantly, compared to the samples baked on parchment paper which resulted in ridges that caused an uneven distribution of tension when stretched (Figure 12), which in turn decreased the tensile strength and elongation at break.

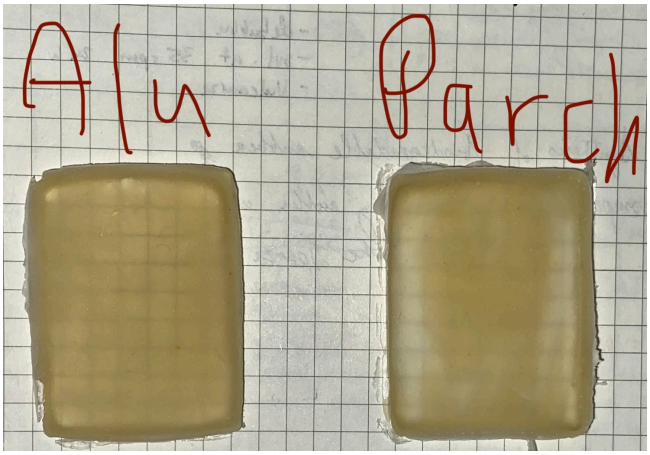


**Figure 11**. *LNR baked on aluminum sheets vs. parchment paper*

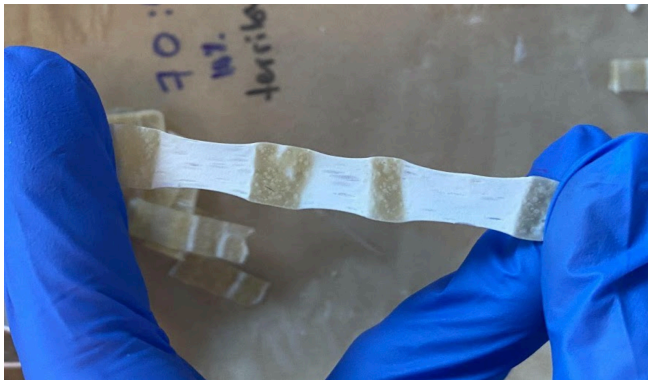

**Figure 12**. *Uneven tensile distribution observed in LNR samples baked on parchment paper*

## 5. Conclusion

This study found that Carboxymethyl cellulose functions strongly as a processing agent for biodegradable rubber by acting as a compatibilizer with starch and strengthening its properties, which in turn aids in the breakdown. CMC itself also improves the mechanical properties of the material due to its surface-exclusive crosslinking capacity. A concentration of 15 pph provided the most optimal quality, elasticity, and elongation at break. The addition of cassava starch to rubber blends in combination with glycerol and carboxymethyl cellulose improved the material's solubility significantly while maintaining its mechanical properties due to CMC's tensile capacities. It was also discovered that Ipomoea pes-caprae in the rubber blend displays similar attributes, such as increased elasticity and malleability, to the ancient Mesoamerican rubber blends which included Ipomoea alba.

The study succeeded in creating a material that displays patterns of potential biodegradability and has the mechanical properties and endurance required for the production of rubber bands.

In the future, full biodegradability tests will need to be conducted over several months in organic matter containing microorganisms under a variety of changing conditions (turbulency, moisture, temperature, etc.) to truly see the full spectrum of the potential that this material has in the field of green materials chemistry and its ecological applications. FTIR and NMR spectroscopy of the samples will also need to be conducted to see how the molecular structures are impacted by the addition of the processing agents – what bonds are formed. Another potential test to determine the quality of solubility of the samples would be UV-vis spectroscopy of the solution that the samples dissolved in to see how the concentration of latex content in the solution changed. It will also be insightful to conduct testing on a higher quantity of samples and compare properties of synthesized samples to those of commercial rubber band products.

Special thanks to Dr. William Grubbs for his support and supervision throughout the project, as well as Mr. Adam Benoit for recommending me to use a bell jar.

## References

[1] H. Chittella, L. W. Yoon, S. Ramarad, and Z.-W. Lai, "Rubber waste management: A review on methods, mechanism, and prospects," *Polymer Degradation and Stability*, vol. 194, p. 109761, 2021, doi: 10.1016/j.polymdegradstab.2021.109761.

[2] R. Prior, "Why sea birds regurgitated thousands of rubber bands on an uninhabited British island." [Online]. Available: https://www.cnn.com/2019/10/23/world/sea-birds-worms-scn-trnd/index.html

[3] Freudenrich, "How Rubber Works." [Online]. Available: https://science.howstuffworks.com/rubber.htm

[4] W. Tessanan, P. Phinyocheep, and T. Amornsakchai, “Sustainable Materials with Improved Biodegradability and Toughness from Blends of Poly(Lactic Acid), Pineapple Stem Starch and Modified Natural Rubber,” *Polymers*, vol. 16, no. 2, p. 232, 2024, doi: 10.3390/polym16020232.

[5] “New study reveals waxy starches in sorghum have negative impact on gut microbiome,” *Gut Microbes*, vol. 15, no. 1, p. 2178799, 2023, doi: 10.1080/19490976.2023.2178799.

[6] N. Leksawasdi *et al.*, “Corn starch reactive blending with latex from natural rubber using Na+ ions augmented carboxymethyl cellulose as a crosslinking agent,” *Scientific Reports*, vol. 11, no. 1, p. 19250, 2021, doi: 10.1038/s41598-021-98807-x.

[7] W. Wongvitvichot, S. Pithakratanayothin, S. Wongkasemjit, and T. Chaisuwan, “Fast and practical synthesis of carboxymethyl cellulose from office paper waste by ultrasonic-assisted technique at ambient temperature,” *Polymer Degradation and Stability*, vol. 184, p. 109473, 2021, doi: 10.1016/j.polymdegradstab.2020.109473.

[8] D. Hosler, S. L. Burkett, and M. J. Tarkanian, “Prehistoric Polymers: Rubber Processing in Ancient Mesoamerica,” *Science*, vol. 284, no. 5422, pp. 1988–1991, 1999, doi: 10.1126/science.284.5422.1988.

[9] “Young's modulus.” [Online]. Available: https://en.wikipedia.org/w/index.php?title=Young%27s_modulus&oldid=1282966396

[10] “NMR Chemical Shifts of Impurities.” [Online]. Available: https://www.sigmaaldrich.com/MX/en/technical-documents/technical-article/genomics/cloning-and-expression/blue-white-screening

Open Access | https://doi.org/10.62329/cvfp9555

Morganton Scientific

*North Carolina School of Science and Mathematics*

Journal of Student STEM Research

# Optimizing Photovoltaic Output Through the Integration of Passive Optical Tools for Enhanced Photon Capture in Solar Cells

**Prahas Ramidi**[1], and **Akhilesh Karthik**[2]

[1]North Carolina School of Science and Mathematics, [2]NCSSM

## Abstract

Solar panels utilize light energy from the sun through their solar cells to generate electricity. However, during nighttime or when the weather is disrupting the sun, they may not be as efficient in producing electricity because there is not enough energy to knock electrons from their bond and generate power. This experiment's purpose was to increase the efficiency of solar panels through focusing and reflective materials. The hypothesis was tested by focusing light through a magnifying glass onto a solar panel, by using a mirror to reflect light towards another panel, and finally comparing those two to a control. These experiments occurred on a sunny day, cloudy day, and during sunset for 1 minute per trial with a total of 3 trials per sunlight condition. Vernier Graphical Analysis devices collected quantitative current & voltage measurements, which were then analyzed through comparative graphs created for the 3 different conditions listed. Due to the optical tools' influence, the test panels showed a voltage and a current increase of up to 2.1%-14.6% during each scenario. The hypothesis was correct in the sense that these optical devices produced an increased amount of wattage during all 3 situations, giving a rise in solar efficiency. In conclusion, a wattage increase of up to 25% can be significant when using solar panels during times when solar panel usage is not optimal, essentially seeking to find a solution providing consistent energy with efficiency.

**Keywords** Solar Panels, Renewable Energy, Photovoltaic Cells, Magnifying Glass

## 1. Introduction

As the demand for energy continues to grow, finding sustainable solutions has become one of the most pressing challenges in today's world. While previous generations heavily relied on fossil fuels for their energy needs, the environmental costs make them unsustainable in the long run. Since the Industrial Revolution, our dependence on fossil fuels significantly grew, leading to an increase in carbon dioxide levels in Earth's atmosphere. Over the last two centuries, $CO_2$ has risen by 50%. Since 2002 itself, we have increased by 55 parts per million to 420 ppm, referring to $CO_2$ molecules per 1 million molecules of dry air [1]. Carbon dioxide being a greenhouse gas essentially traps the sun's solar radiation within the atmosphere and causes surface temperatures to rise. While this greenhouse effect is a natural process critical for maintaining Earth's habitable climate, anthropogenic activities since the 1800s have intensified it far beyond protective levels. This resulting global warming poses harmful threats to human health, wildlife, agriculture, and our environment as a whole [2].

Renewable energy offers a promising path forward. Unlike fossil fuels, they are abundant, clean, and naturally replenished in a small period of time, making them critical in the transition to sustainable energy systems. Hydroelectric and wind energy both use moving streams to spin a turbine and generate electricity, achieving renewability, but they aren't

**Published** Jun 27, 2024

**Correspondence to**
Prahas Ramidi
ramidi26r@ncssm.edu

consistent worldwide. Solar energy, unlike the others, has the ability to revolutionize global power generation. Throughout history, the sun has been a constant, powerful source of light and energy. Despite its potential, there's still the challenge in efficiency and reliability, especially under variable conditions. Overcoming these challenges is essential to realizing its full promise as a leading energy source. By utilizing passive devices, meaning those that are not taking extra energy from outside, and enhancing that for energy capture and conversion, can significantly improve the performance of solar panels. This experiment integrates optical tools, specifically, magnifying glasses and mirrors to achieve this.

It is hypothesised that on sunny days, neither magnifying glasses nor mirrors can further optimize solar panel performance. This is because as photons strike the PV cells and dislodge electrons, fewer electrons remain available for displacement, limiting the impact of additional light. As a result, when more photons are reflected onto the solar panel through passive optical devices, the likelihood of dislodging more electrons decreases as fewer remain available to be displaced. Thus the wattage output of a standalone panel may closely match one using optical devices. However, on days when it is cloudy or during sunrise/sunset, it is predicted that flat mirrors and magnifying glasses could be utilized to increase a solar panel's wattage output. This is hypothesized because when there are not many photons hitting the photovoltaic cells, the mirror will be able to direct additional photons that would have otherwise missed the solar panel back towards the panel, and similarly magnifying glasses would be able to concentrate more photons directly onto the solar panel. For that reason both optical tools would be able to create enough electron-hole pairs to increase the flow of electricity. Furthermore, it is predicted that a magnifying glass will be able to outperform a flat mirror in directing photons to the PV cell, resulting in higher wattage output. This is because flat mirrors reflect light at an angle equal to the angle of incidence so all of the light will not necessarily be reflected directly onto the solar panel. That would make the magnifying glass be more efficient, but these mirrors are still way better to use than a solar panel standing alone.

A big societal impact of this experiment is more frequent usage of solar panels and lesser use of fossil fuels for energy. Solar panels can also be set up easier than long energy lines when trying to provide energy to remote areas. Finally, in regions with limited sunlight, reflectors and concentrators can help achieve efficiency levels comparable to areas with abundant sunlight. Enhancing their performance could lower costs while improving their reliability and effectiveness as a renewable energy solution.

## 2. Background

Solar panels are used to harness the power of the sun, a renewable source of energy. These panels are made from silicon or a semiconductor which is installed between conductive layers. Silicon is an element where its atoms have 14 electrons, 4 of which are on the outermost shell. Since silicon tends to fill up that shell, it will share electrons with four nearby atoms, forming a crystalline structure. This is the exact kind of structure needed in photovoltaic cells. PV cells use 2 different layers of semiconductor material– an N type which has extra electrons and a P type which has extra spaces for electrons. When the two types of semiconductor meet, electrons can drift across the P/N junction, leaving a positive charge on the layer with the holes and a negative charge on the layer with excess electrons. The role of the sun is to release small particles called photons. If they can strike a solar cell with enough energy, it can knock electrons from their bond, leaving a hole. The negatively charged electron moves in one direction to fill the positively charged hole. Along the way, the moving electrons are collected by thin metal conductors which use them to generate electrical energy as they move on their path. The cell's electric field generates voltage, driving electron flow to create current. The product of the two is

wattage, or the power needed for electrical work. Once the electrons fill in the holes, they essentially go back to where they came from so this same process can be repeated for many years, hence, renewable energy [3].

Of course, this is only if the photon strikes the solar cell with enough energy. This may not always be the case, such as cloudy days or when the sun isn't up. By using magnifying glasses, the goal is to concentrate sunlight right on the solar panel. This explanation draws from the science behind the optics used in magnifying glasses. A magnifying lens is made of a mix of two different types of surfaces coming from either convex, concave, or flat. Lens' also have focal points which is where all the light rays converge after passing through. With this attribute, magnifying glasses have the opportunity to concentrate sunlight to any desired location. As a result, more photons will be directed at a single point to knock electrons loose from their atoms, and overall, harness more energy. Similarly, the incorporation of mirrors allows the solar panel to maximize its photon absorption. By reflecting additional sunlight onto the panel's surface, the mirrors enhance its ability to harness energy from both direct and reflected solar radiation [4].

On average, a solar cell can produce 0.5-0.6 volts. The main factors that can play a role in the power generated, which is the product of both current & voltage, is efficiency, surface area, and its proportionality to the intensity of light striking the solar cell. Under optimal sunlight conditions, a standard PV panel with a surface area of 160 $cm^2$ can generate about 2 watts at 100% intensity. During days where this is not the case, wattage can drop significantly. Studies indicate that incorporating passive devices can substantially increase the efficiency and output of PV cells. Passive devices that would work in this situation include reflectors, cooling systems, solar tracking mounts, concentrators, etc. Without drawing the need of additional external energy, these mechanisms are valuable in optimizing solar cell performance [5].

## 3. Experiment

### *3.1. Project Materials*

- AK52X52: 52mm x 52mm Solar Panels - 3
- Double Concave Magnifying Glass - 1
- Mirror - 1
- Vernier Graphical Analysis Voltage Probes - 3
- Vernier Light Sensor - 1
- Vernier LabQuest Mini Interface - 1
- 330 Ohm Resistors - 1
- Red LED Lights - 1

### *3.2. Methodology*

1. Find a outdoor spot around noon on a sunny day to set up to record data
2. Place solar panels on a table (keep them flat) such that they are right in the sun
3. Connect the positive end of the voltage probe to the positive wire of the solar panel and the negative end of the voltage probe to the negative wire of the solar panel
4. Repeat step 3 for the other two solar panels
5. Place the mirror behind one of the solar panels and angle it downwards so that the light rays fall in an ellipse surrounding the panel to the best of its ability
6. Place magnifying glass in front of another panel so that it focuses the light onto it
7. The solar panel should be viewable through the magnifying glass
8. Connect all 3 voltage probes to the Vernier LabQuest Mini Interface

9. Open Vernier's Graphical Analysis software and set it up to collect data for 180 seconds at a rate of 20 samples per second
10. Run the software to collect data for 180 seconds and save the data
11. Take a 330 Ohm resistor and wrap one end of the resistor around the anode of an LED (the longer lead)
12. Take one solar panel with the voltage probe and wrap the positive wire around the other end of the resistor
13. Connect the negative wire from the solar to the other lead on the LED
14. Take the light probe and place it to face the same direction as the solar panel
15. Disconnect the voltage probe from the other two solar panels, and connect the voltage probe and the light sensor from this solar panel to the Vernier LabQuest Mini Interface
16. Open Vernier's Graphical Analysis software and set it up to collect data for 60 seconds at a rate of 20 samples per second
17. Run the software to collect data for 60 seconds and save the data
18. Repeat steps 16 & 17 two more times under the mirror & magnifying glass
19. Repeat steps 16-18 two more times for a total of three trials under all three conditions
20. Repeat steps 1-19 at noon on a cloudy day, and once around sunset

### *3.3. Results/Data Analysis*

Data Output Done by Vernier Graphical Analysis Voltage Probe, Graphical Analysis Software, and Light Sensor

#### 3.3.1. *Data From The Test Without The Red LED Circuit:*

**Sunny**

This graph (Figure 1) of the voltage output of each solar panel shows when they were tested at noon on a sunny day. This graph along with the statistics in the table above show that the voltage outputs in a sunny light condition were very similar. The Control and Mirror followed a similar trend while the Magnifying Glass had a very inconsistent trend. That is likely due to the many variables that could affect the output of the solar panel like the heat, because solar panels do not work well when hot, and a magnifying glass can concentrate light causing the heat to also rise which could be a possible explanation for the Magnifying Glass's voltage output trend.

**Cloudy**

| Time of Day | Solar Panel Type | Average Voltage (V) |
|---|---|---|
| Sunny | Control | 3.326 |
| Sunny | Mirror | 3.278 |
| Sunny | Magnifying Glass | 3.324 |
| Cloudy | Control | 3.430 |
| Cloudy | Mirror | 3.524 |
| Cloudy | Magnifying Glass | 3.452 |
| Sunset | Control | 1.758 |
| Sunset | Mirror | 1.830 |
| Sunset | Magnifying Glass | 1.765 |

**Table 1**. *Voltage for Time of Day and Solar Panel Type*

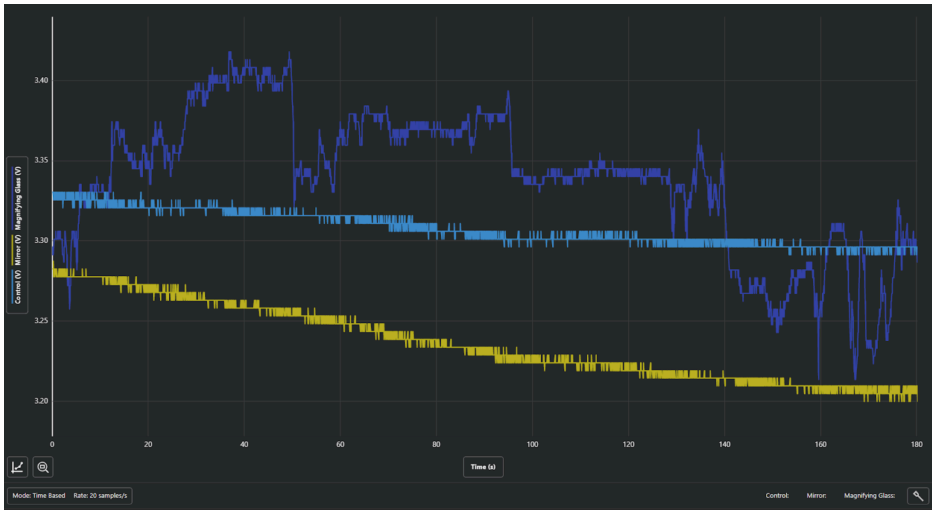


**Figure 1.** *Voltage output of solar panel at noon on a sunny day*

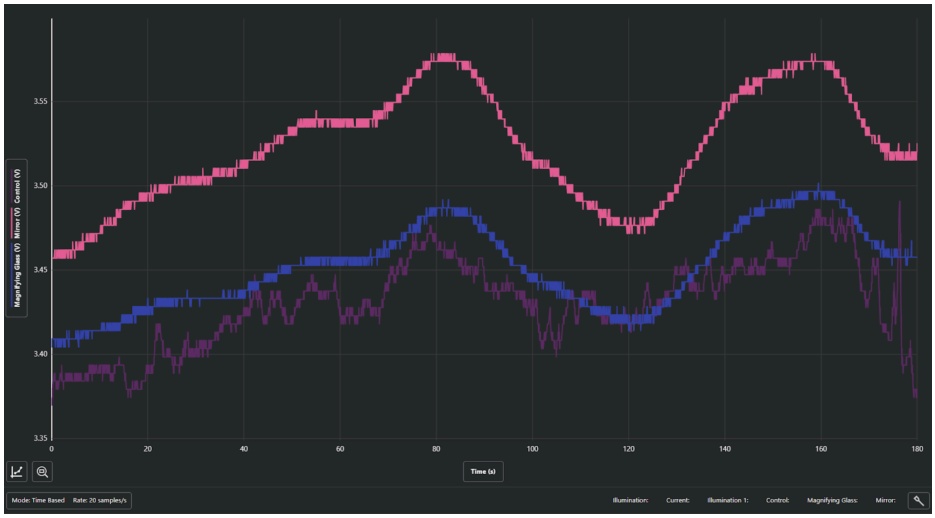


**Figure 2.** *Voltage output of solar panel at noon on a cloudy day*

This graph (Figure 2) of the voltage output of each solar panel shows when they were tested on a cloudy day. The voltages for all 3 light modifying conditions seem to have followed a similar wave like trend that was likely caused by a change in lighting as the clouds moved. The graph clearly shows how the solar panel which utilized the mirror had a greater voltage output for the entirety of the test while the control and the magnifying glass solar panels were very similar in voltage output with only a 0.022V difference in average. The mirror solar panel was able to output a voltage that was 0.096V greater than the control on average which is shown by the statistics in the table above.

### Sunset

This graph (Figure 3) of the voltage output of each solar panel shows when they were tested during a sunset. The voltages for all 3 light modifying conditions seem to have followed the same declining trend which was likely caused by the sun going down as it set. This graph shows the mirror solar panel having the greatest voltage output followed by the magnifying glass solar panel, which is followed by the control solar panel that that is not experiencing any light modification. The mirror likely was able to produce the greatest voltage output as the mirror was situated behind the solar panel allowing the

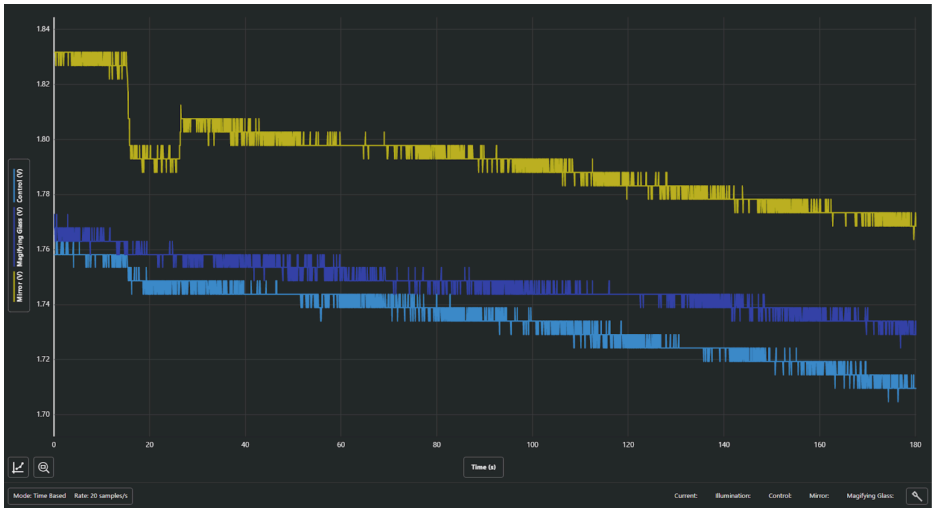


**Figure 3**. *Voltage output of solar panel during sunset*

solar panel to get hit by the photons that reach the panel direction, in addition to the photons that are reflected onto the solar panel by the mirror. The statistics in the table on above show that the mirror solar panel was able to produce an output that was 0.072V greater than the output of the control on average.

3.3.2. *Data From Trials With The LED Circuit:*

*Trial Data Calculations:*

**Equations:**

V = Voltage (Volts)

R = Resistance (Ohms)

I = Current (Amps)

P = Electrical Power (Watts)

$I = \frac{V}{R}$

$P = IV$

Average = $\frac{a_1+a_2+a_3+\cdots+a_n}{n}$

Percent Change = $\frac{New-Original}{Original} * 100\%$

*Resistance is 330 Ohms due to the 330 Ohm Resistor

This chart (Figure 4) displays the output voltage measured during each of the 27 trials where the red dot is the average of the respective 3 trials. This chart shows how the voltage output for all 3 optical devices was relatively the same in the sunny sunlight condition, the mirror and the magnifying glass are slightly greater than control for the sunset scenario, and the mirror and magnifying glass are much greater than the control for the cloudy sunlight condition. The difference between control and the optical devices were greatest during the cloudy sunlight condition with it being greater for the mirror.

This chart (Figure 5) displays the current generated during each of the 27 trials based on the calculations done with Ohm's Law. The red points show the average current generated during the respective set of 3 trials. This chart is very similar to the voltage chart with the only difference being the scale because current & voltage are directly proportional. For

| Time of Day | Solar Panel Type | Trial Number | Avg Voltage per Trial (V) | Illuminance (Lux) |
|---|---|---|---|---|
| Noon & Sunny | Control | Trial 1 | 3.276 | 119313 |
| Noon & Sunny | Control | Trial 2 | 3.170 | 118753 |
| Noon & Sunny | Control | Trial 3 | 3.287 | 118565 |
| Noon & Sunny | Mirror | Trial 1 | 3.349 | 118894 |
| Noon & Sunny | Mirror | Trial 2 | 3.310 | 118041 |
| Noon & Sunny | Mirror | Trial 3 | 3.279 | 117258 |
| Noon & Sunny | Magnifying Glass | Trial 1 | 3.321 | 118800 |
| Noon & Sunny | Magnifying Glass | Trial 2 | 3.214 | 118753 |
| Noon & Sunny | Magnifying Glass | Trial 3 | 3.235 | 117821 |
| Cloudy | Control | Trial 1 | 3.393 | 47260 |
| Cloudy | Control | Trial 2 | 2.476 | 42250 |
| Cloudy | Control | Trial 3 | 1.846 | 38261 |
| Cloudy | Mirror | Trial 1 | 3.201 | 44530 |
| Cloudy | Mirror | Trial 2 | 3.045 | 42340 |
| Cloudy | Mirror | Trial 3 | 2.592 | 39764 |
| Cloudy | Magnifying Glass | Trial 1 | 3.420 | 45670 |
| Cloudy | Magnifying Glass | Trial 2 | 3.143 | 41380 |
| Cloudy | Magnifying Glass | Trial 3 | 1.848 | 40200 |
| Sunset | Control | Trial 1 | 1.867 | 544.321 |
| Sunset | Control | Trial 2 | 1.652 | 542.331 |
| Sunset | Control | Trial 3 | 1.701 | 542.935 |
| Sunset | Mirror | Trial 1 | 1.827 | 544.459 |
| Sunset | Mirror | Trial 2 | 1.836 | 541.454 |
| Sunset | Mirror | Trial 3 | 1.855 | 541.493 |
| Sunset | Magnifying Glass | Trial 1 | 1.841 | 545.961 |
| Sunset | Magnifying Glass | Trial 2 | 1.826 | 542.931 |
| Sunset | Magnifying Glass | Trial 3 | 1.805 | 540.348 |

**Table 2**. *Voltage and Illuminance for Time of Day and Solar Panel Type*

that reason all the points seem to be in the same position relative to each other and similar observations and conclusions to those made for the voltage graph can be made here.

| Time of Day | Solar Panel Type | Trial Number | Avg Voltage per Trial (V) | Avg Voltage (V) | Avg Current per Trial (mA) | Avg Current (mA) | Avg Wattage per Trial (W) | Avg Wattage (W) | % Δ Voltage & Current from Control | % Δ Wattage from Control |
|---|---|---|---|---|---|---|---|---|---|---|
| Sunny | Control | Trial 1 | 3.276 | 3.244 | 9.927 | 9.831 | 0.03252 | 0.03190 | 0 | 0 |
| | | Trial 2 | 3.170 | | 9.606 | | 0.03045 | | | |
| | | Trial 3 | 3.287 | | 9.961 | | 0.03274 | | | |
| | Mirror | Trial 1 | 3.349 | 3.313 | 10.15 | 10.04 | 0.03399 | 0.03326 | 2.106 | 4.237 |
| | | Trial 2 | 3.310 | | 10.03 | | 0.03320 | | | |
| | | Trial 3 | 3.279 | | 9.936 | | 0.03258 | | | |
| | Magnifying Glass | Trial 1 | 3.321 | 3.257 | 10.06 | 9.869 | 0.03342 | 0.03215 | 0.3802 | 0.7555 |
| | | Trial 2 | 3.214 | | 9.739 | | 0.03130 | | | |
| | | Trial 3 | 3.235 | | 9.803 | | 0.03171 | | | |
| Cloudy | Control | Trial 1 | 3.393 | 2.572 | 10.28 | 7.793 | 0.03489 | 0.02126 | 0 | 0 |
| | | Trial 2 | 2.476 | | 7.503 | | 0.01858 | | | |
| | | Trial 3 | 1.846 | | 5.594 | | 0.01033 | | | |
| | Mirror | Trial 1 | 3.201 | 2.946 | 9.700 | 8.927 | 0.03105 | 0.02650 | 14.56 | 24.64 |
| | | Trial 2 | 3.045 | | 9.227 | | 0.02810 | | | |
| | | Trial 3 | 2.592 | | 7.855 | | 0.02036 | | | |
| | Magnifying Glass | Trial 1 | 3.420 | 2.804 | 10.36 | 8.496 | 0.03544 | 0.02524 | 9.021 | 18.71 |
| | | Trial 2 | 3.143 | | 9.524 | | 0.02993 | | | |
| | | Trial 3 | 1.848 | | 5.600 | | 0.01035 | | | |
| Sunset | Control | Trial 1 | 1.867 | 1.740 | 5.658 | 5.273 | 0.01056 | 0.009200 | 0 | 0 |
| | | Trial 2 | 1.652 | | 5.006 | | 0.008270 | | | |
| | | Trial 3 | 1.701 | | 5.155 | | 0.008768 | | | |
| | Mirror | Trial 1 | 1.827 | 1.839 | 5.536 | 5.574 | 0.01011 | 0.01025 | 5.709 | 11.44 |
| | | Trial 2 | 1.836 | | 5.564 | | 0.01021 | | | |
| | | Trial 3 | 1.855 | | 5.621 | | 0.01043 | | | |
| | Magnifying Glass | Trial 1 | 1.841 | 1.824 | 5.579 | 5.527 | 0.01027 | 0.01008 | 4.828 | 9.589 |

**Table 3**. *Statistics Calculated from Trial Data*

This chart (Figure 6) displays the wattage output generated during each of the 27 trials. The red points show the average wattage generated during the respective 3 trials. This chart shows the data for the sunny condition trials and the sunset condition trials as being very clean and constant when compared to the cloudy condition trials which look like a mess of random points. However, the mess of random points makes sense for the cloudy trials as the sunlight conditions are not too constant when it is cloudy resulting in there not being a consistent line of points. Still the chart shows that the mirror performed better than the control in all the sunlight conditions with the difference not being very significant in sunny conditions. The magnifying glass performed similarly as shown by the chart, but its difference in wattage output when compared to the control was not as much as the mirror.

## 4. Conclusion

To conclude, the original hypothesis proved to be partially correct. At first, it was thought that on a sunny day, with the sun being at its highest point, the tools we use–a magnifying glass and mirror–wouldn't show significant changes in voltage & current. This is because, with an additional light source beyond the sun at peak intensity, fewer electrons remain

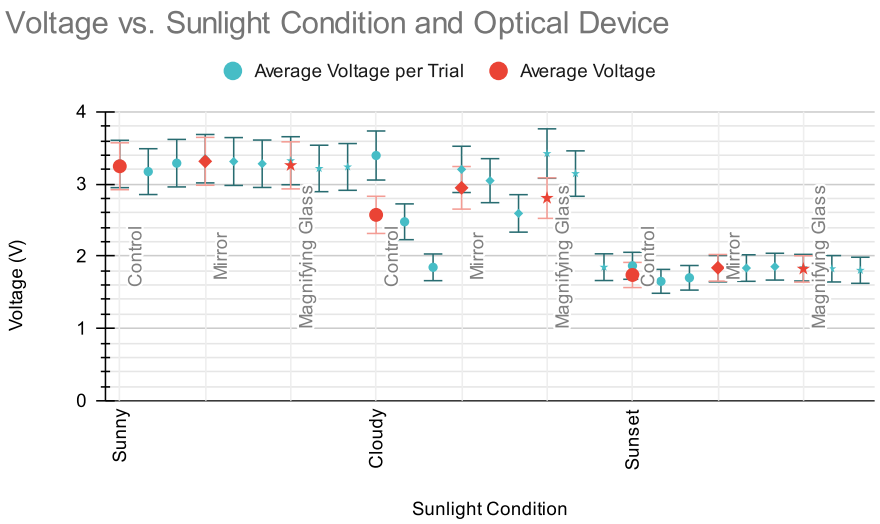


**Figure 4.** ● = *Control* | ◆ = *Mirror* | ★ = *Magnifying Glass*

available for photons to strike, reducing the likelihood of dislodging more electrons. The final results show that with a magnifying glass on a sunny day, current & voltage have a 0.3802% increase and wattage has a 0.7555% increase. With a mirror under the same conditions, current & voltage have a 2.106% increase and wattage as a 4.237% increase. Since these percent changes were under 5% and really minimal, it's safe to assume that this part of the hypothesis was correct in the sense that there weren't any significant changes regarding voltage & current, and therefore, wattage as well.

The second part of the hypothesis, however, was not as accurate as initially thought. Flat mirrors reflect light at the angle of incidence, so not all light was predicted to hit the panel directly. However, the magnifying glass concentrated photons in one region, dislodging electrons only there and limiting voltage. In contrast, the mirror directed sunlight onto the panel while it also received light directly from the sun. Ultimately, directing light with the mirror proved more effective than concentrating it.

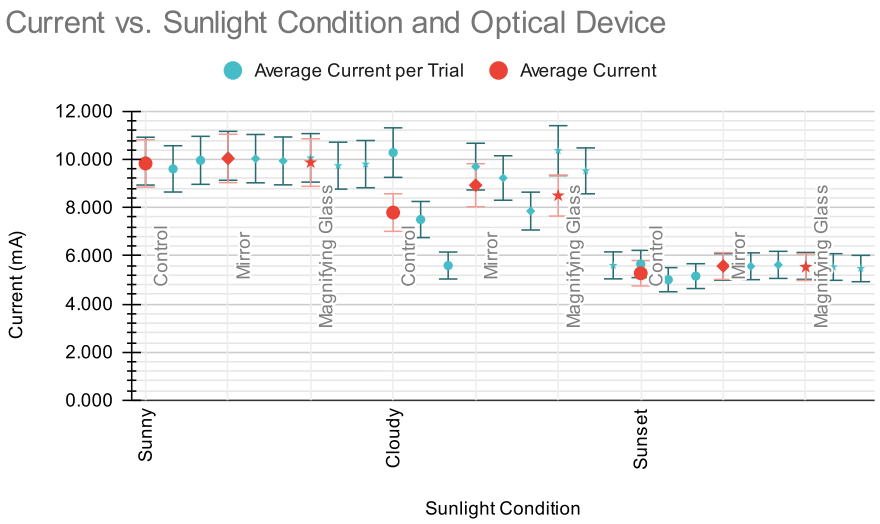


**Figure 5.** ● = *Control* | ◆ = *Mirror* | ★ = *Magnifying Glass*

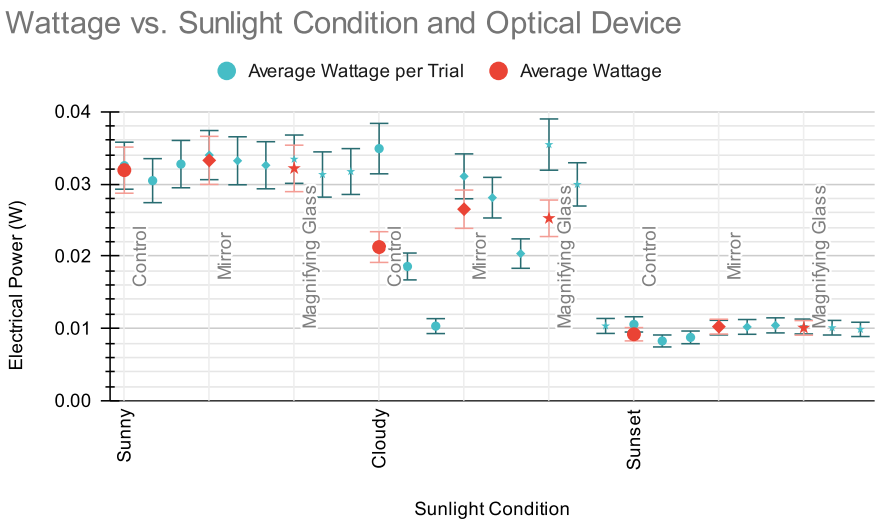


**Figure 6.** ● = *Control* | ◆ = *Mirror* | ★ = *Magnifying Glass*

Ultimately, the purpose of this experiment was achieved because both the solar panel with a mirror reflecting light on it and the solar panel with the magnifying glass concentrating light on it performed better than the solar panel standing alone. In all 3 situations, this was proven to be true but primarily the percent increase was way bigger in the conditions under cloudy weather and during sunset. The voltage & current percent change for the mirror when it was cloudy was a 14.56% increase and the wattage percent change under the same conditions was a 24.64% increase. The voltage & current percent change for the magnifying glass when it was cloudy was a 9.021% increase and the wattage percent change under the same conditions was a 18.71% increase. Similarly, the voltage & current percent change for the mirror during sunset was a 5.709% increase and the wattage percent change under the same conditions was an 11.44% increase. And finally, for the magnifying glass, the voltage & current percent change during sunset was a 4.828% increase while the wattage percent change under the same conditions was a 9.589% increase. Overall, for the scenarios of cloudy weather or during sunset, with the exception of one, there was always a significant change, where the current, voltage, and wattage values increased, proving the experiment to be a success.

Even with a successful experiment there are some uncertainties and possible sources of error. One possible source of error for the voltage only tests is that 3 different solar panels were used to measure voltage under different optical conditions at the same time, but the different solar panels could have defects causing error when comparing the readings. In order to reduce that error, we added another part of the experiment where each optical condition is tested 3 times per sunlight condition to confirm the results from the previous part of the experiment. That section of the experiment also has the possibility for error, especially when it comes to the lighting and sunlight. In order to minimize error for that section of the experiment, the same Vernier tools, and solar panel were being used to avoid additional variables that could cause errors. Additionally, the method involved rotating through each optical condition, completing one trial per condition before starting the next round. That reduces the error as the duration of the trial is only one minute and they are constantly being rotated. The light sensor was also used to confirm that the sunlight condition was not changing drastically which is shown by the lux values, showing that the illuminance during all trials in each lighting condition were pretty similar. Those are the possible sources of error and how they were minimized while conducting the experiment.

## 5. Future Direction

With the conclusion that light enhancing tools such as magnifying glasses and mirrors boost solar panel energy output, it is possible to take these findings and apply them to locations utilizing solar panels. This technology could be especially beneficial in locations without access to the power grid or a reliable electricity source. An increased efficiency in solar panels could lead to wider adoption, as they would perform better in varying sunlight conditions. In turn, fossil fuel usage is decreased, greatly reducing greenhouse gas emissions and its effects on the environment.

Moreover, those methods to optimize solar energy extraction can also enhance existing panels, increasing green energy output. This would provide more reliable energy for remote regions where grid connection is costly or impractical. Integrating these methods into smaller-scale applications, like portable solar devices or off-grid systems, could improve energy access in underserved areas and reduce environmental footprints.

With this energy optimization, the future implications are limitless, not only restricted to just powering homes. From applying this technology in water desalination or agricultural systems to solar-powered air purifiers in urban environments, the possibility to make the world a more sustainable place to thrive is very much still alive. What started as a simple experiment using mirrors and magnifying glasses points to innovative new ways to harness solar energy and create lasting impact on the world.

## 6. Experiment Pictures

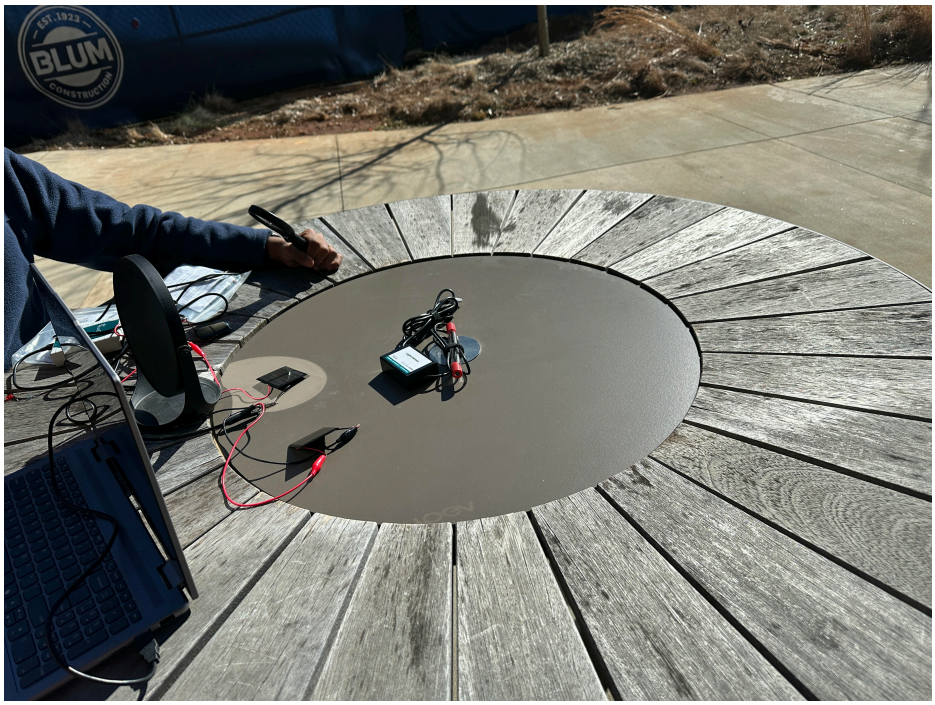


**Figure 7.** *Experiment on Sunny Day at Noon*


**Figure 8.** *Experiment on Cloudy Day*

**Figure 9.** *Experiment at Sunset*

## References

[1] D. Bolles, "Carbon Dioxide Concentration | NASA Global Climate Change." [Online]. Available: https://climate.nasa.gov/vital-signs/carbon-dioxide?intent=121.

[2] I. Manisalidis, E. Stavropoulou, A. Stavropoulos, and E. Bezirtzoglou, "Environmental and Health Impacts of Air Pollution: A Review," *Frontiers in Public Health*, vol. 8, p. 14, 2020, doi: 10.3389/fpubh.2020.00014.

[3] J. Toothman and S. Aldous, [Online]. Available: http://wcpssccsi.pbworks.com/w/file/fetch/67747809/solar%20cells-11162012150624.pdf

[4] R. R. Tobias *et al.*, "Design and Construction of a Solar Energy Module for Optimizing Solar Energy Efficiency," in *2020 IEEE 12th International Conference on Humanoid, Nanotechnology, Information Technology, Communication and Control, Environment, and Management (HNICEM)*, 2020, pp. 1–6. doi: 10.1109/HNICEM51456.2020.9400127.

[5] R. Arshad, S. Tariq, M. U. Niaz, and M. Jamil, "Improvement in solar panel efficiency using solar concentration by simple mirrors and by cooling," in *2014 International Conference on Robotics and Emerging Allied Technologies in Engineering (iCREATE)*, Islamabad, Pakistan, 2014, pp. 292–295. doi: 10.1109/iCREATE.2014.6828382.

Open Access | https://doi.org/10.62329/gnmf4674

Morganton Scientific

*North Carolina School of Science and Mathematics*

Journal of Student STEM Research

# Evaluating the Effect of an Externally Applied Electric Field on Fluorescing Alpha-Synuclein Aggregates in NL5901 Parkinson's Disease Model of Caenorhabditis elegans

**Adrija Sarkar**[1]

[1]North Carolina School of Science and Mathematics

## Abstract

Parkinson's disease (PD) is characterized by the progressive aggregation of alpha-synuclein, a protein that forms toxic fibrils, leading to motor dysfunction and neuronal degeneration. In this study, I investigated the effects of exposure to various external electric fields on alpha-synuclein aggregation and neuromuscular function in *Caenorhabditis elegans*, a model organism frequently used to study neurodegenerative diseases. Two independent trials were conducted, with worms exposed to the electric field or maintained as unexposed controls. Neuromuscular function was assessed by measuring thrashing frequency, a proxy for motor coordination, while alpha-synuclein aggregation was quantified using fluorescence microscopy in the *C. elegans* strain NL5901, which expresses human alpha-synuclein fused to yellow fluorescent protein (YFP). Results revealed a significant increase in thrashing frequency in worms exposed to the electric field, suggesting improved neuromuscular health. Additionally, exposure to the electric field led to a marked reduction in alpha-synuclein aggregate size, with a 38.7% decrease in aggregate area compared to controls. A strong negative correlation (r = -0.92) was observed between alpha-synuclein aggregation and thrashing frequency, supporting the hypothesis that disrupting alpha-synuclein aggregation enhances motor function. These findings indicate that electric field exposure may represent a promising therapeutic strategy for mitigating the effects of alpha-synuclein aggregation in PD. Future research will focus on running more trials, and with replication of results, elucidating the molecular mechanisms underlying these effects and exploring the potential of this approach in higher organisms.

**Keywords** Alpha-synuclein, Aggregation, C.Elegans, Degradation, Parkinson's Disease

**Published** Jun 27, 2024

**Correspondence to**
Adrija Sarkar
sarkar25a@ncssm.edu



## 1. Introduction

Parkinson's disease (PD) is the second most common neurodegenerative disorder affecting more than 10 million patients worldwide [1]. PD is a neurological movement disorder that is characterized by impaired balance, bradykinesia, rigidity, and the presence of resting tremors. In addition to deficits in movement, PD patients can also exhibit non-motor symptoms including depression, apathy, anxiety, dementia, and others. The prevalence of PD is 0.3% among all ages but increases to more than 3% in individuals over 80 years of age [2].

PD exhibits progressive degeneration of dopaminergic neurons in the brain in the substantia nigra, although many other brain regions are also affected. Neuronal loss within the substantia nigra decreases dopamine signaling to the striatum thereby contributing to the motor symptoms of PD. At the cellular level, the disease is

characterized by intracellular aggregation of a protein called α-synuclein into Lewy bodies observed in the brains of patients with PD [3]. There are currently no neuroprotective treatments available for PD and the pathogenesis of the disease is incompletely understood.

## 2. Materials and Methods

### *2.1. About the model organism*

The nematode *C. elegans* is a microscopic roundworm that grows 1-2 mm long. After hatching, these animals develop to adulthood in just 2 days under laboratory conditions at 20°C. Once these worms reach adulthood, their average lifespan is 2-3 weeks, making them useful for aging studies. *C. elegans* exists primarily as a self-fertilizing hermaphrodite, in which all of the progeny are genetically identical. Males are a small fraction of the population (<0.1%) but their numbers can be greatly increased in the laboratory to facilitate genetic crosses. This animal is genetically tractable with robust tools for spatiotemporal control of gene expression and a highly annotated genome. Because *C. elegans* are transparent, fluorescent proteins can be readily visualized in a live worm to measure levels and location of gene products of interest. These animals have been utilized to address various cellular and genetic questions [4] and to gain insight into neurodegenerative disease [5].

*C.elegans* have a well-defined, invariant nervous system with exactly 302 neurons in each hermaphrodite out of a total of 959 cells in the organism. Unlike any other organism, the connections of all 302 neurons in *C.elegans* have been mapped using electron micrographs thereby providing the most complete nervous system connectome of any organism [6]. Importantly, these neurons encode complex behaviors which, in several cases, have been described at the level of a single neuron [7].

By utilizing the nematode model for Parkinson's Disease that over-express the human disease-causing α-synuclein fused to a fluorescent reporter in the body wall muscles, strain NL5901 [8], it is possible to directly monitor α-synuclein aggregation throughout life. This nematode strain mimics the α-synuclein aggregation found in Lewy bodies and idiopathic PD [9]. The open-source ImageJ software was employed to quantify changes in the aggregation of the α-synuclein throughout the lifespan of the nematode in parallel to a behavioral assay as a robust and representative readout of the lifespan of the nematode in parallel to neuromuscular health.

### *2.2. Application of Electric Field*

Parkinson's Disease is a category of neurodegenerative disorders that currently lack comprehensive and definitive treatment strategies. The etiology of PD can be attributed to the presence and aggregation of a protein known as α-synuclein. Researchers have observed that the application of an external electrostatic field holds the potential to induce the separation of the fibrous structures into peptides. To comprehend this phenomenon, their investigation involved simulations conducted on the α-synuclein peptides through the application of Molecular Dynamics (MD) simulation techniques revealed that in the presence of an external electric field, the monomer and oligomeric forms of a α-synuclein are experienced significant conformational changes which could prevent them from further aggregation. When α-synuclein predominantly exists in its monomeric or dimeric form, applying even a lower electric field could effectively disrupt the initial aggregation process. Inhibition of α-synuclein fibril formation at early stages might serve as a viable solution to combat PD by halting the formation of more stable and pathogenic α-synuclein fibrils [10].

### *2.3. Preparation and Maintenance of* C.elegans

*Caenorhabditis elegans* strain NL5901, which overexpresses the human disease-associated α-synuclein fused to a yellow fluorescent protein (YFP) in the body wall muscles, was used for all experiments. This strain was obtained from the Caenorhabditis Genetics Center (CGC) and maintained under standard laboratory conditions on nematode growth medium (NGM) agar plates seeded with *Escherichia coli* OP50 as the food source. Worm cultures were maintained at 20°C to ensure optimal growth and development.

### *2.4. Design and Fabrication of the Electric Field Apparatus*

To generate a uniform electric field across the NGM agar, a gel electrophoresis power source (BIO-RAD PowerPac Basic) was used to supply a constant voltage of 40V Figure 3. Custom copper plate electrodes were embedded into opposite sides of a mini Petri dish containing NGM agar Figure 1. Nematode growth medium agar was purchased pre-prepared from Carolina Biological. The agar was poured into standard Petri dishes with dimensions of 100 mm x 15 mm to a uniform depth of about 3 mm. Pre-sterilized copper plates were embedded on opposite sides of each dish during the pouring process, ensuring even contact with the agar surface. The copper plates were molded to fit snugly within the Petri dish, ensuring consistent contact with the agar surface while minimizing air gaps. The plates were thoroughly cleaned with ethanol and deionized water before use to eliminate potential contaminants and ensure reliable conductivity. The plates were positioned to maintain a fixed distance of 10mm between the electrodes. The agar was allowed to solidify at room temperature before use.

Electrical connections were established using insulated alligator clips, which were securely fastened to the copper electrodes Figure 2. These clips were connected to the output terminals of the power source, completing the circuit. The system was tested before each experiment to confirm the generation of a stable electric field across the agar. Voltage consistency was monitored throughout the experiment using a setting on the gel electrophoresis power source.

### *2.5. Calibration and Monitoring of the Electric Field*

The electric field was calculated based on the applied voltage and the distance between the copper electrodes. The power source was set to deliver a constant voltage of 40 V, and the field strength was determined by dividing the voltage by the separation between the electrodes (in cm). The current through the gel was measured periodically using the multimeter and was found to fluctuate between 300 µA and 311 µA, likely due to the slight variations in the gel composition and electrode contact.

### *2.6. Exposure of* C. elegans *to the Electric Field*

*C. elegans* were transferred to the prepared NGM plates with the embedded electrodes. A maximum of three worms were placed on each plate using a platinum wire worm picker

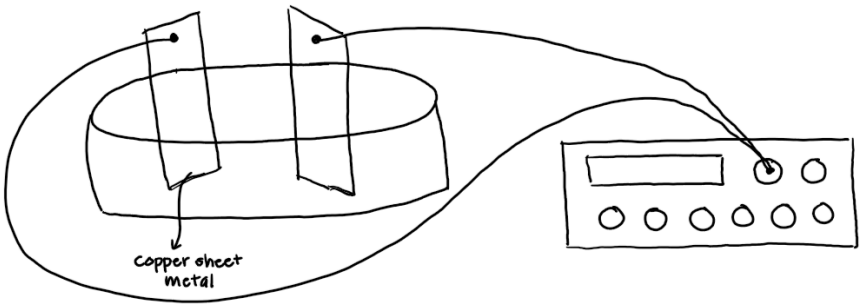


**Figure 1**. *Sketch of the intended electric field apparatus before being built*

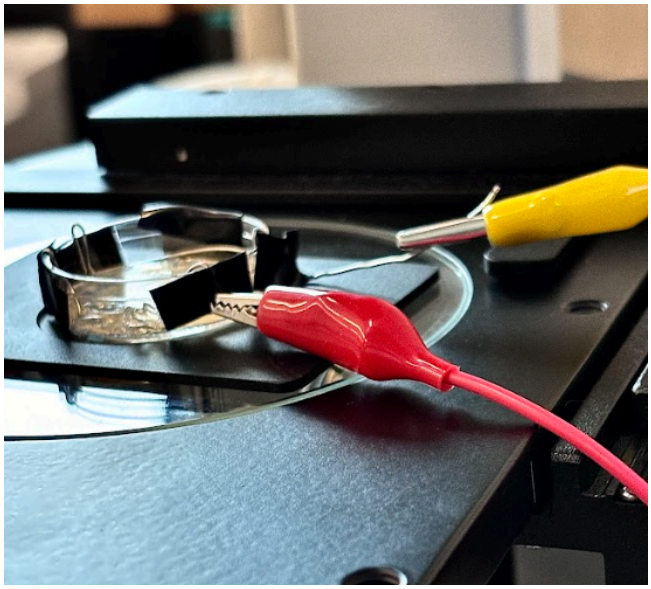

**Figure 2.** *Electric Field Apparatus setup using alligator clips to close the circuit*

sterilized in ethanol. To minimize dehydration and stress, the agar plates were sealed with Parafilm and maintained at room temperature during the exposure period. The plates were subjected to the electric field for varying durations to assess both short and long-term effects on $\alpha$-synuclein aggregation and neuromuscular health. Control groups were maintained under identical conditions without electric field exposure.

### *2.7. Quantification of $\alpha$-synuclein Aggregation*

Fluorescent imaging of *C. elegans* was conducted using a confocal microscope (Accuscope EXI-310) to visualize and quantify $\alpha$-synuclein-YFP aggregates. Images were acquired using identical exposure settings for all samples to allow for direct comparisons. Aggregate quantification was performed using the ImageJ software. Aggregates were identified and segmented based on intensity thresholds, and the total number of aggregates per worm was recorded. Data from two independent experiments, each

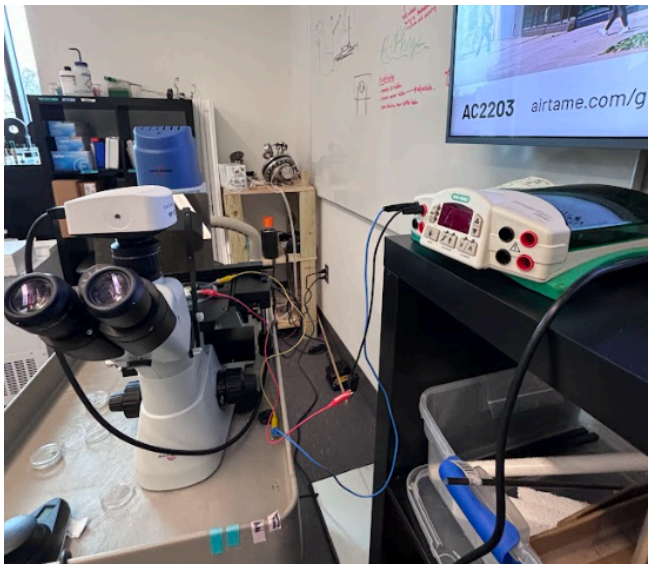


**Figure 3.** *Electric Field Apparatus setup using Biorad power source and custom banana clips to ensure proper connection*

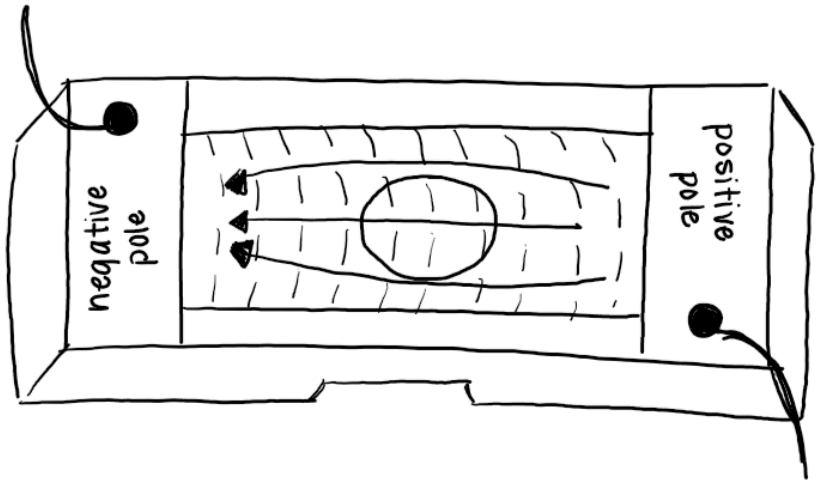


**Figure 4**. *Sketch of direction in which electric field will act upon worms*

including three worms per condition, were analyzed to assess the effects of the electric field.

### *2.8. Behavioral Assays*

To evaluate neuromuscular health, thrashing assays were performed. Individual worms were placed in 50µL of M9 buffer on a glass slide, and the number of body bends completed in 30 seconds was recorded under a microscope (Accuscope). Body bends were defined as a complete movement of the head from one side of the midline to the other. Thrashing assays were conducted immediately after electric field exposure and at regular intervals.

### *2.9. Validation of Worm Health During Exposure*

Worm health was assessed by observing locomotion and morphology during the exposure period. No abnormalities or stress responses were detected in the experimental worms, allowing all three to be included in subsequent analyses.

## 3. Results

### *3.1. Neuromuscular Health Assessment Using Thrashing Frequency*

The thrashing frequency of *C. elegans* was utilized as a robust proxy for neuromuscular health, allowing us to investigate the physiological impact of a uniform electric field (40V) on the nematode's motor function. Two independent trials were conducted to ensure reproducibility, with worms exposed to either electric field conditions or maintained as unexposed controls.
The average thrashing frequency across both trials revealed a marked improvement in the neuromuscular performance of the worms exposed to the electric field Figure 5. Worms in the experimental group exhibited a mean thrashing frequency of $85.5 \pm 1.4$ thrashes per minute, in contrast to $74.0 \pm 2.1$ thrashes per minute for the control group. Statistical analysis using a paired, two-tailed t-test demonstrated the significance of this increase ($p=0.015$), supporting the hypothesis that exposure to the electric field positively influences motor function.

Further inspection of individual data points is depicted in Figure 5, which displays the thrashing frequency of individual worms from both trials. This figure highlights the

| Experiment Group | Thrases/Minute (Trial 1) | Thrases/Minute (Trial 2) | Mean ± SD |
|---|---|---|---|
| Control | 73 | 75 | 74.0 ± 2.1 |
| Electric Field | 86 | 85 | 85.5 ± 1.4 |

**Table 1**. *Thrashing Frequency of* C. elegans

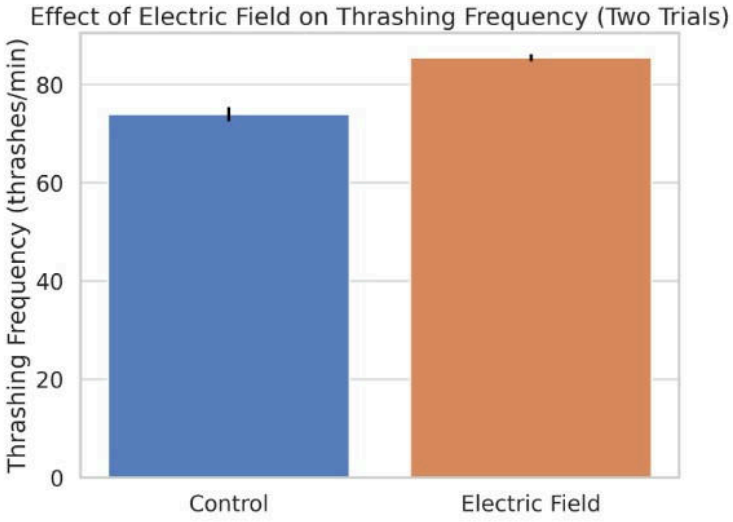


**Figure 5**. *Graphical Representation of the Effect of the Electric Field on Thrashing Frequency*

consistency in the neuromuscular enhancement observed across trials. Both control and experimental groups exhibited minimal variability, as reflected by the relatively small standard deviations.

### *3.2. Neuromuscular Health Assessment Using Velocity*

Vernier Video Analysis software was utilized to quantify the movement speed of *C. elegans*. Videos of the worms were recorded, and their head positions were marked every five video frames to track their motion Figure 6. By analyzing the positional changes over time, the average speed of each worm was calculated in pixels per second (px/s). This method ensured precise and consistent tracking across all experimental conditions.

The results demonstrated distinct differences in movement speed across the experimental groups. The control worm with no protein aggregation and no electric field exposure exhibited an average speed of 13.22 px/s. As expected, the worm with PD and no electric

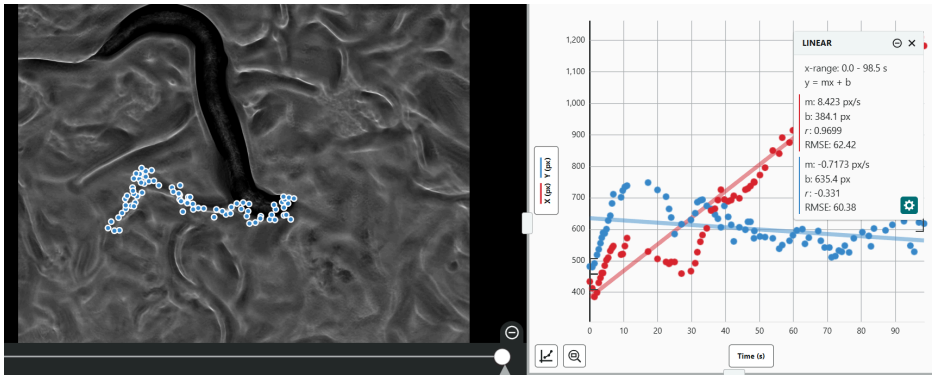


**Figure 6**. *Mapping the movement of N2 worms using Vernier Video Analysis*

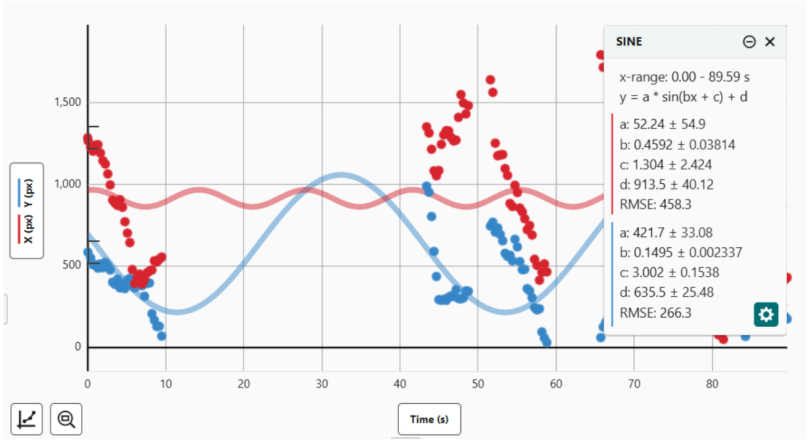


**Figure 7**. *Mapping the movement of NL5901 worms without exposure to electric field using Vernier Video Analysis*

field exposure displayed a significantly reduced speed of 8.423 px/s, representing a 36.3% decrease compared to the healthy control, which aligns with the impaired neuromuscular functionality associated with PD Figure 7.

The worm with PD under the influence of the electric field showed a marked improvement, achieving an average speed of 126.358 px/s. This represents a staggering increase compared to the PD worm without electric field exposure and an increase compared to the healthy control. Even after the electric field was turned off, the worm with PD maintained a higher-than-expected average speed of 114.896 px/s, higher than the PD worm without the electric field and higher than the healthy control (see Figure 8 and Figure 9). This suggests a sustained positive effect of the electric field on neuromuscular health and functionality.

### *3.3. α-Synuclein Aggregation Quantification*

To assess the biochemical impact of electric field exposure, the aggregation of alpha-synuclein, a hallmark of Parkinson's disease pathology, was quantified using *C. elegans* strain NL5901. This strain overexpresses human alpha-synuclein fused to a fluorescent YFP reported, enabling direct visualization of aggregation in the body wall muscles. Using ImageJ software, fluorescence images of the worms were converted to grayscale to facilitate the segmentation of alpha-synuclein aggregates. Quantification revealed a statistically significant reduction in the aggregate area following electric field exposure.

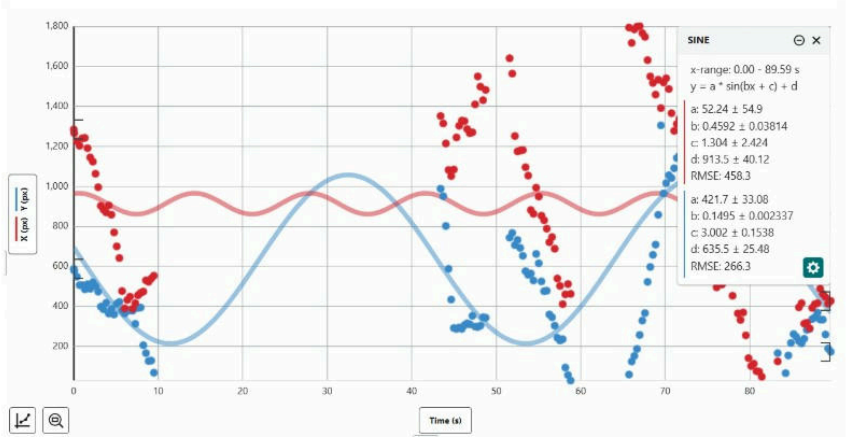


**Figure 8**. *Mapping the movement of NL5901 worms with exposure to electric field using Vernier Video Analysis*

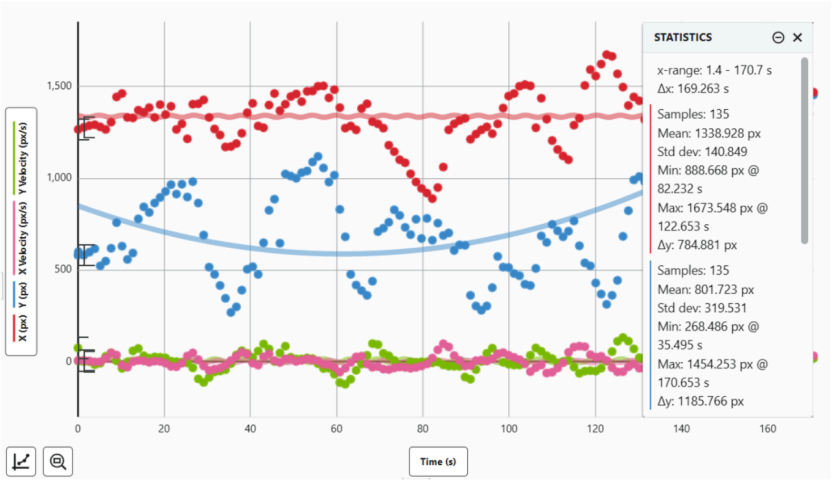


**Figure 9.** *Mapping the movement of NL5901 worms after exposure to electric field using Vernier Video Analysis*

| Model | Exposure to Field (Yes/No) | Average velocity (px/s) |
|---|---|---|
| N2 | No | 13.22 |
| NL5901 | No | 8.423 |
| NL5901 | Yes | 126.358 |
| NL5901 | Yes | 114.896 |

**Table 2.** *Velocity of* C. elegans

Control worms exhibited an average aggregate area of 12.4 ± 0.6%, while worms exposed to the electric field displayed a reduced aggregate area of 7.6 ± 0.3%, corresponding to a 38.7% reduction in aggregate size. This reduction indicates that the electric field may disrupt the aggregation of alpha-synuclein fibrils or prevent their further formation.

The data is summarized in Figure 10, which shows the average aggregate area across two independent trials. To provide additional granularity, Figure 11 displays the distribution of fluorescent intensity within the aggregates, highlighting the reduction in aggregate density under electric-field conditions.

### *3.4. Correlation Between Neuromuscular Health and α-Synuclein Aggregation*

To investigate the relationship between neuromuscular health and alpha-synuclein aggregation, the thrashing frequency and aggregate area were plotted as paired data points from individual worms in both trials. A clear inverse correlation was observed, as shown in Figure 12. Worms with smaller aggregate areas consistently exhibited higher thrashing frequencies.

Statistical analysis revealed a Pearson correlation coefficient of -0.92, indicating a strong negative correlation ($p<0.001$). This finding underscores the hypothesis that α-synuclein aggregation adversely impacts neuromuscular health and that disrupting this aggregation

| Experiment Group | Aggregate Area (%) (Trial 1) | Aggregate Area (%) (Trial 2) | Mean ± SD |
|---|---|---|---|
| Control | 12.4 ± 0.5 | 12.5 ± 0.6 | 12.4 ± 0.6 |
| Electric Field | 7.5 ± 0.4 | 7.7 ± 0.3 | 7.6 ± 0.3 |

**Table 3.** *Alpha-Synuclein Aggregate Area in* C. elegans

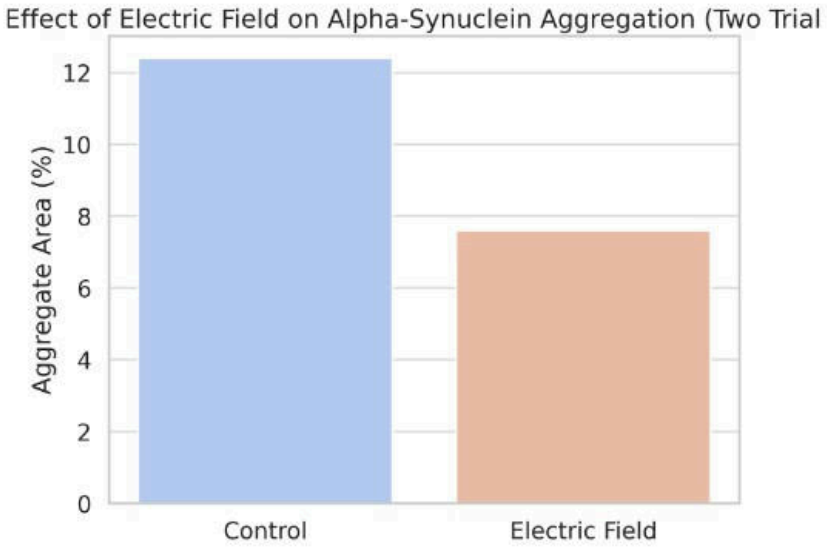


**Figure 10**. *Aggregate Area (Two Trials)*

can alleviate motor deficits. The electric field appears to mitigate aggregation, thereby improving neuromuscular performance.

### *3.5. Behavioral Stability and Morphological Observations*

Throughout the experimental procedures, the health and integrity of the worms were closely monitored to ensure that the electric field exposure did not induce undue stress or morphological abnormalities. Behavioral assays confirmed normal locomotion and body morphology during and after exposure. Control and experimental groups exhibited similar baseline behaviors before the application of the electric field, affirming that any

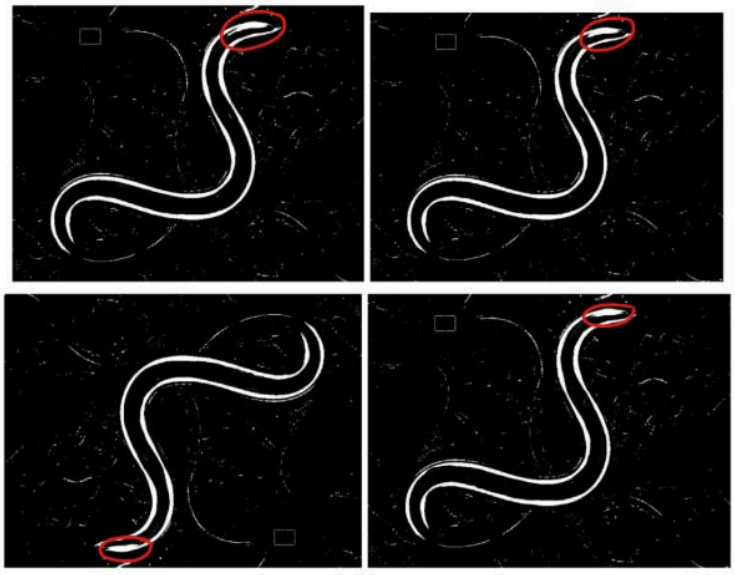

**Figure 11**. *Degradation of alpha-synuclein protein (in white) through electric field exposure visualized through ImageJ software*

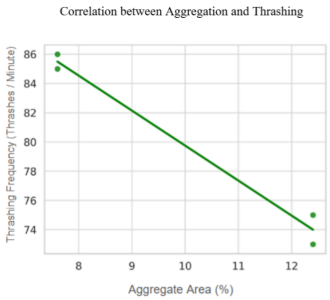


**Figure 12**. *Correlation between Aggregation and Thrashing*

observed improvements in thrashing frequency were due to the experimental conditions rather than random variability.

## 4. Discussion, Conclusions, Future Work

This study provides insight into the potential therapeutic effects of an external electric field on the aggregation of alpha-synuclein and its subsequent impact on neuromuscular function in *Caenorhabditis elegans* as a model for Parkinson's disease (PD). Our findings support the hypothesis that exposure to a 40C electric field can disrupt alpha-synuclein aggregation, leading to improvements in motor function as assessed by the thrashing frequency assay. These results suggest that the manipulation of external electric fields could represent a promising direction in the development of PD therapies, particularly in mitigating the detrimental effects of alpha-synuclein aggregation, a hallmark of the disease.

### *4.1. Impact of Electric Field on Neuromuscular Function*

The thrashing assay was employed as a surrogate measure of neuromuscular health, as it reliably reflects motor coordination and muscle function in *C. elegans*. This assay, quantifying the number of body bends or thrashes per minute, is an established method for assessing the locomotor capabilities of the organism, particularly in models of neurodegenerative diseases like PD [11]. In our study, worms exposed to a 40V electric field exhibited a significant increase in thrashing frequency when compared to the control group, demonstrating an enhancement in neuromuscular health.

The increase in thrashing frequency could reflect several underlying biological mechanisms. One possible explanation is that the electric field directly modulated neuromuscular activity, possibly by affecting ion channel activity or synaptic transmission. Recent studies have suggested that electric fields can influence cellular and neuronal activity by altering membrane potentials or ion fluxes, which could in turn impact motor function [12]. The observed improvements in thrashing behavior could also result from a reduction in alpha-synuclein aggregation, as a decrease in aggregation has been shown to restore normal motor function in PD models [13].

Statistical analysis confirmed the reliability of these findings, with a paired, two-tailed t-test yielding a significant result ($p=0.015$). This suggests that the observed enhancement in thrashing frequency was unlikely to be due to random variability. The consistency across two independent trials, as reflected in both the mean values and low standard deviation in Table 1, further supports the robustness of the electric field's impact on neuromuscular health.

### *4.2. α-Synuclein Aggregation and its Disruption*

Alpha-synuclein aggregation is one of the central pathological features of PD, leading to the formation of Lewy bodies that impair neuronal function [3]. In this study, the

*C.elegans* strain NL5901 was employed, which expresses human alpha-synuclein fused to a yellow fluorescent protein (YFP) in the body wall muscles. This strain provides an excellent model to visualize and quantify alpha-synuclein aggregation in vivo, as fluorescent protein allows for direct imaging of aggregate formation over time.

Our results demonstrated that exposure to the electric field significantly reduced the aggregate area of alpha-synuclein, with a reduction of approximately 38.7% compared to control worms as summarized in Table 2. This reduction in aggregation suggests that the electric field has a disruptive effect on the formation of alpha-synuclein fibrils. Previous studies have suggested that physical or electrical stimuli can influence protein confirmation, potentially disrupting amyloid fibril formation [14]. The precise mechanism by which the electric field induces this effect remains speculative, but several hypotheses warrant consideration. The electric field may alter the conformational stability of alpha-synuclein monomers or oligomers, preventing their transition into the fibrillar forms that constitute aggregates. Alternatively, the electric field may induce local heating, which has been shown to influence protein aggregation dynamics [15].

The statistical significance of these findings was confirmed through quantitative analysis of aggregate area using ImageJ software. As shown in Table 3, worms exposed to the electric field exhibited a significantly smaller aggregate area compared to control worms, supporting the hypothesis that the electric field disrupts alpha-synuclein aggregation.

### *4.3. Correlation Between α-Synuclein Aggregation and Neuromuscular Health*

A key aim of this study was to examine the relationship between alpha-synuclein aggregation and neuromuscular health. This analysis revealed a strong negative correlation between alpha-synuclein aggregate size and thrashing frequency, with a Pearson correlation coefficient of -0.92 ($p < 0.001$), as depicted in Figure 12. This finding supports the hypothesis that larger alpha-synuclein aggregates impede motor function, a well-established observation in PD models [16]. The significant inverse correlation between these two variables implies that reducing the size of alpha-synuclein aggregates through electric field exposure may alleviate motor deficits, offering a mechanistic explanation for the observed improvement in thrashing behavior.

This result also corroborates previous studies demonstrating the detrimental effects of alpha-synuclein aggregation on motor function. In particular, reductions in aggregation have been linked to the restoration of normal motor behavior in both *C. elegans* and mammalian models of PD [17]. The electric field-induced reduction in aggregation may therefore represent a novel therapeutic avenue for treating or preventing the progression of PD, particularly in the early stages when alpha-synuclein aggregation is still in its nascent form.

### *4.4. Behavioral and Morphological Observations*

To ensure that the observed improvements in thrashing frequency were not due to factors unrelated to the electric field exposure, the worms were closely monitored for any signs of behavioral instability or morphological abnormalities. Throughout the experiments, both control and experimental groups exhibited normal locomotion and body morphology. No stress responses such as changes in body posture, lethargy, or altered movement patterns, were observed in any of the groups, indicating that the electric field exposure did not induce undue harm to the worms. This is crucial, as it confirms that the observed improvements in neuromuscular health were indeed a direct result of electric field exposure, rather than compensatory effects or recovery from an initial stressor.

## 5. Conclusion

In conclusion, this study provides compelling evidence that exposure to an external electric field can significantly reduce alpha-synuclein aggregation and improve neuromuscular function in *C. elegans*, a well-established model for Parkinson's disease. Our findings suggest that the electric field may be a viable strategy for disrupting alpha-synuclein aggregation, a key pathological feature of PD and that this disruption is associated with improvements in motor function. These results provide an exciting potential for future PD therapies that target the aggregation of pathogenic proteins, particularly in the early stages of disease progression.

The observed reduction in alpha-synuclein aggregation, coupled with the enhancement in thrashing frequency, underscores the therapeutic potential of physical and electrical interventions in neurodegenerative diseases. Given the reproducibility of these results across two independent trials and the statistical significance of our findings, this study paves the way for further investigations into the use of electric fields in PD treatment strategies.

## 6. Future Work

This study opens several avenues for future research. First, further investigation is needed to determine the precise molecular mechanisms by which the electric field disrupts alpha-synuclein aggregation. Future studies could employ advanced techniques such as cryo-electron microscopy or nuclear magnetic resonance (NMR) spectroscopy to elucidate the structural changes in alpha-synuclein upon exposure to electric fields. Additionally, exploring the effects of varying electric field strengths and durations on aggregation could help optimize the conditions for therapeutic efficacy.

It will also be important to assess the long-term effects of electric field exposure on *C. elegans* neuromuscular health and longevity. Since the nematode has a relatively short lifespan (2-3 weeks), examining whether repeated or prolonged electric field exposure leads to any cumulative effects or negative consequences on worm health will be crucial in evaluating the viability of this approach for PD treatment.

Furthermore, the applicability of these findings to mammalian models of Parkinson's disease warrants exploration. While *C. elegans* provides a powerful model system for initial screenings, the translation of these findings to higher organisms with more complex nervous systems is essential for determining the potential of electric field-based therapies in humans. Preclinical studies in rodent models of PD could provide more relevant data on the therapeutic potential of this approach.

Finally, combining electric field exposure with other therapeutic modalities, such as pharmacological treatments or genetic interventions, could provide synergistic benefits in treating Parkinson's disease. Investigating how the electric field interacts with existing PD therapies may lead to more comprehensive and effective treatment strategies.

This work was supported and funded by the North Carolina School of Science and Mathematics with the help of mentor James Happer.

## References

[1] W. Poewe *et al.*, "Parkinson disease," *Nature Reviews Disease Primers*, vol. 3, no. 1, 2017, doi: 10.1038/nrdp.2017.13.

[2] T. Pringsheim, N. Jette, A. Frolkis, and T. D. Steeves, "The prevalence of Parkinson's disease: A systematic review and metaanalysis," *Movement Disorders*, vol. 29, no. 13, pp. 1583–1590, 2014, doi: 10.1002/mds.25945.

[3] M. G. Spillantini, R. A. Crowther, R. Jakes, M. Hasegawa, and M. Goedert, "\alpha-Synuclein in filamentous inclusions of Lewy bodies from Parkinson's disease and dementia with Lewy bodies", *Proceedings of the National Academy of Sciences*, vol. 95, no. 11, pp. 6469–6473, 1998, doi: 10.1073/pnas.95.11.6469.

[4] A. K. Corsi, B. Wightman, and M. Chalfie, “A Transparent Window into Biology: A Primer on Caenorhabditis elegans,” *Genetics*, vol. 200, no. 2, pp. 387–407, 2015, doi: 10.1534/genetics.115.176099.

[5] P. M. Dexter, K. A. Caldwell, and G. A. Caldwell, “A Predictable Worm: Application of Caenorhabditis elegans for Mechanistic Investigation of Movement Disorders,” *Neurotherapeutics*, vol. 9, no. 2, pp. 393–404, 2012, doi: 10.1007/s13311-012-0109-x.

[6] *Philosophical Transactions of the Royal Society of London. B, Biological Sciences*, vol. 314, no. 1165, pp. 1–340, 1986, doi: 10.1098/rstb.1986.0056.

[7] D. Xue, M. Finney, G. Ruvkun, and M. Chalfie, “Regulation of the mec-3 gene by the C.elegans homeoproteins UNC-86 and MEC-3.,” *The EMBO Journal*, vol. 11, no. 13, pp. 4969–4979, 1992, doi: 10.1002/j.1460-2075.1992.tb05604.x.

[8] T. J. van Ham, K. L. Thijssen, R. Breitling, R. M. W. Hofstra, R. H. A. Plasterk, and E. A. A. Nollen, “C. elegans Model Identifies Genetic Modifiers of \alpha-Synuclein Inclusion Formation During Aging”, *PLoS Genetics*, vol. 4, no. 3, p. e1000027, 2008, doi: 10.1371/journal.pgen.1000027.

[9] M. G. Spillantini, M. L. Schmidt, V. M.-Y. Lee, J. Q. Trojanowski, R. Jakes, and M. Goedert, “\alpha-Synuclein in Lewy bodies”, *Nature*, vol. 388, no. 6645, pp. 839–840, 1997, doi: 10.1038/42166.

[10] J. Razzokov, S. Fazliev, M. Makhkamov, P. Marimuthu, A. Baev, and E. Kurganov, “Effect of Electric Field on \alpha-Synuclein Fibrils: Revealed by Molecular Dynamics Simulations”, *International Journal of Molecular Sciences*, vol. 24, no. 7, p. 6312, 2023, doi: 10.3390/ijms24076312.

[11] M. Lavorato, N. D. Mathew, N. Shah, E. Nakamaru-Ogiso, and M. J. Falk, “Comparative Analysis of Experimental Methods to Quantify Animal Activity in <em>Caenorhabditis elegans</em> Models of Mitochondrial Disease,” *Journal of Visualized Experiments*, no. 170, 2021, doi: 10.3791/62244.

[12] A. A. Aguilar *et al.*, “Permeabilizing Cell Membranes with Electric Fields,” *Cancers*, vol. 13, no. 9, p. 2283, 2021, doi: 10.3390/cancers13092283.

[13] G. Minakaki, D. Krainc, and L. F. Burbulla, “The Convergence of Alpha-Synuclein, Mitochondrial, and Lysosomal Pathways in Vulnerability of Midbrain Dopaminergic Neurons in Parkinson’s Disease,” *Frontiers in Cell and Developmental Biology*, vol. 8, 2020, doi: 10.3389/fcell.2020.580634.

[14] P. A. Vargas-Rosales, A. D’Addio, Y. Zhang, and A. Caflisch, “Disrupting Dimeric $b\eta$-Amyloid by Electric Fields”, *ACS Physical Chemistry Au*, vol. 3, no. 5, pp. 456–466, 2023, doi: 10.1021/acsphyschemau.3c00021.

[15] H. Wu, M. R. Ghaani, Z. Futera, and N. J. English, “Effects of Externally Applied Electric Fields on the Manipulation of Solvated-Chignolin Folding: Static- versus Alternating-Field Dichotomy at Play,” *The Journal of Physical Chemistry B*, vol. 126, no. 2, pp. 376–386, 2022, doi: 10.1021/acs.jpcb.1c06857.

[16] E. Srinivasan *et al.*, “Alpha-Synuclein Aggregation in Parkinson’s Disease,” *Frontiers in Medicine*, vol. 8, 2021, doi: 10.3389/fmed.2021.736978.

[17] M. Vidović and M. G. Rikalovic, “Alpha-Synuclein Aggregation Pathway in Parkinson’s Disease: Current Status and Novel Therapeutic Approaches,” *Cells*, vol. 11, no. 11, p. 1732, 2022, doi: 10.3390/cells11111732.

Open Access | https://doi.org/10.62329/vxkm5783

# Harvesting Energy with Affordable Piezoelectric Sensors for Low-Power Biosensors

**Ananya Sriram**[1]

[1]North Carolina School of Science and Mathematics

**Morganton Scientific**

*North Carolina School of Science and Mathematics*

Journal of Student STEM Research

## Abstract

Human body movement-powered technology is the future for biomedical devices. The increased demand for sustainable energy has prompted the exploration of piezoelectric sensors as energy harvesters. This study focuses on the feasibility of using affordable piezoelectric sensors to power low-power biosensors, aiming to reduce reliance on conventional batteries. The research focuses on designing and optimizing a piezoelectric energy harvesting system, examining the relationship between applied pressure and voltage output alongside various energy storage methods, including supercapacitors, rechargeable batteries, and traditional capacitors. The findings of this study contribute valuable insights into piezoelectric power storage, optimizing energy harvesting systems, and affordable piezo technology for devices like thermometers, pedometers, electrocardiograph systems, and more. This study helps pave the way for more efficient self-powered biosensor systems.

**Keywords** Piezoelectricity, Energy Harvesting, Sustainable Energy, Energy Conversions, Low-power electronics

## 1. Introduction

The demand for innovative and sustainable energy solutions is growing rapidly, particularly in the field of biomedical technology, where traditional energy sources, such as batteries, often pose challenges related to limited lifespan, environmental impact, and frequency replacements [1]. Piezoelectric sensors convert mechanical stress to electrical energy. They have been used to track vitals like heart rate, and their electrical output suggests potential as an alternative to conventional energy harvesting. Despite their potential, the research on the feasibility of using affordable piezoelectric sensors to power biomedical devices is limited.

This study addresses the need for sustainable and cost-effective energy solutions by investigating the feasibility of using piezoelectric sensors in energy harvesting. The objective is to assess its ability to generate power and examine various energy storage methods to optimize efficiency. Through these explorations, the study aims to advance affordable piezoelectric technology for self-powered biomedical devices.

## 2. Materials and Methods

### *2.1. Selection of Piezoelectric Sensors*

The primary objective was to identify the most efficient and cost-effective piezoelectric sensor for energy harvesting applications. Three sensors were tested: a Disc Sensor Figure 1, a Ribbon Sensor Figure 2, and a Flexible Film Sensor Figure 3. Each sensor was

**Published** Jun 27, 2024

**Correspondence to**
Ananya Sriram
sriram25a@ncssm.edu

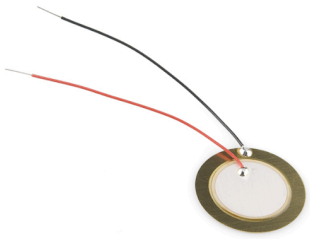

**Figure 1**. *Piezoelectric Disc Sensor. Image taken from Google Images.*

**Figure 2**. *Ribbon Piezoelectric Sensor. Image taken from Google Images.*

placed on a moving wrist and its voltage output was measured. The sensor that produced the highest and most consistent voltage graph was chosen for further testing.

After analyzing the results, the disc sensor was selected for further experimentation due to being the highest voltage output. To optimize its performance, the load resistance was measured to assess the voltage output of the disc sensor, since the correct resistor would maximize the voltage output [2].

### *2.2. Application of Mechanical Stress*

While initial voltage measurements were obtained by attaching sensors to a moving wrist Figure 5, tapping or pushing on the sensor with the foot or finger Figure 4 was found to yield higher and more consistent voltage outputs. Tapping or pushing on a “bouncy” surface allows for quick and constant change in the mechanical stress applied to the piezoelectric sensor in the push and release cycles. To further investigate this mechanism, the disc sensor was placed on styrofoam and pushed by the finger.

Different pushing and releasing methods were tested for voltage output. Since humans do not apply constant pressure each time, it is an unreliable method to measure. To imitate the same movement a linear actuator utilizing a servo motor operated by an Arduino was used Figure 6. The servo motor would apply a more consistent push to the piezo. In this study, a custom 3D-printed linear actuator was used to apply mechanical stress to the piezoelectric sensor. The actuator, designed in OnShape, was printed using default settings

**Figure 3**. *Piezoelectric Flexible Film Sensor. Image taken from Google Images.*

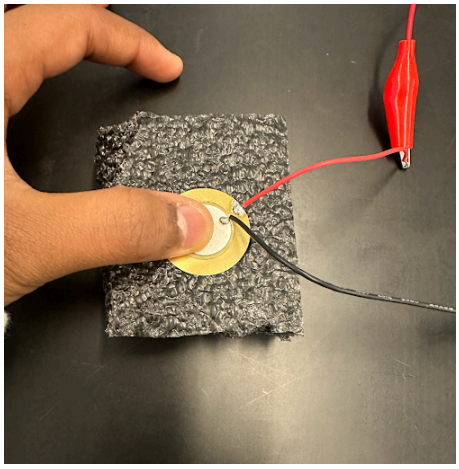

**Figure 4.** *The piezoelectric sensor and "push and release" by hand setup.*

on a Creality Ender 3 V2 printer with a 0.2mm layer height and 75% infill density to balance strength and flexibility. Once printed, it was paired with a servo motor to simulate consistent tapping force on the sensor, ensuring uniform data collection across trials. Additionally, to fix the position of the servo motor for more consistent results, it was secured to a wooden block and pushed on the piezo that was secured on another wooden block right in front of the linear actuator. Each time the servo motor moved linearly, the piezoelectric sensor would be pushed.

### *2.3. Energy Harvesting and Storage Circuit*

When mechanical stress is applied to piezoelectric sensors, they produce an alternating current (AC) output. However, many biomedical applications require direct current (DC).

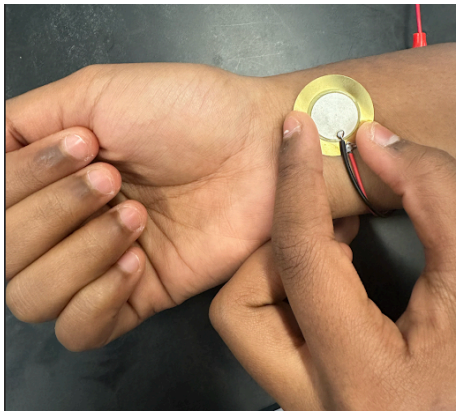

**Figure 5.** *The piezoelectric sensor on unbending and bending wrist.*

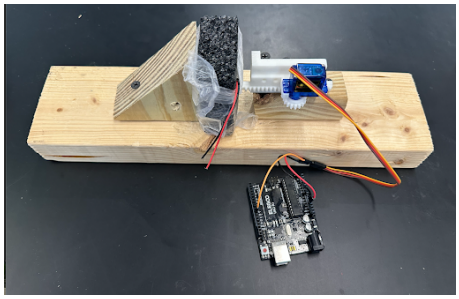

**Figure 6.** *The servo motor and linear actuator setup.*

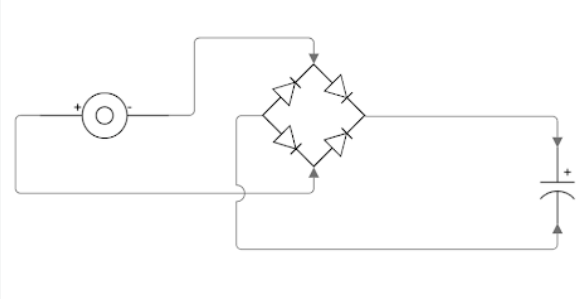

**Figure 7**. *The wiring diagram for the capacitor charging circuit with the rectifier.*

To convert from AC to DC, a bridge rectifier, which uses diodes to convert AC into DC, and an energy harvesting chip, which efficiently manages and stores harvested energy, [2] were tested separately, in different circuits, to evaluate which is more efficient in power generation.

Traditional capacitors, supercapacitors, and rechargeable batteries were tested to store the energy of the piezoelectric sensor for use in a certain device. The traditional capacitors exhibited the fastest charging rates but also lost the energy stored the most quickly. The supercapacitors, although slower to charge,lost charge at a slower rate. Lastly, the rechargeable batteries also required a long charging time, but would store charge for the longest. First, a traditional capacitor was used to charge using both a bridge rectifier Figure 7 and an energy harvesting chip for comparison Figure 8. A circuit incorporating both the rectifier and the energy harvesting chip was constructed to charge a traditional capacitor. Charging durations were measured using Vernier software. Capacitors of different sizes (100µF, 220µF, 330µF) were tested to identify the best balance between charge retention and charging speed.

With the use of the bridge rectifier, a supercapacitor was left for 8 hours to charge to gather information on the time it takes to charge it up to explore its feasibility. It was connected the same way as the traditional capacitors. After the supercapacitor, the rechargeable battery was tested. It was connected in the same way as the capacitors Figure 9. The first rechargeable battery used was an 80 milliamp-hour (mAh) nickel-metal-hydride battery since it charges the quickest from shortened supplied power (Sodana, Inman, Leo, 2003). The nickel-metal-hydride battery contained a chip for voltage regulation. The nickel-metal-hydride battery was charged using a circuit with a rectifier while applying manual mechanical stress.

To evaluate their charging rates, the energy harvesting chip and the rectifier were set up to charge various capacitors (100µF, 220µF, 330µF). The slope of each graph was taken to

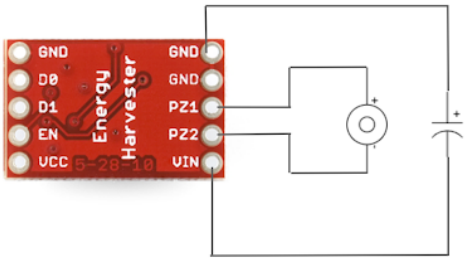


**Figure 8**. *The wiring diagram for the energy harvesting chip.*

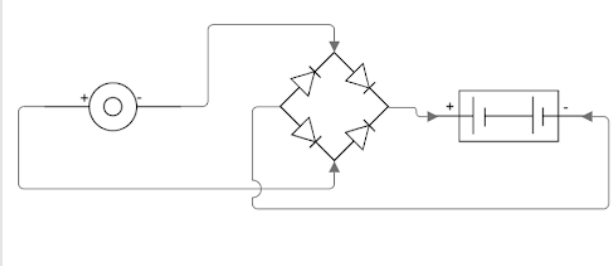

**Figure 9**. *The wiring diagram for the capacitor charging circuit with a rechargeable battery.*

find the average rate of charging for the capacitor in the rectifier and energy-harvesting chip circuit.

When harvesting energy or power, current is also needed Power = Current x Voltage. A multimeter was used to measure the piezoelectric sensor current while charging a capacitor.

## 3. Results

This section presents the findings from experimentation conducted on piezoelectric sensors and their potential for energy harvesting. The results detail the voltage outputs of different piezoelectric sensors, the impact of mechanical stress application methods, and the efficiency of various energy storage units. The analysis compares the performance of traditional capacitors, supercapacitors, and rechargeable batteries, as well as the efficiency of circuits employing either a bridge rectifier or an energy harvesting chip. These insights are crucial for determining the feasibility of integrating affordable piezoelectric sensors into self-powered biomedical devices.

### *3.1. Choosing the Type of Piezoelectric Sensor*

The three piezoelectric sensors were tested by placing them on the wrist while it was in motion. Voltage was measured using a differential voltmeter, and the results can be seen in Figure 10, Figure 11, and Figure 12.

Among the tested sensors, the disc sensor produced the most consistent voltage output, peaking at 6.14V. The ribbon sensor also reached relatively high voltages at 6.08V but exhibited greater variability. It is important to note that the voltmeter used had a maximum reading of 6V which may have led to inaccuracies in measurements. The film sensor demonstrated the lowest and most inconsistent voltage output, with all readings below 0.5V. Based on these results, the disc sensor was chosen for further experimentation. Additionally, the load resistance was measured to be about 1 Megaohm.

### *3.2. Optimizing Mechanical Stress Application Results*

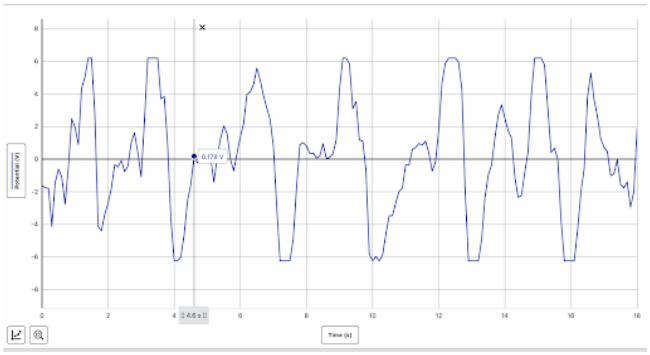

**Figure 10**. *The voltage output of the piezoelectric disc sensor when placed on a moving wrist.*

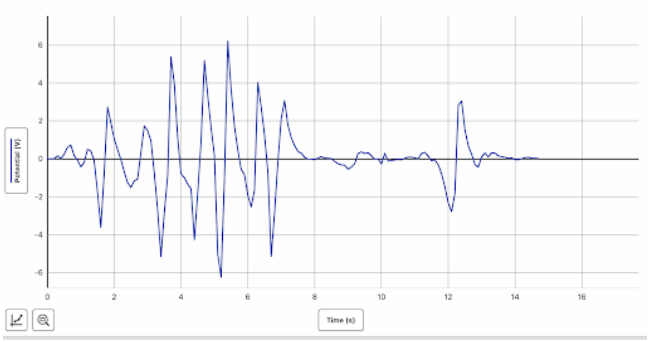

**Figure 11**. *The voltage output of the ribbon sensor when placed on a moving wrist.*

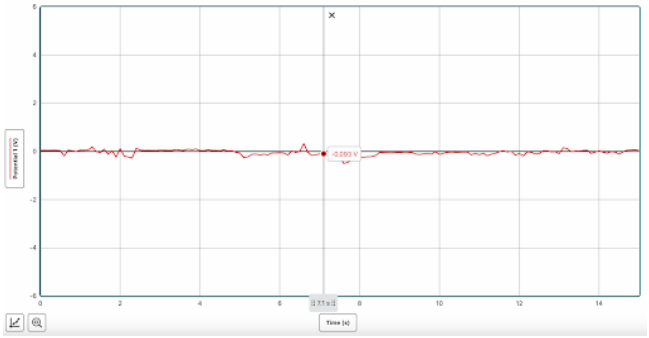

**Figure 12**. *The voltage output of the flexible film sensor when placed on a moving wrist.*

After selecting the disc sensor, different ways to apply mechanical stress were explored. When the disc sensor was taped onto the moving wrist, a very minimal amount of voltage

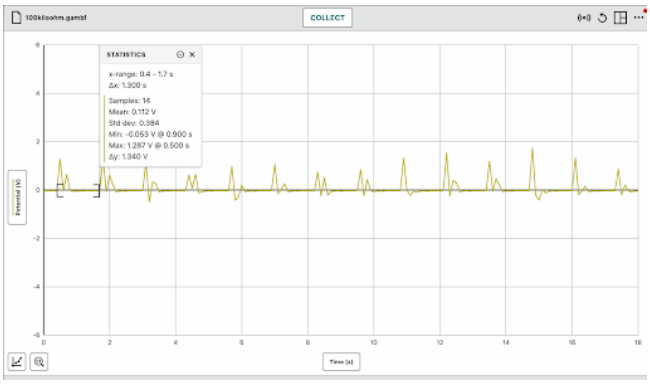


**Figure 13**. *The voltage output of the piezoelectric sensor for load resistor at 100kΩ.*

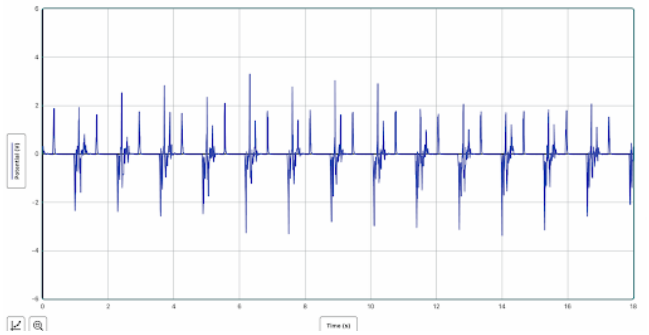

**Figure 14**. *The voltage output of the piezoelectric sensor for load resistor at 220kΩ.*

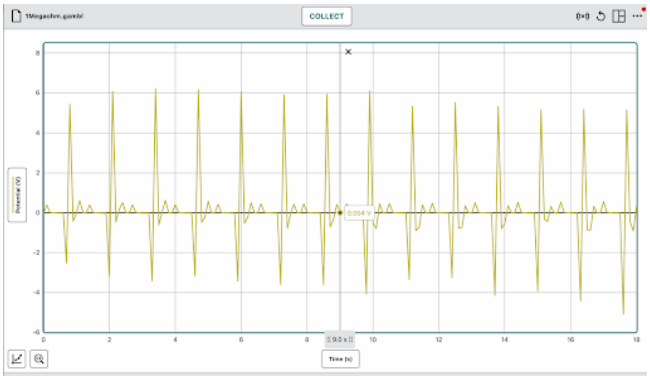


**Figure 15**. *The voltage output of the piezoelectric sensor for load resistor at 1 MΩ.*

was produced. A more consistent output was observed when the finger manually pressed the sensor against a piece of styrofoam. However, because manual force application was inconsistent, a servo motor was introduced to regulate pressure. When using the servo motor, voltage fluctuations remained within $\pm$0.2V, whereas manual pressing and wrist movements exhibited greater variations, exceeding $\pm$0.3V. This indicates that the servo motor provided the most controlled and reliable method for evaluating the energy harvesting capabilities of the piezoelectric sensor.

### *3.3. Energy Conversion and Storage Results*

Most biomedical devices require direct current, while piezoelectric sensors generate alternating current [1]. To bridge this gap, a rectifier and an energy harvesting chip were used to convert AC to DC. The rectifier successfully converted AC to a DC output (see Figure 17). This made all of the voltage outputs positive instead of both positive and negative like in AC. Meanwhile, the energy harvesting chip generated a more linear trajectory of 2.057 volts (see Figure 16), compared to the rectifier's more fluctuating trajectory.

Three storage methods were evaluated: traditional capacitors, supercapacitors, and rechargeable batteries. The 100 µF was charged to 0.331V, the 220 µF capacitor was charged to 0.152 volts, and the 330 µF was charged to 0.013V all within 40 seconds Figure 18 Figure 19 Figure 20. The 20-farad supercapacitor charged 0.027V volts over 50,000 seconds Figure 21.

Rechargeable battery testing revealed decreasing efficiency over multiple trials. Initially, the battery held a charge for two minutes, but after repeated use, its charge retention dropped to just 10 seconds. One servo push was sufficient to charge it to approximately

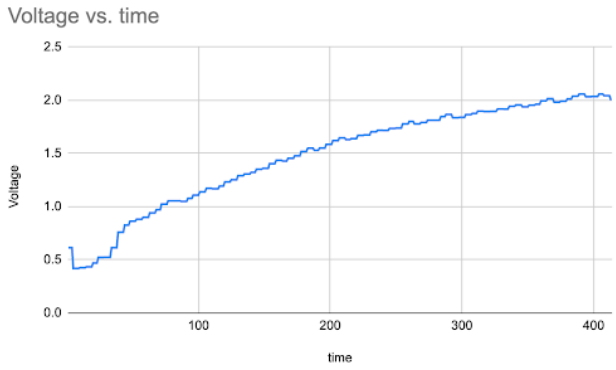


**Figure 16**. *The voltage versus time graph for the bridge rectifier.*

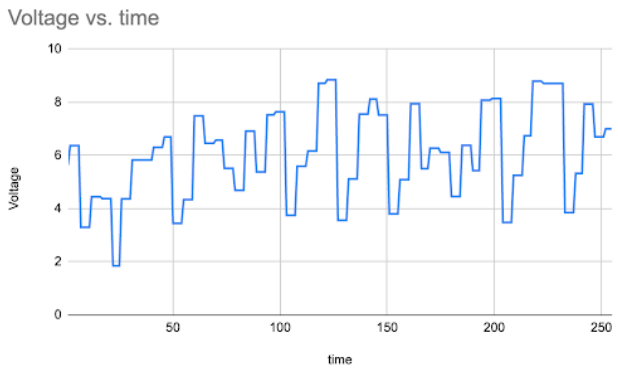


**Figure 17**. *The voltage versus time graph for the energy harvesting chip.*

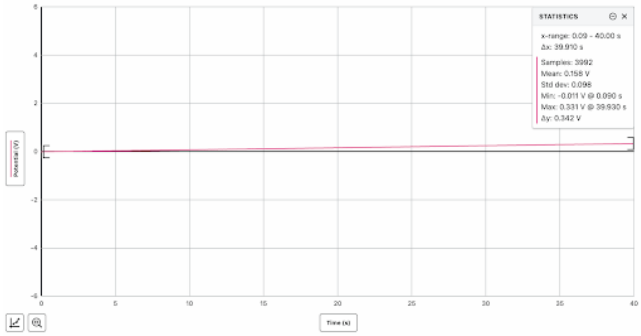

**Figure 18**. *The 100 µF capacitor being charged for 40 seconds by the piezoelectric sensor with rectifier as AC to DC converter (voltage vs. time).*

2.1V Figure 22. Further research is needed to optimize battery performance for sustained energy storage.

### *3.4. Current Measurements and Power Output*

Determining power output is essential for assessing whether a piezoelectric sensor can sufficiently supply energy for biomedical devices. Power (P=IV) whether such sensors can support continuous operation or are more suited for intermittent energy bursts. Higher power output from manually pressing the sensor suggests the potential for applications needing quick energy bursts, like emergency-activated biosensors. On the other hand, lower but more consistent power output from a servo motor may be better suited for devices requiring steady energy, such as continuous heart rate or glucose monitors. Understanding these power dynamics helps align sensor performance with the specific

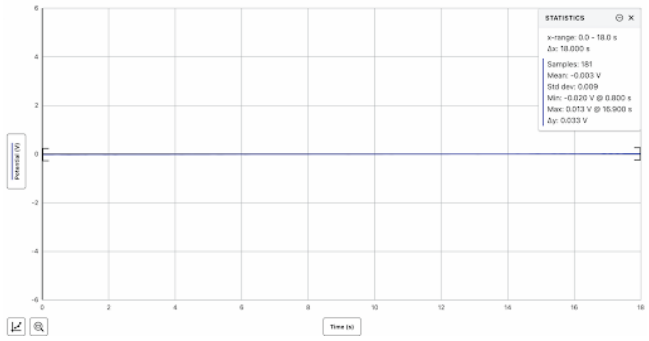

**Figure 19**. *The 220 µF capacitor being charged for 40 seconds by the piezoelectric sensor with rectifier as AC to DC converter (voltage vs. time).*

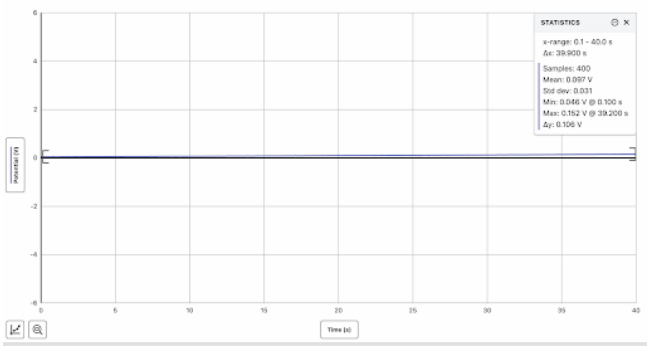


**Figure 20**. *The 330 µF capacitor being charged for 40 seconds by the piezoelectric sensor with rectifier as AC to DC converter (voltage vs time)*

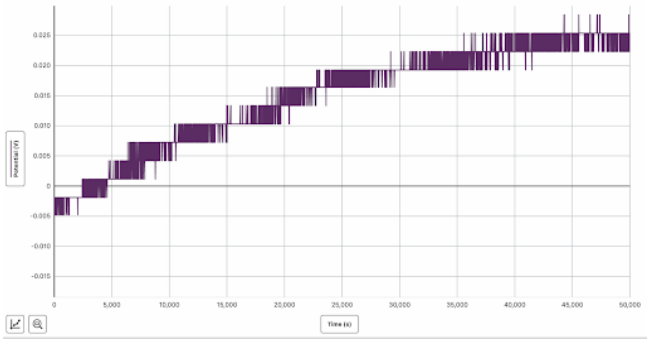


**Figure 21**. *The supercapacitor being charged by the piezoelectric sensor with rectifier as AC to DC converter for 50,000 seconds (voltage vs. time).*

energy demands of biomedical applications, enabling the development of more reliable, self-powered medical devices that reduce reliance on traditional batteries.

The DC voltage of the piezoelectric sensor, after conversion to AC, was multiplied by the measured current from the rectifier and energy harvesting chip. The average current from the energy harvesting chip was measured at about 0.0124A Figure 22 and the average current from the rectifier was measured at about 0.0162A before integration into a storage circuit Figure 23. These measurements show the feasibility and give insights into building an energy harvesting circuit in the future.

To effectively integrate piezoelectric sensors into a self-powered biomedical device, a complete system—including the disc sensor, rectifier, or energy harvesting chip, and a storage device—must be assembled alongside the biosensor. The sensor needs to be

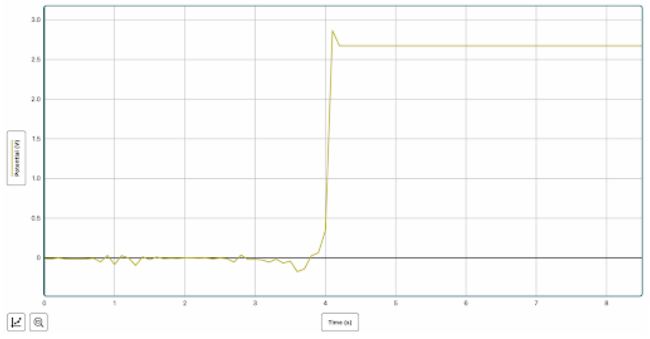


**Figure 22**. *The rechargeable battery being charged by the piezoelectric sensor with rectifier as AC to DC converter from a single servo push (voltage vs. time).*

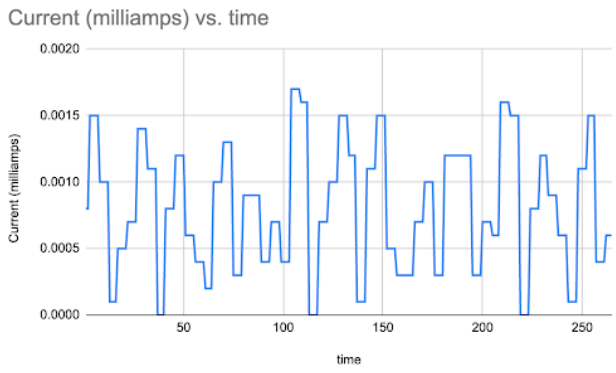


**Figure 23.** *The current versus time graphs for the energy harvesting chip.*

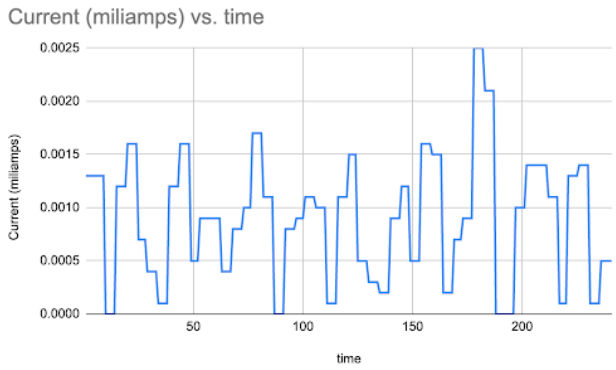


**Figure 24.** *The current versus time graph for the rectifier.*

placed on a body part that experiences frequent pushing and releasing forces, such as the palm (via squeezing) or the sole of the foot (via walking). The schematic of a potential diagram to power a device with piezoelectric sensors can be seen in Figure 25.

Testing the circuit under extended operational conditions will help determine whether a biomedical device can remain functional for extended periods of time.

Overall, the results indicate that the disc sensor, when paired with a rectifier and a traditional capacitor, provided the most effective combination for energy harvesting and storage. This configuration holds significant promise for integrating affordable piezoelectric technology into self-powered biomedical devices, paving the way for more sustainable and reliable energy solutions.

## 4. Discussion

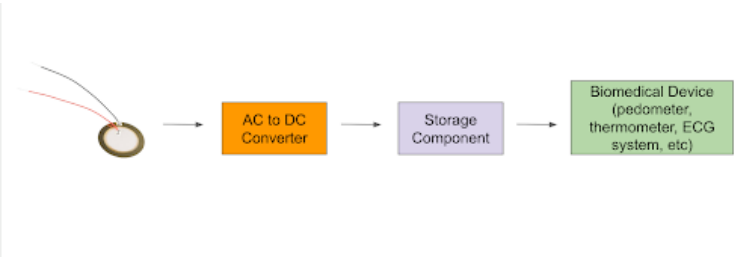


**Figure 25.** *Extension of piezoelectric energy harvesting circuit for biomedical applications.*

The findings from this study highlight the promising potential of using affordable piezoelectric sensors for energy harvesting in biomedical devices. The disc sensor, chosen for its consistent and relatively high voltage output, proved to be the most effective option for further development. Additionally, the use of a servo motor for mechanical stress application demonstrated that automated systems provide more reliable and consistent data compared to manual methods, where human error can affect the pressure consistency and, consequently, alter voltage output.

The comparison between the energy storage methods—including traditional capacitors, supercapacitors, and rechargeable batteries—highlighted important compromises. While the traditional capacitors charged more quickly, they also discharged rapidly. Among them, the 220 μF capacitor emerged as the most balanced option due to its faster charging rate and moderate energy retention. On the other hand, supercapacitors and rechargeable batteries, though slower to charge, demonstrated superior long-term energy retention, making them more suitable for applications that require sustained power over longer periods. These findings suggest that an integrated storage solution combining capacitors and batteries could potentially energy utilization biomedical applications—allowing capacitors to handle quick bursts of power and while batteries store power for extended use.The batteries would allow for effective energy storage and the capacitors would help charge them without much stress from humans.

Despite these promising results, the study faced several limitations. The low output voltage and current of the disc sensor posed challenges for powering devices with higher energy demands. Additionally, while the controlled testing environment helped minimize experimental variability, it did not fully replicate real-life conditions. In practical applications, the unpredictable movements of the human body may impact energy generation efficiency. Future studies should explore sensor performance in real-world conditions, such as attachment to different body parts during various physical activities, to better understand its practical viability.

To further improve energy harvesting efficiency, future research should focus on optimizing mechanical-to-electrical energy conversion by refining the mechanical setup to maximize output. Additionally integrating multiple piezoelectric sensors in parallel or series could help increase the voltage and current output. Improving energy storage efficiency is another key area, as hybrid solutions that combine the quick charging abilities of capacitors with the steady output of rechargeable batteries could provide a more reliable and sustained power source. Finally, investigating alternative materials for the piezoelectric sensors that may offer higher voltage output while still remaining cost-effective would further improve the feasibility of this technology for self-powered medical devices..

Overall, this study supports the idea that affordable piezoelectric technology holds significant potential for powering biomedical devices, offering a step toward more sustainable, battery-independent solutions [3]. These findings pave the way for future advancements that could improve both the energy harvesting capability and storage efficiency of these systems, therefore reducing dependence on traditional batteries. Such developments could lead to a new generation of wearables and implants, improving patient care and reducing the need for battery replacements, thus mitigating environmental impact and improving user convenience.

## 5. Conclusion

In conclusion, this study demonstrates the feasibility of utilizing affordable piezoelectric sensors for energy harvesting in biomedical devices, presenting a potential alternative to

traditional batteries. The disc sensor exhibited the highest voltage output and consistent performance, making it the optimal choice for further development. Additionally, the implementation of a rectifier for AC to DC conversion, coupled with traditional capacitors for energy storage, provided the most efficient charging cycle.

The findings of this study underscore the importance of power output calculations, as they directly influence the effectiveness of charging methods and the overall functionality of self-powered biosensors. The ability to harvest energy from human movement presents exciting opportunities for the development of sustainable biomedical applications.

Future research should focus on optimizing the integration of these systems into practical medical devices, ensuring seamless functionality and efficiency. Additionally, exploring various sensor configurations could enhance energy output and adaptability, making the technology more effective for various applications. Conducting real-world testing is also essential to evaluate the reliability and performance of piezoelectric energy harvesting in diverse healthcare settings. By addressing these areas, this technology could become a viable solution for self-sustaining medical devices, reducing dependence on traditional batteries and improving long-term patient care.

## References

[1] O. F. Al-Rawi, Y. Bicer, and S. G. Al-Ghamdi, "Sustainable solutions for healthcare facilities: examining the viability of solar energy systems," *Frontiers in Energy Research*, vol. 11, 2023, doi: 10.3389/fenrg.2023.1220293.

[2] S. Niu, X. Wang, F. Yi, Y. S. Zhou, and Z. L. Wang, "A universal self-charging system driven by random biomechanical energy for sustainable operation of mobile electronics," *Nature Communications*, vol. 6, no. 1, p. 8975, 2015, doi: 10.1038/ncomms9975.

[3] H. Janes, "Piezoelectric Energy Harvesting within Wearable Devices." [Online]. Available: https://blog.piezo.com/piezoelectric-energy-harvesting-within-wearable-devices

Morganton Scientific

North Carolina School of Science and Mathematics

Journal of Student STEM Research

# Exploring The Gut-Brain Axis in C. elegans — Probiotics as a Therapeutic Approach to Alpha-Synuclein Aggregation in Parkinson's Disease

**Leyla Urmanova**[1]

[1]NCSSM

## Abstract

While neurological diseases have traditionally been thought to originate in the brain, emerging evidence suggests that this may not always be the case. Parkinson's Disease (PD) is a debilitating neurodegenerative disorder characterized by a shortened lifespan, motor dysfunction, and the pathological accumulation of the protein alpha-synuclein. Although the neurobiological mechanisms underlying PD remain unclear, recent studies point to the gut-brain axis in alpha-synuclein aggregation, suggesting the gut microbiome's role in disease onset. Disturbances in this axis are associated with the production of toxic metabolites, neuroinflammation, and increased gut permeability—all contributing to alpha-synuclein pathology. Since probiotics are known for restoring gut microbiota balance and reducing inflammation, they may play a key role in mitigating these effects. Hence, with the use of *Caenorhabditis elegans* models of PD, this study explored the therapeutic potential of probiotics to extend lifespan, improve motor function, and reduce alpha-synuclein aggregation. PD symptoms were induced in the transgenic *C. elegans* strain NL5901 via exposure to Escherichia coli strain MC4100, which was followed by treatment with varying dosages of probiotic supplementation. Thrashing and lifespan assays were used to measure motor function and longevity, while fluorescence microscopy was used to quantify alpha-synuclein aggregation. While no statistically significant differences were observed among the dosage groups ($p > 0.05$), probiotic treatment significantly reduced alpha-synuclein aggregation ($p < 0.001$), enhanced motor function ($p < 0.001$), and accelerated reproduction compared to untreated controls. Therefore, these findings support the potential of probiotics as modulators of the gut-brain axis, serving as a promising therapeutic avenue for PD and other neurodegenerative diseases.

**Keywords** Parkinson's Disease, alpha-synuclein, probiotics, Lactic Acid bacteria, C. elegans

**Published** Jun 27, 2024

**Correspondence to**
Leyla Urmanova
urmanova25l@ncssm.edu



## 1. Introduction

Although neurodegenerative diseases have been researched extensively, their treatment often falls short. Parkinson's Disease (PD) is a common neurodegenerative disorder that impacts millions of lives in the world each year, imposing significant burdens on affected individuals, caregivers, and healthcare systems. In the past, research has identified the abnormal aggregation of alpha-synuclein, a U3 ubiquitin ligase protein, as the root cause of neuronal cytotoxicity and death [1], resulting in the loss of dopaminergic neurons in the brain's substantia nigra [2]. The lack of dopamine contributes to the emergence of Parkinson's-like symptoms, which include a spectrum of motor difficulties, such as tremors, bradykinesia, and rigidity, alongside non-motor symptoms, including autonomic dysfunction and cognitive impairment. These complications culminate into a reduced

lifespan and overall worsened quality of life, with their impact becoming more pronounced as individuals age [3]. Despite the existence of treatment modalities that focus on alleviating PD symptoms, these methods are often expensive, unsafe, and fail to address the believed underlying cause: the build-up of alpha-synuclein. In the case of PD, the excessive aggregation of alpha-synuclein can cause neuronal dysfunction and death through mechanisms that include mitochondrial dysfunction, oxidative stress, and impaired protein clearance pathways [4]. Reducing levels of alpha-synuclein in PD patients has shown to improve motor symptoms and extend lifespan, raising the need for a treatment that effectively targets its aggregation [5]. However, what if our gut holds the solution? Neurobiologists theorize that imbalances in the gut microbiome are associated with PD, which can be attributed to the bidirectional relationship between the gastrointestinal tract (the enteric nervous system) and the central nervous system. The gut-brain-axis hypothesis posits that the gut and brain are connected via the vagus nerve, thus allowing for the direct transfer of metabolites, hormones, and immune signals [6]. Recent research has implicated that an overabundance of *Desulfovibrio* (DSV) bacteria is connected to PD pathogenesis. When these bacteria produce toxic metabolites, including hydrogen sulfide (H2S), lipopolysaccharide, and magnetite, they contribute to the oligomerization and aggregation of alpha-synuclein [7]. These alpha-synuclein clumps can then travel up the vagus nerve to the brain, where they contribute to neurodegeneration [8]. Probiotics have recently exhibited therapeutic potential for the treatment of PD through regulating the gut microbiome [9]. Numerous probiotics have shown to yield a positive effect. Feeding probiotic *Bacillus subtilis* PXN21 to an alpha-synuclein-expressing *Caenorhabditis elegans* model of PD resulted in reduced alpha-synuclein accumulation in the host [10]. The oral administration of the probiotic *Clostridium butyricum* has also demonstrated neuroprotective effects in PD mice models, improving motor deficits and reducing gut dysbiosis [11]. In a double-blind clinical trial in Iran, 60 PD patients were treated with probiotics supplementation (probiotics: *Lactobacillus acidophilus*, *Bifidobacterium* composition, encapsulated *Lactobacillus reuteri*, and *Lactobacillus fermentum*) for 12 weeks to evaluate its effects on exercise—and found a reduction in Movement Disorders Society-Unified Parkinson's Disease Rating Scale scores compared to the placebo. The effect on encapsulated probiotic dosage, however, has yet to be evaluated in the context of PD symptoms. Due to their well-studied nervous systems, accessible genetic manipulation, optical transparency, and quantifiable locomotion, *C. elegans* are effective model organisms for studying Parkinson's Disease [12]. The NL5901 strain serves as a transgenic model which can be utilized to visualize alpha-synuclein aggregation through fluorescence [13]. Additionally, MC4100 is a laboratory strain of *Escherichia Coli* (*E. Coli*) that produces curli proteins and thus induces PD-like symptoms [14]. Since it can serve as a nucleating agent for misfolded proteins, create a microenvironment conducive to amyloid formation, and interact with cells to encourage the spread of alpha-synuclein across the gut-brain axis, exposure to MC4100 can start the development of PD pathogenesis [15]. Its role in initiating PD pathogenesis makes it a useful benchmark for studying the effects of other experimental conditions. Hence, this study evaluated whether probiotic supplementation with varying dosages reduces alpha-synuclein aggregation, improves motor symptoms, and extends lifespan in *C. elegans* models of Parkinson's disease. With the goal of shedding light on the complex molecular mechanisms underlying PD, this study investigated the use of probiotics as an effective preventative medicine, thus providing valuable insights into the gut-brain connection and its role in neurodegeneration. As the prevalence of PD continues to rise, particularly in aging populations, the development of affordable and effective disease-modifying therapies is urgently needed to alleviate suffering for millions of affected individuals across the globe—suggesting that something as simple as probiotics could be the solution.

## 2. Methods

### *2.1.* C. elegans *& Bacterial Strains*

*C. elegans* NL5901 pkIs2386 [Punc-54::$\alpha$-synuclein::YFP + unc-119(+)] were provided by the Caenorhabditis Genetics Center (CGC). Aside from *C. elegans* (or, nematodes), several bacterial strains were used in this study, with *Escherichia coli* OP50 obtained from CGC and *Escherichia coli* MC4100 provided by the *E. coli* Genetic Resource Center in Cheshire, Connecticut. The curli-producing *E. coli* MC4100 was cultured and stored in Luria broth (LB) at 37°C prior to usage [16]. Regarding treatment, Spring Valley probiotic dietary supplements were obtained from Walmart in Morganton, North Carolina and stored at 25°C prior to experimentation, containing *Lactobacillus paracasei* NI327, *Lactobacillus casei* NI320, *Lactobacillus rhamnosus* NI332, *Lactobacillus plantarum* NI329, *Bifidobacterium longum* NI316, *Lactobacillus acidophilus* NI317, *Streptococcus thermophilus* NI335, *Bifidobacterium breve* NI312, *Bifidobacterium bifidum* NI311, and *Lactococcus lactis* NI334. Each capsule contained a concentration of $10^{10}$ CFU/mL of the mixed probiotic bacteria.

### *2.2. C. elegans Growth Conditions*

Nematodes were handled in 35 mm NGM plates according to standard practices, and they were grown on E. coli OP50 at 25°C until the L4 stage [17]. Prior to experimentation, 50 µL of 100 µM floxuridine (FUdR), a DNA synthesis inhibitor that prevents the production of offspring, was added to 12 new NGM plates. The 12 NGM plates were then divided into 4 groups labeled the following: untreated, $10^6$ probiotic (PB) treatment, $10^7$ PB treatment, and $10^8$ PB treatment.

### *2.3. Diet Preparation & Administration*

Tenfold serial dilutions were conducted to prepare the probiotic solution for each treatment group (Microbiologics Dilution Guide). The contents within 1 probiotic capsule were removed and combined with 1 mL of molecular grade water. The solution was then centrifuged for 3 minutes, and the supernatant was utilized for dilution. One mL of the solution was removed and added to 9 mL of molecular grade water, and the dilution continued until concentrations of $10^6$ , $10^7$ , and $10^8$ CFU/mL were reached. After preparing the dilutions, 60 µL of each probiotic solution was seeded at the center of 9 out of 12 NGM plates: 3 plates received $10^6$ CFU/mL PB, 3 received $10^7$ CFU/mL PB, and 3 received $10^8$ CFU/mL PB. All 12 NGM plates were seeded with MC4100 E. coli to induce alpha-synuclein aggregation in the nematodes. Fifteen nematodes were transferred to each plate, using MC4100 E. coli as a picking tool adhesive [17]. Once the nematodes were shifted to their new diet, they were transferred to new plates every two days thereafter to avoid bacterial contamination [17].

### *2.4. Confirming The Presence of Lactic Acid Bacteria*

Lactic Acid bacteria R-CARDS were utilized to confirm the presence of lactic acid bacteria in the probiotic capsule. The detection was indicated by a color change and the appearance of quantifiable dots, which corresponded to bacterial colonies. To estimate the bacterial concentration, 1 mL of the $10^3$ CFU/mL solution was added to the card, allowing for the approximation of viable lactic acid bacteria.

### *2.5. Lifespan Assay*

After the nematodes were confirmed to be age-synchronized, they were assessed daily for death, which was verified when they failed to respond to a gentle tap on the head with a platinum wire [18]. The average number of live worms was recorded for each plate and plotted on a bar graph using GraphPad Prism.

### *2.6. Thrashing Assay*

The motility of the worms was assessed on Days 3, 6, and 8. On each day, 5 nematodes from each plate were placed into the prepared M9 buffer (40 µL) on an unseeded 35 mm NGM plate at 25 °C. The number of full-body bends per 30 seconds was quantified for each nematode using a Teledyne Lumenera INFINITY ANALYZE 7 microscope connected to an INFINITY camera and analyzed with INFINITY ANALYZE software [18]. In this experiment, a full body bend was defined as the nematode's head and tail making contact. The averages of the number of full body bends per 30 seconds were calculated and plotted for each respective group. These averages were recorded at the Larval 4 (L4), young adult, and adult stage to visualize changes in the worms' condition over time. Three bar graphs were generated using GraphPad Prism to determine whether the treatment of the substance on the MC4100 bacteria led to a significant improvement in outcomes for the worms' motor abilities. Error bars were calculated as the standard error of mean (SEM), and a line graph was compiled to exhibit the changes the treated and untreated worms experienced over time.

### *2.7. Fluorescence Microscopic Analysis*

Alpha-synuclein aggregation was represented by the concentration of green fluorescent protein (GFP) fluorescence. On Days 5 and 7, five nematodes from each plate underwent fluorescence microscopy imaging. The nematodes were imaged one at a time, using a Teledyne Lumenera INFINITY ANALYZE 7 microscope at 40× magnification. Maximal projections of confocal images were captured with INFINITY ANALYZE 7 Software at peak exposure in the single GFP channel. To determine the extent of the aggregation, ImageJ v1.51 was used with no additional plugin. The drawing feature within ImageJ was utilized to outline the nematode and obtain the area, mean, integrated density (IntDensity), and the raw integrated density (RawIntDensity). The same parameters were obtained from the surrounding environment by outlining portions of the image background (of any size). The nematode's Corrected Total Cell Fluorescence (CTCF) was then calculated with the following formula: CTCF = Integrated density - (Area of selected cell x Mean fluorescence of background readings) The average of the calculated values was derived from each group (Measuring cell fluorescence using ImageJ). Bar graphs were generated using GraphPad Prism to visually represent the data across different groups, and t-tests were employed to compare means between treatment conditions and assess the significance of any observed differences. Error bars were calculated as the standard error of mean (SEM).

## 3. Results & Discussion

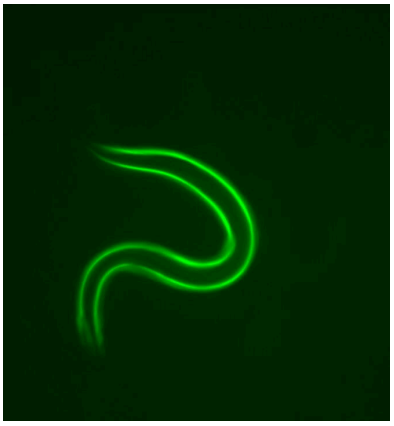

**Figure 1**. *Untreated nematode (did not receive probiotic treatment) imaged with fluorescence microscopy and INFINITY ANALYZE X software.*

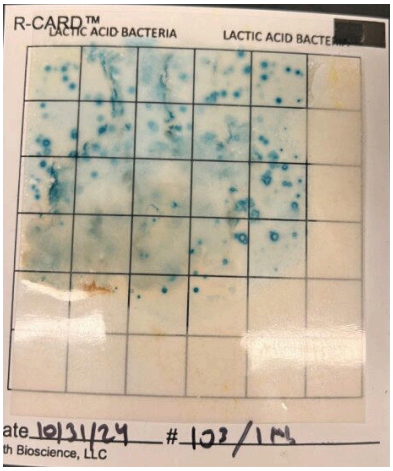


**Figure 2**. *A Lactic Acid Bacteria R-CARD displaying the presence of Lactic Acid bacteria obtained from $10^3$ CFU/mL of 1 Spring Valley probiotic capsule. Each blue dot represents a colony of bacteria, and the dots in each square were quantified to yield a total concentration of approximately $10^3$. This confirmed the accuracy of the serial dilutions.*

### *3.1. Confirming The Presence of Lactic Acid Bacteria*

The presence of Lactic Acid bacteria in the probiotic capsules was confirmed by the appearance of colored dots on the R-CARDs, as shown in Figure 2. The concentration derived from the card was approximated as $10^3$ CFU/mL, which confirmed the reliability of the serial dilutions.

### *3.2. Lifespan Assay*

Despite the presence of FUdR in all the plates, the worms were observed reproducing during the experiment. The nematodes in the PB treatment groups reproduced on Day 7, and the untreated nematodes reproduced on Day 8. As a result, the lifespan assay could not be conducted. Differences in the timing of reproduction between the untreated and treated groups were noted; however, the possibility of probiotics extending nematode lifespan could not be determined in this assay.

### *3.3. Thrashing Assay*

As shown in Figure 3, Figure 4, and Figure 5, the untreated groups exhibited a significantly lower average number of thrashes compared to the PB treatment groups on Days 3, 6, and 8. No statistically significant difference was observed across the probiotic treatment groups throughout the course of the experiment. These conclusions were determined through the implementation of t-tests and calculation of p-value.

### *3.4. Fluorescence Microscopic Analysis*

Based on the differences in CTCF levels, the treated nematodes exhibited a lower level of alpha-synuclein aggregation compared to the untreated nematodes, regardless of what PB concentration they received. This trend was recorded on Day 5 and continued on Day 7, where an even larger disparity in GFP fluorescence was observed. On Day 7, however, $10^6$ and $10^7$ PB treatment groups displayed the lowest CTCF levels. No statistically significant difference was observed in the CTCF levels across treatment groups. These conclusions were determined through implementing t-tests and calculating p-value.

These results showcase the potential of probiotic supplementation in improving motility and decreasing alpha-synuclein aggregation in nematodes. The probiotics may have countered the pathogenesis of PD, resulting in improved physiological resilience and reduced disease progression. These findings, in turn, support the emerging theory that probiotics hold potential beneficial effects on molecular and cellular pathways, as well as

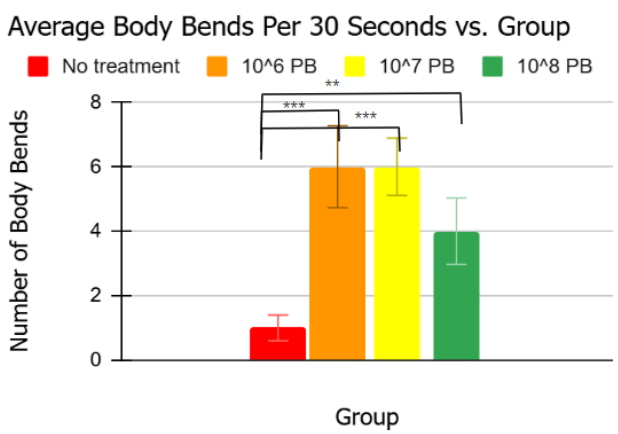


**Figure 3**. *Probiotic treatment increased thrashing behavior in Day 3 worms. The solid red bar represents the untreated worms, which were solely exposed to MC4100 E. coli. The orange bar represents the treated worms, which were exposed to $10^6$ CFU/mL probiotic supplementation alongside MC4100. The yellow and green bars represent the treated worms exposed to the $10^7$ and $10^8$ concentrations of the probiotic supplementation, respectively. The treated worms experienced a significant (p<0.01) number of thrashes per 30 seconds compared to the untreated worms and experienced an insignificant difference in thrashes amongst themselves. In terms of p-value, one star signifies p<0.05, two stars signifies p<0.01, and three stars signifies p<0.001.*

behavioral outcomes, in preclinical and clinical studies of PD [19]. Although the lifespan assay could not be conducted and the application of FUdR had not demonstrated efficacy, the nematodes that received PB treatment reproduced approximately 24 hours earlier than the untreated nematodes, which suggests an underlying relationship between probiotics and vitality. This study also confirmed the use of MC4100 bacteria as a positive control in PD experimentation. Future studies can continue to rely on this bacteria to initiate alpha-synuclein aggregation and evaluate the efficacy of potential therapeutic agents, such as probiotics, in mitigating the associated neurodegenerative effects. In this case, the dosage did not impact the efficacy of the probiotic treatment. This calls for further experimentation to determine the minimum dosage that yields a statistically

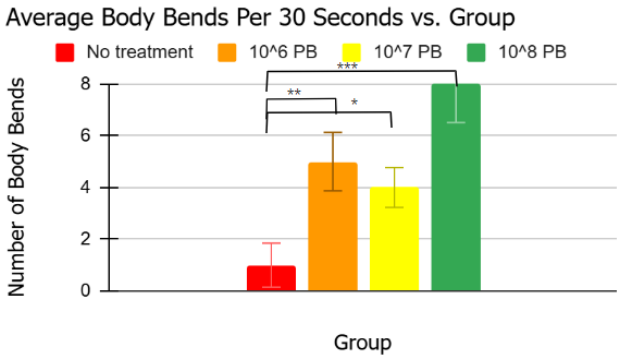


**Figure 4**. *Probiotic treatment continued to increase thrashing behavior in Day 6 worms. The solid red bar represents the untreated worms, which were solely exposed to MC4100 E. coli. The orange bar represents the treated worms, which were exposed to $10^6$ CFU/mL probiotic supplementation alongside MC4100. The yellow and green bars represent the treated worms exposed to the $10^7$ and $10^8$ concentrations of the probiotic supplementation, respectively. The $10^8$ worms presented the most statistically significant difference in the number of thrashes per 30 seconds, with p<0.001. Overall, the treated worms experienced a significant (p<0.05) number of thrashes compared to the untreated worms and experienced an insignificant difference in thrashes amongst themselves. In terms of p-value, one star signifies p<0.05, two stars signifies p<0.01, and three stars signifies p<0.001.*

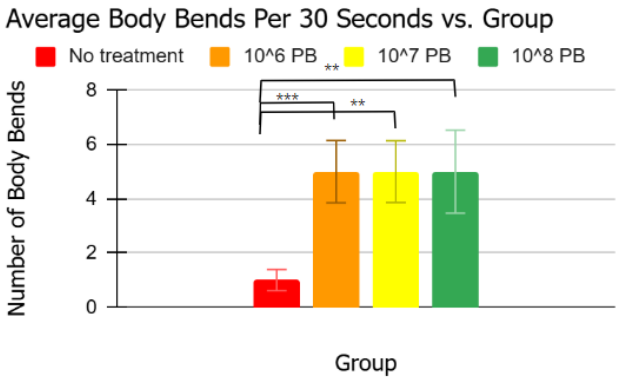


**Figure 5**. *Probiotic treatment remained consistent with increasing thrashing behavior in Day 8 worms. The solid red bar represents the untreated worms, which were solely exposed to MC4100 E. coli. The orange bar represents the treated worms, which were exposed to $10^6$ CFU/mL probiotic supplementation alongside MC4100. The yellow and green bars represent the treated worms exposed to the $10^7$ and $10^8$ concentrations of the probiotic supplementation, respectively. Overall, the treated worms experienced a significant ($p<0.05$) number of thrashes per 30 seconds compared to the untreated worms and experienced an insignificant difference in thrashes amongst themselves. The worms in treatment groups yielded the same average number of thrashes, presenting no statistically significant difference ($p>0.05$). In terms of p-value, one star signifies $p<0.05$, two stars signify $p<0.01$, and three stars signify $p<0.001$.*

significant difference. Additionally, future studies should confirm the presence of MC4100 bacteria and the probiotic bacteria within the nematodes' gut microbiomes through microscopy or sequencing techniques. This imaging will assist with determining the localization and interaction of the probiotics within the host's gut. Such follow-up interventions will enable us to understand the mechanisms at play and refine probiotic-based strategies for neuroprotection. Overall, this study adopted a different approach with studying PD pathogenesis. Targeting the imbalances within the gut microbiome, utilizing a widely available ingestible product as preventative treatment, and focusing on the impact on various dosages provides a unique lens that emphasizes the gut-brain connection and its potential for therapeutic interventions. These findings align with the

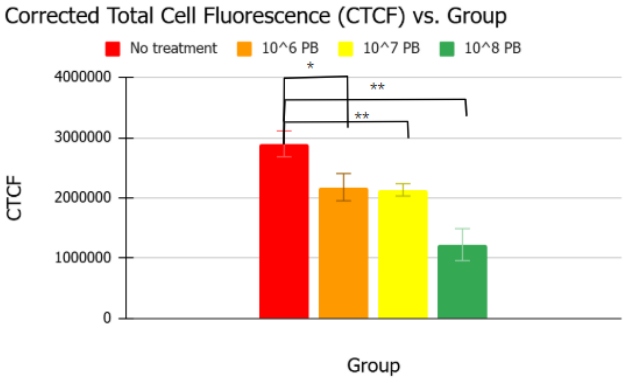


**Figure 6**. *Probiotic treatment presented lower levels of alpha-synuclein aggregation for Day 5 worms. The solid red bar represents the untreated worms, which were solely exposed to MC4100 E. coli. The orange bar represents the treated worms, which were exposed to $10^6$ CFU/mL probiotic supplementation alongside MC4100. The yellow and green bars represent the treated worms exposed to the $10^7$ and $10^8$ concentrations of the probiotic supplementation, respectively. The group that received the highest probiotic concentration presented the lowest average CTCF value—a value significantly lower than that of the untreated group ($p<0.01$). Overall, all treatment groups experienced significantly lower levels of aggregation compared to the untreated group ($p<0.05$). In terms of p-value, one star signifies $p<0.05$, two stars signify $p<0.01$, and three stars signify $p<0.001$.*

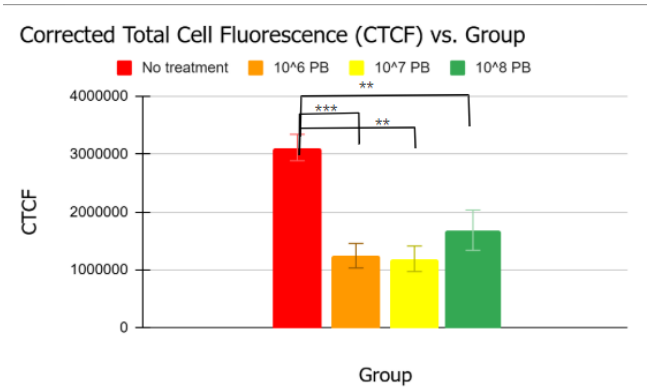


**Figure 7**. *Probiotic treatment presented lower levels of alpha-synuclein aggregation for Day 7 worms. The solid red bar represents the untreated worms, which were solely exposed to MC4100 E. coli. The orange bar represents the treated worms, which were exposed to $10^6$ CFU/mL probiotic supplementation alongside MC4100. The yellow and green bars represent the treated worms exposed to the $10^7$ and $10^8$ concentrations of the probiotic supplementation, respectively. Overall, all treatment groups experienced significantly lower levels of aggregation compared to the untreated group ($p<0.01$). The group that received the lowest probiotic concentration presented the lowest average CTCF value, greatly differing from the untreated group's ($p<0.001$). In terms of p-value, one star signifies $p<0.05$, two stars signify $p<0.01$, and three stars signify $p<0.001$.*

growing claim that probiotics wield neuroprotective effects—offering promising avenues for non-invasive treatment strategies. It is crucial to acknowledge, however, that the study faced several limitations. The inability to conduct a lifespan assay and the lack of efficacy in FUdR application limited comprehensive analysis, which left certain potential effects unexplored. Since the study also could not confirm bacterial presence in the gut microbiomes, it lacked verification that the probiotics successfully reached their target location. The viability of the probiotics may also have been impacted by environmental conditions, such as fluctuations in temperature, inadequate nutrient availability, and prolonged storage times, which may have compromised bacterial integrity and limited their impact on nematode health.

## 4. Conclusion

Ultimately, the administration of probiotic supplementation in *C. elegans* resulted in accelerated reproduction, greater motility, and reduced alpha-synuclein aggregation. The difference in dosage did not result in a statistically significant difference in any of the three factors across the probiotic treatment groups; however, these groups showed improved PD symptoms compared to the untreated group. Thus, the presence of probiotics (in concentrations of $10^6$, $10^7$, and $10^8$ CFU/mL) is sufficient to discourage PD pathogenesis. Administration of the probiotic treatments at the start of the experiment allowed for the evaluation of probiotics as a preventative treatment, providing insight into its ability to address the issue of alpha-synuclein aggregation—the root cause of PD. However, numerous questions remain unanswered. What are the specific properties that enable probiotics to alleviate PD symptoms on a neurological level? Would a probiotic mixture be more effective in treating PD compared to isolated Lactic Acid bacteria? What if probiotics were administered post-pathogenesis? Most importantly, though, how can probiotics be leveraged to prevent neurodegeneration and enhance human health? Although this study provides valuable insights into their efficacy in treating PD, future studies will hopefully produce answers to these questions—enabling us to determine effective therapeutic strategies for PD and other neurodegenerative diseases. Since current treatment methods remain expensive and largely inaccessible for the time being,

the possibility of probiotics as preventative medicine offers a promising solution—in neurodegenerative treatment and beyond.

## References


[1] J. Lotharius and P. Brundin, "Pathogenesis of parkinson's disease: dopamine, vesicles and \alpha-synuclein", *Nature Reviews Neuroscience*, vol. 3, no. 12, pp. 932–942, 2002, doi: 10.1038/nrn983.

[2] D. J. Surmeier, "Determinants of dopaminergic neuron loss in Parkinson's disease," *The FEBS Journal*, vol. 285, no. 19, pp. 3657–3668, 2018, doi: 10.1111/febs.14607.

[3] L. I. Golbe and C. E. Leyton, "Life expectancy in Parkinson disease," *Neurology*, vol. 91, no. 22, pp. 991–992, 2018, doi: 10.1212/wnl.0000000000006560.

[4] A. Picca, R. Calvani, H. J. Coelho-Junior, F. Landi, R. Bernabei, and E. Marzetti, "Mitochondrial Dysfunction, Oxidative Stress, and Neuroinflammation: Intertwined Roads to Neurodegeneration," *Antioxidants*, vol. 9, no. 8, p. 647, 2020, doi: 10.3390/antiox9080647.

[5] H. Park, T.-I. Kam, V. L. Dawson, and T. M. Dawson, "\alpha-Synuclein pathology as a target in neurodegenerative diseases", *Nature Reviews Neurology*, vol. 21, no. 1, pp. 32–47, 2024, doi: 10.1038/s41582-024-01043-w.

[6] Y. Han *et al.*, "Vagus Nerve and Underlying Impact on the Gut Microbiota-Brain Axis in Behavior and Neurodegenerative Diseases," *Journal of Inflammation Research*, pp. 6213–6230, 2022, doi: 10.2147/jir.s384949.

[7] V. A. Huynh, T. M. Takala, K. E. Murros, B. Diwedi, and P. E. J. Saris, "Desulfovibrio bacteria enhance alpha-synuclein aggregation in a Caenorhabditis elegans model of Parkinson's disease," *Frontiers in Cellular and Infection Microbiology*, vol. 13, 2023, doi: 10.3389/fcimb.2023.1181315.

[8] S. Holmqvist *et al.*, "Direct evidence of Parkinson pathology spread from the gastrointestinal tract to the brain in rats," *Acta Neuropathologica*, vol. 128, no. 6, pp. 805–820, 2014, doi: 10.1007/s00401-014-1343-6.

[9] A. H. Tan, J. W. Hor, C. W. Chong, and S. Lim, "Probiotics for Parkinson's disease: Current evidence and future directions," *JGH Open*, vol. 5, no. 4, pp. 414–419, 2020, doi: 10.1002/jgh3.12450.

[10] M. E. Goya *et al.*, "Probiotic Bacillus subtilis Protects against \alpha-Synuclein Aggregation in C. elegans", *Cell Reports*, vol. 30, no. 2, pp. 367–380, 2020, doi: 10.1016/j.celrep.2019.12.078.

[11] J. Sun *et al.*, "Probiotic Clostridium butyricum ameliorated motor deficits in a mouse model of Parkinson's disease via gut microbiota-GLP-1 pathway," *Brain, Behavior, and Immunity*, vol. 91, pp. 703–715, 2021, doi: 10.1016/j.bbi.2020.10.014.

[12] Y.-L. Tseng *et al.*, "Degradation of neurodegenerative disease-associated TDP-43 aggregates and oligomers via a proteolysis-targeting chimera," *Journal of Biomedical Science*, vol. 30, no. 1, 2023, doi: 10.1186/s12929-023-00921-7.

[13] Shamsuzzama, L. Kumar, and A. Nazir, "Modulation of Alpha-synuclein Expression and Associated Effects by MicroRNA Let-7 in Transgenic C. elegans," *Frontiers in Molecular Neuroscience*, vol. 10, 2017, doi: 10.3389/fnmol.2017.00328.

[14] J. Y. Lim, J. M. May, and L. Cegelski, "Dimethyl Sulfoxide and Ethanol Elicit Increased Amyloid Biogenesis and Amyloid-Integrated Biofilm Formation in Escherichia coli," *Applied and Environmental Microbiology*, vol. 78, no. 9, pp. 3369–3378, 2012, doi: 10.1128/aem.07743-11.

[15] T. R. Sampson *et al.*, "A gut bacterial amyloid promotes \alpha-synuclein aggregation and motor impairment in mice", *eLife*, vol. 9, 2020, doi: 10.7554/elife.53111.

[16] M. S. Son and R. K. Taylor, "Growth and Maintenance of Escherichia coli Laboratory Strains," *Current Protocols in Microbiology*, vol. 27, no. 1, 2012, doi: 10.1002/9780471729259.mc05a04s27.

[17] "Maintenance of C. elegans," 2019, [Online]. Available: http://www.wormbook.org/chapters/www_strainmaintain/strainmaintain.html

[18] S. Hughes, M. van Dop, N. Kolsters, D. van de Klashorst, A. Pogosova, and A. M. Rijs, "Using a Caenorhabditis elegans Parkinson's Disease Model to Assess Disease Progression and Therapy Efficiency," *Pharmaceuticals*, vol. 15, no. 5, p. 512, 2022, doi: 10.3390/ph15050512.

[19] V. Leta *et al.*, "Neurogenic and anti-inflammatory effects of probiotics in Parkinson's disease: A systematic review of preclinical and clinical evidence," *Brain, Behavior, and Immunity*, vol. 98, pp. 59–73, 2021, doi: 10.1016/j.bbi.2021.07.026.

Open Access | https://doi.org/10.62329/mhkn9486

**Morganton Scientific**

*North Carolina School of Science and Mathematics*

Journal of Student STEM Research

# Computationally Modeling Factors of Aging that Affect the Population of T-cells and B-cells of Humans Age 60 and Older

**Felice Zhu**[1]

[1]NCSSM

## Abstract

The study of T-cell and B-cell population dynamics concerning the effects of aging presents significant challenges due to various factors. Individual variations in health conditions and the complex interrelations within the immune system can lead to diverse outcomes. To address these complexities, we implemented a systematic approach to create computational models, which simulate the long-term population dynamics of T-cells and B-cells under conditions of aging. These models encompass essential physiological processes, including thymic output, bone marrow production, cellular activation, senescence, and natural cell death. Additionally, we generated graphical representations from the models to facilitate a clearer visualization of the observed trends. Age 60 was selected as the initial point for this analysis, as the effects of the aging immune system become increasingly evident at this stage, making previous facts by other studies more recognizable. This study underscores the potential of computational modeling capabilities in advancing our comprehension of the immune system, providing valuable insights for tracking and visualizing population dynamics. The modeling done here can be added upon to reach higher complexities to models that can accurately reflect what occurs in real life.

**Keywords** T-cell and B-cell Computational Model, Stella Architect, Immune System Aging, T-cells and B-cells dynamics

## 1. Introduction

Aging is an inevitable process characterized by a gradual decline in the human body's functionality, including the immune system's efficiency. While some mechanisms of aging are well-documented, such as thymic involution, the specific factors underlying these processes are not yet fully understood. As individuals age, the responsiveness of T-cells and B-cells to pathogens decreases, and there is also an increased risk of autoimmune complications. No table alterations in the immune system typically commence around the age of 60 [1]. It is essential to clarify that both T-cells and B-cells are produced in the bone marrow; however, T-cells migrate to the thymus to undergo maturation, enabling them to effectively combat pathogens. This research emphasizes computational modeling to study the effects of aging on the behavior, dynamics, and interactions of T-cell and B-cell populations, which contribute to the overall decline of the immune system.

The thymus gland is responsible for generating naive T-cells, which are crucial for activating the immune response. This maturation process is meant to prevent and eliminate self reactive T-cells in the body. Thymic involution, the process by which the thymus gland progressively shrinks, begins as one is born and continues throughout an individual's life [2]. In younger individuals, this involution occurs at a gradual rate, allowing for efficient regeneration of thymic cells and maintaining a robust population of

**Published** Jun 27, 2024

**Correspondence to**
Felice Zhu
zhu26f@ncssm.edu

naive T-cells. However, this process poses significant challenges as individuals reach approximately 60 years of age, at which point the rate of cell regeneration decreases markedly. Consequently, there is a pronounced decline in the population of naive T-cells over subsequent years, which adversely affects the immune response to pathogens and increases the susceptibility to autoimmune complications[2]. It is important to note that the rate of thymic involution varies widely among individuals, influenced by factors such as lifestyle, genetics, and gender. Furthermore, with our advancement in healthcare, people can seek thymus therapy which regenerates thymus cells to increase naive T-cell count. Therefore, developing a universal model applicable to all individuals is complex. This study will account for thymic involution in the modeling of T-cell populations, but it's worth noting that its rate may vary among individuals and will not reflect possible therapy interventions.

The bone marrow plays a crucial role in the production of both B-cells and T-cells; however, it primarily serves as the site for B-cell maturation. The maturation process occurring within the bone marrow resembles that of the thymus, wherein self-reactive B-cells are identified and eliminated. As individuals age, the bone marrow undergoes deterioration, leading to decreased cellularity and a corresponding reduction in the production of naive B-cells [3]. This decline becomes increasingly evident around the age of 60 and older. Activated B-cells, which possess the capacity to generate billions of antibodies, tend to reach a state of exhaustion slightly more rapidly than T-cells. This phenomenon is attributable to the considerable amount of energy and resources expended at the cellular level. Furthermore, the aging process exacerbates this exhaustion, resulting in diminished antibody production and a heightened likelihood of B-cells entering a state of senescence. Senescence is the aging of cells, rendering them dysfunctional, long-lasting, and space-occupying. Similar to the thymus, the rate of bone marrow deterioration varies among individuals, influenced by a variety of factors. Bone marrow transplantation represents one of the most effective, albeit challenging, methods for regenerating bone marrow; this procedure is generally more complex than thymus therapy. Such variability complicates the endeavor to accurately model bone marrow function across diverse individuals. This study will incorporate considerations of bone marrow deterioration into the modeling of B-cell populations; however, it will not reflect the individual differences in deterioration rates or account for the potential effects of bone marrow transplants.

The rates in the research were chosen to help reflect that of a 60-year-old's immune system. Some rates considered in this paper are death rate, activation rate, and senescence rate. Additionally, age accelerates the senescence rate of all populations and declines the activation rate weakening the immune response. Each population and cell type will present different rates.

Activation in the immune system resembles a domino effect. Age does affect the rate at which T-cells and B-cells are activated, and as stated before the rates of these decline over time which weakens the immune response (aligns with the fact that older people have weaker immune systems). For example, helper T-cells are often seen as the activator for B-cells [4] but that rate decreases as the population of naive T-cells decreases. On the other hand, the senescence rate will accelerate over time leading to a more dominant population of senescent cells seen later in the older ages.

The frequencies of death and senescence of naive T-cells and B-cells are lower than those observed in other immune cell populations. These naive cells are not subject to exhaustion or prolonged activation resulting from combating infections, which contributes to their low turnover rates concerning death and senescence. Naive has selective signaling T-cells engage via their IL-7R receptors [noauthor_t_2025], while naive

B-cells utilize BAFF receptors [4] and both promote cellular survival and inhibit premature apoptosis, provided they do not encounter an activating antigen. In contrast, the activated cell population exhibits the highest turnover rates for both death and senescence. This phenomenon arises from their constant activity, which involves the production of significant quantities of cytokines that deplete their energy and resources, ultimately leading to exhaustion. Consequently, these activated cells may undergo apoptosis or become senescent. This state of exhaustion is increasingly prevalent in older human immune systems, resulting in elevated rates of death and senescence within this population. Memory cells represent a specialized subset of activated cells that retain the capacity to recognize and respond to previously encountered pathogens. Given their lower activity levels and reduced cytokines production compared to activated cells, memory cells exhibit a diminished death rate and can persist in the body for extended periods. Nonetheless, they are not entirely immune to exhaustion, which may result in low levels of senescence turnover. Senescent cells are characterized by a loss of functionality and an inability to replicate, yet they tend to persist over time. Various factors, including cellular exhaustion, DNA damage, and chronic inflammation—each of which is associated with the aging process—can induce their formation [1]. These senescent cells accumulate within the body and may compromise immune responses as well as the efficacy of vaccinations A primary reason for their prolonged existence is their inherent resistance to apoptosis [noauthor_senescent_2021]. However, senescent cells remain unstable and unpredictable, as numerous factors may influence the senescence process. Consequently, it is increasingly common to observe a substantial rise in senescent cells among the elderly, leading to their eventual dominance over other immune cell populations. The modeling process will take into account most of these facts, except a few like inflammation, and produce a quantitative reflection.

## 2. Computational Approach

In order to effectively model population dynamics, differential equations are particularly utilized for representing the changes within biological populations. This study will formulate and utilize the sets of equations to reflect the dynamics of both T-cells and B-cells. Specifically, we will focus on four distinct populations: naive, activated, memory, and senescent cells. The analysis will cover a 50-year period, beginning at age 60 and continuing until age 110.

This model will operate under the following assumptions: chronic inflammation is absent, no regenerative procedures have been conducted on the thymus or bone marrow, all types of activated cells are grouped into one active population, all types of memory cells are grouped into one memory population, and the model initiates with no activated adaptive immune cells. Furthermore, there exists a relatively low quantity of naive cells, coupled with a presence of memory and senescent cells, as a result of a slightly compromised immune system, and the rates incorporated in the model will aid in reflecting these specified conditions. ChatGPT was used to help develop differential equations, sub-formulas (Fig. 1), and rate parameters that describe the population dynamics of different T-cell subsets.

$$dT_{naive}(t) = p(t) - \alpha_{NS}(t) * T_{naive}(t) - r_{activation}(t) * T_{naive}(t) - \sigma * T_{naive}(t) \tag{1}$$

$$dT_{activated}(t) = r_{activation}(t) * T_{naive} - \alpha_{AS}(t) * T_{activated} - \delta_{AM}(t) * T_{activated}(t) - \sigma_{activated} * T_{activated}(t) \tag{2}$$

$$dT_{memory}(t) = \delta_{AM} * T_{activated}(t) - \sigma_{MS} * T_{memory}(t) - \sigma_{memory} * T_{memory}(t) \tag{3}$$

$$dT_{senescent}(t) = \alpha_{NS} * T_{naive}(t) + \alpha_{AS} * T_{activated}(t) + \alpha_{MS} * T_{memory}(t) - \sigma_{senescent} * T_{senescent}(t) \tag{4}$$

Equation (1) represents the dynamics of naive T cells, while Equation (2) represents the dynamics of activated T-cells. Additionally, Equation (3) represents the population dynamics of memory T-cells, and Equation (4) represents the dynamics of senescent T-

**Formulas and Values (T-cells)**

(All rates were converted to display values in years.)

NS represents naive to senescent

AS represents active to senescent

MS represents memory to senescent

AM represents activated to memory

**-Thymus output-**

$$P(t) = P_0 e^{-\beta t}$$

P(t) represents the thymus output

$P_0$ represents the initial population of naive T-cells (3.65 x $10^9$ Naive cells)

$\beta$ represents the rate of thymic involution (5%)

**-Activation of Naive T-cells to Active-**

$$r_{activation} = r_0 e^{-\sigma t}$$

$r_{activation}(t)$ represents the activation rate from naive to active

$r_0$ represents the initial activation rate from naive to active (70%)

$\sigma$ represents the declination of the rate (3%)

**-Senescent Transition Rates-**

$$\alpha_{(NS,AS,MS)}(t) = \alpha_{(NS0,AS0,MS0)} e^{\gamma_{(NS,AS,MS)} t}$$

$\alpha(t)$ represents the transition to senescent

$\alpha_0$ represents the initial transition rate

$\gamma$ represents the the acceleration of transition rate to senescent

EACH $\alpha_0$ RATE IN RESPECTIVE ORDER (1%, 10%, 3%)

EACH $\gamma$ IN RESPECTIVE ORDER (1%, 5%, 2%)

**-Death Rates-**

$$\sigma_{(naive,activated,memory,senescent)}$$

$\sigma_{naive}$ represents the death rate of naive T-cells (1%)

$\sigma_{activated}$ represents the death rate of activated T-cells (60%)

$\sigma_{memory}$ represents the death rate of memory T-cells (5%)

$\sigma_{senescent}$ represents the death rate of senescent T-cells (7%)

**-Memory Activation-**

$$\delta_{AM}(t) = \delta_{AM0} e^{-\gamma t}$$

$\delta_{AM0}$ represents the inital transtion from active to memory (40%)

$\gamma$ represents the declination of active to memory (3%)

**Figure 1**. *Rates and sub-formulas of T-cell population*

cells. All rates are expressed in terms of years. ChatGPT offered reasonable rates for constructing the model, which reflects a moderately compromised immune system. Although the relationship is nonlinear and does not precisely adhere to an exponential form, exponential functions were selected as the most suitable approach for modeling these dynamics [5].

Next, we tasked ChatGPT to help craft a set of equations that would reflect the B-cell population dynamics. It crafted similar equations to the T-cells and sub-formulas (Fig. 2) also followed the same structure; however, the rates differed from the T-cells to reflect the unique dynamics the B-cell population undergoes.

$$dB_{naive}(t) = Q(t) - \alpha_{senescence}(t) * B_{naive}(t) - r_{activation}(t) * B_{naive}(t) - \alpha_{naive} * B_{naive}(t) \quad (5)$$

$$dB_{activated}(t) = r_{activation}(t) * B_{naive}(t) - \alpha_{AS}(t) * B_{activated}(t) - \delta_{AM}(t) * B_{activated}(t) - \sigma_{activated} * B_{activated}(t) \quad (6)$$

$$dB_{memory}(t) = \delta_{AM}(t) * B_{activated}(t) - \alpha_{MS} * B_{memory}(t) - \sigma_{memory} * B_{memory}(t) \quad (7)$$

$$dB_{memory}(t) = \alpha_{NS} * B_{naive}(t) + \alpha_{AS} * B_{activated}(t) + \alpha_{MS} * B_{memory}(t) - \sigma_{Senescent} * B_{Senescent}(t) \quad (8)$$

Equation (5) represents the dynamics of naive B cells, while Equation (6) represents the dynamics of activated B-cells. Additionally, Equation (7) represents the population dynamics of memory B-cells, and Equation (8) represents the dynamics of senescent B-cells. Following the development of differential equations, it is important to select an appropriate computational tool to visualize the dynamics to gain a deeper understanding

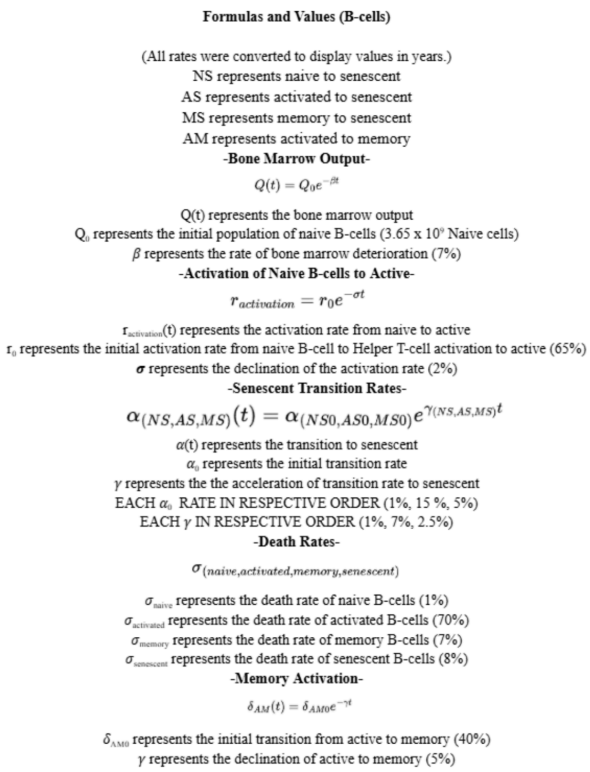


**Figure 2.** *Rates and sub-formulas of B-cell population*

of the relationships between the various rates. Stella Architect has been identified as a suitable platform for this purpose, owing to its strong capabilities in system dynamics modeling. The interface of Stella facilitates the creation of stock-and-flow diagrams, which effectively illustrate the transitions among different cell states and the underlying physiological processes. In this framework, stocks denote populations of naive, activated, memory, and senescent cells, while flows represent the transition of activation, senescence, and cell death. Additionally, converters and connectors are utilized to incorporate the various rates into the model. The simulation was conducted using the RK4 method (Runge-Kutta Method), which is recognized for its precision and higher-order capabilities in evaluating differential equations accurately. The models constructed can be seen in Figure 3 and Figure 4. In preparation for the generation of the graphs, the axes have been labeled appropriately, with the x-axis denoting the years following the age of 60 and the y-axis representing the population.

## 3. Results and Discussion

The models ran and two line graphs were produced for each population to display their respective dynamics with each line graph showing the four unique populations. The results accurately reflect the long-term effects of aging on T-cells and B-cells, activation, death, and turnover.

In the context of T-cells, as illustrated in Figure 5, the population of naive T-cells exhibits a gradual decline over time, ultimately approaching zero. After 50 years, the quantity of naive T-cells is significantly lower than at the outset, with only a few million remaining. This reduction can primarily be attributed to thymic involution. Naive T-cells show a lower propensity for apoptosis, and their turnover to senescent cells is relatively minimal in comparison to the overall T-cell population. The decline in naive T-cells has a major

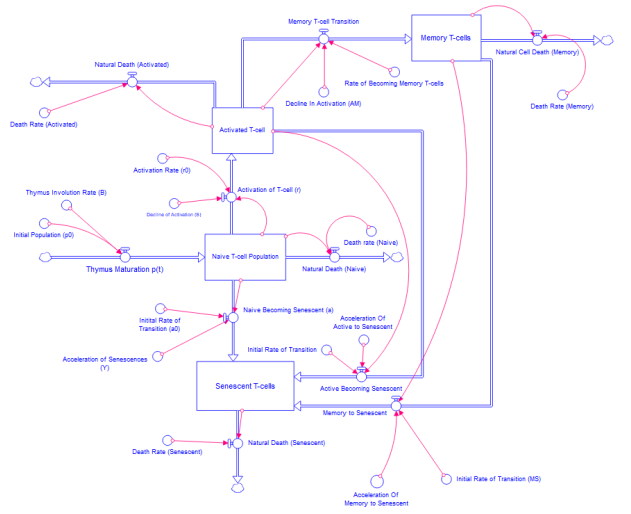


**Figure 3**. *Constructed Stella model of T-cell population dynamics*

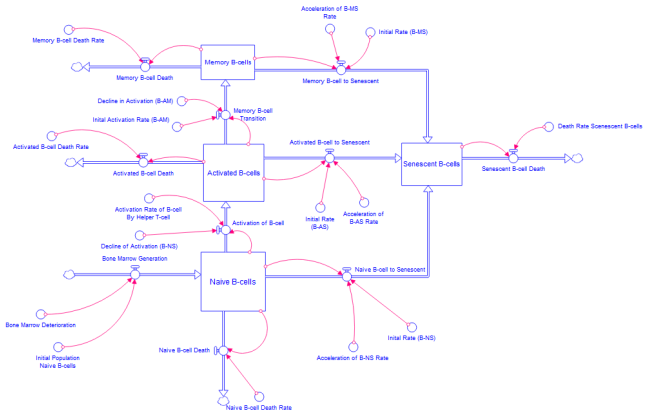


**Figure 4**. *Constructed Stella model of B-cell population dynamics*

effect on all T-cell populations, particularly the active T-cells. As the population of naive T cells diminishes, the population of active T-cells also decreases. The rates selected within this model accurately reflect these dynamics. The elevated death rate, declining activation rate, and increased turnover rate to senescent cells in activated T-cells suggest a significant decline over time, illustrating that the immune response weakens as one ages. Furthermore, it is important to note that activated T-cells transition to the senescent state at a faster rate than other T-cell populations. The memory T-cell population, being the second most abundant in the model, reflects a low senescent turnover rate and death rate. This phenomenon explains why the decline in the populations of naive and activated T-cells does not significantly impede the number of memory T-cells. Nevertheless, a trend exists indicating a reduction in memory T-cell population over time, due in part to the decreased activation rate of active T-cells converting to memory T-cells, as well as the mortality and senescence of older T-cells. This trend further underscores the weakening of the immune system. Ultimately, senescent T-cells emerge as the dominant population as time progresses, as all other T-cell populations, particularly the active T-cells, contribute to this accumulation. Senescent T-cells do not undergo rapid apoptosis and thus accumulate within the body, subsequently diminishing immune responses. This relationship is evidenced by the substantial increase in senescent T-cells alongside the decline in the active T-cell population.

In the context of B-cells, having very similar trends as illustrated in Figure 6, the population of naive B-cells experiences a gradual decline over time, ultimately approaching zero. After 50 years, the quantity of naive B-cells is markedly reduced compared to the initial count, with only a few million remaining. This reduction is primarily attributable to diminished bone marrow output. Naive B-cells, like naive T-cells, exhibit a lower propensity for apoptosis and their turnover. The decline in naive B cells has a major impact on all B-cell populations, particularly active B-cells. As the population of naive B-cells diminishes, there is a corresponding decrease in the active B-cell population. The rates selected within this model accurately reflect these dynamics. The elevated death rate, declining activation rate, and increased turnover to exhausted cells in active B cells indicate a substantial decline over time, illustrating the weakening of the adaptive immune response as individuals age. Furthermore, it is noteworthy that active B-cells transition to an exhausted state at a faster rate than other B-cell populations. The memory B-cell population, the second most abundant in this model for a while, demonstrates a low turnover and death rate concerning exhaustion. This observation elucidates why the decline in naive and active B-cells does not significantly hinder the number of memory B-cells. Nevertheless, there exists a discernible trend indicating a gradual reduction in the memory B-cell population over time, attributable in part to the decreased activation rate of naive B cells converting into memory B-cells, as well as the mortality and exhaustion of older B-cells. However, towards the end of the graph, the naive B-cells gain the second most abundance as theactive B-cells population has significantly decreased and the active to memory rate has declined a large amount. Conclusively, senescent B-cells emerge as the predominant population as time progresses, since all other B-cell populations, particularly active B-cells, contribute to this accumulation. Senescent B-cells do not undergo rapid apoptosis, leading to their accumulation within the body and subsequently diminishing immune responses. This relationship is evidenced by a marked increase in exhausted B-cells alongside the decline in the active B-cell population. These graphical figures demonstrate the active differences between T-cells and B cells as B-cells exhaust faster due to their function.

The results accurately reflect existing scientific evidence/knowledge. Both graphical figures demonstrate a declining trend in the function and population of T-cells and B-cells. The population of naive T-cells is crucial for maintaining the balance of other immune cell populations, except for senescent cells. As indicated by the graphs, the decline in naive T-cells over time will inevitably lead to a decrease in memory and active cell populations. This illustrates the negative effects of thymic involution and bone marrow deterioration on these immune cell populations. The results also show that the rates of senescent cells accelerate over time, making the senescent cell population the most dominant among individuals aged 60 and older which aligns with the fact that senescent T-cells and B-cells will dominate the other populations and weaken immune responses. While the model offers valuable insights, its simplified assumptions may not fully capture the complexities associated with immune aging. Future iterations of the model could enhance predictive accuracy by incorporating more non-linear dynamics, environmental influences, and factors from earlier life stages. Despite these limitations, the findings highlight the potential to mitigate the impacts of immunosenescence and improve health outcomes for aging individuals. This model has effectively reflected information corroborated by other studies, which is valuable as it paves the way for future models.

The findings of this study present significant opportunities for future research focused on addressing immune aging and its associated consequences. One particularly promising area involves the development of interventions aimed at mitigating immune senescence. Strategies such as thymic rejuvenation, stem cell therapies, and pharmacological agents designed to enhance bone marrow output could be beneficial in maintaining populations

of naive T-cells and B-cells. Additionally, targeting the pathways involved in T-cell senescence and B-cell exhaustion may provide therapeutic avenues to support immune function in the aging population. Furthermore, it is essential to explore the influence of environmental and lifestyle factors on immune dynamics. Research may investigate how dietary choices, physical exercise, and exposure to pathogens impact immune aging. Moreover, studies examining whether interventions such as caloric restriction or customized exercise programs can improve immune resilience over time will be valuable. Future research should also consider the intricate interactions between T-cells and B-cells. Analyzing how fluctuations in one population affect the other, particularly about cytokine signaling, could yield critical insights into the maintenance of balanced immune responses. Investigation on inflammation was missing from this model and could be a factor incorporated in future research as the majority of elderly suffer from chronic inflammation and this factor has effects on T-cells and B-cells. Finally, investigations into age-related diseases and the efficacy of vaccinations among older populations may have substantial applications. A deeper understanding of how immune senescence contributes to conditions such as cancer or chronic infections could guide the development of targeted treatments. Additionally, optimizing vaccine design may enhance protective measures for aged individuals. These factors could all be possible future studies that could generate more accurate models of the immune system and enhance our understanding of the interconnectedness of certain factors and cell population dynamics.

## 4. Conclusions

In conclusion, this research aimed to address the question of how to computationally model the factors of aging that influence the populations of T-cells and B-cells in humans aged 60 years and older. The study successfully developed differential equations, aided by contributions from ChatGPT, to facilitate the modeling of these cellular dynamics that accurately reflect factual information. In addition, Stella models were constructed which closely correspond to established scientific knowledge regarding the impact of the aging process on the immune system. The findings reveal that while the population dynamics of T-cells and B-cells exhibit nonlinear characteristics, a systematic approach can still produce accurate models aligning with factual ideas. However, the modeling process underscores the inherent complexity of population dynamics, due to the involvement of multiple factors that vary significantly among individuals. Consequently, the creation of a single universal model that accurately represents all individuals remains unfeasible. Nevertheless, this research presents opportunities for expansion by incorporating

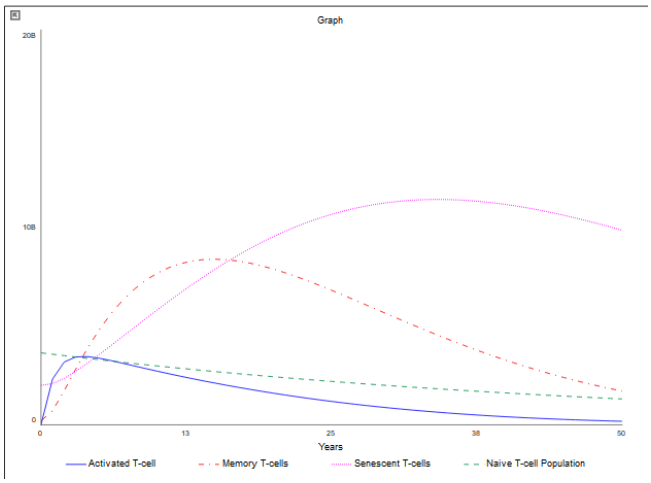


**Figure 5**. *T-cell population graph 50 years later (after 60)*

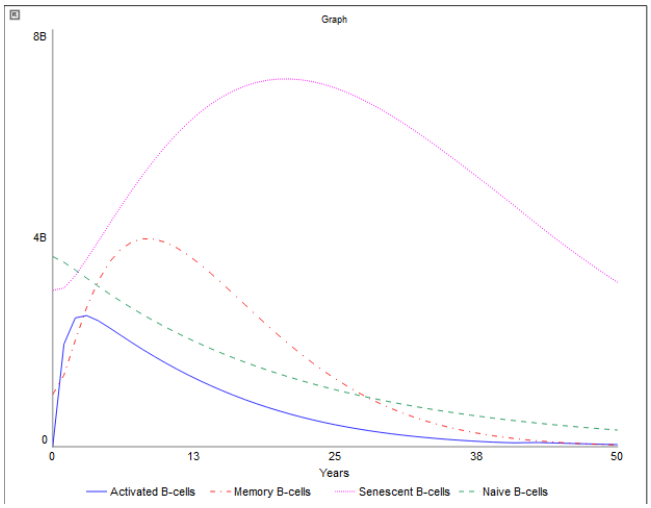


**Figure 6**. *B-cell population graph 50 years later (after 60)*

additional factors and real-life scenarios into the model. It could give us insights into understanding age-related immune decline, developing better therapies, or personalizing medicine and its effects on the immune system.

In conclusion, this research provides a comprehensive quantitative modeling and analysis of the aging immune system, establishing a foundational framework for subsequent studies aimed at enhancing health outcomes within aging populations. It emphasizes the significance of computational models in informing interventions designed to study, potentially mitigating the immune decline in older humans while expand knowledge and uncovering mysteries of immune science.

We sincerely thank Mr. Robert Gotwals for his invaluable guidance and support throughout this project, and course, and for allowing this independent research. Special thanks to the North Carolina School of Science and Mathematics for providing the software necessary for our research. We acknowledge the authors of the sources that contributed valuable background information. Additionally, the author is grateful to personal instructors for their feedback on this paper. Finally, heartfelt thanks go to friends and family for their unwavering support during the process of conducting the research.

## References

[1] C. M. Weyand and J. J. Goronzy, "Aging of the Immune System. Mechanisms and Therapeutic Targets," *Annals of the American Thoracic Society*, vol. 13, no. Supplement_5, pp. S422–S428, 2016, doi: 10.1513/AnnalsATS.201602-095AW.

[2] "Thymic involution." [Online]. Available: https://en.wikipedia.org/w/index.php?title=Thymic_involution&oldid=1267397385

[3] E. Reitman, "Yale Study Finds Aging of Bone Marrow Accelerates Atherosclerotic Plaque Formation." [Online]. Available: https://medicine.yale.edu/news-article/yale-study-finds-aging-of-bone-marrow-accelerates-atherosclerotic-plaque-formation/

[4] "B cell." [Online]. Available: https://en.wikipedia.org/w/index.php?title=B_cell&oldid=1279553599

[5] "ChatGPT." [Online]. Available: https://chatgpt.com/